The Study of Macrophage Heterogeneity in the Peritoneal Cavity

CHIA-TE LIAO

Thesis presented for the degree of
Doctor of Philosophy

2015

Institute of Infection and Immunity

School of Medicine
Cardiff University

Dedication

To my parents, Lynn and Vera

Acknowledgements

First of all, I would like to thank my supervisors, Professor Philip Taylor, Professor Donald Fraser and Professor Nicholas Topley, for their fantastic supervision and continuous support during my PhD study. Their enormous enthusiasm and great expertise not only guide me throughout the project, also help me building up my competence in conducting basic and translational research.

I am very delighted to work with all the members within Phil's lab. Especially, I would like to express my gratitude to Dr. Marcela Rosa for her wealth of advice and continued support in my laboratory work. Additionally, I would like to thank Dr. Luke Davies for his help in the beginning of my animal work, Nicola and Dina for their technical assistance, Rob and Leah for the mutual support in the lab.

Cardiff University has a great research community/platform in the field of peritoneal dialysis. It is my pleasure to involve in this big family and I would like to thank all the participants within this network. I am extremely grateful to Dr. Matthias Eberl, Dr. Chan-Yu Lin, Dr. Ann Kift-Morgan and Dr. Chantal Colmont for their contribution in setting up and maintaining the PD research framework. I would also like to express my sincere gratitude to Professor Simon Jones for his kindly sharing the expertise in the experimental peritonitis model and valuable opinions on my research project. Beyond these, I would like to thank Dr. Mohd Wajid A. Khan for his assistance in the human antigen presentation assay. I am also very grateful to the PD nurses at University Hospital of Wales and all the PD patients for their excellent cooperation throughout the project.

Last but not least, I would like to thank my family and friends here and in Taiwan. Without their constant support, I would not be able to complete this thesis.

Summary

Mononuclear phagocytes play a key role in tissue homeostasis and in host defense against pathogen invasion. However, the phenotypic identities and functional properties of this heterogeneous population within the peritoneal cavity remains poorly elucidated. In the context of peritoneal dialysis, it is hypothesized that the modification of macrophage/dendritic cell biology by the dialysis process would alter tissue homeostasis, host susceptibility to infection and local immunity, compromising long-term outcomes of the patients. The research work carried out in this thesis has tested this hypothesis by examination of the immunobiology (mainly phenotype and function) of human and murine peritoneal macrophage and dendritic cell subsets. Moreover, the potential link between the altered immunobiology of peritoneal mononuclear phagocytes and clinical outcomes of the dialysis patients has been investigated. Several key findings were generated during these studies: 1) multiple discrete peritoneal macrophage and dendritic cell subsets have been phenotypically identified in humans (from different clinical settings of peritoneal dialysis) and in mice (from naïve and inflamed conditions); 2) in humans, the phenotypes and the activation/maturation status of peritoneal macrophages and dendritic cells are modified throughout the dialysis course and also during acute peritonitis; some characteristic alterations are associated with adverse patient outcomes; 3) in mice, the distinctive kinetics of the respective peritoneal macrophage and dendritic cell subsets in clinically relevant acute peritonitis models have been characterized; 4) individual peritoneal macrophage and dendritic cell subsets (human and mice) display differences in their phagocytic capacity and the ability to process and present antigen.

Publications and Presentations

Publications

Davies LC, Rosas M, Jenkins SJ, **Liao CT**, Scurr MJ, Brombacher F, Fraser DJ, Allen JE, Jones SA, Taylor PR. (2013) Distinct bone marrow-derived and tissue-resident macrophage lineages proliferate at key stages during inflammation. *Nat Commun* 4:1886.

Fielding CA, Jones GW, McLoughlin RM, McLeod L, Hammond VJ, Uceda J, Williams AS, Lambie M, Foster TL, **Liao CT**, Rice CM, Greenhill CJ, Colmont CS, Hams E, Coles B, Kift-Morgan A, Newton Z, Craig KJ, Williams JD, Williams GT, Davies SJ, Humphreys IR, O'Donnell VB, Taylor PR, Jenkins BJ, Topley N, Jones SA. (2014) Interleukin-6 signaling drives fibrosis in unresolved inflammation. *Immunity* 40(1):40-50.

Rosas M, Davies LC, Giles PJ, **Liao CT**, Kharfan B, Stone TC, O'Donnell VB, Fraser DJ, Jones SA, Taylor PR. (2014) The transcription factor Gata6 links tissue macrophage phenotype and proliferative renewal. *Science* 344(6184):645-648.

Presentations

Annual Congress of European Renal Association- European Dialysis Transplantation Association (EDTA-ERA), Paris, France, 24th -27th May, 2012 **(poster presentation)**
Title: Immunophenotyping of Peritoneal Macrophages and Their Surface Markers in Peritoneal Dialysis Patients

Institute of Infection and Immunity Annual Meeting, Cardiff, United Kingdom, 12th September, 2012 **(poster presentation)**
Title: Characterisation of peritoneal dendritic cells in mouse and human

MITReG Postgraduate Research Day, Cardiff, United Kingdom, 21 September, 2012 **(oral presentation)**
Title: Characterisation of peritoneal dendritic cells in mouse and human

Institute of Infection and Immunity Research Seminar, Cardiff, United Kingdom, 18 February, 2013 **(oral presentation)**
Title: Heterogeneity of macrophage and dendritic cells in the peritoneal cavity

EuTRiPD spring school, Cardiff, United Kingdom, 14 March, 2014 **(oral presentation)**
Title: Characterisation of peritoneal dendritic cells in peritoneal dialysis patients and its potential clinical implications

Institute of Infection and Immunity Research Seminar, Cardiff, United Kingdom, 20 October, 2014 **(oral presentation**)
Title: Characterisation of peritoneal macrophages and dendritic cells in mice and humans

Abbreviations

A (as in A405, A488, 647 etc.) – Alexa-Fluor
APC – Allophycocyanin
APCs – Antigen presenting cells
APD – Automated peritoneal dialysis
APF – 3'-(p-aminophenyl) fluorescein
BATF3 – Basic leucine zipper transcription factor ATF-like 3
BM – Bone marrow
BSA – Bovine serum albumin
CAPD – Continuous ambulatory peritoneal dialysis
CBS – Centre Biotechnology Service
CCPD – Continuous cyclic peritoneal dialysis
CD – Cluster of differentiation
cDC – Conventional dendritic cell
CDP – Common dendritic cell precursor
CKD – Chronic kidney disease
CLR – C-type lectin receptor
CR – Complement receptor
CTL – Cytotoxic T lymphocytes
Cy – Cyanine
DAPI – 4',6-diamino-2-phenylindole
DC – Dendritic cell
DDAO – 7-Hydroxy-9*H*-(1,3-Dichloro-9,9-Dimethylacridin-2-One)
D/P – Ratio of dialysate to plasma
dH2O – deionised H2O
DNA – Deoxyribonucleic acid
ds – double stranded
EDTA – Ethylenediaminetetraacetic acid
EGF-TM7 – Epidermal growth factor receptor 7 pass trans-membrane
EPS – Encapsulating peritoneal sclerosis
ER – Endoplasmic reticulum
ESRD – End-stage renal disease
FACS – Fluorescence-activated cell sorting
FcR – Fc receptor
FCS – Foetal calf serum
FITC – Fluorescein isothiocyanate
FLT3 (L) – FMS-like tyrosine kinase 3 (ligand)

FSc – Forward scatter
G (phase) – Gap
GDP – Glucose degradation product
GFR – Glomerular filtration rate
GM-CSF – Granulocyte/macrophage colony stimulating factor
GPCR – G-protein coupled receptor
h – hours
HD – Haemodialysis
HLA – Human leukocyte antigen
IFN – Interferon
IL – Interleukin
Inf MØ – Inflammation associated or inflammatory macrophage
IRF4 – Interferon-regulatory factor 4
LPS – Lipopolysaccharides
M (phase) – Mitosis
mAb – monoclonal antibody
CAM – 'Classically activated' macrophage
AAM – 'Alternatively activated' macrophage
MCP-1 – Monocyte chemoattractant protein-1
M-CSF – Macrophage colony stimulating factor
MDP – Macrophage and dendritic cell precursor
MFI – median fluorescent intensity
MHC – Major histocompatibility complex
min – minutes
MoP – Monocyte precursor
MPS – mononuclear phagocyte system
MØ – Macrophage
NIPD –Night intermittent peritoneal dialysis
PAMPs – Pathogen associated molecular patterns
PBMC – Peripheral blood mononuclear cells
PBS – Phosphate buffered saline
PD – Peritoneal dialysis
pDC – Plasmacytoid dendritic cell
PE – Phycoerythrin
PerCP – Peridinin chlorophyll
PET – Peritoneal equilibration test
phH3 – phospho-histone H3
PRP – Pathogen recognition receptor

RES – Reticuloendothelial system
Res MØ – Resident macrophage
RKF – Residual kidney function
RPMI – Roswell Park Memorial Institute medium
ROS – Reactive oxygen species
ROX – 6-carboxyl-x-rhodamine
rpm – revolutions per minute
RT – Room temperature
SEM – Standard error of mean
SES – *Staphylococcus epidermidis* supernatant
S (phase) – synthesis
SR – Scavenger receptor
SSc – Side scatter
TGF- β – transforming growth factor β
Th1 – type 1 helper T lymphocytes
Th2 – type 2 helper T lymphocytes
Th17 – type 17 helper T lymphocytes
Tim-4 – T cell immunoglobulin and mucin domain-containing protein 4
TipDC –Tumor necrosis factor (TNF) and inducible nitric oxide synthase (iNOS)-producing dendritic cell
TLR – Toll-like receptors
TNF – tumour necrosis factor
Treg – Regulatory T cells

Contents

Chapter 1 – General Introduction…… 1

1.1 Overview…… 2

1.2 Peritoneal cavity and peritoneal membrane…… 3

1.2.1 Anatomy of peritoneal cavity……...…… 3

1.2.2 Peritoneal membrane physiology…… 4

1.3 Peritoneal dialysis……...…… 6

1.3.1 Background…….. 6

1.3.2 Peritoneal dialysis technique…… 7

1.3.3 Peritoneal equilibration test (PET)…….…….. 9

1.3.4 Complications…….……. 10

1.4 Heterogeneity of monocytes, macrophages and dendritic cells…….……12

1.4.1 Historical background…….…. 12

1.4.2 Origins and developmental pathways…….……. 14

1.4.3 Surface receptors and molecules……..… 19

1.4.4 Functional specialization……..... 22

1.4.5 Macrophage activation and polarization……..24

1.5 Macrophages and dendritic cells in the peritoneal cavity……...…25

1.5.1 Leukocyte compositions in human peritoneal cavity……...25

1.5.2 The role of peritoneal macrophages in PD patients……..27

1.5.3 The role of peritoneal dendritic cells in PD patients……30

1.5.4 Mononuclear phagocytes in mouse peritoneal cavity…….. 31

1.6 Scope of the thesis……...34

Chapter 2 – Materials and methods……35

2.1 Human study……..… 36

2.1.1 Ethical approval……36

2.1.2 Study populations……36

2.1.3 Isolation of human peritoneal cells from PD effluent fluids……39

2.1.4 Isolation of human mononuclear cells from peripheral bloods of PD patients and healthy individuals…….……..39

2.1.5 Cell counting…….…40

2.1.6 Flow cytometry…….…40

2.1.6.1 General staining procedures…….....40

2.1.6.2 Standarisation, calibration and quality control……42

2.1.7 Cell cycle analysis and proliferation assay…….…..43

2.1.8 *Ex vivo* microbial product stimulation and cytokine production assay.....43

2.1.9 *Ex vivo* phagocytosis and respiratory burst assay…….44

2.1.10 Fluorescence-activated cell sorting of human peritoneal monocytic cells……..... 45

2.1.11 Morphological analysis…….……45

2.1.12 Antigen processing and presentation assay……..46

2.2 Mouse study…….....47

2.2.1 Animals……..... 47

2.2.2 Experimental peritonitis models……...…47

2.2.3 Adoptive transfer experiments……. 48

2.2.4 Flow cytometry…… 48

2.2.5 Cell cycle analysis and proliferation assay……...…50

2.2.6 *Ex vivo* microbial products stimulation and cytokine production assay...50

2.2.7 Apoptotic thymocyte clearance assay…….51

2.2.7.1 Generation of apoptotic thymocytes……..51

2.2.7.2 Quantification of apoptotic thymocytes……51

2.2.7.3 *In vivo* apoptotic thymocyte clearance assay……..…. 52

2.2.8 Fluorescence-activated cell sorting of mouse peritoneal MØ/DC subsets…….. 53

2.3 Statistical analysis……...53

Chapter 3 – Phenotypic and functional characterisation of peritoneal macrophages and dendritic cells in peritoneal dialysis patients……...… 54

3.1 Introduction…….....55

3.2 Results…….....57

3.2.1 Flow-cytometric analysis of human peritoneal cells– basic principles…57

3.2.2 Identification of peritoneal myeloid cells from PD effluent fluids based on CD116 (GM-CSF receptor alpha) expression…….59

3.2.3 Phenotypic identification of two major peritoneal monocytic subsets ($CD14^{+}CD1c^{-}$ and $CD14^{low/-}CD1c^{+}$) from PD effluent fluids……..61

3.2.4 Phenotypic comparisons between peritoneal $CD14^{+}$ MØ and $CD1c^{+}$ DC from PD patients…….. 64

3.2.5 Heterogeneous activation and maturation of peritoneal MØ and DC.....68

3.2.6 Phenotypic comparisons between human blood monocytic subsets and peritoneal monocytic subsets from PD patients……...… 71

3.2.7 Cytokine response to *ex vivo* stimulation with microbial products……..75

3.2.8 Phagocytosis and respiratory burst response after *ex vivo* challenges with fluorescence-conjugated zymosan particles or bacteria……...…77

3.2.9 Flow-cytometric cell sorting of human peritoneal MØ and DC subsets…….. 80

3.2.10 Antigen processing and presenting assay……81

3.3 Discussion……...82

Chapter 4 – Kinetics and distributions of peritoneal myelomonocytic cells during the course of peritoneal dialysis therapy……....85

4.1 Introduction……86

4.2 Results……88

4.2.1 Clinical outcomes of new-starter PD patients with 1-year follow-up…..88

4.2.2 Kinetic changes of major peritoneal myeloid cells during the 1st year of PD therapy……90

4.2.3 Kinetic changes of peritoneal MØ and DC subsets during the 1st year of PD therapy……93

4.2.4 Minimal local proliferation of peritoneal MØs and DCs alongside post-surgery inflammatory recruitment……96

4.2.5 Is the catheter-induced peritoneal inflammatory response associated with early non-peritonitis technique failure in new-starter PD patients?.....98

4.2.6 Association between peritoneal immune characteristics and the risk for developing first episode of peritonitis during the 1st year of PD therapy ……102

4.2.7 Differential distributions of peritoneal myeloid cells and MØ/DC subsets between infected PD effluents from acute peritonitis patients

and uninfected fluids from stable dialysis patients…….....104

4.2.8 Differential distributions of peritoneal myeloid cells and MØ/DC subsets between patients with and without treatment failure upon acute bacterial peritonitis……...107

4.2.9 Pathogen-specific distributions of peritoneal myeloid cells and MØ/DC subsets during acute bacterial peritonitis……..…110

4.2.10 Impact of peritonitis history on the distributions of peritoneal myeloid cells and MØ/DC in patients under stable dialysis……..…….115

4.3 Discussion…….…..118

Chapter 5 – Characterisation of "dendritic cell-like" subsets in the murine peritoneal cavity…….……...121

5.1 Introduction…….…....122

5.2 Results…….....124

5.2.1 Phenotypic identification of murine peritoneal 'DC-like' subsets under steady state……....124

5.2.2 Phenotypic discrimination between murine peritoneal 'DC-like' subsets and recruited monocyte-derived macrophages during inflammation…...129

5.2.3 Cellular kinetics of different peritoneal macrophage and 'DC-like' subsets during acute experimental peritonitis……...132

5.2.4 Peritoneal 'DC-like' subsets are recruited from the periphery during acute experimental peritonitis……...135

5.2.5 Limited evidence of local proliferation of peritoneal 'DC-like' subsets during acute experimental peritonitis……...138

5.2.6 CCR2-dependent homeostasis and inflammatory recruitment of

peritoneal DC-like subsets……141

5.2.7 The role of IL-10 on the inflammatory recruitment of peritoneal 'DC-like' subsets and MØs……...146

5.2.8 Differential cytokine responses among distinct peritoneal MØ/DC subsets upon *ex vivo* microbial product stimulation…….149

5.2.9 Differential capacity for *in vivo* apoptotic thymocyte clearance among distinct peritoneal MØ/DC subsets……...153

5.2.10 Fluorescence activated cell sorting and morphological analysis of murine peritoneal MØ/DC subsets……...157

5.3 Discussion…….……..159

Chapter 6 – General discussion……162

6.1 The identities of peritoneal MØ/DC subsets……...163

6.1.1 Peritoneal MØs: "resident" *versus* "recruited"…….....163

6.1.2 Peritoneal DC population…….…166

6.1.3 Comparisons between human and murine peritoneal MØ/DC subsets....169

6.1.4 Future directions……...170

6.2 Alterations of peritoneal MØ/DC phenotypes and activation/maturation status during PD therapy……...172

6.2.1 Altered distribution of peritoneal MØ/DC during PD therapy…….172

6.2.2 Altered activation/maturation status of peritoneal MØ during PD therapy……..174

6.2.3 Future directions……...176

6.3 From peritonitis to peritoneal fibrosis: defining the roles of peritoneal MØ and DC in PD patients……...178

Bibliography…….181

Appendix

1. Clinical characteristics of the study patients…….……200

2. Antigen processing and presentation assay in mice……..201

Lists of figures

Figure 1.1 Renal replacement therapy (RRT) modality in incident patients……... 6
Figure 1.2 Different modes of peritoneal dialysis……... 8
Figure 1.3 Origins and renewal of tissue-resident macrophages……..……..…….....15
Figure 1.4 Hematopoietic origins of tissue macrophages and dendritic cells…….17
Figure 2.1 PD patient recruitment and the timescale of PD fluid sampling……38
Figure 3.1 Flow-cytometric strategies to exclude doublets, cellular debris and dead cells during data analysis……..58
Figure 3.2 Flow-cytometric gating strategies to identify different peritoneal myeloid subsets from PD effluent fluids……..60
Figure 3.3 Phenotypic identification of two major mononuclear phagocyte subsets in the peritoneal effluent fluids from PD patients……62
Figure 3.4 HLA-DR^{+}CD14$^{low/-}$ cells are potentially peritoneal dendritic cells……..63
Figure 3.5 Phenotypic comparisons between human peritoneal CD14^{+} MØ and CD1c^{+} DC…….65
Figure 3.6 Quantitative comparisons of receptor expression between human peritoneal CD14^{+} MØ and CD1c^{+} DC under stable status and during acute bacterial peritonitis……..66
Figure 3.7 Human peritoneal MØ/DC could be subdivided into six cell subtypes based on the differential expression of CD16 and CD206……...69
Figure 3.8 Differential marker expression on six distinct peritoneal monocytic subsets under stable status or during acute bacterial peritonitis……...70
Figure 3.9 Phenotypic characterisation of three major monocytic subsets in peripheral bloods from PD patients…….....72
Figure 3.10 Major monocytic subsets (based on CD14 *versus* CD16 expression) in peripheral bloods and in the peritoneal cavity from PD patients…….73
Figure 3.11 Phenotypic identification of blood CD1c^{+} DC precursors…… 73
Figure 3.12 Cytokine production by peritoneal MØ and DC after *ex vivo* stimulation with SES or LPS……...75
Figure 3.13 Quantification of intracellular cytokine production by peritoneal MØ/DC after *ex vivo* stimulation with SES or LPS…….76
Figure 3.14 Phagocytosis and respiratory burst responses following *ex vivo* challenges with zymosan particles……... 78
Figure 3.15 Phagocytosis and respiratory burst responses following *ex vivo* challenges with *staphylococcus epidermidis* (S.E)…….. 79
Figure 3.16 Cell sorting of human peritoneal MØ/DC and their morphology……. 80

Figure 3.17 Human antigen processing and presenting assay…….. 81
Figure 4.1 Flow diagram of longitudinal outcomes of new-starter PD patients during 1-year follow-up……... 89
Figure 4.2 Changes in the numbers of major peritoneal myeloid cells during the 1st year of PD therapy……91
Figure 4.3 Kinetic changes of major peritoneal myeloid subsets during the 1st year of PD therapy……92
Figure 4.4 Differential kinetic changes of $CD14^+$ MØ sand $CD1c^+$ DC during the 1st year of PD therapy……...94
Figure 4.5 Individual kinetic changes of six peritoneal monocytic subsets during the 1st year of PD therapy……95
Figure 4.6 Minimal proliferative activity of peritoneal MØ/DC during post-surgery inflammation……... 97
Figure 4.7 Comparisons of peritoneal myeloid cells from the 1st flush PD effluents between new-starter PD patients without early technique failure *versus* those with catheter-related technique failure……99
Figure 4.8 Differential distributions of peritoneal MØ/DC subsets from the 1st flush PD effluents between new-starter PD patients with and without catheter failure……..…100
Figure 4.9 Comparisons of kinetic changes of peritoneal myeloid cells during pre-dialysis period between new-starter PD patients with and without non-peritonitis technique failure…….……..101
Figure 4.10 Comparisons of major peritoneal myeloid cells between infected PD effluents from day 1 acute bacterial peritonitis and uninfected fluids from stable dialysis patients……. ...105
Figure 4.11 Differential distributions of peritoneal MØ/DC subsets between PD patients with bacterial peritonitis *versus* the stable dialysis patients…...106
Figure 4.12 Comparisons of major peritoneal myeloid cells between bacterial peritonitis episodes with treatment success *versus* those with treatment failure…….…..108
Figure 4.13 Differential distributions of peritoneal MØ/DC subsets between bacterial peritonitis with treatment success *versus* treatment failure…..109
Figure 4.14 Comparisons of major peritoneal myeloid cells between culture-negative *versus* culture-positive peritonitis……111
Figure 4.15 Differential distributions of peritoneal MØ/DC subsets between culture-negative and culture-positive bacterial peritonitis……...112
Figure 4.16 Comparisons of major peritoneal myeloid cells between gram-positive, gram-negative and mixed type bacterial peritonitis……113

Figure 4.17 Differential distributions of peritoneal MØ/DC subsets between gram-positive, gram-negative and mixed type bacterial peritonitis……..114
Figure 4.18 Comparisons of major peritoneal myeloid cells and MØ/DC subsets between stable dialysis patients without history of peritonitis, with only one episode of peritonitis and with more than one episode of peritonitis ……116
Figure 4.19 Differential distributions of peritoneal MØ/DC subsets between stable dialysis patients without history of peritonitis and those with history of peritonitis…….…….117
Figure 5.1 Phenotypic identification of peritoneal 'DC-like' subsets in the naïve murine peritoneal cavity……...126
Figure 5.2 Phenotypic comparisons between peritoneal resident MØs and three 'DC-like' subsets from naïve mice…….……..128
Figure 5.3 Phenotypic discrimination of 'DC-like' cells from monocyte-derived inflammatory MØs during peritoneal inflammation……....130
Figure 5.4 Phenotypic comparisons between peritoneal resident MØs, inflammatory MØs and three 'DC-like' subsets from inflamed mice…..131
Figure 5.5 Cellular kinetics of peritoneal myelomonocytic subsets during acute SES-induced peritoneal inflammation……..133
Figure 5.6 Cellular kinetics of peritoneal myelomonocytic subsets during acute zymosan-induced peritoneal inflammation……...134
Figure 5.7 Peritoneal 'DC-like' cells are recruited from the periphery during acute SES-induced peritonitis……136
Figure 5.8 Limited evidence of proliferation during peritonitis of murine peritoneal 'DC-like' subsets……..139
Figure 5.9 Myeloid cell compositions in the naïve peritoneal cavity of *Ccr2*$^{-/-}$ mice, compared to wild-type *Ccr2*$^{+/+}$ mice……142
Figure 5.10 Myeloid cell compositions in the peritoneal cavity from 72h post-SES challenge *Ccr2*$^{-/-}$ mice and wild-type *Ccr2*$^{+/+}$ mice……144
Figure 5.11 IL-10 limits inflammatory response in acute SES-induced peritonitis model……147
Figure 5.12 Peritoneal MØ/DC subsets exhibit differential pro-inflammatory cytokine production following SES or LPS exposure……..150
Figure 5.13 Peritoneal MØ/DC subsets exhibit differential IL-10 production following SES or LPS exposure……...152
Figure 5.14 Glucocorticoid-induced thymocyte apoptosis *ex vivo*…….…..154
Figure 5.15 Peritoneal MØ/DC subsets from naïve status exhibit differential capability of apoptotic thymocyte clearance……155

Figure 5.16 Peritoneal MØ/DC subsets from 72h after SES-induced peritonitis exhibit differential capability of apoptotic thymocyte clearance…….156
Figure 5.17 Flow-cytometric cell sorting and morphological analysis of individual peritoneal MØ/DC subset……..158

Lists of tables

Table 1.1 Description of 'three pores' of peritoneal capillary endothelium…… 5

Table 1.2 Peritoneal membrane characteristics of different transport status……... 9

Table 1.3 Summary of select surface receptors and molecules on mononuclear phagocytes in mice and humans…….….21

Table 1.4 Phenotypic definition of peritoneal mononuclear phagocyte subsets (steady state and inflamed state) used in the current literature……...33

Table 2.1 Fluorochrome-conjugated anti-human monoclonal antibodies for surface antigen staining in this project……41

Table 2.2 Fluorochrome-conjugated anti-mouse monoclonal antibodies used in this project…….….49

Table 3.1 Phenotypic comparisons of select receptor expressions between major monocytic subset in peripheral blood and in the peritoneal cavity…….74

Table 4.1 Comparisons of clinical and peritoneal immune characteristics at the start of PD between patients free from peritonitis and patients developing first peritonitis episode within the 1st year of PD therapy…. 103

Table 5.1 Differentially expressed genes between peritoneal F4/80^{low}MHCII^{+} MØs and F4/80^{int}MHCII^{+} MØs during thioglycollate peritonitis……. 127

Chapter One

General introduction

1.1 Overview

The overall purpose of the work carried out during my PhD research project was to understand the heterogeneity of peritoneal mononuclear phagocytes (macrophages and dendritic cells) and to define their respective immune characteristics (phenotypes and functional properties) in peritoneal dialysis patients.

In order to introduce this subject, I will first describe the anatomy of the peritoneal cavity and the physiology of the peritoneal membrane, before considering peritoneal dialysis (PD) as a therapy. The overview of PD will provide a broad insight of the historical background, basic techniques and most importantly, its complications. Subsequently, I will introduce the current understanding of monocyte/macrophage/DC biology, particularly focusing on their ontogeny/development as well as their roles in tissue homeostasis and the body's defences against pathogens. Finally, I will review the state of knowledge about the immunobiology of this heterogeneous population in the peritoneal cavity, encompassing PD patients and mouse models.

1.2 Peritoneal cavity and peritoneal membrane

1.2.1 Anatomy of peritoneal cavity

The earliest description of the peritoneal cavity can be dated back to 3000 B.C., when the Egyptian morticians described it as a "definitive entity in which the viscera were somehow suspended" (Cunningham et al., 1926). The peritoneum is derived from mesenchyme and composed of a thin connective tissue layer covered by a monolayer of mesothelial cells. The largest serous membrane of human body, the peritoneum supports the abdominal viscera and serves as a conduit for the blood vessels, lymphatic vessels and nerves. The peritoneal membrane has a surface area ranging between 1-2 m^2 in human adults (Esperanca et al., 1966; Pawlaczyk et al., 1996). About 80-90% of this total membrane area consists of visceral peritoneum (including that covering the liver, mesenteries and omentum), and 10-20% is parietal peritoneum (Pawlaczyk et al., 1996; Albanese et al., 2009). The space between parietal and visceral peritoneum is the peritoneal cavity, normally filled with a small amount (~50 mL) of serous fluid that permits the two layers to slide freely over each other.

The submesothelial connective tissue layer (interstitium) primarily comprises cells (fibroblasts, mast cells and macrophages) and collagen fibres embedded in an amorphous substance (Hruza et al., 1977). The peritoneal membrane has extensive blood vessel coverage, with the visceral peritoneum supplied by the mesenteric arteries and the parietal peritoneum supplied by epigastric, intercostal and lumbar arteries. Another substantial component of the peritoneum is the lymphatic system, which drains a wide range of materials including water, proteins, cells, from the interstitial compartment and the peritoneal cavity (Mactier et al., 1987).

1.2.2 Peritoneal membrane physiology

In 1877, a German investigator, Georg Wegner, by working on animal models, first depicted the concept of "peritoneal ultrafiltration". His observations revealed that injection of hypertonic fluids into the peritoneal cavity led to increased intraperitoneal volume while hypotonic solutions resulted in a reduced intraperitoneal volume (Wegner 1877). Two English researchers then specifically determined that fluid and solute transport across the peritoneal membrane could be 'bi-directional', noting that solute exchange was primarily between solutions in the peritoneal cavity and blood compartment (Starling and Tubby 1894). Subsequently, Putnam defined the peritoneum as a semi-permeable membrane that allowed water and solute transport based on the principles of osmosis and diffusion, in his published paper "The living peritoneum as a dialyzing membrane" in the *American Journal of Physiology* (Putnam 1923).

Structurally, the peritoneum constitutes three major components involved in the water and solute transport between the peritoneal space and the plasma:

1. Mesothelial cell monolayer
2. Interstitial space
3. Capillary endothelium

Notably, it is the capillary wall (endothelium) that appears to be the primary filter determining the solute transport, as both mesothelial layer and interstitial space only provide minor resistance to the flow of solutes. Several theoretical models have been proposed to determine the transport of solutes across the peritoneal capillary bed. Of them, the **"three pore model"** is the most commonly described clinical model (Rippe 1993). In this model, the capillary endothelial cells are postulated as having three

kinds of "pores" that allow for the movement of solute and water across the capillary. These three pores are the large pores, small pores and ultra small (transcellular) pores. Their characteristics are summarised in Table 1.1 as below.

Table 1.1 Description of 'three pores' of peritoneal capillary endothelium

	Large pores	**Small pores**	**Ultra small pores**
Size	Up to 250 angstroms	40-55 angstroms	2.3-15 angstroms
Density (% surface area)	Few in number (<1%)	Most numerous (>95%)	Many in numbers (~ 2%)
Molecules transported	Macromolecules (ex. Proteins)	Small solutes (ex. sodium) and water	Water only
Localization	Inter-endothelial clefts	Inter-endothelial clefts (?)	Aquaporins (AQP1) on endothelium

Modified from Rippe B. Perit Dial Int.13:S35-8, 1993

The movement of water and solutes of varying sizes occurs due to two physiological processes that happen simultaneously:

1. **Diffusion**- occurs when solutes move down a concentration gradient between two compartments
2. **Convection**- occurs when dissolved solutes are small enough to move through the pores as water is moving across the capillary, in response to an osmotic force.

1.3 Peritoneal dialysis

1.3.1 Background

End-stage renal disease (ESRD), is the point at which kidney function has permanently declined to a level which no longer supports the body's needs. This may be as a final consequence of progressive loss of function in a patient with Chronic Kidney Disease, or following irreversible Acute Kidney Injury. Patients with ESRD require replacement therapy (RRT) to maintain their lives. Currently, diabetic renal disease remains the single most common cause of ESRD in the UK (UK Renal Registry 2013). The distribution of the modality choices for newly initiated RRT is shown in Fig 1.1 A. About 20% of new adult ESRD patients are treated with peritoneal dialysis (PD) and about 70 % with haemodialysis (HD). The number of the incident adult patients treated with each dialysis modality (HD *versus* PD) in 2012 by age group is shown in Figure 1.1 B. [data recruited from UK Renal Registry (2013): https://www.renalreg.org/reports/2013-the-sixteenth-annual-report/]

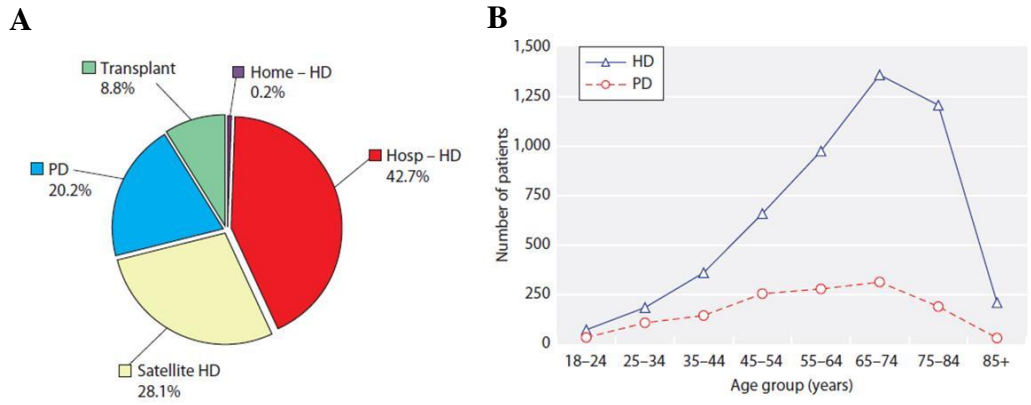

Figure 1.1 Renal replacement therapy (RRT) modality in incident patients

(A) Pie chart showing the RRT modality at 90 days from incident patient cohort in UK (1/10/2011–30/09/2012) (B) Number of incident dialysis patients in 2012, by age group and initial dialysis modality. [Adapted from UK Renal Registry 2013]

PD has several advantages over HD such as greater patient independence, no need for vascular access and needles, fewer dietary restrictions, relatively stable haemodynamics during continuous ultrafiltration (suitable for cardiac failure patients), and better preservation of residual kidney function (RKF) (Tokgoz 2009). The latter has been suggested to confer some survival benefits over HD in the short term (first 2-3 years) (Chaudhary et al., 2011). However, long-term PD is limited with less than one-third able to maintain PD beyond 3 years due to a significant dropout rate. The main reasons for dropout, according to UK Renal Registry 2013, include: receiving kidney transplantation (~30%), deaths from any cause (~20%) and non-death technique failures resulting in modality shifting to HD (~20%). The one absolute contraindication to chronic PD is an unsuitable peritoneum owing to the presence of malignancy, severe fibrosis or extensive adhesions. Other situations not recommended for PD include abdominal hernias, presence of colostomy, ileostomy or nephrostomy, recurrent severe backache with pre-existing disc disease.

1.3.2 Peritoneal dialysis technique

PD has been a widely accepted RRT for treating ESRD patients since late 1970s (Teitelabaum et al., 2003). It involves using the peritoneum as a filter membrane. Before the commencement of PD, a small flexible catheter is surgically inserted in the abdomen. Maintenance dialysis ensued after catheter wound healed and appropriate training. During PD therapy, sterile “dialysis fluid” is filled by gravity into the peritoneal cavity. During the dwell, blood circulates through the peritoneum, so waste products and excess fluid are moved from the blood into the dialysis fluid. After variable dwell time, the dialysis fluid is then drained out into the “effluent bag”.

PD has two basic modes of choice (Fig. 1.2). Continuous ambulatory peritoneal dialysis (CAPD), which is done manually, normally consists of three fluid exchanges during daytime and one long dwell overnight. The alternative approach is to use a machine with settings for cyclic exchanges in the night time (automated peritoneal dialysis, APD), either with a long dwell during the daytime as Continuous Cycling Peritoneal Dialysis (CCPD) or free from dialysis in the daytime as Nocturnal Intermittent Peritoneal Dialysis (NIPD). The dose and the frequency of dialysis exchanges primarily depend on the adequacy of the patient's dialysis.

Figure 1.2 Different modes of peritoneal dialysis

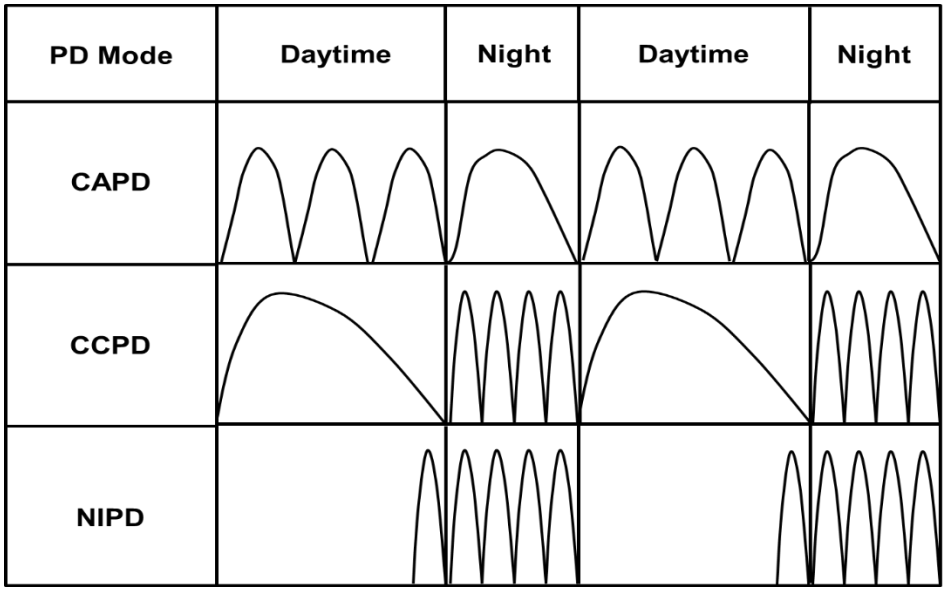

CAPD: continuous ambulatory peritoneal dialysis, CCPD: continuous cyclic peritoneal dialysis, NIPD: nocturnal intermittent peritoneal dialysis (Modified from Chiu et al., 2002)

The most common form of PD solutions are traditional dextrose-based solutions with varying concentrations of glucose (1.5-4.25%) used to create osmotic gradients to drive ultrafiltration and convection. Other types of PD fluid include solutions containing lower glucose degradation products (GDPs) and/or neutral pH, and non-dextrose solutions (icodextrin) using polymers to create a colloidal osmotic pressure (García-López et al., 2012).

1.3.3 Peritoneal equilibration test (PET)

A patient's peritoneal membrane transport status can be assessed by measuring the creatinine equilibration curve and the glucose absorption curve during a standardized peritoneal equilibration test (Twardowski et al., 1987). The standardized 4-hour PET involves a 2-liter 2.5% dextrose dwell. During the dwell, dialysate samples are taken at 0, 2, and 4 hours and a plasma sample at 2 hours. The dialysate to plasma (D/P) ratios for creatinine and glucose are measured. Based on 4-hour dialysate and plasma creatinine level (D/P creatinine), patients can be classified into one of four transport categories: high (fast), high-average, low-average, and low (slow) transporter. The characteristics of different transporters are summarised below (Twardowski 1990):

Table 1.2 Peritoneal membrane characteristics of different transport status

Transport status	D/P creatinine	Solute clearance	Ultrafiltration
High (fast)	> 0.80	Excellent	Poor
High average	0.65-0.80	Adequate	Adequate
Low average	0.55-0.64	Borderline	Good
Low (slow)	< 0.55	Inadequate	Excellent

Based on PET, clinicians can prescribe a suitable regimen for individual patient. For example, high transporters should be better on regimens with frequent, short-dwell exchanges (CCPD/NIPD), whereas low transporters are suitable for long-dwell exchange (CAPD). It has been recommended that an evaluation of peritoneal membrane characteristics should routinely be repeated at least once per year or when new clinical problems (overhydration, malnutrition, metabolic disturbance) are noticed (van Biesen et al., 2010).

1.3.4 Complications

In general, the complications of PD therapy can be categorised into "catheter-related" and "dialysis-related" conditions.

Catheter-related complications

Catheter-related complications include catheter dysfunction, external cuff extrusion, pericatheter leak, exit site or pericatheter infection and early peritonitis (Kathuria et al., 2009). The following conditions would lead to catheter dysfunction: 1) intra-luminal obstruction with blood/fibrin clot, 2) catheter tip migration or kinking, 3) omental tissue encasement ('omental wrapping'). Most of them can be reversed through medical or surgical interventions (Diaz-Buxo et al., 1998), however, in cases of severe irreversible occlusion, catheter removal is necessary. In fact, catheter dysfunction is one of the major reasons for early technique failure.

Dialysis-related complications

(1) Non-infectious complications –

These include abdominal hernias (due to increased intraperitoneal pressure), hydrothorax, haemoperitoneum, and chyloperitoneum. Abdominal hernias and hydrothorax can be repaired and the patients can choose to return to PD after surgery. The underlying aetiologies of haemoperitoneum ('bloody effluent') and chyloperitoneum ('milky effluent') are complex, ranging from benign conditions (i.e., menstruation, lymphatic vessel trauma) to serious situations (i.e., cancer metastasis with intra-peritoneal seeding, intraperitoneal tumours resulting in extrinsic obstruction of lymphatic vessels). For malignant cases, withdrawal from PD therapy may be necessary (McCormick et al., 2007).

(2) Peritonitis –

Despite treatment advance, peritonitis remains a major cause for morbidity and mortality in PD patients. The diagnosis of acute peritonitis is based on the presence of abdominal pain and cloudy peritoneal effluent with >100 WBC/mm^3 (Li et al., 2010). Generally, broad-spectrum antibiotics covering Gram-positive and Gram-negative bacteria are prescribed intraperitoneally after the sampling of PD fluid ("cloudy effluent") for microbiological examination. The choice of antibiotics is subsequently refined to narrower-spectrum cover, according to the culture results. Normally, the entire treatment course takes 14 to 21 days (Li et al., 2010). Refractory peritonitis, defined as failure of the effluent to clear after 5 days of appropriate antibiotics, should be managed by catheter removal (Choi et al., 2004). In cases of recurrent/relapsing peritonitis, catheter removal may prove necessary (Szeto et al., 2009).

(3) Peritoneal membrane fibrosis –

Peritoneal membrane fibrosis resulting in ultrafiltration failure is one of the major complications in long-term PD patients. Two forms of membrane fibrosis are often classified: a slowly progressive 'simple fibrosis' and a fulminant 'encapsulating peritoneal sclerosis (EPS)' (Davies et al., 2011). The underlying mechanism appears to be complex (Kim et al., 2009), but it has been argued that severe or multiple peritonitis episodes and the usage of non-physiological PD solutions (prolonged exposure to glucose and glucose degradation products) could be the key contributing factors (Davies 2014). A recent study showed that local inflammatory status, measured as intraperitoneal IL-6 level, correlated with peritoneal membrane function over time and can be a surrogate biomarker to predict membrane outcome (Lambie et al., 2013).

1.4 Heterogeneity of monocytes, macrophages and dendritic cells

1.4.1 Historical background

It has been widely recognized that Russian biologist Élie Metchnikoff first introduced the term 'macrophage (MØ)' (which means "big eater") in late 19th century to describe the large mononuclear phagocytes in tissues, which was distinguished from another phagocytosing cell type, called 'microphage' ("small eater", now known as polymorphonuclear leukocytes or neutrophils) (Metchnikoff 1892). In 1924, Aschoff assigned MØs to the 'reticuloendothelial system (RES)'; a system also comprising of reticular cells, endothelial cells, fibroblasts, which were considered to have a common tissue origin at that time (Aschoff 1924). Subsequently, Ebert and Florey (1939), using rabbit ear chamber experiments, demonstrated that mammalian blood monocytes actively migrating towards sites of injury and differentiating into MØs *in vivo*. With the aid of thymidine autoradiography, Volkman and Gowans (1965) showed that these tissue-infiltrating MØs actually originated from the bone marrow (BM). Because of the involvement of non-monocyte/ MØ cells leading to the argument that RES did not truly represent a cell lineage, a group of scientists including Ralph van Furth, James G. Hirsch and Zanvil A. Cohn, proposed the 'mononuclear phagocyte system (MPS)' to replace the 'RES', on the basis that MØs shared important functional characteristics *in vivo* and were derived from monocytes, whereas reticular cells, endothelial cells and fibroblasts were not (van Furth et al., 1972). The MPS represented a linear model in which committed bone marrow precursors give rise to circulating monocytes from which tissue MØs are derived. The MPS paradigm has been disputed due to the evidences of MØ proliferation and maintenance in the tissues (Sawyer et al., 1982; Parwaresch et al., 1984; Czernielewski et al., 1987; Melnicoff et al., 1988), and also

the presence of MØ populations in the yolk sac before primitive haematopoiesis (Naito et al., 1996). Very recently, mouse studies have demonstrated that most tissue-resident MØs can be of embryonic origins and primarily independent of haematopoietic supply (Chorro et al., 2009; Ginhoux et al., 2010; Hoeffel et al., 2012; Schulz et al., 2012).

On the other hand, Ralph M. Steinman and Zanvil A. Cohn (1973) first identified a novel cell type from mouse peripheral lymphoid organs – dendritic cells (DCs). Functionally, these classical DCs were professional in processing and presenting antigen to naïve T lymphocytes, initiating the adaptive immune response (Steinman et al., 1978). Shortly after its discovery, DCs were incorporated into MPS by Ralph van Furth (1980) and widely accepted by other researchers. Of note, the original Steinman-Cohn's DCs were restricted in lymphoid tissues, but subsequently DC networks were also recognised in non-lymphoid tissues in mice and humans (Schlitzer et al., 2014). The developmental origin and differentiation pathways of DC subsets will be discussed in the next section.

Several breakthroughs in the past decade have advanced our understanding of monocyte/MØ/DC biology (Davies et al., 2013; Schlitzer et al., 2014; Ginhoux et al., 2014; Guilliams et al., 2014). Firstly, the application of polychromatic flow cytometry has permitted the exploration of reliable surface markers on discrete cell populations, which enabled the clear discrimination between DCs and MØs in tissue compartments. Secondly, with the aids of novel cell lineage tracing strategies, the developmental pathways of distinct monocyte/MØ/DC subsets under homeostatic or inflamed conditions could now be mapped in mice. Thirdly, the potential corresponding cell subsets between mice and humans could be identified through detailed gene expression profiling and the cross-species mapping.

1.4.2 Origins and developmental pathways

Mononuclear phagocytes are broadly segregated into two main populations based on their developmental sources: 'embryonic origin' and 'haematopoietic origin'. Recent evidences unveiled that part of adult tissue-resident MØs are basically originated from yolk sac and/or fetal liver during embryonic period (Fig. 1.3) (Davies et al., 2013; Ginhoux et al., 2014). Initial fate-mapping works confirmed that adult microglia and Langerhans cells were established prenatally (Chorro et al., 2009; Ginhoux et al., 2010). Subsequently, these findings were extended to a 'Myb-independent' population of characteristically F4/80^{high} MØs in several tissues, such as spleen (red pulp MØ), liver (Kupffer cell), brain (microglia), skin (Langerhans cell), pancreas, lung and kidney (Schulz et al., 2012). Additional evidence revealed that these 'prenatally seeded' tissue MØs have substantial self-renewal ability (proliferative expansion) that enables them to maintain tissue homeostasis after birth (Davies et al., 2011; Yona et al., 2013; Hashimoto et al., 2013), and to recover from the 'MØ disappearance' reaction upon specific immune challenges (Davies et al., 2011; Jenkins et al., 2011). However, others also suggested that microglia and Langerhans cells can derive from blood monocyte under certain conditions after birth (Merad et al., 2002; Ajami et al., 2007). Very recently, new evidence confirms that BM-derived precursors or circulating monocytes could constantly contribute to the steady-state tissue MØ pools, although this hematopoietic supply has been suggested with tissue-specific variation, for example, mostly tissue MØs in the steady-state intestine are hematopoietic in origin. (Zigmond et al., 2012; Bain et al., 2014). Additional evidence implies that the embryonic MØs in tissues are gradually replaced by BM-derived MØs under steady-state conditions after birth, such as cardiac tissues (Molawi et al., 2014).

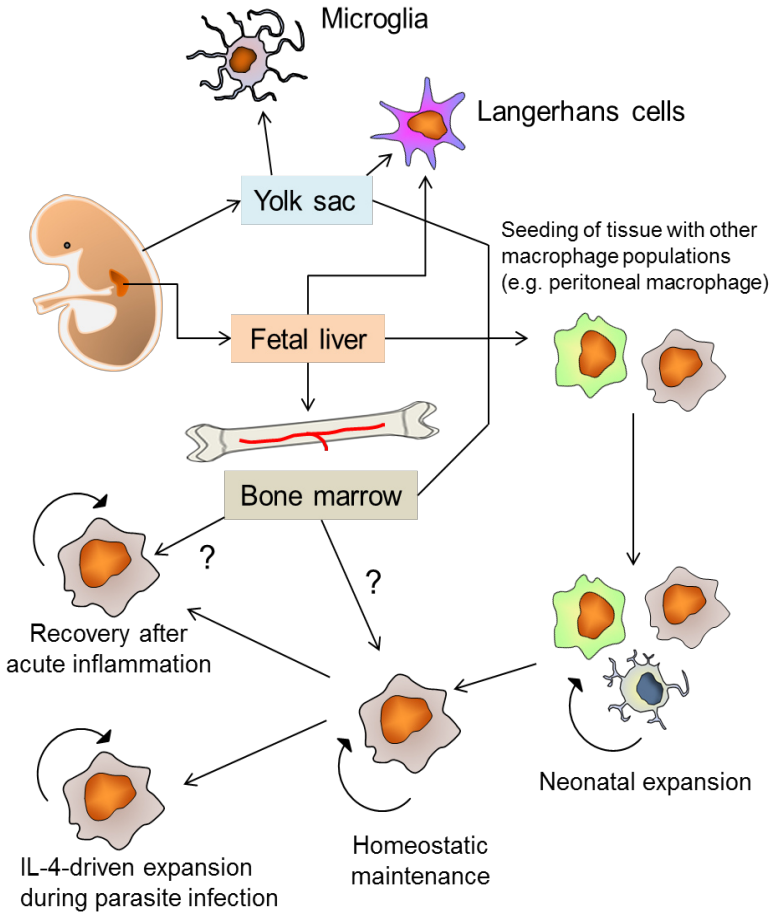

Figure 1.3 Origins and renewal of tissue-resident macrophages.

Recent fate-mapping studies and single-cell analyses in mice indicate that MØs derived early in embryogenesis from the yolk sac can contribute to adult pools of tissue MØs, such as Langerhans cells and microglia. Other tissues may be similarly seeded or established after definitive haematopoiesis in the fetal liver or bone marrow. Proliferative local expansion of tissue MØs in the neonatal period, followed by low-level self-renewal during adulthood appears sufficient to maintain many tissue resident populations. During the resolution of acute inflammation, local proliferation can be enhanced to help restore homeostatic tissue-resident MØs. In the context of the Th2 cell environment associated with parasite infection, substantial IL-4–dependent proliferation can expand numbers of tissue-resident MØs beyond that normally seen in the tissue (Jenkins et al., 2011). This post-inflammatory proliferative expansion of resident MØs can also be found in acute zymosan-induced peritonitis model (Davies et al., 2011), although this is IL-4 receptor-independent. The exact contribution of BM–derived inflammatory MØs to these tissue-resident pools is still unclear, but it appears likely to happen, although perhaps with tissue-specific variation.

(Modified from Davies et al., *Nat Immunol* 14:987, 2013)

The haematopoietic lineages of monocyte/MØ/DC have been elucidated in mice recently (Fig. 1.4) (Geissmann et al., 2010; Guilliams et al., 2014). In the BM, the haematopoietic stem cells (HSC) produce common lymphoid progenitors (CLP) and common myeloid progenitors (CMP). The latter gives rise to MØ and DC precursors (MDP). It has been suggested that monocyte-MØ lineage (Monocyte precursors, MoP) (Hettinger et al., 2013) and DC lineage (common DC precursors, CDP) (Liu et al., 2009) are separated from MDP. MoP give rise to Ly-6C$^+$ classical monocytes and Ly-6C$^-$ non-classical monocytes; both of them leave BM and enter into blood circulation. Ly-6C$^+$ monocytes are the predominant subset in the blood and poised to migrate to the inflamed sites (Geissmann et al., 2003; Serbina et al., 2008), whereas Ly-6C$^-$ monocytes (also called 'patrolling monocytes') serve to clear endothelial cell debris as 'intravascular housekeepers'(Geissmann et al., 2003; Auffray et al., 2007). Notably, Ly-6C$^+$ monocytes might constitute the steady-state precursors of Ly-6C$^-$ monocytes (Yona et al., 2012). As previously mentioned, circulating monocytes could also contribute to the steady-state 'tissue MØ pool' with tissue-specific variation (Bain et al., 2013; Molawi et al., 2014). On the other hand, CDP give rise to plasmacytoid DCs precursors (pre-pDC) and conventional DC precursors (pre-cDC); both of them leave BM and enter into blood circulation (Diao et al., 2004; Naik et al., 2007; Onai et al., 2007). Under homeostatic conditions, pre-pDC and pre-cDC locally differentiate into pDC and cDC, respectively, either reside in lymphoid tissues or enter into non-lymphoid tissues (Naik et al., 2006; Liu et al., 2009; Ginhoux et al., 2009; Onai et al., 2013). Of note, some pDC might originate from a lymphoid precursor (Corcoran et al., 2003; Pelayo et al., 2005). During inflammation, Ly-6C$^+$ monocytes are the major sources of recruited 'inflammatory MØs' in the tissues and could differentiate into 'inflammatory DCs' such as tumour necrosis factor (TNF) and inducible nitric oxide synthase (iNOS)–producing DCs (TipDCs) (Serbina et al.,

2006). However, it has been suggested that monocytes do not give rise to cDC and pDC both at steady state and during inflammation (Fogg et al., 2006; Liu et al., 2009).

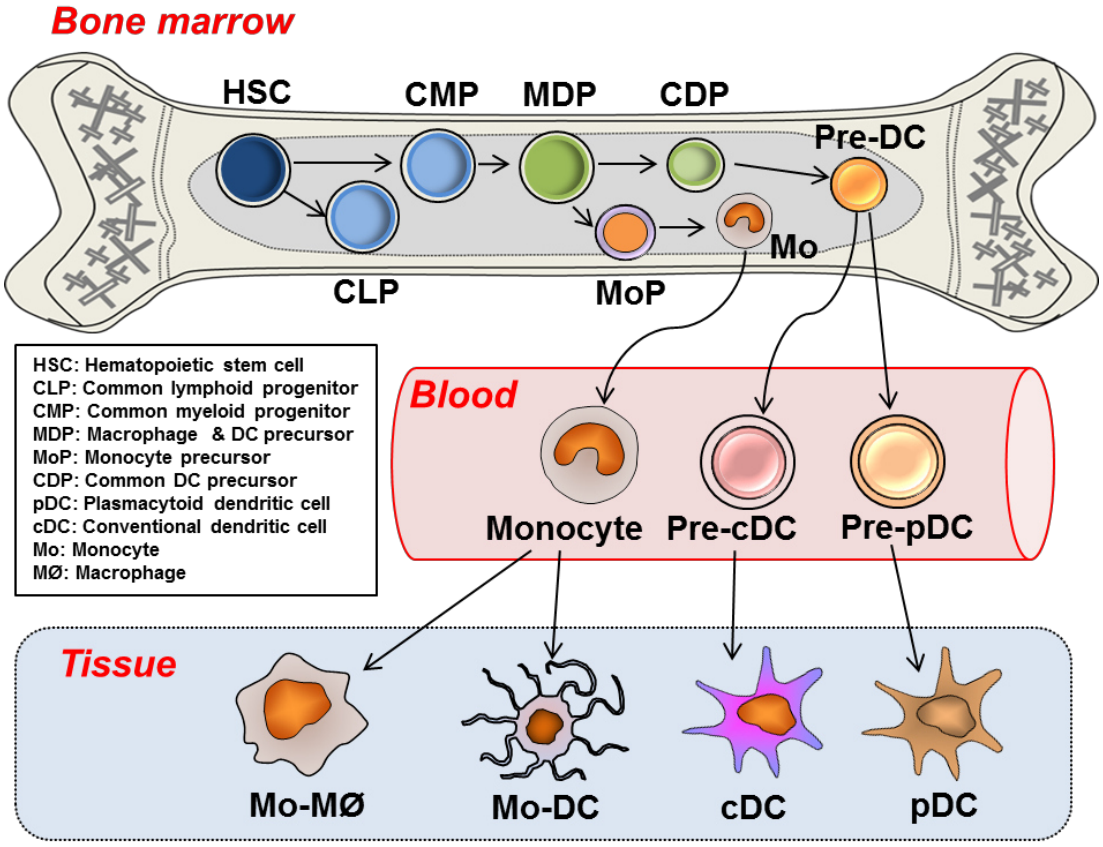

Figure 1.4 Hematopoietic origins of tissue macrophages and dendritic cells

Simplified model showing the hematopoietic development of monocyte (Mo)/MØ/DC. In the bone marrow (BM), the haematopoietic stem cells (HSC) produce common lymphoid progenitors (CLP) and common myeloid progenitors (CMP). The latter give rise to MØ/DC precursors (MDP). MDP give rise to common DC precursors (CDP) and monocyte precursors (MoP), respectively. Monocytes arise from MoP leave BM and enter into the blood circulation. Circulating monocytes (mostly Ly-6C$^+$ classical monocytes) contribute to the steady-state 'tissue MØ pool' (monocyte-derived MØ, 'Mo-MØ') with tissue-specific variation. On the other hand, CDP give rise to precursors of plasmacytoid DCs (pre-pDC) and conventional DCs (pre-cDC); both enter into the blood circulation. Under homeostatic condition, pre-pDC and pre-cDC locally differentiate into pDC and cDC, respectively, either reside in lymphoid tissues or enter into non-lymphoid tissues. During inflammation, Ly-6C$^+$ monocytes are the major sources of recruited 'inflammatory MØs' and could also differentiate into 'inflammatory DCs' or 'monocyte-derived DC, Mo-DC' in the inflamed tissues.

The lineage commitment and differentiation of monocyte/MØ/DC are controlled by several key cytokines or growth factors (Geissmann et al., 2010; Ginhoux et al., 2014; Guilliams et al., 2014). Macrophage-colony-stimulating factor (M-CSF or CSF-1), interleukin-34 (IL-34) and their receptor, CSF1R (also known as c-fms, M-CSFR, CD115) are important in MØ development, proliferation and survival (Hamilton et al., 2008; Pollard et al., 2009; Greter et al., 2012; Wang et al., 2012) as well as in DC development (Fancke et al., 2008). FMS-like tyrosine kinase 3 (FLT3) and its ligand (FLT3L) are critical for the pan-DC development (McKenna et al., 2000; Waskow et al., 2008). The differentiation into each DC subtype is regulated by distinct sets of transcription factors. For example, basic leucine zipper transcription factor ATF-like 3 (BATF3) is important for the development of $CD8\alpha^+/CD103^+$ cDC subset (Hildner et al., 2008), whereas $CD8\alpha^-/CD11b^+$ cDC subset is controlled by IFN-regulatory factor 4 (IRF4) (Suzuki et al., 2004; Schlitzer et al., 2013). The development of pDCs is regulated by E2-2 (Cisse et al., 2008; Ghosh et al., 2010). Granulocyte/macrophage-colony-stimulating factor (GM-CSF or CSF-2) and its receptor CSF2R (also known as GM-CSFR or CD116) also play a key role in DC development under steady state, and more importantly during inflammation (Zhan et al., 2012; van de Laar et al., 2012).

Recently, through the cross-species gene expression profiling, the corresponding monocyte/MØ/DC subsets between mice and humans could be mapped. For example, mouse $Ly\text{-}6C^+$ monocytes may correspond to human $CD14^+CD16^-$ "classical" monocytes, while $Ly\text{-}6C^-$ monocytes are similar to human $CD14^{dim}CD16^+$ "non-classical" monocytes. In terms of DC subsets, mouse $CD8\alpha^+$ (lymphoid)/ $CD103^+$ (non-lymphoid) cDCs correspond to human $CD141^+$ cDCs, whereas mouse $CD8\alpha^-$ (lymphoid)/$CD11b^+$ (non-lymphoid) cDCs are akin to human $CD1c^+$ cDCs (Schlitzer et al., 2014).

1.4.3 Surface receptors and molecules

Mononuclear phagocytes contain a broad repertoire of surface receptors and molecules, which determine a wide range of cellular activities such as growth, differentiation, activation, maturation, migration, endocytosis, phagocytosis, pathogen recognition, antigen presentation and cell-cell interaction. Some of these receptors or molecules are not only restricted to monocyte/MØ/DC subsets but also shared by other cell types. Here, a select of surface receptors/molecules relevant to this thesis are summarised below and in Table 1.3.

(1) Fc receptors (FcRs) –

Binding of the Fc portion of immunoglobulin molecules to the Fc receptors can trigger various functions such as endocytosis, phagocytosis, transmembrane signal generation and secretion of potent mediators (Guilliams et al., 2014).

(2) Complement receptors (CRs) –

These are involved in the binding complement components (either in free form or as part of an immune complex) and ingestion of opsonized particles (van Lookeren Campagne et al., 2007).

(3) Pathogen recognition receptors (PRRs) –

These receptors mediate binding and endocytosis/phagocytosis of pathogens. They also act as sensors to recognize pathogen associated molecular patterns (PAMPs) and induce a pro-inflammatory cascade which leads to many anti-microbial effector responses (Gordon et al., 2002). PRRs include toll-like receptors (TLRs), C-type lectin receptors (CLRs), and scavenger receptors (SRs).

(4) Cytokine receptors –

The receptor-ligand (cytokine) interactions mediate a variety of cellular activities such as growth and differentiation, proliferation, migration, activation and anti-microbial effector responses (Miyajima et al., 1992).

(5) Chemokine receptors –

Following interaction with their specific ligands (chemokines), these receptors trigger a process known as chemotaxis that traffics the cell to a desired location within the organism (Mantovani et al., 2004).

(6) Cell adhesion molecules –

These molecules involve in cell-cell interaction (NK/T/B cell activation), cell-matrix interaction, and leukocyte trafficking

(7) Molecules involved in antigen presentation –

These consists of MHC class I and II molecules and costimulatory molecules.

Some surface markers have been adopted for phenotypic purpose due to their unique expressions on distinct cellular subsets (Gordon and Taylor, 2005). For example, **F4/80** is the best known phenotypic marker for mouse tissue MØs (Austyn and Gordon, 1981). However, EGF-like module-containing mucin-like hormone receptor-like 1 (EMR1), the human homolog of F4/80, is an eosinophil-specific marker, not for human MØs (Hamann et al., 2007) and mouse F4/80 is not so specific to human MØs. Instead, **CD14**, a co-receptor for LPS, has long been used as a surrogate marker for human monocyte/MØs, though $CD14^{dim}$ monocyte subset has been characterised recently (Ziegler-Heitbrock et al., 1993). In mice, DCs are traditionally defined as $CD11c^{high}MHCII^{+}$ cells (Metlay et al., 1990), however, **CD11c** expression is also noted on activated monocytes/MØs, NK cells and other granulocytes, arguing its specificity for DC recognition.

Table 1.3 Summary of select surface receptors and molecules on mononuclear phagocytes in mice and humans

Fc receptor
FcγRI (CD64), FcγRII (CD32), FcγRIII (CD16), FcγRIV*, FcεRI, FcεRII (CD23)
Complement receptors
CR1 (CD35), CR3 (Mac-1, CD11b/CD18), CR4 (gp150/95, CD11c/CD18)
Pattern recognition receptors
Toll-like receptors: TLR-1, TLR-2, TLR-4 (with CD14 as co-receptor for LPS-binding protein), TLR-5, TLR-6, TLR-10, TLR-11*,TLR-12*
C-type lectin receptors: DC-SIGN (CD209), Langerin (CD207), MGL (CD301, CLEC10A), MDL1 (CLEC5A), Dectin-1 (CLEC7A), MICL (DCAL2, CLEC12A), DNGR1 (CLEC9A), DCIR (CLEC4A), DCAR (CLEC4B), BDCA-2 (CD303, CLEC4C)[#], Mincle (CLEC4E), Dectin-2 (CLEC6A), Mannose receptor (CD206), DEC205 (LY75, CD205), Thrombomodulin (CD141, BDCA-3)[#]
Scavenger receptors: SR-AI/II, MARCO, CD36, SR-BI, CD68 (Macrosialin), CD163, LOX-1
Cytokine receptors
IL-2R, IL-3R, IL-4R, IL-6R, IL-7R, IL-10R, IL-13R, IL-16R, IL-17R, IL-23R, leptin receptor, HGF receptor, TNF-αR, TGF-βR, IFN-α, β, γ receptors, M-CSFR (c-fms, CSF1R, CD115), GM-CSF (CSF2R, CD116)
Chemokine receptors
CCR1, CCR2, CCR5, CCR8, CCR9, CXCR1, CXCR2, CXCR4, CX_3CR1
Cell adhesion molecules
L-selectin (CD62L), ICAM-1 (CD54), LFA-1 (CD11a/CD18), VLA-4 (CD49d/CD29)
Molecules involved in antigen presentation
MHC class I, MHC class II, CD1 family (a/b/c/d/e, CD1c = BDCA-1)[#], CD40, CD80, CD86
Surface antigens important for monocyte/MØ subset identification
EGF-TM7 family (F4/80 or EMR1), Ly-6 family (Ly-6B or 7/4 antigen, Ly-6C) *
Others
hormone receptors (binding to insulin, glucocorticoids), fibronectin receptors, laminin receptors, transferrin and lactoferrin receptors, advanced glycation endproduct (AGE) receptors, lipoprotein lipid receptors, receptors for peptides and small molecules (i.e., 1,2,5-Dihydroxy vitamin D3) and receptors for coagulants/anti-coagulants (i.e., fibrinogen/fibrin, α1-antithrombin, heparin)

* Receptors/molecules only expressed in mice

[#] Receptors/molecules only expressed in humans

(modified from Ross JA and Auger MJ. The biology of the macrophage. In Burke B, Lewis CE: *The Macrophage*. 2nd edition, p12, 2002, Oxford University Press)

1.4.4 Functional specialisation

To date, diverse functional properties of mononuclear phagocytes have been elucidated. From a simplified viewpoint, MØs are the powerful phagocytes efficiently engulfing and killing the encountered microorganisms, while DCs are the professional antigen-presenting cells which could activate naïve T lymphocytes to initiate the adaptive immune response. However, it should be noted that these two cell types do share lots of biological functions, which could be explained by their phenotypic similarity as well as plasticity (Geissmann et al., 2010). Below are the principal functions of MØ and DC:

(1) Phagocytosis and killing of microorganisms

The phagocytic and microbicidal activities begin with the recognition and opsonisation of the pathogens. The opsonins (IgG or C3 fragments) coated on the organisms bind to the related Fc receptors or complement receptors on MØs, initiating the subsequent microbicidal activity such as release of reactive oxygen intermediates (respiratory burst) and arachidonic acid metabolites (Rouzer et al., 1980). On the other hand, particle ingestion is followed by the fusion of the phagosomes (containing ingested materials) with primary lysosomes (containing a variety of enzymes), forming secondary lysosomes or phagolysosomes necessary for the degradation of ingested pathogens (Myers et al., 1985).

(2) Apoptotic cell clearance

In many tissues, apoptosis of cells is an integral component of cell turnover. Proper clearance of apoptotic cells ensures tissue homeostasis being maintained appropriately in multicellular organisms. The process of apoptotic cell clearance is complex, generally involving several steps: sensing and recognition of the

apoptotic cells, engulfment and degradation (Poon et al., 2014). Unlike microbial phagocytosis, the phagocytosis of apoptotic cells is typically considered nonphlogistic. The defects in this process are thought to be the aetiology of a variety of diseases, such as autoimmune diseases, cancers (Elliott et al., 2010).

(3) Antigen processing and presentation

Antigen processing and presentation is a fundamental step to bridging innate and adaptive immunity. Most endogenous antigens are degraded by non-lysosomal proteolytic mechanisms. The processed peptides are associated with MHC class I molecules in endoplasmic reticulum (ER), transported to cell surfaces and presented to $CD8^+$ T cells (Nuchtern et al., 1989). For exogenous proteins, the ingested antigens are degraded in endosomes (containing protease) and the processed peptides are transported into ER, associated with MHC class II molecules and presented on to $CD4^+$ T cells (Cresswell et al., 1985). A third route called "cross-presentation", in which APCs (especially DCs) uptake, process and present extracellular antigens with MHC class I molecules to $CD8^+$ T cells, is important for induction of cytotoxic immunity against most tumours and against viruses that do not readily infect APCs (Heath et al., 2001; Joffre et al., 2012). Recent evidence shows that distinct DC subsets exhibit preferential antigen processing and presentation *in vivo* (Dudziak et al., 2007; Merad et al., 2013).

Furthermore, MØ/DCs play important roles in mediating tissue inflammation through producing distinct inflammatory cytokine profiles to drive specific T cell polarisation (i.e., IL-12 for Th1; TGF-β/IL-6/IL-23 for Th17) (Damsker et al., 2010). Additionally, distinct MØ subsets have been postulated to participate in the resolution of tissue inflammation or tissue repair/wound healing process (Lucas et al., 2010; Duffield et al., 2013)

1.4.5 Macrophage activation and polarisation

MØ activation or polarization has been a key area of immunological research in the past two decades, starting from *in vitro* experimental conditions then gradually translating into human diseases (Mantovani et al., 2005; Mosser et al., 2008; Gordon et al., 2010; Wynn et al., 2012; Martinez et al., 2014). MØs, as a frontline immune effector cells, display remarkable plasticity and can generate a diverse response to environmental signals or exogenous agents, as well as interact with different lymphocyte subsets (Stout et al., 2005; Biswas et al., 2010). In the early 1990s, the distinctive 'alternative activation' was described for the effect of interleukin-4 (IL-4) or interleukin-13 (IL-13) on MØs, compared to the interferon γ (IFN-γ) and/or lipopolysaccharide (LPS)- induced 'classical activation' (Stein et al., 1992; Doyle et al., 1994). Later on, Mills proposed the 'M1/M2 dichotomy', suggesting an intrinsic transition from pro-inflammatory M1 to wound-healing M2-MØs (Mills et al., 2000). Subsequent works by others have further extended this paradigm into a spectrum including further subdivisions, namely M1 (IFN-γ ± LPS), M2a (IL-4 or IL-13), M2b (immune complex), M2c (IL-10 or glucocorticoid ± TGF-β) (Stout et al., 2005; Mantovani et al., 2005; Edwards et al., 2006; Biswas et al., 2010; Martinez et al., 2014). However, a lot of challenges have been faced when attempting to reconcile the biological properties and expression patterns derived from *in vitro* activated/polarized MØs with data from *in vivo* MØ activation/polarization. The main problems included the non-unified definitions, non-standardised experimental protocols and inconsistent biochemical or genetic markers used for characterization (Murray et al., 2014). The fact that M1 and M2 stimuli do not exist alone in tissues imply that the real situation of MØ activation/polarisation *in vivo* (mouse models or human diseases) could be far more complicated than the proposed scheme (Xue et al., 2014; Lavin et al., 2014).

1.5 Macrophages and dendritic cells in the peritoneal cavity

1.5.1 Leukocyte composition in human peritoneal cavity

The leukocyte composition in human peritoneal cavity was first described as early as 1960s, when the cytologic examinations of pelvic cavity by peritoneal washings or aspiration through cul-de-sac were performed in women with benign and malignant diseases (Marcus 1962, McGowan et al., 1967 & 1969). Soon after the launch of PD therapy in 1970s, the peritoneal leukocyte biology became an important research topic in the PD field. Initially, researchers tried to identify different leukocyte subpopulations from the PD effluents and to determine how the dialysis process altered their distributions (Fakhri et al., 1978; Ganguly et al., 1980; Cichocki et al., 1983; Goldstein et al., 1984). It has been revealed that the leukocyte populations within the PD effluents mainly consist of MØs, granulocytes (neutrophils and eosinophils) and lymphocytes (McGregor et al., 1989; Valle et al., 1989; Lewis et al., 1991). Here, the characteristic features of each peritoneal immune cell type from PD effluents are depicted, except for MØs (detailed in the next section).

Neutrophils

When uninfected, the percentage of peritoneal neutrophils normally decreases to less than 5% of total peritoneal leukocytes after dialysis intervention for more than six months (McGregor et al., 1989). Upon acute peritonitis episodes, a substantial number of neutrophils rapidly accumulate in the peritoneal cavity and become the major effector immune cells executing the microbicidal activity (Hurst et al., 2002; Davey et al., 2011). In patients with good treatment response, neutrophils plummet back to normal status 5-7 days after antibiotics prescribed (Flanigan et al., 1985).

Eosinophils

Increased peritoneal eosinophils in the PD effluents were initially noted in patients complicating with 'sterile peritonitis' (Lee et al., 1967). In most reported cases, 'peritoneal fluid eosinophilia' appears to occur very soon after catheter insertion and initiation of PD (Gokal et al., 1981; Humayun et al., 1981), is relatively asymptomatic and does not require antibiotic therapy. It has been suggested that peritoneal fluid eosinophilia is related to intraperitoneal air (Daugirdas et al., 1987) or allergy to some constituents of the PD system, i.e., catheter tubing (Ejaz et al., 1998). Mostly, eosinophil counts spontaneously decrease to low level (<5%) after continued dialysis. However, recurrent eosinophilia did occur in some cases (Quinlan et al., 2010).

Lymphocytes

The majority of peritoneal lymphocytes within the PD effluents are T cells (Lewis et al., 1993). Recently, the differential role of T cell subsets such as T helper cells, cytotoxic T cells and γδ-T cells, during peritonitis have been explored (Wang et al., 2003; Eberl et al., 2009; Roberts et al., 2010; Davey et al., 2011). Of note, PD-associated peritonitis is characterized with increased TNF-α, IL-1β, IL-12 and IL-18, followed by IFN-γ production, suggesting a predominant Th1-response (Wang et al., 2005). Furthermore, a progressive decrease of CD4/CD8 T cell ratio in serial PD effluents from peritonitis patients correlated with a persistent expression of TGF-β, linking to the deterioration of peritoneal membrane function (Wang et al., 2003). More recently, the role of γδ-T cell in the drive of inflammatory responses during acute peritonitis was noted (Eberl et al., 2009; Davey et al., 2011) and importantly, the increased frequency of peritoneal γδ-T cells on day 1 peritonitis is associated with poor outcomes in peritonitis patients (Davey et al., 2011; Lin et al., 2013).

1.5.2 The role of peritoneal macrophage in PD patients

It has been revealed that MØs are the major cellular constituent within the uninfected PD effluents from maintenance PD patients (Fakhri et al., 1978; Ganguly et al., 1980). Due to its accessibility, PD fluids provide a major source of human peritoneal MØs, which has enabled the broad study of its immunobiology, including cytochemical (peroxidase, nonspecific esterase activity), biochemical (arachidonate metabolism) and functional properties (phagocytosis, hydrogen peroxidase generation and bactericidal activity) (Maddox et al., 1984; Goldstein et al., 1984; Adolfs et al., 1985; Peterson et al., 1985).

Several groups investigated on the functional profiles of peritoneal MØs from uninfected PD effluents and also from healthy volunteers (mainly women receiving laparoscopic examination) (Goldstein et al., 1984; Peterson et al., 1985). They identified that these two cell types had similar capability of bacterial phagocytosis (Goldstein et al., 1984), however, peritoneal MØs from uninfected PD effluents posed superior respiratory burst response and intracellular bacterial killing than those from healthy volunteers (Peterson et al., 1985). Subsequently, it has been demonstrated that conventional glucose-based dialysates might have suppressive effect on the phagocytosis and respiratory burst activity of peritoneal MØs (Alobaidi et al., 1986; McGregor et al., 1987). In fact, this suppressive effect could be due to low pH, high osmolarity, high glucose concentration, and high sodium lactate in the conventional PD fluids (Alobaidi et al., 1986; Topley et al., 1988) or poor opsonizing activity (low IgG, complement and fibronectin) in the dialysates (Davies et al., 1990). Evidences also showed that the phagocytosis index, bactericidal activity, and TNF-α/IL-1β/IFN-γ production of peritoneal MØs were progressively decreased during the course of PD

therapy (Lin et al., 1990; McGregor et al., 1996), suggesting that long-term usage of conventional dialysates would compromise the host defence system in PD patients. Additionally, patients with history of peritonitis had significantly suppressed MØ function under uninfected status, compared to those free from peritonitis. Moreover, patients with 'low occurrence of peritonitis' had better peritoneal MØ function than those with 'high occurrence of peritonitis' (Lin et al., 1990).

In 1990s, several new 'biocompatible' PD fluids were developed and were examined whether 'new dialysis fluids' are better than conventional fluids in terms of maintaining the peritoneal immunocompetence (Jörres et al., 1993; de Fijter et al., 1993; Schenk et al., 1994; MacKenzie et al., 1998 & 2000, Jones et al., 2002). Notably, it has been shown *in vitro* as well as *in vivo* that new pH neutral, bicarbonate-buffered or bicarbonate/lactate-buffered PD solutions might provide better preservation of peritoneal MØ immune effector functions than conventional acidic, lactate-buffered solutions (MacKenzie et al., 1998 & 2000; Jones et al., 2002).

In 1990s, researchers began to look at the immunophenotypes and activation status of peritoneal MØs in PD patients. Benefits from the application of contemporary flow cytometers in biomedical research, a variety of surface markers expressed on peritoneal MØs could be examined and differential expression patterns could be analysed from various clinical settings. The initial work revealed that peritoneal MØs from PD effluents expressed higher HLA-DR, RFD7 (mature phagocyte marker), IL-2R and surface IgG levels, compared to peripheral blood monocytes, suggesting peritoneal MØs have features of maturation and activation (Davies et al., 1989). Others reported that increased Fc and C5a receptor and CD14 expression (Lewis et al., 1990) as well as transferrin receptors on peritoneal MØs (Moughal et al., 1991). During PD-related peritonitis, peritoneal MØs expressed higher ICAM-1 (CD54), Fc

gamma RI (CD64), Fc gamma RII (CDw32), Fc gamma RIII (CD16), transferrin receptors (CD71) and tissue factor, while lower levels of complement receptors such as CR1 (CD35), CR3 (CD11b/CD18), compared to blood monocytes (Hart et al., 1992). On the other hand, longitudinal follow-up studies demonstrated that peritoneal MØs became increasingly immature with time on PD, represented by decreasing expression levels of CD11b, CD11c, CD14, CD16, CD64 (McGregor et al., 1996; Cárcamo et al., 1996). These findings highlighted the phenotypic plasticity of peritoneal MØs during the treatment course of PD and the status of MØ activation and maturation in the particular clinical scenario might reflect how tissue MØs respond to the local environmental changes.

Recently, it has been suggested that peritoneal MØs from uninfected PD patients had features of M2 type MØs (*in vitro* polarised M-CSF–driven MØs), represented by positive CD163 expression but lack of CD16 expression. Functionally, like M2-MØs, they preferentially took up early apoptotic cells and could generate large amounts of IL-10 after LPS stimulation (Xu et al., 2007). However, there is some argument regarding M-CSF-driven M2-MØs (Murray et al., 2014). Another recent study showed that peritoneal MØs were phenotypically similar to IL-4–driven alternatively activated MØs (or pro-fibrotic M2-MØs), as they expressed surface markers such as CD206 and CD163. Of note, mRNA levels of TGF-β, MMP9 and CCL18 in peritoneal MØs were close to M2-MØs, and high dialysate CCL18 level was correlated with decreased peritoneal membrane function (high D/P Cre and poor ultrafiltration capacity), implying that peritoneal MØs might participate in the pathogenesis of peritoneal fibrosis (Bellon et al., 2009).

1.5.3 The role of peritoneal dendritic cells in PD patients

In contrast to peritoneal MØs, the phenotypic and functional identity of dendritic cells in human peritoneal cavity is much less characterized. Traditionally, DCs are characterized by high MHCII expression, dendritic morphology and superior ability to induce a strong allogeneic T cell proliferation (mixed lymphocyte reaction). However, these features could be easily confused with MØs in the same tissue compartment. A serial of studies from Betjes and colleagues reported that distinctive intracellular staining patterns of CD68 could discriminate peritoneal DCs ('juxtanuclear spot-like staining') from peritoneal MØs ('pan-cytoplasmic staining') (Betjes et al., 1991 & 1993). These newly identified DCs were superior APCs for allo-antigen, Candida albicans antigen or purified protein derivative (PPD) (Betjes et al., 1993). Subsequently, McCully and colleagues published another peritoneal DC population from uninfected PD effluents with characteristic $CD14^{+}CD4^{+}$ phenotype, arguing they were one of DC precursor subsets (McCully et al., 2005). They suggested that $CD14^{+}$ monocytes could differentiate into $CD14^{+}CD4^{+}$ pre-DCs or $CD14^{+}CD4^{-}$ MØs in the peritoneal cavity, and the former were more potent allo-stimulators than the latter. Interestingly, both Betjes et al., and McCully et al., observed the increased accumulation of peritoneal DC number during acute PD-related peritonitis, however, what they called 'peritoneal DC' may not be the same cell entity. These limited data point out that the immunobiology (particularly immunophenotype) of peritoneal DC in the context of PD remains unclear and its role in the human peritoneal pathologies such as peritonitis and peritoneal fibrosis needs to be further investigated.

1.5.4 Mononuclear phagocytes in mouse peritoneal cavity

Murine peritoneal MØs are one of the best-studied non-lymphoid tissue MØs (Whitby et al., 1959; Jenkin et al., 1960). Substantial works done by Cohn and colleagues in 1960s unveiled the unique monocyte-like peritoneal mononuclear phagocytes from either unstimulated animals or LPS-stimulated animals (Cohn et al., 1965). Importantly, they set up an *in vitro* culture system to comprehensively investigate the morphologic and biochemical changes during the differentiation process of peritoneal mononuclear phagocytes (Cohn et al., 1966). However, it should be kept in mind that these peritoneal mononuclear phagocytes are a mixed population. The tremendous breakthrough in murine tissue MØ biology is the discovery of F4/80 antigen as a marker for mature tissue MØs (Austyn and Gordon, 1981). This antigen is a G protein -coupled receptor (GPCR), a member of the epidermal growth factor-seven-pass transmembrane (EGF-TM7) family, which also includes EMR1 (human F4/80 homolog) (McKnight et al., 1998). Using the application of anti-F4/80 monoclonal antibody has enabled the identification of resident MØ populations in the wide range of mouse tissues/organs such as kidney, liver, lung, endocrine organs, bone, red pulp of spleen and brain (Hume et al., 1983; Perry et al., 1985; Gordon et al., 1986).

In the naïve peritoneal cavity, our group has shown via flow-cytometric analysis that two resident monocytic-like subsets coexist; the major population is F4/80^{high} cells with CD11b^{high} and MHCII$^{low/-}$ phenotype, while the minor subset is F4/80$^{int\text{-}low}$ cells with CD11b^{+} and MHCII^{high} phenotype (Rosas et al., 2007; Dioszeghy et al., 2008). The former was the classical ‘resident MØs’ whereas the latter was tentatively called ‘DC-like’ cells as their superior ability of processing and presenting antigen (ovalbumin) and stimulating naïve T cell proliferation and IL-2 production

(Dioszeghy et al., 2008). However, these 'DC-like' cells seemed to be a heterogeneous population according to their non-uniform expression of CD11c (traditional DC marker). Additionally, our group was unable to discriminate "DC-like" cells from recruited monocyte-derived MØs during experimental peritonitis, due to the overlapping immunophenotypes (F4/80$^{int\text{-}low}$MHCII^{high}). Soon after this paper published, another group also identified two MØ subsets in naïve peritoneal cavity: 'large MØs' (phenotypically identical to F4/80^{high}MHCII$^{low/-}$ resident MØs) and 'small MØs' with F4/80$^{int\text{-}low}$MHCII^{high} phenotype (Ghosn et al., 2010). Notably, these 'small MØs' were gated after the exclusion of CD11c^{+}MHCII^{high} cells (called "DCs" here). Functionally, 'large MØs' and 'small MØs' exerted differential nitric oxide (NO) production in response to LPS stimulation *in vitro* and *in vivo*. The group also suggested 'small MØs', which predominated in the peritoneal cavity after LPS or thioglycollate stimulation, were basically from circulating Ly-6C^{+} monocytes, not from 'large MØs', although there was no direct evidence supporting this statement. More recently, the transcriptional profiling of distinct murine tissue MØs published as part of Immunological Genome Project (ImmGen) provided substantial information regarding the molecular signatures of murine tissue MØ subsets such as splenic red pulp MØs, lung MØs, peritoneal MØs and microglia (Gautier et al., 2012). On the basis of identified 39 'core-MØ genes', all peritoneal mononuclear phagocyte subsets, either from the steady state (F4/80^{high}MHCII$^{low/-}$ and F4/80^{low}MHCII^{high}) or from day 5 after thioglycollate stimulation (MHCII^{+} and MHCII^{-}), segregated together within the 'MØ entity', and none of them was close to the 'DC entity'. Hence, the identity of peritoneal DC subsets in mice remains ambiguous, both at steady-state and during inflammation, and their exact role needs to be further elucidated (Gautier et al., 2012). Table 1.4 summaries the phenotypes of peritoneal MØ/DC subsets described in the literature (Dioszeghy et al., 2008; Ghosn et al., 2010; Gautier et al., 2012).

Table 1.4 Phenotypic definition of peritoneal mononuclear phagocyte subsets (steady state and inflamed state) used in the current literature

	Dioszeghy et al (2008)	Ghosn et al (2010)	Gautier et al (2012)
Steady state	$F4/80^{high}MHCII^{low/-}$ 'resident' MØs	$CD11b^{high}F4/80^{high}MHCII^{low/-}$ 'large MØs'	$F4/80^{high}MHCII^{low/-}$ MØs
	$F4/80^{int/low}MHCII^{+}$ 'DC-like' cells	$CD11b^{+}F4/80^{+}MHCII^{+}$ 'small MØs'	$F4/80^{low}MHCII^{+}$ MØs
		$CD11b^{int/low}CD11c^{+}MHCII^{+}$ classical DCs	
Inflamed state	$F4/80^{high}MHCII^{low/-}$ resident MØs	$CD11b^{high}F4/80^{high}MHCII^{low/-}$ 'large MØs'	$F4/80^{high}MHCII^{low/-}$ MØs
	$F4/80^{int/low}MHCII^{+/-}$ 'inflammatory' MØ/DCs	$CD11b^{+}F4/80^{+}MHCII^{+/-}$ 'Inflammatory' MØs	$F4/80^{int}MHCII^{+/-}$ MØs
			$F4/80^{low}MHCII^{+}$ MØs
	(unable to discriminate between MØs and DCs)	*(unclear identity of DCs during inflammation)*	*(unclear identity of DCs during inflammation)*

Experimental peritonitis models used in each paper as follow:

- Dioszeghy et al (2008): staphylococcus epidermidis supernatant-induced peritonitis (day 3)
- Ghosn et al (2010): LPS-induced peritonitis (9 hours and day 2);
  thioglycollate-induced peritonitis (day 1 and day 4)
- Gautier et al (2012): thioglycollate-induced peritonitis (day 5);

1.6 Scope of the thesis

Despite general acceptance that the mononuclear phagocytes play key roles in tissue homeostasis and defence against pathogens, the immunobiology of this heterogeneous population in the peritoneal cavity remains poorly elucidated. In the context of PD, peritonitis and peritoneal fibrosis due to repeated infections remain major reasons for mortality and morbidity. It is hypothesized that the modification of MØ/DC biology by the dialysis process alters tissue homeostasis, host susceptibility to infection and local immunity, thus compromising long-term patient outcomes. The key objectives of the present study are to characterize human peritoneal MØ/DC, to investigate how these cells are modified by the dialysis treatment, and to delineate the specific roles of different MØ/DC subsets in peritoneal immunity, using clinically relevant mouse models.

The specific aims of each chapter in this thesis are as follows:

Chapter 3: To characterize the immunophenotypes and functional properties of peritoneal MØ/DC subsets in PD patients

Chapter 4: To assess the cellular distribution/kinetics and phenotypic alterations of peritoneal MØ/DC subsets during the course of PD therapy, and examine their correlations with clinical outcomes

Chapter 5: To identify the corresponding subsets between humans and mice, in order to clarify the differential roles of the respective MØ/DC subsets in the development of peritoneal immunity

Chapter Two

Materials and methods

2.1 Human study

2.1.1 Ethical approval

This study was approved by the South East Wales Local Ethics Committee (COREC: 04WSE04/27). All patients gave written, informed consent for the collection of PD fluids and peripheral bloods before the enrolment. The study was undertaken according to principles described in the Declaration of Helsinki and under the local ethic guidelines (Bro Taf Health Authority, Wales).

2.1.2 Study populations

Patients were recruited from the PD unit at University Hospital of Wales in Cardiff, United Kingdom between October 2010 and December 2014 and categorized into three cohorts defined by the clinical status of the patients at the time of enrollment. The definition of each patient category and the respective plan of PD fluids sampling are described below and summarised in Fig. 2.1:

New starters

Patients with end-stage renal disease (ESRD) who had chosen PD as renal replacement therapy (RRT) were recruited. These patients were followed from the time when PD catheter was surgically inserted to 1 year after PD treatment or until the discontinuation of dialysis due to any reason. Typically 1 week after catheter surgery the catheter was flushed ("1st Flush") to check its patency. The catheter was checked again approximately 1 week before the start of dialysis ("2nd Flush"). The timing of the "2nd Flush" varied, but normally occurred after 3 weeks. When PD commenced,

an initial 'training bag' is used ("1st PD exchange-PD start"). Thereafter, PD effluent samples were collected at 3 months, 6 months and 1year after the start of PD therapy. A total of 50 new-starter PD patients were enrolled in this project. The reasons for discontinuation of PD therapy such as deaths, non-death technique failure (i.e., catheter dysfunction, ultrafiltration failure, peritonitis), kidney transplantation or transfer to other institutes were recorded.

Stable patients

Patients under maintenance PD therapy for more than one year with or without history of peritonitis were recruited. These patients were free from peritonitis for at least three months at the time of PD fluid sampling. A total of 37 uninfected PD effluent samples were collected from 37 stable patients in this project.

Peritonitis patients

Dialysis patients presenting with acute PD-related peritonitis were recruited. The diagnosis of acute peritonitis was based on the presence of abdominal pain and cloudy peritoneal effluent with >100 WBC/mm^3 (Li et al., 2010). The day of the first appearance of cloudy effluent was defined as "day 1 peritonitis". In this study, only PD effluents from day 1 peritonitis were collected for analysis. A total of 42 peritonitis episodes from 37 patients (5 patients having two episodes of peritonitis) were analysed. Of them, 37 episodes were 'culture-positive' peritonitis with documented causative organisms and 5 episodes were 'culture-negative' peritonitis as no bacterial growth from cultures. The treatment of PD-related peritonitis followed the most updated ISPD Guidelines/Recommendations (Li et al., 2010). The outcome of each peritonitis episode was categorised into 'treatment success' or 'treatment failure' (defined as peritonitis-related mortality or technique failure).

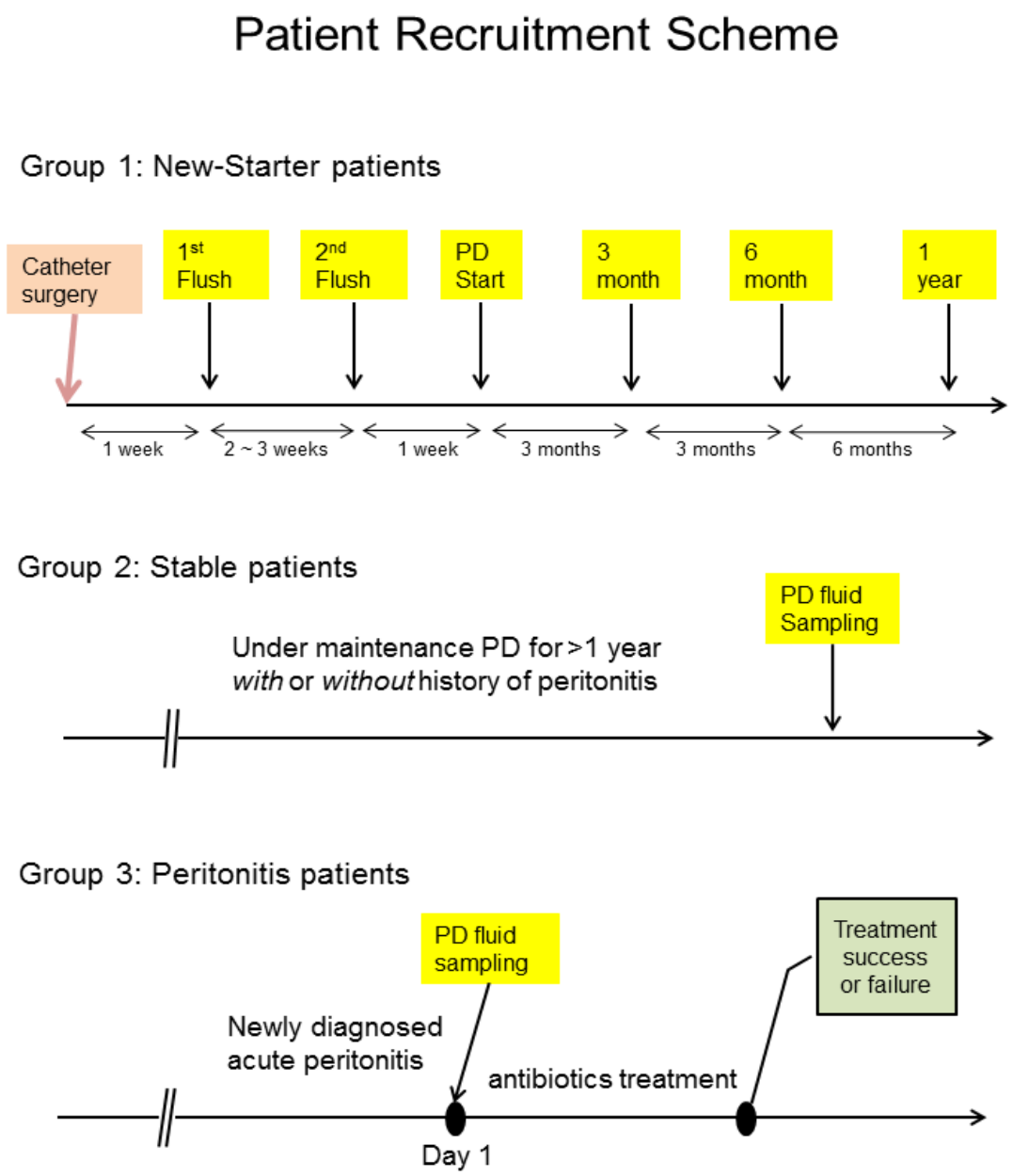

Figure 2.1 PD patient recruitment and the timescale of PD fluid sampling

Schematic plans of the recruitment of three categorised PD patients in this study. For new-starter PD patients (group 1), PD fluid samples were collected at specified time points during the course of PD therapy. For stable patients (group 2), non-infected overnight PD fluid samples were collected from patients under regular PD for at least 1 year (free from peritonitis for at least 3 months). For peritonitis patients (group 3), PD fluid samples from day 1 peritonitis were collected.

2.1.3 Isolation of human peritoneal cells from PD effluent fluids

PD effluent bags were collected from consented PD patients either at clinic or at the patients' homes. Samples were kept in an ice box during transport to reduce cell adhesion to the PD bags and maintain cell quality. The dwell time and the type of dialysate of each collected PD bag were recorded. In the laboratory, the total volume of each PD effluent bag was measured, drained fluids were aliquoted into 500 ml centrifuge tube (Corning Inc., New York, USA) and centrifuged at 2000 rpm (863 *g*) at 4°C for 25 minutes (Sorvall Legend RT). The cell pellet was resuspended in 50 ml phosphate buffered saline (PBS) (Invitrogen), transferred to 50 ml Falcon tubes, and centrifuged at 1300 rpm (365 *g*) at 4°C for 8 minutes. The pellet was resuspended in PBS at 1-2×10^7 cells/ml, kept on ice prior to use.

2.1.4 Isolation of human mononuclear cells from peripheral bloods of PD patients and healthy individuals

Total 5-10 ml venous bloods were withdrawn from new-starter PD patients (at the time of '1st PD flush') as well as healthy volunteers and collected in conventional EDTA tubes. PBMC were isolated by layering whole blood over 10-15 ml of Lymphprep™ containing sodium diatrizoate 9.1% (w/v) and polysaccharide 5.7% (w/v) (Axis-Shield) and centrifuged at 1680 rpm (609 *g*), at 18°C for 20 minutes with minimal acceleration and deceleration. Granulocytes and erythrocytes have a higher density and sediment through the Lymphoprep™ layer during centrifugation. Mononuclear cells remained at the plasma:Lymphoprep™ interface and were aspirated to a 50 ml Falcon tube. After washing with PBS twice, the cell pellet was resuspended in PBS (~10^7/ml) and kept on ice prior to use.

2.1.5 Cell counting

Cells were counted with a dual chamber Neubauer haemocytometer. The cells in four large squares at corners were counted and the number was divided by 4 to gain an average number of cells in 0.0001 cm^3. This cell number was multiplied by 10^4 to give the number of cells *per* ml (1 cm^3). Therefore, in each PD effluent sample:

Total peritoneal cell counts = number of cells *per* ml x total volume of the bag (ml)

2.1.6 Flow cytometry

2.1.6.1 General staining procedures

The isolated cells were stained with LIVE/DEAD Fixable Aqua Stain kit (Life technologies) for 15 minutes at room temperature in the dark. After washing with FACS wash buffer (0.5% w/v BSA, 5 mM EDTA, 2 mM NaN_3 in PBS), the cells were aliquoted to a v-bottom 96-well plate (1-1.5 x10^6 cells in 100 µl per well) and blocked for 15 minutes with normal mouse serum (1 % v/v) to prevent non-specific binding, before the addition of a variety of anti-human monoclonal antibodies; together with appropriate isotype controls (Table 2.1). The antibody mixtures were incubated for 30 minutes on ice in the dark. If a biotin-conjugated antibody was used, then the cells were washed with FACS wash buffer and stained with a streptavidin conjugated with PerCP, APC or Alexa-Fluor 405 (BD Biosciences) for another 30 minutes. The cells were washed three times with FACS wash buffer and transfer into microtitre tubes. Finally, the samples were acquired on a 3-laser, 9-colour Cyan ADP flow cytometer, and data analyzed with Summit software (Beckman-Coulter, Fullerton, CA, USA).

Table 2.1. Fluorochrome-conjugated anti-human monoclonal antibodies for surface antigen staining in this project

Antigen	Fluorochrome	Clone	Isotype	Company
CD1a	PerCP	HI149	Mouse IgG1, k	abcam
CD1c	Biotin or APC	AD5-8E7	Mouse IgG2a, k	Miltenyi Biotec
CD3	FITC	SK7	Mouse IgG1, k	BD Biosciences
CD4	APC-H7	SK3	Mouse IgG1, k	BD Biosciences
CD8	PE-Cy7	SK1	Mouse IgG1, k	BD Biosciences
CD11b	V450	ICRF44	Mouse IgG1, k	BD Biosciences
CD11c	V450	B-ly6	Mouse IgG1, k	BD Biosciences
CD14	ECD	RMO52	Mouse IgG2a, k	Beckman Coulter
CD15	APC	HI98	Mouse IgM, k	BD Biosciences
CD16	PE-Cy7	3GB	Mouse IgG1, k	BD Biosciences
CD19	PerCP	HIB19	Mouse IgG1, k	BD Biosciences
CD36	APC	5-271	Mouse IgG2a, k	BioLegend
CD40	PE	5C3	Mouse IgG1, k	BD Biosciences
CD45	APC	2D1	Mouse IgG1, k	eBioscience
CD56	PE	MY31	Mouse IgG1, k	BD Biosciences
CD62L	V450	DREG-56	Mouse IgG1, k	BD Biosciences
CD64	APC	10.1	Mouse IgG1, k	BioLegend
CD66	PE	B1.1	Mouse IgG2a, k	BD Biosciences
CD73	APC	606112	Mouse IgG2b, k	R&D Systems
CD80	PE	2D10	Mouse IgG1, k	BioLegend
CD83	PE	HB15e	Mouse IgG1, k	BD Biosciences
CD86	PE-Cy5	2331	Mouse IgG1, k	BD Biosciences
CD115	Biotin	12-3A3-1B10	Rat IgG1	eBioscience
CD116	FITC	4H1	Mouse IgG1, k	eBioscience
CD141	APC	AD5-14H12	Mouse IgG1, k	Miltenyi Biotec
CD163	Biotin	GH1/61	Mouse IgG1, k	BioLegend
CD206	PE	3.29B1.10	Mouse IgG1, k	Beckman Coulter
CD209	PerCP	120507	Mouse IgG2b, k	R&D Systems
CD226	APC	11A8	Mouse IgG1, k	BioLegend
CD301	APC	H037G3	Mouse IgG2a, k	BioLegend
CD303	APC	AC144	Mouse IgG1, k	Miltenyi Biotec
CCR2	APC	48607	Mouse IgG2b, k	R&D Systems
CCR3	APC	5E 8	Mouse IgG2b, k	BioLegend
CCR7	PE	3D12	Rat IgG2a	eBioscience

HLA-A2	APC	BB7.2	Mouse IgG2b, k	BD Biosciences
HLA-DR	APC-H7	L243	Mouse IgG2a, k	BD Biosciences
Dectin-1	PE	259931	Mouse IgG2b, k	R&D Systems
Dectin-2	Alexa-Fluor 647	IMG3D1	Mouse IgG3, k	IMGENEX
Siglec-8	PE	7C9	Mouse IgG1, k	BioLegend
Tim4	PE	9F4	Mouse IgG1, k	BioLegend
FceR1	APC	AER-37	Mouse IgG2b, k	eBioscience
MerTK	APC	125518	Mouse IgG1, k	R&D Systems

2.1.6.2 Standardisation, calibration and quality control of flow cytometry

To ensure the data generated from flow cytometric analysis are as accurate and as reliable as possible, several steps have been undertaken:

1. The performance of components of flow cytometer such as lasers, photomultiplier tubes (PMTs), optical filters and log and linear amplifiers is regularly checked by qualified service personnel.
2. Internal quality control is implemented regularly (normally once a week) by our Centre Biotechnology Service (CBS) staffs. This includes routine calibration of the instrument's response to fluorescence signals using reference microbeads (SPHERO^{TM} Ultra Rainbow Fluorescent Particles, Spherotech Inc.) to determine that the performance parameters from each fluorescence channel are within the acceptable ranges.
3. When running on flow cytometer, the concentration of the sample would normally keep in the ranges of 10^5-10^6 cells *per* 100 µl. The acquisition flow rate is maintained around 1000 to 3000 event per second. The total events acquired are normally at least 50,000 events per sample and increased when the rare cell populations (i.e., peritoneal DC subsets) needed to be identified.

2.1.7 Cell cycle analysis and proliferation assay

After surface staining, human peritoneal cells were washed with FACS wash buffer, fixed in 1% formaldehyde (in PBS) for 20 minutes at room temperature in the dark and permeabilized with FACS wash buffer containing 0.5% (w/v) saponin (Sigma). Following fixation and permeabilisation, cells were stained with anti-human Ki-67-FITC (clone B56, BD Biosciences); together with isotype controls. The antibodies were left on ice for 1 hour in the dark. After washed three times with FACS wash buffer containing 0.5% (w/v) saponin, the cells were stained with DAPI solution (4',6-diamidino-2-phenylindole, a fluorescent stain that binds strongly to A-T rich regions in DNA; Life Technologies) on ice for 30 minutes in the dark. The samples were acquired on the Cyan ADP flow cytometer and analyzed as described above.

2.1.8 *Ex vivo* microbial product stimulation and cytokine production assay

Human peritoneal cells were washed three times with complete RPMI medium (RPMI 1640 medium supplemented with 10% heat-inactivated fetal calf serum (FCS), 10 U/ml penicillin and 10 μg/ml streptomycin). $2x10^5$ cells in 100 μl complete RPMI medium were then aliquoted into 48 well flat-bottomed plates. For TNF-α, IL-1β, IL-6, IL-10 assay, 10% v/v SES (homemade, a cell free supernatant prepared from a clinical isolate of *S. epidermidis*, Hurst et al., 2001) or LPS (100 ng/ml final concentration; from *Salmonella enterica* serotype typhimurium, Sigma) was added in the presence of GolgiStop™ (2 μM final concentration; BD Bioscience) and incubated for 4 hours (TNF-α, IL-1β and IL-6) or 24 hours (IL-10) at 37 °C, 5% CO_2. For IL-12p40/70 assay, cells were primed for 2 hours with recombinant human IFN-γ (10 ng/ml final concentration; PeproTech), then activated with IFN-γ (10 ng/ml final

concentration) and either SES (10% v/v) or LPS (100 ng/ml final concentration) in the presence of GolgiStop™ (2 μM final concentration; BD Bioscience) for an additional 22 hours at 37 °C, 5% CO_2. The cells were carefully recovered using plastic cell lifters, washed with PBS twice, blocked with normal mouse serum (1% v/v) and stained with surface anti-human antibodies. After that, the cells were fixed in 1% formaldehyde (in PBS) for 20 minutes in the dark, permeabilized with FACS wash buffer containing 0.5% (w/v) saponin (Sigma), and then stained with anti-human cytokine antibodies including anti-TNF-α-APC (clone: 6401.1111) from BD Biosciences, anti-IL-1β-APC (8516) from R&D Systems, anti-IL-6-APC (MQ2-13A5) from BD Biosciences, and anti-IL-12(p40/p70)-APC (C8.6) from Miltenyi Biotec; together with appropriate isotype controls. The antibodies were left on ice for 30 minutes in the dark before washing the cells three times with FACS wash buffer. The samples were acquired on the Cyan ADP flow cytometer and data were analyzed as described above.

2.1.9 *Ex vivo* phagocytosis and respiratory burst assay

Human peritoneal cells were washed three times with complete RPMI medium. ~$5x10^5$ cells in 100 μl complete RPMI medium were then aliquoted into 48 well flat-bottomed plates. 3'-(p-aminophenyl) fluorescein (APF), a fluorescent probe designed for the detection of free radicals such as hydroxyl radical (HO•), hypochlorite anion (–OCl), was freshly prepared in complete RPMI medium with the final concentration of 5μM. The cell pellets were resuspended either with 100μl complete RPMI medium containing APF (5μM) or with RPMI medium alone (as controls) and incubated for 30 minutes at 37 °C, 5% CO_2 in the dark. Following APF staining, 100 μl Alexa-Fluor 405-conjugated zymosan particles ($2x10^6$ particles) or

7-Hydroxy-9*H*-(1,3-Dichloro-9,9-Dimethylacridin-2-One)(DDAO)-conjugated *Staphylococcus epidermidis* (~10^8 CFU) were added and incubated for 30 minutes at 37 ^oC, 5% CO_2 in the dark. Then the plates were placed on ice to stop the reaction. After washing with complete RPMI medium twice, the cell pellets were stained as described above (section 2.1.6.1). The samples were acquired on the Cyan ADP flow cytometer and data were analyzed as described above.

2.1.10 Fluorescence-activated cell sorting of human peritoneal monocytic cells

For cell sorting, the same staining protocol as shown in section 2.1.6.1 was undertaken except for using FACS wash buffer without NaN_3. After final wash, the cells were resuspended to ~10^7 cells per ml in FACS wash buffer without NaN_3 and transferred to 5 ml polystyrene round-bottom tubes (BD Falcon). The cells were sorted using FACSAria III according to the instruction. The cells were kept cold in the FACSAria III by using the inbuilt refrigeration system, and collected in pre-labeled 5 ml polypropylene tubes with pre-filled 0.5 ml FCS (Life Technologies) as cell cushion. After sorting, the isolated cell populations were checked for the purity by flow cytometry and immediately used in functional assays.

2.1.11 Morphological analysis

Cytospin preparations were made using ~10^4 purified cells, spun at 300 rpm for 5 minutes (Cytospin 3, Shandon). Cytospun cells were air-dried, stained with Microscopy Hemacolour (Merck), visualized on a Leica DMLB microscope with DFC490 camera (Leica) and processed using QWin Software (Leica).

2.1.12 Antigen processing and presentation assay

Stable PD patients were screened by flow cytometry for their HLA-A2 status (anti-HLA-A2-APC, clone: BB7.2, eBiosicences). Antigen cross-presentation assays were performed as previously described with modifications (Meuter et al., 2010). The purified peritoneal MØ or DC subsets were cultured in 96-well round-bottomed plates ($5x10^4$-$2x10^5$ cells/well). M1-specific $CD8^+$ T cells were generated by stimulating PBMCs with 0.1 nM M1p58-66. Resting cells with >95% M1p58-66-specific cells were used for assays, as determined by PE-tetramer staining (made in-house, performed by Dr. Wajid Khan). Recombinant Influenza M1 protein (1 μM) was added to the APCs for 20 hours at 37°C, 5% CO_2. APCs were washed extensively before co-culturing with responder T cells at a ratio of 1:1-2 (APCs: responder T cells). M1p58-66 peptide (0.1 μM) was added to the APCs for 1 hour at 37°C prior to co-cultured with responder T cells. Responder cells alone and with 10 μg/ml PMA and 1 μM ionomycin were used as negative and positive controls, respectively. The co-cultures were incubated for 5 hours at 37°C, 5% CO_2 in the presence of Brefeldin-A (10 μg/ml; Sigma-Aldrich). In brief, the cells were then stained with LIVE/DEAD Fixable Aqua Stain kit (Life technologies), blocked for 15 minutes with normal human IgG (0.1 mg/ml, KIOVIG, Baxter) and then stained with surface antibodies for 30 minutes on ice. The cells were fixed and permeabilised (as above) for intracellular staining with anti-IFN-γ-FITC (B27, BD Biosciences) for 30 minutes on ice in the dark. The samples were acquired on either the FACSCanto II or CyAn ADP flow cytometers and analyzed with FlowJo (TreeStar) or Summit software.

2.2 Mouse study

2.2.1 Animals

Animals in this study were housed and maintained at Cardiff University. All experiments were aged and sex matched (mostly 6-12 week-old females), unless otherwise stated. C57BL/6 mice were obtained from Harlan Olac. C57BL/6.*Il10*$^{-/-}$ were obtained from Jackson Laboratory. *Ccr2*$^{-/-}$ mice (B6.129S4-*Ccr2*^{tm1Ifc}/J, from Jackson Laboratory Stock: 004999) and C57BL/6.CD45.1 mice (from Jackson Laboratory) were bred from our own colonies. 129S6/SvEv and 129S6/SvEv.CD45.1 (gift from Professor Fiona Powrie, Oxford University) congenic mouse strains were bred from our own colonies. All experiments were performed in accordance with institutional and United Kingdom Home Office guidelines under the project licenses 30/2401 (2010-2012) and 30/2938 (2012-2014).

2.2.2 Experimental peritonitis models

Experimental peritonitis was induced by single intraperitoneal administration of 200 μl of a cell free supernatant prepared from a clinical isolate of *S. epidermidis* (SES) (Hurst et al., 2001) or administration of zymosan particles (0.2-2x10^7, as indicated). Mice were sacrificed at scheduled time points, typically 4 hours or 72 hours after inflammatory insults. Total peritoneal cells were harvested by lavage using a 5 ml syringe (with 21 G hypodermic needle) containing 5 ml ice-cold 5mM EDTA in PBS. The recovered cells were collected in 15 ml labeled centrifuged tubes (Corning Inc., New York, USA), kept on ice await further experiments.

2.2.3 Adoptive transfer experiments

9 to 11-week-old donor naïve 129S6/SvEv.CD45.1 congenic mice were humanely sacrificed and peritoneal cells were recovered by lavage with 1 ml ice-cold PBS. Cells were pooled from several donors and 400µl ($1.8x10^6$ cells) was immediately intraperitoneally injected into host 129S6/SvEv (CD45.2) mice. One day after adoptively transferred, mice were either injected with SES or were left unchallenged then sacrificed on day 3. Total peritoneal cells were harvested and analyzed by flow cytometry as indicated below.

2.2.4 Flow cytometry

Flow cytometry was performed broadly the same as for human cells. Murine peritoneal cells were incubated in blocking buffer (5% v/v heat-inactivated rabbit serum, 0.5% w/v BSA, 5 mM EDTA, 2 mM NaN_3, 4 µg/ml rat anti-mouse 2.4G2 in PBS) for 30 minutes on ice. Fluorochrome-labeled or biotin-conjugated antibodies (Table 2.2) in FACS wash buffer (0.5% w/v BSA, 5 mM EDTA, 2 mM NaN_3 in PBS) were added. After 30 minutes incubation on ice in the dark, the cells were washed three times with FACS wash buffer. When necessary, the cells were incubated for further 30 minutes on ice in the dark with fluorochrome-conjugated streptavidin. After final wash, the samples were acquired and analyzed as previously described.

Table 2.2. Fluorochrome-conjugated anti-mouse monoclonal antibodies used in this project

Antigen	Fluorochrome	Clone	Isotype	Company
F4/80	Biotin	CI:A3-1	Rat IgG2b	Homemade
F4/80	PE-TxR	BM8	Rat IgG2b	Invitrogen
CD11b	FITC	5C6	Rat IgG2b	Homemade
CD11b	APC-Cy7	M1/70	Rat IgG2b	BioLegend
CD11c	PE-Cy7	HL3	Ar Hamster IgG1	BD Biosciences
CD19	V450	1D3	Rat IgG2a	BD Biosciences
CD36	PE	HM36	Armenian Hamster IgG	BioLegend
CD45.1	APC,	A20	Mouse IgG2a	eBiosciences
CD45.2	APC-Cy7	104	Mouse IgG2a	BioLegend
CD64	PE	X54-57.1	Mouse IgG1	BD Biosciences
CD73	eF450	TY/11.8	Rat IgG1	eBiosciences
CD80	Biotin	16-10A1	Ar Hamster IgG2	BD Biosciences
CD86	Biotin	B7-2	Rat IgG2b	BD Biosciences
CD192/CCR2	PE, APC	475301	Rat IgG2b	R&D Systems
CD206	Biotin	5D3	Rat IgG2a	Homemade
CD209a	Biotin	5H10/CIRE	Rat IgG2a	BD Biosciences
CD226	PE, APC, Alexa-Fluor 647	10E5	Rat IgG2b	eBiosciences BioLegend
CD301	Alexa-Fluor 647	ER-MP23	Rat IgG2a	AbD Serotec
Ly6C	Brill.V421	HK1.4	Rat IgG2a	BioLegend
Ly6G	APC-Cy7	1A8	Rat IgG2a	BD Biosciences
MHC-II I-A/I-E	PerCP/PECy5.5	M5/114.15.2	Rat IgG2b	BioLegend
Tim4	PE	RMT4-54	Rat IgG2a	BioLegend
MerTK	APC	108928	Rat IgG2a	R&D Systems
TNF-α	PE	MP6-XT22	Rat IgG1	BD Biosciences
IL-6	PE	MP5-20F3	Rat IgG1	BD Biosciences
IL-10	APC	JES5-2A5	Rat IgG2b	eBiosciences
IL-12(p40/p70)	PE	C15.6	Rat IgG1	BD Biosciences

2.2.5 Cell cycle analysis and proliferation assay

Peritoneal cells were harvested from 6-7 week-old female C57BL/6 mice at 72 hours after low dose zymosan ($2x10^6$ particles) challenge. The cells were fixed in 1% formaldehyde (in PBS) and permeabilized with FACS wash buffer containing 0.5% w/v saponin (Sigma). Following that, the cells were incubated in blocking buffer (5% v/v heat-inactivated rabbit serum, 0.5% w/v BSA, 5 mM EDTA, 2 mM NaN_3, 0.5% w/v saponin, 4 μg/ml rat anti-mouse 2.4G2 in PBS) for 30 minutes on ice, then antibody cocktails including surface antigen staining and anti-human Ki-67-FITC (clone B56, BD Biosciences, cross-reacting with mouse species) antibodies were added; together with isotype controls. The antibody staining was left for 1 hour on ice in the dark. After washing three times with FACS wash buffer, the cells were stained with DAPI solution (Life Technologies) for 30 minutes on ice in the dark. The samples were acquired and analyzed as described above.

2.2.6 *Ex vivo* microbial product stimulation and cytokine production assay

Murine peritoneal cells were washed three times with complete RPMI medium. Cells were plated in 48 well flat-bottomed plates ($2x10^5$ in 200 μl per well) with 0.1% (v/v) Golgi-plug (BD Biosciences). SES (10% v/v) or LPS (100 ng/ml final concentration; from *Salmonella enterica* serotype typhimurium, Sigma) was added as stimulants and complete RPMI medium only controls were performed in parallel. After incubation at 37°C, 5% CO_2 for 6 hours, the cells were carefully recovered using plastic cell lifters and intracellular cytokines including TNF-α, IL-6, IL-10, IL-12(p40/p70) were assessed as previously described.

2.2.7 Apoptotic thymocyte clearance assay

2.2.7.1 Generation of apoptotic thymocytes

The thymus consists of two lobes and lies on the median line of vertebral column, just above the heart. In the young mice, the thymus is well-developed, while those in the adult or in the old age are atrophic and difficult to detect visually. After euthanasia, the rib cages are carefully opened to expose the thymus ("whitish pads"). After removal of thymus, thymocytes were obtained by mechanical dissociation with a 2-ml syringe plunger and the suspensions of cells in PBS were filtered through a sterile cell strainer (40 μm Nylon, BD Falcon) twice to remove residual fibrous tissue. The cells were washed with PBS, resuspended in 50 ml complete RPMI medium in the presence of 1 μM dexamethasone (Sigma-Aldrich) and transferred to Nunclon tissue culture flask, 175 cm^2 (Thermo scientific) and incubated for 4 hours at 37°C, 5% CO_2. The cells were washed and resuspended in PBS (~10^7 cells/100 μl).

2.2.7.2 Quantification of apoptotic thymocytes

A small aliquot of apoptotic thymocyte suspension was diluted with PBS (~10^4 cells/ 100 μl) and cytospin preparations (Cytospin 3, Shandon) were made as previously described. Cytospun cells were air-dried, stained with Microscopy Hemacolour (Merck), visualized on a Leica DMLB microscope with DFC490 camera (Leica) and processed using QWin Software (Leica). Apoptosis was confirmed by characteristic morphological changes including nuclear fragmentation, chromatin condensation, cell shrinkage, and membrane blebbing. The percentage of induced apoptosis was assessed by flow cytometry through NIM-DAPI staining (containing nuclear isolation

medium, NIM-II and 4',6-diamidino-2-phenylindole, DAPI). Specifically, 200 µl cell suspensions (1-3x10^5 cells) were aliquoted to a 1.5ml Eppendorf tube, mixed with 200 µl NIM-DAPI solution and left for 30 minutes in the dark. Following staining, the cells were centrifuged at 2,000 rpm (~700 *g*) at 4°C for 10 minutes. The supernatant was carefully discarded (not to disturb the nuclear pellet). The nuclear pellet was resuspended in ~200 µl PBS. The samples were acquired on the Cyan ADP flow cytometer and data were analysed by summit software. The proportion of 'sub G_0' area on the flow-cytometric plots denoted the percentage of apoptotic thymocytes (see Fig. 5.14). Normally, ~50% of thymocytes become apoptotic after dexamethasone (1 µM) treatment for 4 hours.

2.2.7.3 *In vivo* apoptotic thymocyte clearance assay

Apoptotic thymocytes (~2x10^7 cells in 200 µl PBS) from naive 129S6/SvEv.CD45.1 congenic mice were intra-peritoneally transferred to 129S6/SvEv (CD45.2) mice, either naïve or 72 hours after SES challenge. After 30 minutes retention, mice were humanely sacrificed and peritoneal cells were recovered by lavage with 5 ml of ice cold PBS with 5 mM EDTA. The cells were washed twice with PBS followed by blocking and antibody staining for surface antigens (including anti-mouse CD45.1-V450). After that, the cells were washed, fixed in 1% formaldehyde (in PBS) and permeabilized with FACS wash buffer containing 0.5% (w/v) saponin (Sigma). Intracellular staining was undertaken with anti-mouse CD45.1-APC, together with IgG2a-APC controls, in order to identify the apoptotic thymocytes within the phagocytes, presumably CD45.1-APC$^+$ (intracellular) CD45.1-V450$^-$ (surface). The samples were acquired on flow cytometer and analysed by summit software. The "percentage of phagocytosis" was measured by the subtraction plot (histogram)

between positive CD45.1-APC staining and IgG2a-APC isotype staining on individual MØ/DC subset, restricted to CD45.1-V450^{-} and singlet cell gate to exclude the adhered but not ingested apoptotic cells (see Fig. 5.15 and 5.16).

2.2.8 Fluorescence-activated cell sorting of mouse peritoneal MØ/DC subsets

Subpopulations of peritoneal monocytic phagocytes were isolated from peritoneal lavages using a FACS Aria^{TM} III (BD Bioscience). Typically, cells from 10 C57BL/6 mice (6-7 week-old females), either naïve or 72 hours after SES challenge were pooled, centrifuged and resuspended in blocking buffer (without NaN_3) at a concentration of 10^7 cells/ml for 30 minutes on ice. After that, anti-mouse antibodies were added and incubated for 30 minutes on ice in the dark. The cells were washed twice with FACS wash buffer (without NaN_3) and resuspended in the same buffer at a concentration of 10^7 cells per ml for flow-sorting. The purified cells were collected and checked for the purity as previously described and immediately used in antigen processing and presentation assays (performed by Dr. Marcela Rosas, detailed in Appendix 2). Cytospin preparations were made, stained with Microscopy Hemacolour (Merck), visualized on a Leica DMLB microscope with DFC490 camera (Leica) and processed using QWin Software (Leica).

2.3 Statistical analysis

Statistical analyses were conducted using the GraphPad Prism. The statistical tests used are indicated as appropriate within the text. *P*-values are summarized as follows: *= $P \leq 0.05$, **= $P \leq 0.01$ and ***= $P \leq 0.001$. All analyses performed were two-tailed.

Chapter Three

Phenotypic and functional characterisation of peritoneal macrophages and dendritic cells in peritoneal dialysis patients

3.1 Introduction

The monocytic cell lineage (often called mononuclear phagocyte system) in lymphoid or non-lymphoid tissues comprises macrophages (MØs), dendritic cells (DCs) and other specialized cells, including microglia (brain), osteoclasts (bone), and Kupffer cells (liver) (Hume DA et al., 2002; Gordon and Taylor 2005). Recent progress in MØ/DC biology research has indicated that the heterogeneity of these cell phenotypes is related to different developmental origins, distinct differentiation pathway, and diverse compartmental status i.e., steady state or inflammation (Geissmann et al., 2010; Hashimoto et al., 2011; Satpathy et al., 2012; Merad et al., 2013). Also, studies on the phenotypic and functional attributes of different tissue MØ subsets *in vivo* have highlighted that distinct subset has specialised roles in tissue homeostasis and local innate or adaptive immunity (Villadango et al., 2007; Davies et al., 2013). In the context of peritoneal cavity, however, the immunobiology of human MØ/DCs remains poorly understood, which contrasts with the extensive knowledge derived from their murine counterparts. The requirement for invasive procedures to gain access to peritoneal cells for analysis has limited the biological investigation of human cells. Peritoneal dialysis (PD) as a renal replacement therapy for end-stage kidney failure patients provides a unique opportunity to study peritoneal cell biology in humans via an implanted PD catheter (Popovich et al., 1978; Maddox et al., 1984). In the field of PD research, studies in late 1970s/early 1980s began to examine the cellular composition of dialysis effluent fluids from non-infected PD patients, and revealed that the MØ is the predominant cell type within the PD fluids (Fakhri et al., 1978; Ganguly et al., 1980; Cichocki et al., 1983; Goldstein et al., 1984). Based on *ex vivo* and *in vitro* functional analysis, these studies suggested peritoneal MØs are the frontline player of host peritoneal defence system in PD patients (Verbrugh et al., 1983; Peterson et al., 1985; McGregor et al.,

1987; Lin et al., 1990). Recently, it has been suggested that peritoneal MØs from PD patients phenotypically and functionally resemble the *in vitro* polarised M-CSF–driven 'anti-inflammatory' MØ (Xu et al., 2007) or IL-4–driven alternatively activated MØ (Bellon et al., 2009). However, these findings are relatively simplistic and contrast with recent studies in mice that highlight MØ heterogeneity during inflammation (Davies et al., 2013). Furthermore, the information regarding DC in the human peritoneal cavity is even less owing to the paucity of specific markers permitting the unambiguous identification of this cell type (McCully et al., 2006). Overall, the lack of detailed phenotypic and functional characterisation of human peritoneal MØ/DC has limited the investigation of their specialised roles in the process of initiation/resolution of peritonitis, which would be fundamental with regards to understand how PD therapy modifies the cellular distribution/kinetics and local immunity in patients.

Hence, the specific aims of this chapter are:

1. To establish a novel flow-cytometric gating strategy to specifically identify distinct peritoneal monocytic subsets in PD patients.
2. To examine the expression of a broad range of surface receptors by distinct peritoneal monocytic subsets from PD patients under different clinical scenarios (i.e. new-starters, stable dialysis and during acute bacterial peritonitis).
3. To explore the relationship between blood monocyte subsets and peritoneal monocytic subsets through surface phenotype comparisons.
4. To investigate the specialised function of peritoneal MØ and DC, including:
    a) cytokine production after *ex vivo* microbial product stimulation.
    b) *ex vivo* phagocytic capacity and respiratory burst response.
    c) *in vitro* antigen processing and presentation.

3.2 Results

3.2.1 Flow-cytometric analysis of human peritoneal cells—basic principles

Cells within human peritoneal dialysate comprise mainly leukocytes, with a minority of non-leukocytes such as mesothelial cells. Following appropriate preparation of single cell suspensions and defined staining procedures (detailed in Materials and Methods), total peritoneal cells from PD effluents were run through a multi-colour flow cytometer. In order to accurately identify a target cell population and determine its specific receptor expression, three steps were employed during data analysis (Fig. 3.1). Firstly, the "singlet population" was gated in the density plot of Forward Scatter Linear (FS Lin) against Forward Scatter Area (FS Area). This "doublet discrimination" gating is to exclude aggregated cells and coincidental events, which could lead to false-positive antibody staining. Secondly, the cellular debris, typically located at the extreme left lower corner in the density plot of FS Area against Side Scatter Area (SS Area), was excluded. Thirdly, only "live cells", which were negative for Aqua Live/Dead stain (Life Technologies), were selectively gated to prevent from false-positive or false-negative staining on the dead cells. Altogether, these strategies would ensure the phenotypic characterisation of target cell populations entirely based on single and live cells. These principles applied to all analysed human samples within the whole study.

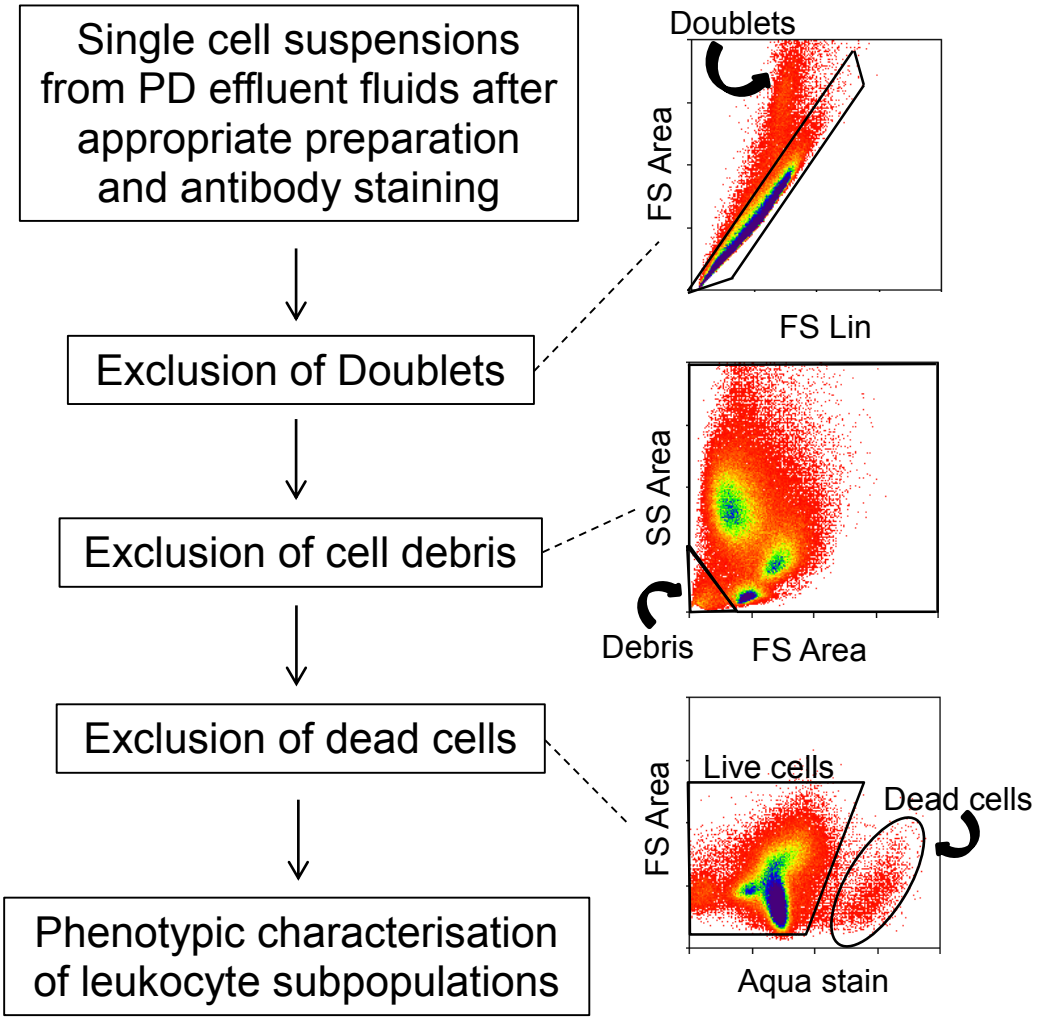

Figure 3.1 Flow-cytometric strategies to exclude doublets, cellular debris and dead cells during data analysis

After appropriate preparation of single cell suspensions and staining procedures, total peritoneal cells from PD effluent samples were examined by multi-colour flow cytometry. Representative density plots showed three-step flow-cytometric strategies including exclusion of doublets, cellular debris and dead cells, before going on phenotypic characterisation of leukocyte subpopulations. Data represent the analysis of peritoneal effluent cells from the first flush bag of a new-starter PD patient, and the same principles applied to all analysed human samples within the whole study.

3.2.2 Identification of peritoneal myeloid cells from PD effluent fluids based on CD116 (GM-CSF receptor alpha) expression

Peritoneal leukocytes from PD effluents comprise mainly neutrophils, eosinophils, macrophages and lymphocytes. Traditionally, the identification of leukocyte composition within PD effluent cells is based on the morphologic features of each cell type demonstrated by cytochemical staining methods (Cichocki et al., 1983). Recently, techniques have become available utilising a wide range of fluorochrome-conjugated antibodies to recognize specific surface antigens, with which the cells of interest within a mixed cell population can be clearly identified through flow-cytometric analysis (Autissier et al., 2010). In this study, I employed a novel gating strategy based on CD116 (GM-CSF receptor alpha) expression, a pan-myeloid lineage cell marker (Fig. 3.2), which has been used effectively in mice (Rosas et al., 2007). Together with HLA-DR (MHC class II molecule) and CD14 (a co-receptor for LPS), $CD116^+$ myeloid cells could be separated into two main subpopulations: mononuclear phagocytes ($HLA\text{-}DR^+CD14^{+/low/-}$) and granulocytes ($HLA\text{-}DR^-CD14^-$). Major granulocytic subsets, such as neutrophils and eosinophils, could be further identified by their unique expression of surface markers, $CD16^+/CD15^+/CD66b^+$ (Moulding et al., 1999; Schmidt et al., 2012) and $CD16^-/CCR3^+/Siglec\text{-}8^+$ (Höchstetter et al., 2000; Floyd et al., 2000), respectively. Additionally, eosinophils could be identified simply by their characteristic FS/SS profile (Davies et al., 2011) after pre-gating on $CD116^+HLA\text{-}DR^-CD14^-CD16^-$ cells. This flow-cytometric gating strategy provides a useful approach not only to identify and quantify major myeloid subsets, but also enables studies to include all the potential mononuclear phagocyte subsets in the human peritoneal cavity.

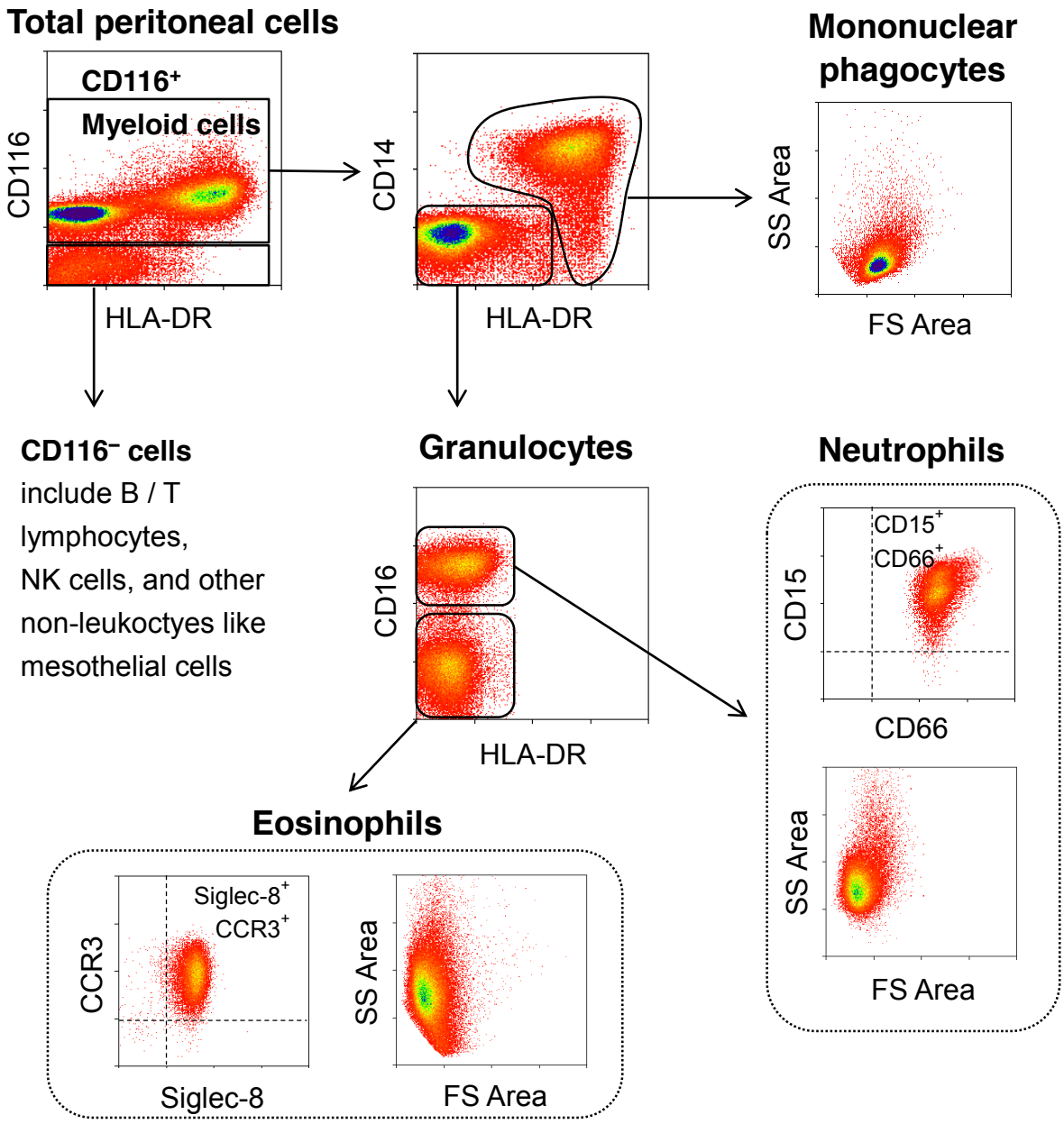

Figure 3.2 Flow-cytometric gating strategies to identify different peritoneal myeloid subsets from PD effluent fluids

Density plots show myeloid cells were pre-gated on $CD116^+$ populations after exclusion of doublets, cellular debris and dead cells. Within these cells, mononuclear phagocytes could be readily identified as $HLA\text{-}DR^+CD14^{+/low/-}$. Granulocytes were $HLA\text{-}DR^-CD14^-$. Other useful surface markers such as CD16, CD15, CD66(b), CCR3, siglec-8, are applied for confirmation of neutrophils ($CD16^+CD15^+CD66b^+$) and eosinophils ($CD16^-CCR3^+siglec\text{-}8^+$). Data represent the analysis of peritoneal effluent cells from the first flush bag of a new-starter PD patient.

3.2.3 Phenotypic identification of two major peritoneal mononuclear phagocyte subsets ($CD14^+CD1c^-$ and $CD14^{low/-}CD1c^+$) from PD effluent fluids

Heterogeneity of tissue mononuclear phagocytes has been widely studied in humans and in mice (Gordon and Taylor 2005; Satpathy et al., 2012; Davies et al., 2013). In the context of human peritoneal cavity, however, mononuclear phagocyte biology remains poorly described. Traditionally, CD14 is adopted as an identifying marker for peritoneal MØs (McCully et al., 2005; Xu et al., 2007). However, this is relatively simplistic as it has neglected the possibility of $CD14^{low/-}$ monocytic subsets, which have been found in peripheral bloods (Ziegler-Heitbrock et al., 1993; Geissmann et al., 2003) and other tissues such as liver (Liaskou et al., 2013), lung (Chana et al., 2013). On the other hand, the identity of peritoneal DCs in humans remains unclear due to lack of DC-specific markers and the highly overlapping marker expression on MØ and DC (McCully et al., 2006). So far, there is no validated flow-cytometric strategy to clearly identify peritoneal MØ/DC subsets in PD effluents. Here, the proposed flow-cytometric gating strategy as shown in Fig. 3.2, has first defined the $CD116^+HLA\text{-}DR^+CD14^{+/low/-}$ mononuclear phagocytes in the PD effluents. These monocytic cells are negative for the following lineage markers: CD3 (T lymphocyte), CD19 (B lymphocyte), CD15 (granulocyte) and CD56 (NK cell) (Fig. 3.3A). Within this population, two major subsets, $CD14^+$ cells and $CD14^{low/-}$ cells, could be readily subdivided (Fig. 3.3B). Interestingly, the majority of $CD14^{low/-}$ cells were $CD16^{low/-}CD206^{high/+}$, and $CD14^+$ cells were notably heterogeneous in the expression of CD16 and CD206. There were only subtle differences between these two cell types regarding the expression of myelomonocytic markers such as CD11b, CD11c, CD115 and CD116 (Fig. 3.3B).

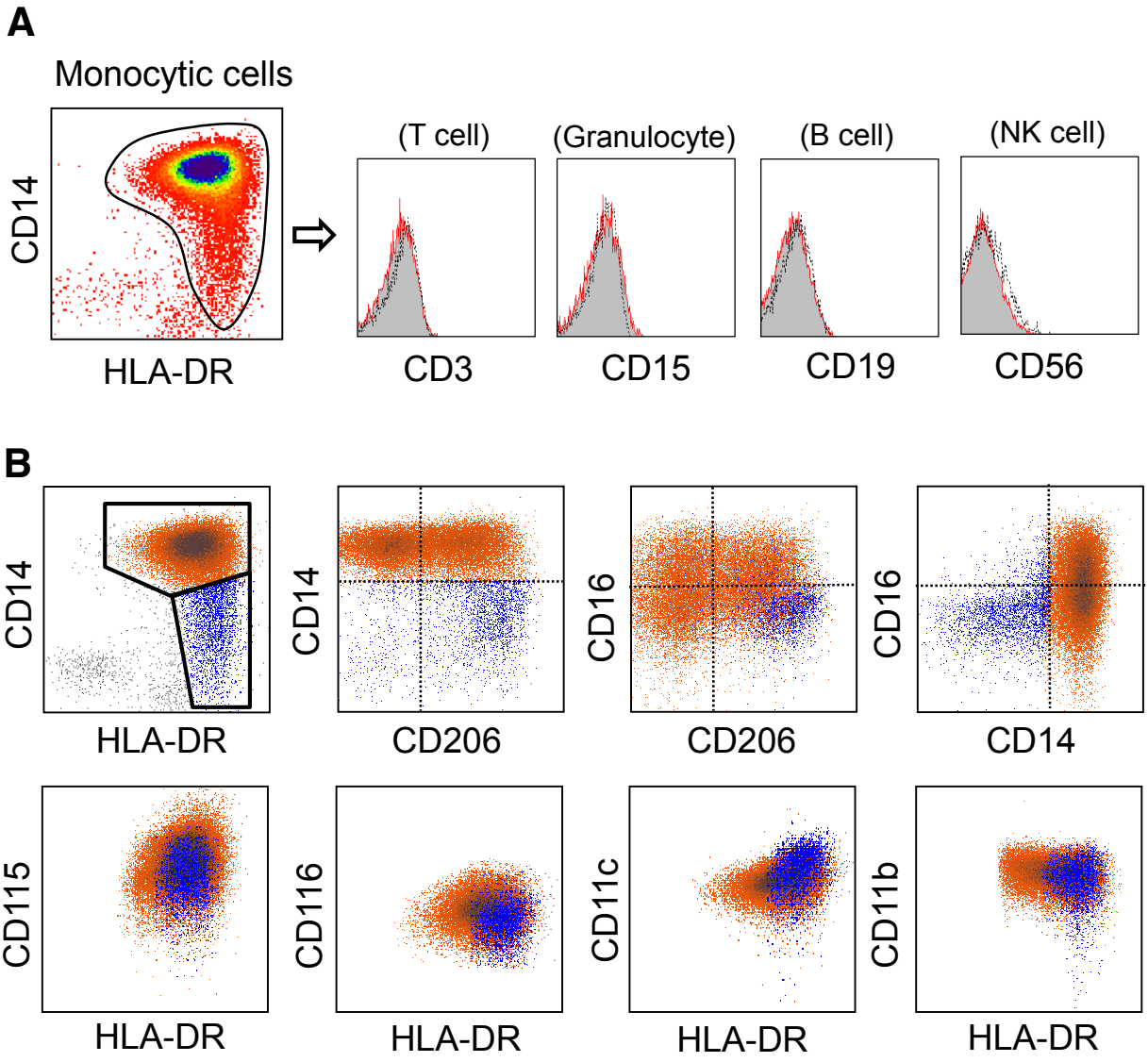

Figure 3.3 Phenotypic identification of two major mononuclear phagocyte subsets in the peritoneal effluent fluids from PD patients

(A) Flow-cytometric analysis of peritoneal effluent cells. Plots shown were pre-gated on $CD116^{+}HLA\text{-}DR^{+}CD14^{+/low/-}$ monocytic cells after exclusion of doublets, debris, dead cells and granulocytes. Histograms display CD3 (T cells), CD15 (granulocytes), CD19 (B cells) and CD56 (NK cells) lineage marker expression by the monocytic cells. Shaded histograms depict receptor specific staining and dotted lines denote isotype control staining. Data represent one of 5 stable PD patients. **(B)** Representative plots showing the separation of the two monocytic subsets, $CD14^{+}$ (orange) and $CD14^{low/-}$ (blue). $CD14^{low/-}$ cells are mainly $CD16^{low/-}CD206^{high}$, and $CD14^{+}$ cells were heterogeneous in the expression of CD16 and CD206 (upper panel). The expression of CD115, CD116, CD11c and CD11b is similar across both subsets (lower panel). Data are derived from one stable PD patient (representative of 37 in total).

Next, to determine whether these two discrete subsets could possibly represent the existence of MØ and DC within the dialysate, additional DC-associated markers, such as CD1c (BDCA-1, myeloid DC marker), CD141 (BDCA-3, myeloid DC marker), CD303 (BDCA-2, plasmacytoid DC marker), CD1a, CD83 and CD209 (DC-SIGN), were examined thoroughly. Interestingly, $CD14^{low/-}$ cells rather than $CD14^{+}$ cells were distinctively found to be $CD1c^{+}$ cells. Hence, phenotypically, $CD14^{+}CD1c^{-}$ cells were suggested to be the contemporary "peritoneal MØs", and $CD14^{low/-}CD1c^{+}$ cells could potentially be "peritoneal DCs".

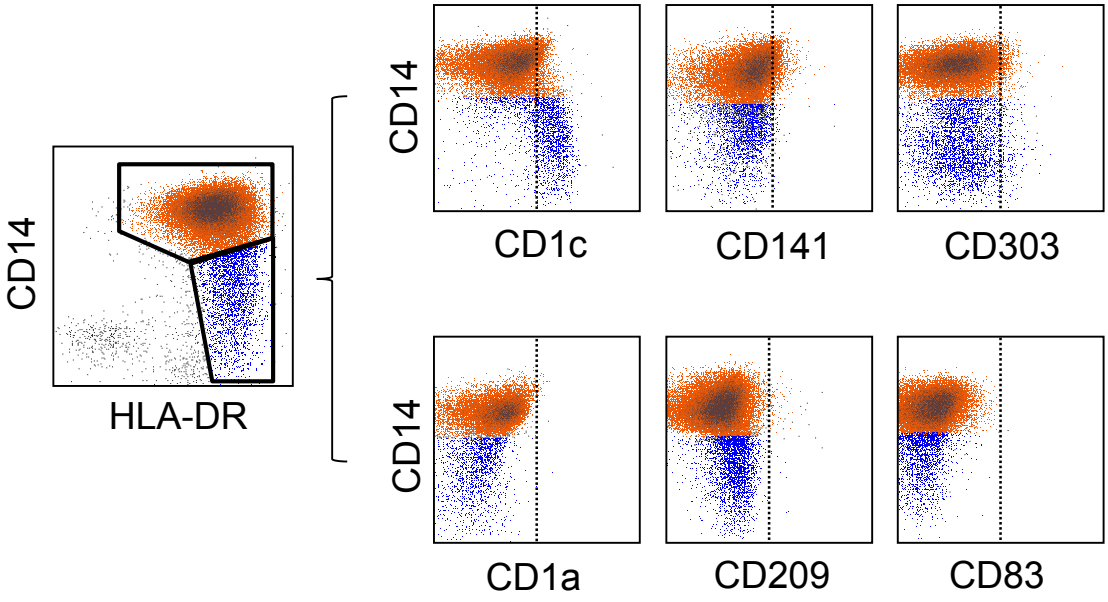

Figure 3.4 $HLA\text{-}DR^{+}CD14^{low/-}$ cells are potentially peritoneal dendritic cells

Flow-cytometric plots showing positive $CD1c^{+}$ expressions on $CD14^{low/-}$ cells (blue), but not on $CD14^{+}$ cells (brown). All other relevant "DC-associated" markers were >98% negative across both cell types. The dotted lines denote the maximal level of the isotype control staining. Data are derived from one stable PD patient (representative of 5 patients in total).

3.2.4 Phenotypic comparisons between peritoneal CD14$^+$ MØ and CD1c$^+$ DC from PD patients

Following identification of CD14$^+$ MØ and CD1c$^+$ DC, a detailed phenotyping on these two monocytic subsets was performed, examining a wide range of surface markers, including receptors involving monocyte transmigration as well as MØ/DC activation/maturation (CD11b, CD11c, CD16, CD36, CD64, CD163, CD206, CD226, FcεR1α), antigen presentation (CD40, CD80, CD86), pathogen recognition (CD301, Dectin-1, Dectin-2), apoptotic cell clearance (MerTK) and chemokine receptors involving MØ/DC recruitment and migration (CCR2, CCR7). In addition, Tim-4 (T cell immunoglobulin and mucin domain-containing protein 4) and CD73 (5'-nucleotidase) were evaluated, as both were found to be highly expressed on murine peritoneal resident MØs (Davies et al., 2011; Rosas et al., 2014). As shown in Fig. 3.5, these surface markers were differentially expressed on peritoneal CD14$^+$ MØs and CD1c$^+$ DCs. Select receptor expressions were quantitatively compared between these two subsets in PD patients under either uninfected status ("clear fluids") or acute bacterial peritonitis ("cloudy fluids") (Fig. 3.6). Notably, CD1c$^+$ DCs were characterized by lower CD11b, CD16, CD36, CD64, CD163, MerTK, CCR2 expression, and higher CD11c, CD206, CD226, FcεR1α, CD301 expression, compared to CD14$^+$ MØs, under either uninfected stable conditions or during acute bacterial peritonitis (Fig. 3.6). In addition, very low expression of CD62L, CD80 and CCR7 were uniformly noted across two subsets in both circumstances. Other surface molecules such as Dectin-1, Dectin-2, Tim-4, and CD73 were similarly expressed by these cells.

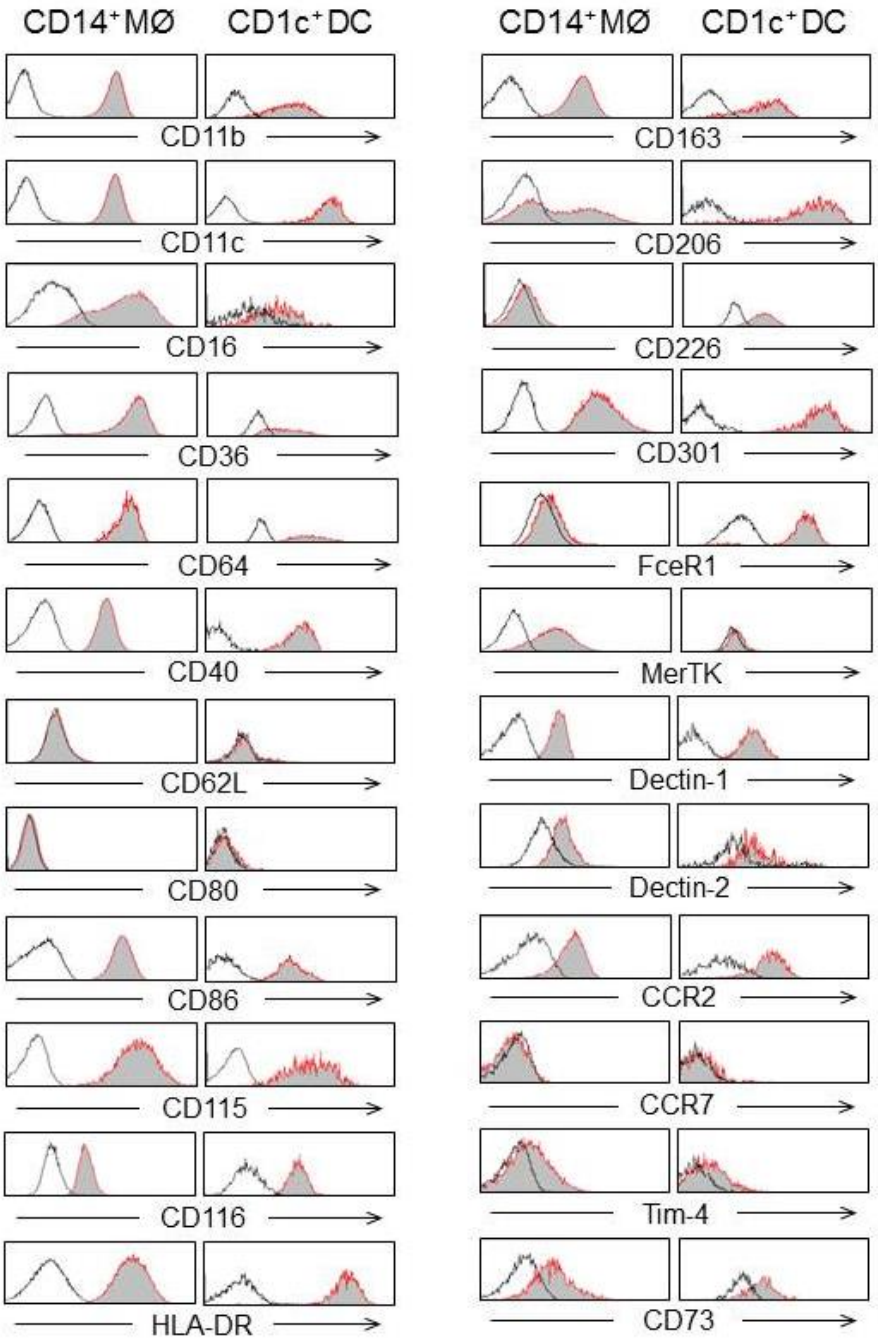

Figure 3.5 Phenotypic comparisons between human peritoneal CD14⁺ MØ and CD1c⁺ DC

Flow-cytometric analysis of select marker expression by peritoneal $CD14^+$ MØ and $CD1c^+$ DC. Representative histogram plots were pre-gated on $CD116^+HLA\text{-}DR^+$ cells after exclusion of doublets, debris, dead cells and granulocytes, then gated on the respective $CD14^+$ MØ and $CD1c^+$ DC subset. Shaded histograms depict receptor specific staining and bold lines denote isotype control staining. Data are representative of 4 stable PD patients.

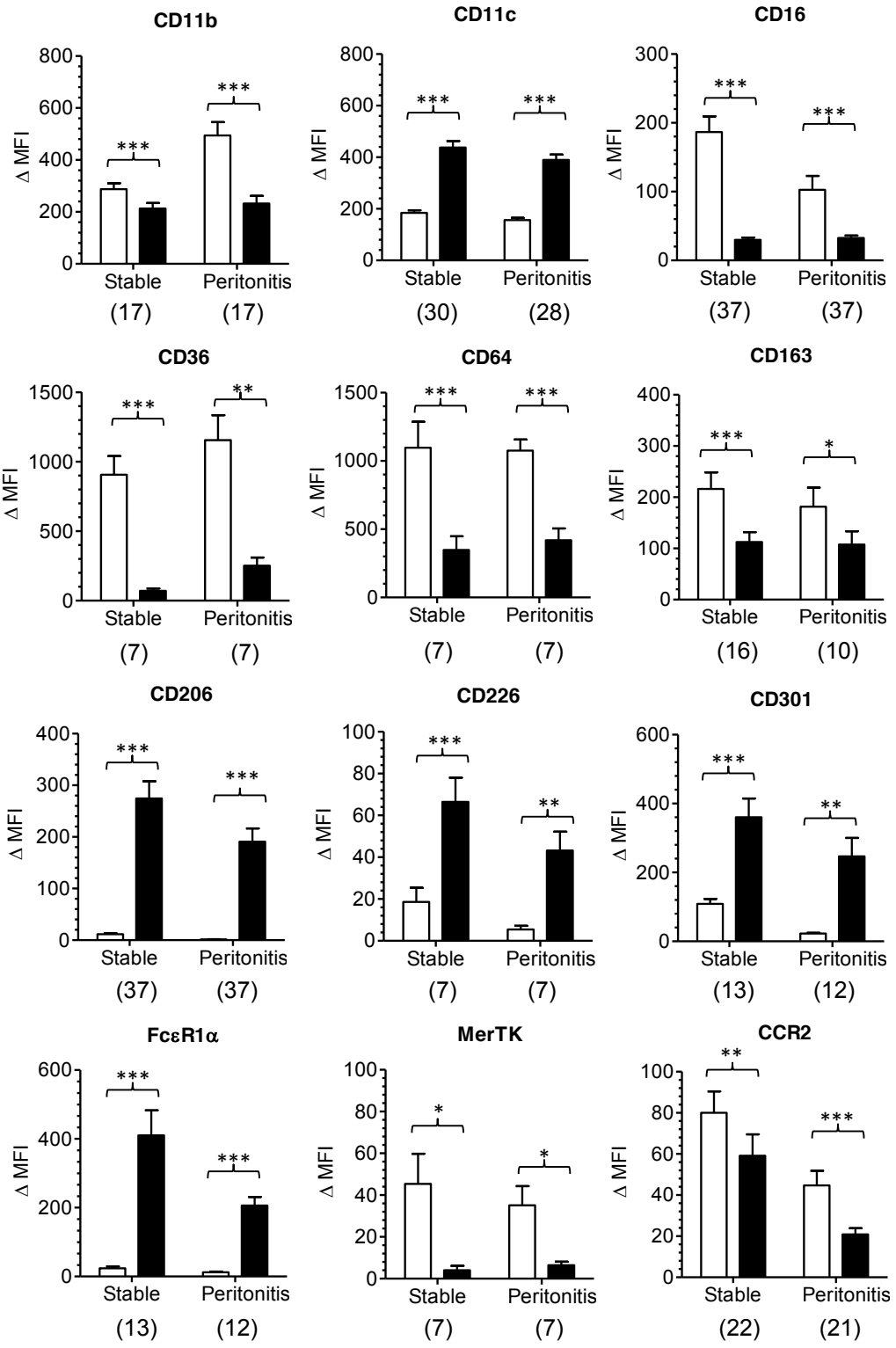

(Figure legend in the next page)

Figure 3.6 Quantitative comparisons of receptor expression between human peritoneal $CD14^+$ MØ and $CD1c^+$ DC under stable status and during acute bacterial peritonitis

Bar graphs shown were quantification of select receptor expression, measured as difference in medium fluorescence intensity (MFI) between receptor specific and isotype control staining. White bars denote $CD14^+$ MØ and black bars are $CD1c^+$ DC. Data are shown as mean ± SEM of the indicated number of patients (n) and was analysed using paired *t*-test. *P*-values are summarized as follows: *= $P \leq 0.05$, **= $P \leq 0.01$ and ***= $P \leq 0.001$.

3.2.5 Heterogeneous activation and maturation of peritoneal MØ and DC

Previous study has noticed that peritoneal MØs from infected or uninfected PD effluents express variable levels of CD16 (FcγRIIIa/IIIb) and CD206 (macrophage mannose receptor) (Bellon et al., 2009). Our data, consistent with these observations, also demonstrated heterogeneous expression levels of CD16 and CD206 on peritoneal mononuclear phagocytes (Fig. 3.3B). Both CD16 and CD206 have been adopted as markers indicative of monocyte-to-macrophage activation or maturation (Mokoena et al., 1985; Andreesen et al., 1990; Noorman et al, 1997). Notably, based on the expression levels (high/+ *versus* low/–) of CD16 and CD206, peritoneal MØ/DC could be sub-categorized into six cell subtypes (Fig. 3.7). Specifically, $CD14^+$ MØs could be separated into $CD16^{high/+}$ and $CD16^{low/-}$ cells, each with $CD206^+$ and $CD206^-$. $CD1c^+$ DCs were basically $CD16^{low/-}$, which consist of $CD206^+$ (majority) and $CD206^-$ (rare). Interestingly, individual subtype displayed differential expression of HLA-DR, CD86 and CD163 from PD patients under stable conditions (Fig. 3.8A) or during acute bacterial peritonitis (Fig. 3.8B). These differential expression profiles most likely reflect different stages of MØ/DC activation or maturation within the peritoneal cavity. Of note, peritoneal MØ with $CD16^+CD206^+$ ('double positive') subtype expresses the highest levels of HLA-DR, CD86 and CD163, among $CD14^+$ MØs, whereas $CD16^-$ $CD206^-$ ('double negative') subtype expresses the lowest levels of these surface antigens.

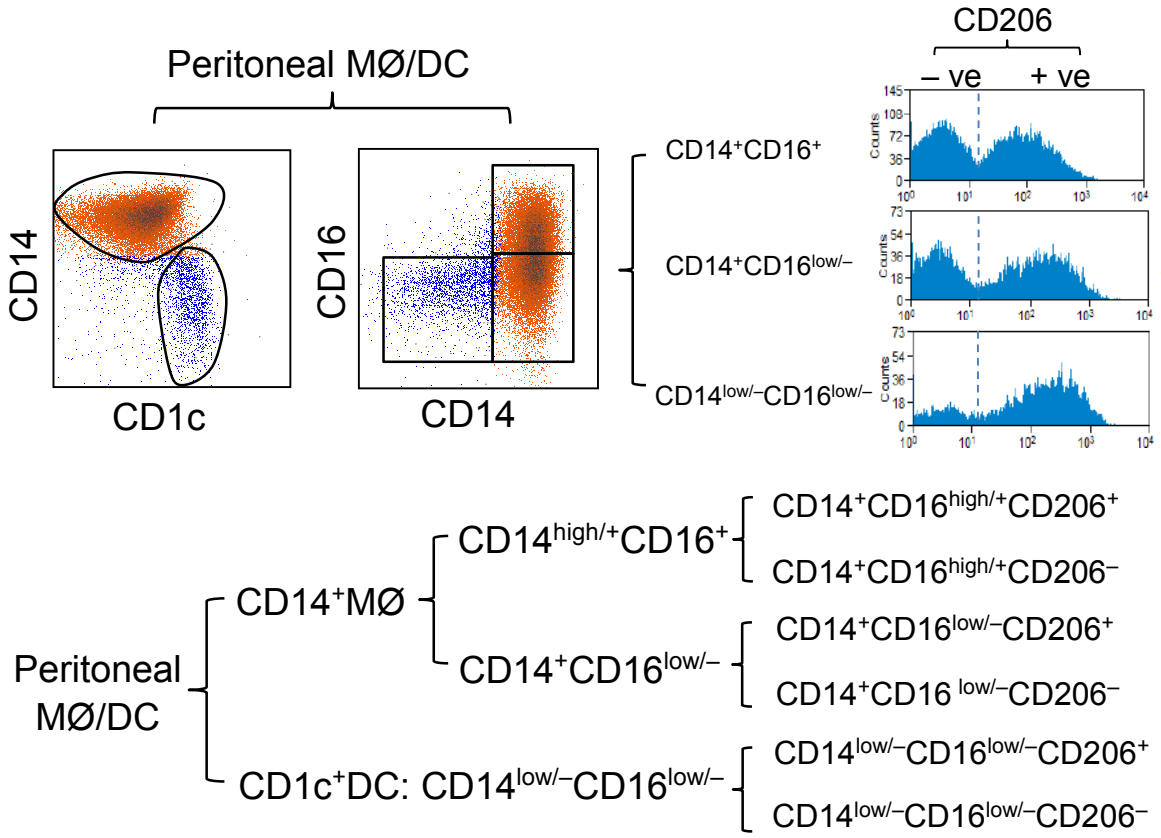

Figure 3.7 Human peritoneal MØ/DC could be subdivided into six cell subtypes based on the differential expression of CD16 and CD206

Flow-density plots (upper left) and histogram plots (upper right) showing $CD14^+$ MØs (orange) and $CD1c^+$ DCs (blue) could be subdivided into six subtypes according to their differential CD16 and CD206 expression. Data represent one stable PD patient. The expression of these two markers have been studied in all patients' effluent samples. Variations in the distribution of each subtype in the individual samples are analysed and discussed in Chapter 4.

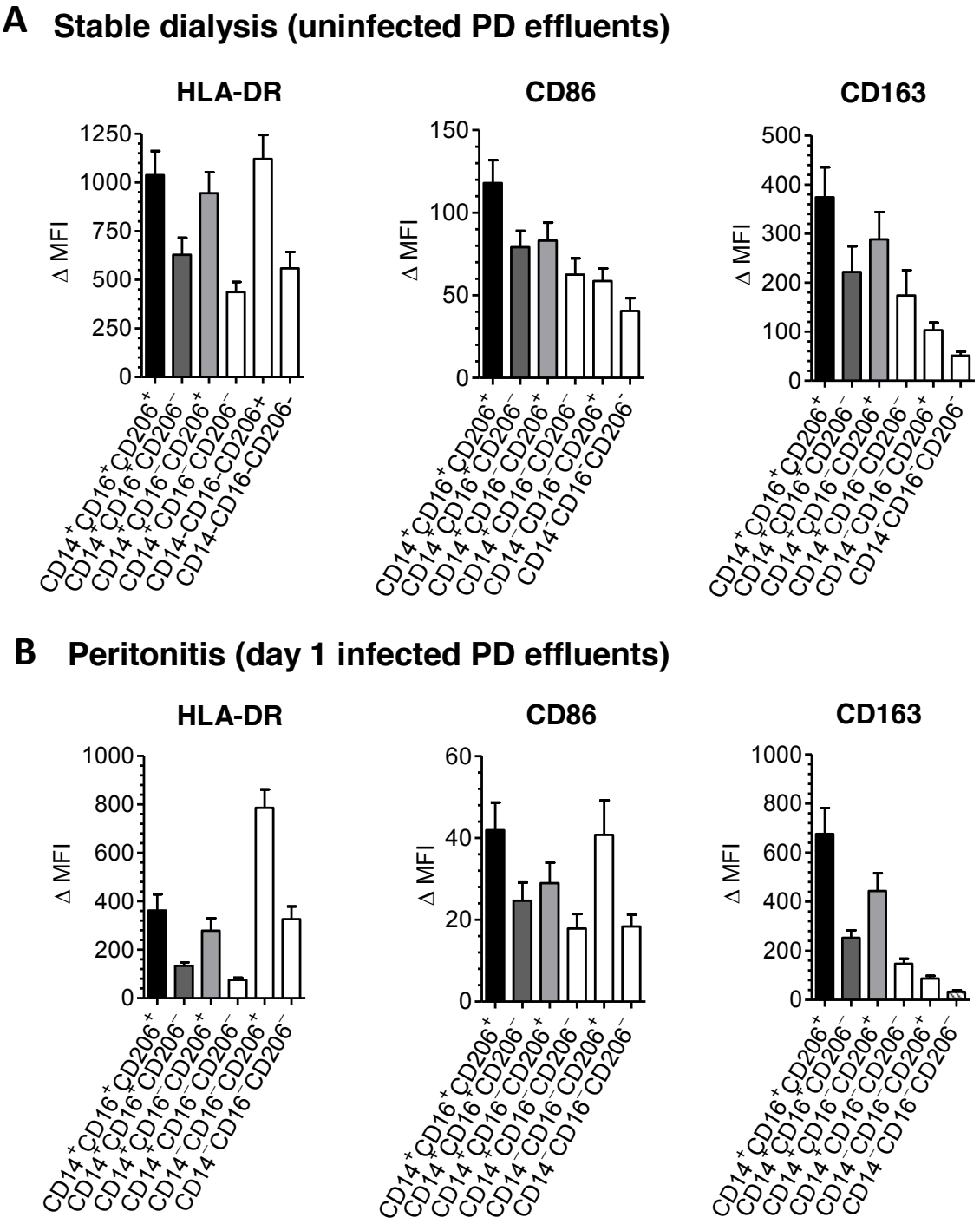

Figure 3.8 Differential marker expression on six distinct peritoneal monocytic subsets under stable status or during acute bacterial peritonitis

Bar graphs comparing select receptor expression (HLA-DR, CD86, CD163), measured as difference in medium fluorescence intensity (MFI) between receptor specific and isotype control staining, among individual six subsets from PD patients under stable status (n = 10, upper panel **A**) and during acute bacterial peritonitis (n = 10, lower panel **B**). Data is shown as mean ± SEM.

3.2.6 Phenotypic comparisons between human blood monocytic subsets and peritoneal monocytic subsets from PD patients

To understand the potential lineage relationship between blood monocytic subsets and peritoneal mononuclear phagocyte subsets, it would be of interest to phenotypically compare the monocytic cells of two compartments. For this purpose, a similar flow-cytometric gating approach was applied to peripheral blood mononuclear cells (PBMC) to identify $CD116^{+}HLA\text{-}DR^{+}$ cells and perform a detailed immunophenotyping of blood monocytic subsets in new-starter PD patients (Fig. 3.9). The results were in agreement with previous reports displaying three major cell types (stratified by CD14 vs. CD16 expression) and their differential receptor expressions. By concomitantly analysing peritoneal mononuclear phagocytes from the same patients at the same time point (1st peritoneal flush), monocytic cells of different origins could be phenotypically compared. The most notable finding was minimal $CD14^{low/-}CD16^{+}$ cells in the peritoneal cavity, while the proportion of $CD14^{low/-}CD16^{low/-}$ cells ($CD1c^{+}$ DC) was much increased, compared to peripheral bloods (Fig. 3.10). Of note, $CD14^{low/-}$ $CD16^{low/-}$ cells in blood comprise rare $CD1c^{+}$ myeloid DC precursors (Fig. 3.11 and Cros J et al, 2010).

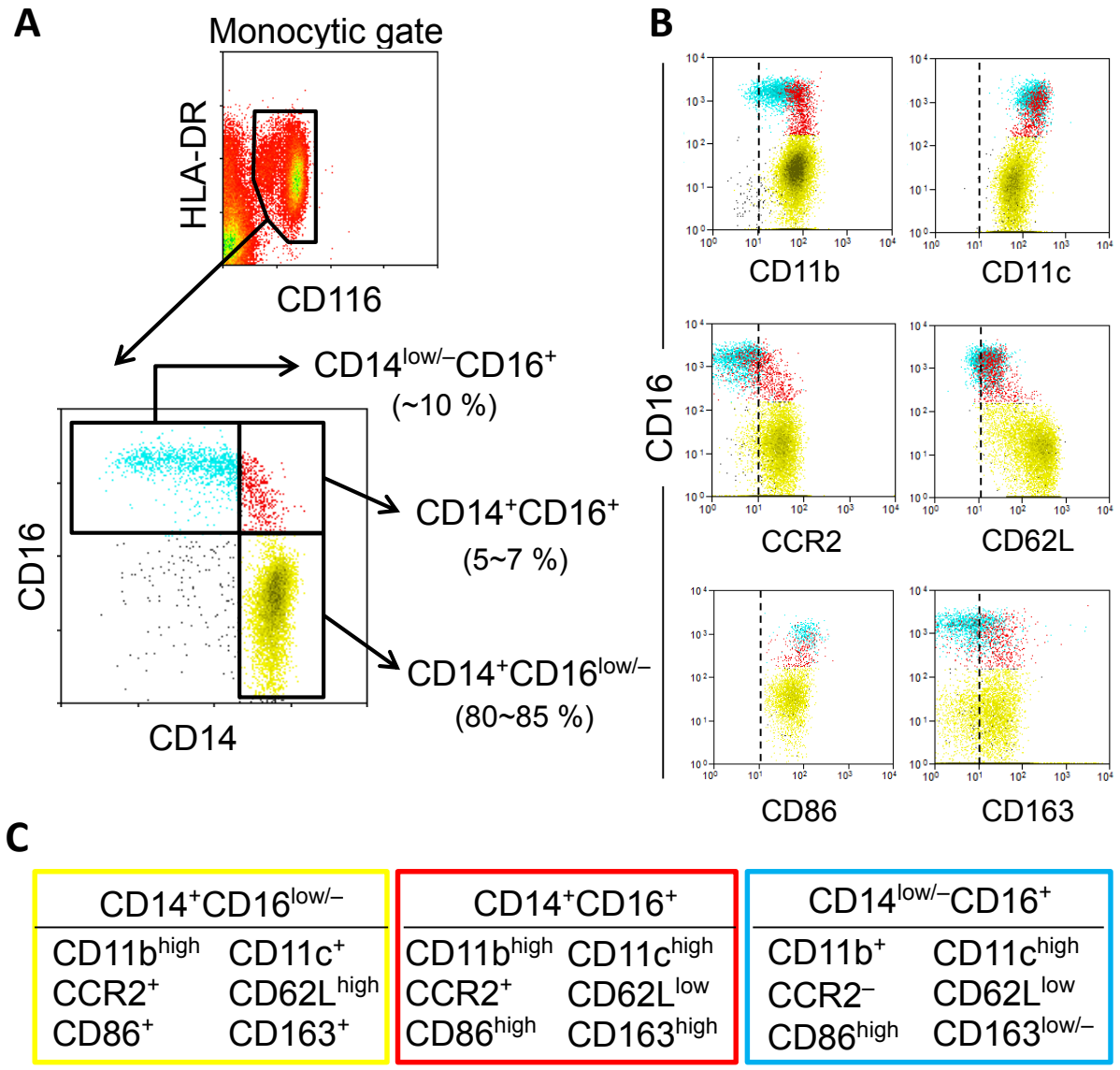

C

$CD14^+CD16^{low/-}$	
$CD11b^{high}$	$CD11c^+$
$CCR2^+$	$CD62L^{high}$
$CD86^+$	$CD163^+$

$CD14^+CD16^+$	
$CD11b^{high}$	$CD11c^{high}$
$CCR2^+$	$CD62L^{low}$
$CD86^{high}$	$CD163^{high}$

$CD14^{low/-}CD16^+$	
$CD11b^+$	$CD11c^{high}$
$CCR2^-$	$CD62L^{low}$
$CD86^{high}$	$CD163^{low/-}$

Figure 3.9 Phenotypic characterisation of three major monocytic subsets in peripheral bloods from PD patients

(A) Representative density plots show blood monocytic cells. Cells were pre-gated on $CD116^+HLA\text{-}DR^+$ populations after exclusion of doublets, cellular debris and dead cells. These cells are readily subdivided into three major subsets ($CD14^+CD16^{low/-}$, $CD14^+CD16^+$, $CD14^{low/-}CD16^+$). $CD14^{low/-}CD16^{low/-}$ cells comprise rare myeloid DC precursors (Cros J et al, 2010). **(B)** Plots depict differential receptor expressions by distinct monocytic subsets. Dashed lines denote the maximal level of isotype control staining. **(C)** Summary of the phenotypic comparison among three subsets. Data are derived from the analysis of PBMC from one new-starter PD patient (representative of 10 patients in total).

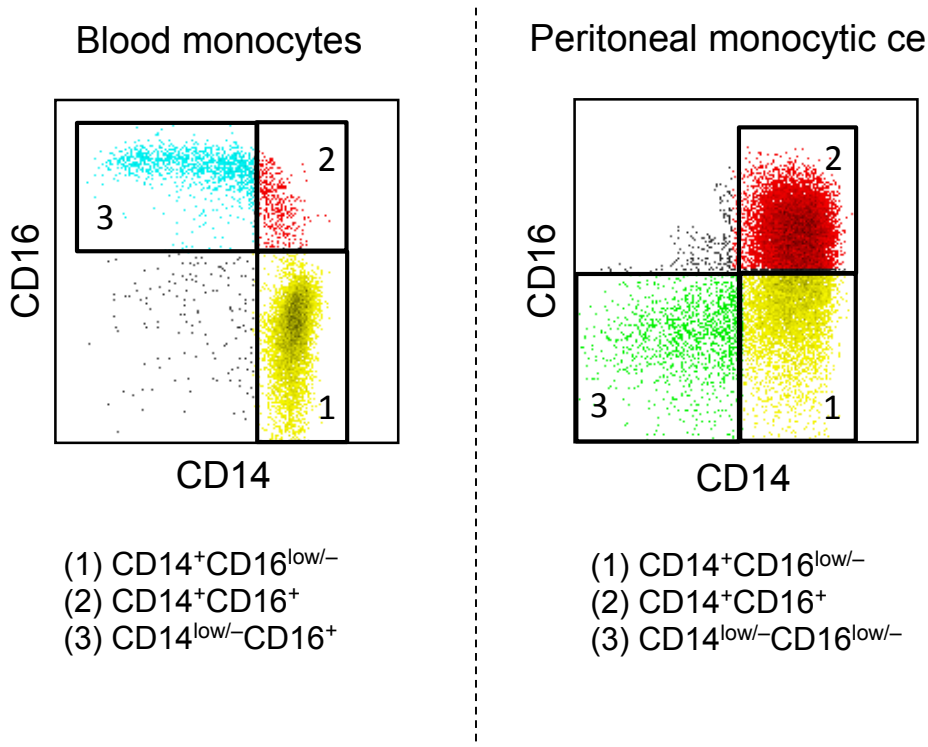

Figure 3.10 Major monocytic subsets (based on CD14 *versus* CD16 expression) in peripheral bloods and in the peritoneal cavity from PD patients

Representative density plots showing three major blood monocyte subsets (left) and peritoneal monocytic cells (right) according to the differential CD14/CD16 expression. Plots shown were pre-gated on $CD116^{+}HLA\text{-}DR^{+}$ cells after exclusion of doublets, debris, dead cells and granulocytes in both circumstances. Data are derived from the flow-cytometric analysis of PBMC and peritoneal cells from one PD patient at the time of 1st peritoneal flush (representative of 10 new-starter patients in total).

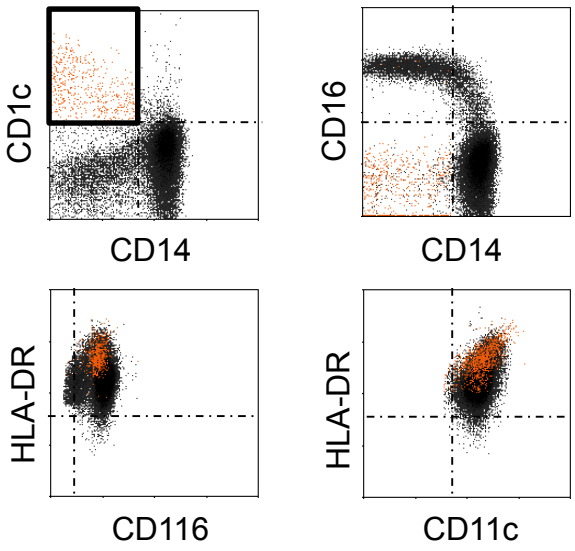

Figure 3.11
Phenotypic identification of blood $CD1c^{+}$ DC precursors

Flow-cytometric density plots showing $CD1c^{+}$ DC precursors (orange) in peripheral bloods are $CD116^{+}HLA\text{-}DR^{high}CD11c^{+}$ and $CD14^{low/-}CD16^{low/-}$. Data are derived from one healthy individual (representative of 4 in total).

Table 3.1 summarises the quantification of receptor expressions in blood and peritoneal monocytic subsets (stratified by CD14 vs CD16 expression). Remarkably, all subsets of blood monocytes have very low expression of CD206, a marker mainly expressed on mature MØs and DCs (Noorman et al., 1997). Within peritoneal monocytic cells, $CD14^{+}CD16^{-}$ cells are phenotypically similar with their counterparts in peripheral blood ($CD206^{low/-}CCR2^{+}CD86^{+}CD163^{low}$) except for a very low CD62L expression, which might be due to shedding of CD62L when blood monocytes migrate into the peritoneal cavity (Smalley 2005). Peritoneal $CD14^{+}CD16^{+}$ subsets have broadly higher expression of CD11b, CD86 and CD163, while $CD14^{low/-}CD16^{-}$cells (basically CD1c+ DCs) have higher expression of CD11c, HLA-DR and CD206.

Table 3.1 Phenotypic comparisons of select receptor expressions between major monocytic subset in peripheral blood and in the peritoneal cavity

	Blood monocytes			Peritoneal monocytic cells		
	$CD14^{+}CD16^{-}$	$CD14^{+}CD16^{+}$	$CD14^{low/-}CD16^{+}$	$CD14^{+}CD16^{-}$	$CD14^{+}CD16^{+}$	$CD14^{low/-}CD16^{-}$
CD11b	269.4 ± 46.28	265.2 ± 34.31	88.62 ± 10.62	307.8 ± 42.36	401.6 ± 53.79	195.9 ± 38.42
CD11c	83.53 ± 6.579	161.2 ± 10.94	198.2 ± 13.81	178.2 ± 21.10	219.4 ± 27.44	401.3 ± 39.90
CD62L	127.7 ± 29.56	20.13 ± 3.351	11.36 ± 2.066	4.742 ± 0.548	7.665 ± 1.669	4.994 ± 0.732
CD86	38.34 ± 3.282	80.48 ± 6.400	94.08 ± 9.342	42.81 ± 4.399	103.0 ± 10.91	40.85 ± 4.389
CD163	25.18 ± 3.148	36.38 ± 7.587	3.511 ± 1.140	33.51 ± 5.117	172.3 ± 31.22	16.35 ± 2.645
CCR2	37.56 ± 4.941	26.31 ± 3.438	4.628 ± 0.416	36.39 ± 5.972	19.83 ± 2.398	17.65 ± 2.249
HLA-DR	51.99 ± 11.92	299.0 ± 35.93	192.7 ± 25.32	197.2 ± 35.50	338.5 ± 45.30	461.8 ± 33.21
CD206	0.683 ± 0.195	2.051 ± 0.275	1.568 ± 0.192	13.38 ± 2.751	63.91 ± 20.39	199.2 ± 24.69

Data represent mean ± SEM of median fluorescence intensity (MFI), measured as difference between receptor specific and isotype control staining, and are derived from the analysis of PMBC and peritoneal effluent cells from 10 new-starter PD patients (at the time of 1st peritoneal flush). The monocytic cell type with the highest receptor expression in each compartment is denoted in red colour.

3.2.7 Cytokine response to *ex vivo* stimulation with microbial products

To understand functional profiles of human peritoneal $CD14^+$ MØ and $CD1c^+$ DC in the dialysis effluents from PD patients, several assays were conducted. Firstly, to test the cellular responses to microbial stimuli, the production of the pro-inflammatory cytokines (TNF-α, IL-1β, IL-6, IL-12p40/p70) and anti-inflammatory cytokine (IL-10) were measured by intracellular flow cytometry after *ex vivo* stimulation with LPS or SES (See the details in section 2.1.8). Both $CD14^+$ MØ and $CD1c^+$ DC could generate significant amounts of TNF-α, IL-1β, IL-6, as well as small amounts of IL-10 and IL-12p40/p70 after stimulation (Fig. 3.12).

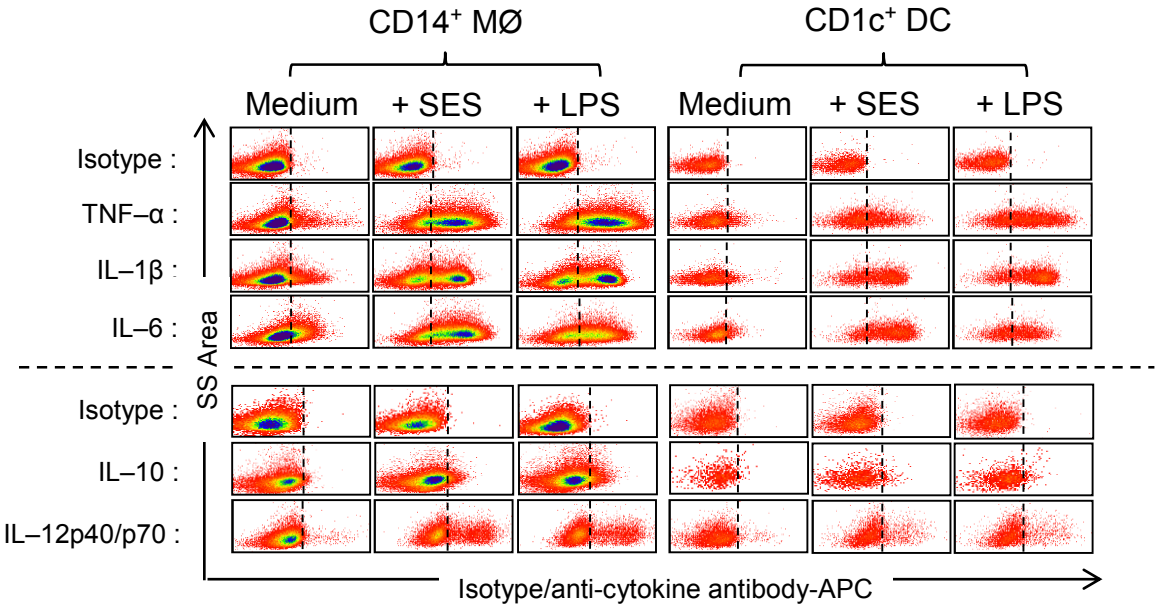

Figure 3.12 Cytokine production by peritoneal MØ and DC after *ex vivo* stimulation with SES or LPS

Representative density plots illustrating the flow-cytometric determination of intracellular cytokine production by peritoneal MØ/DC from stable PD patients, after *ex vivo* stimulation with SES (1:10 dilution) or LPS for 4 hours (TNF-α, IL-1β, IL-6), 24 hours (IL-10), or 22 hours (IL-12p40/p70, in addition to 2 hours IFN-γ priming), in parallel with medium only as unstimulated control. Data from one patient representative of 7 stable PD patients giving similar results.

There was no significant difference between $CD14^+$ MØ and $CD1c^+$ DC regarding the pro-inflammatory/anti-inflammatory cytokine productions at basal condition (medium only) (Fig. 3.13). Notably, upon either *ex vivo* SES or LPS stimulation, $CD14^+$ MØs could generate higher TNF-α and IL-6 than $CD1c^+$ DC. With regards to IL-1β, IL-10 and IL-12p40/p70, no difference after stimulation between MØs and DCs was found.

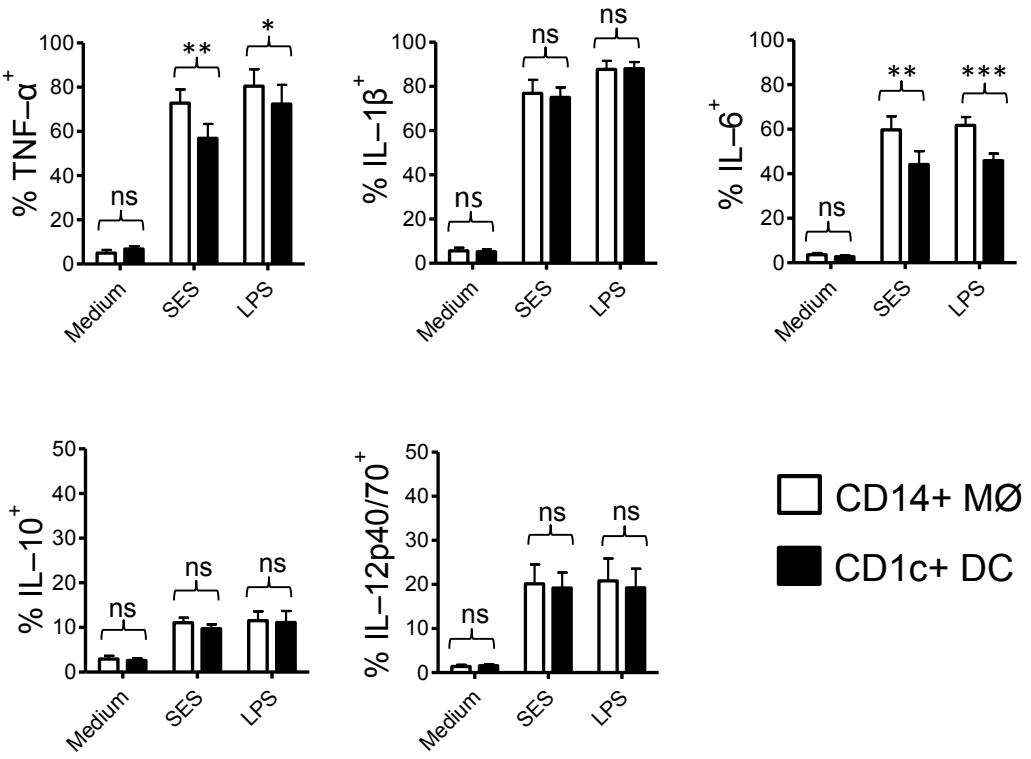

Figure 3.13 Quantification of intracellular cytokine production by peritoneal MØ/DC after *ex vivo* stimulation with SES or LPS

Bar graphs comparing the intracellular cytokine production between peritoneal $CD14^+$ MØ (white bars) and $CD1c^+$ DC (black bars). Cells were cultured in medium alone or stimulated *ex vivo* with SES or LPS for 4 hours (TNF-α, IL-1β, IL-6), 24 hours (IL-10), or 22 hours (IL-12p40/p70, in addition to 2 hours IFN-γ priming), . Positive intracellular cytokine production was determined by comparison with isotype controls (see Fig. 3.12). Data represent mean ± SEM and are derived from 7 stable PD patients. Statistical analysis was performed by paired *t*-tests. (*= $P \leq 0.05$, **= $P \leq 0.01$, ***= $P \leq 0.001$, and ns= non-significant).

3.2.8 Phagocytosis and respiratory burst response after *ex vivo* challenges with fluorescence-conjugated zymosan particles or bacteria

Phagocytosis of pathogens or microbial products is a major host defence function of peritoneal mononuclear phagocytes, a process leading to generation of various reactive oxygen species (ROS) for use in oxygen-dependent killing of microbes (Underhill and Ozinsky 2002). To examine their phagocytic capacity and their potential for generation of ROS, peritoneal cells were incubated with 3'-(p-aminophenyl) fluorescein (APF), a fluorescent probe designed for the detection of free radicals such as hydroxyl radical (HO•), hypochlorite anion ($^{-}$OCl), then challenged with Alexa Fluor 405–conjugated zymosan particles or DDAO–conjugated *Staphylococcus epidermidis* (detailed in Materials and Methods). Zymosan is a cell wall extract from *Saccharomyces cerevisiae* (DiCarlo and Fiore 1958). It has been shown that it has ligands bind to TLR2/6 (Underhill 2003) and C-type lectin receptors such as Dectin-1 (Brown et al., 2001 & 2002) on monocytic cells. This assay was analysed by flow cytometry.

As shown in Fig. 3.14, without zymosan particle loading (no phagocytosis), both $CD14^{+}$ MØ and $CD1c^{+}$ DC generated minimal ROS as low spontaneous activation (Fig. 3.14A, upper second panel). Through the process of zymosan particle uptake, these monocytic cells produced significant amounts of ROS, detected by APF (Fig. 3.14A, lowest panel). The preliminary results revealed $CD14^{+}$ MØ had a better phagocytic capacity for zymosan particles and that they generated a significantly higher respiratory burst response than $CD1c^{+}$ DC (Fig. 3.14B).

Similar results were observed when the same assay using DDAO–conjugated *Staphylococcus epidermidis* (DDAO-S.E) as inciting agents instead (Fig. 3.15).

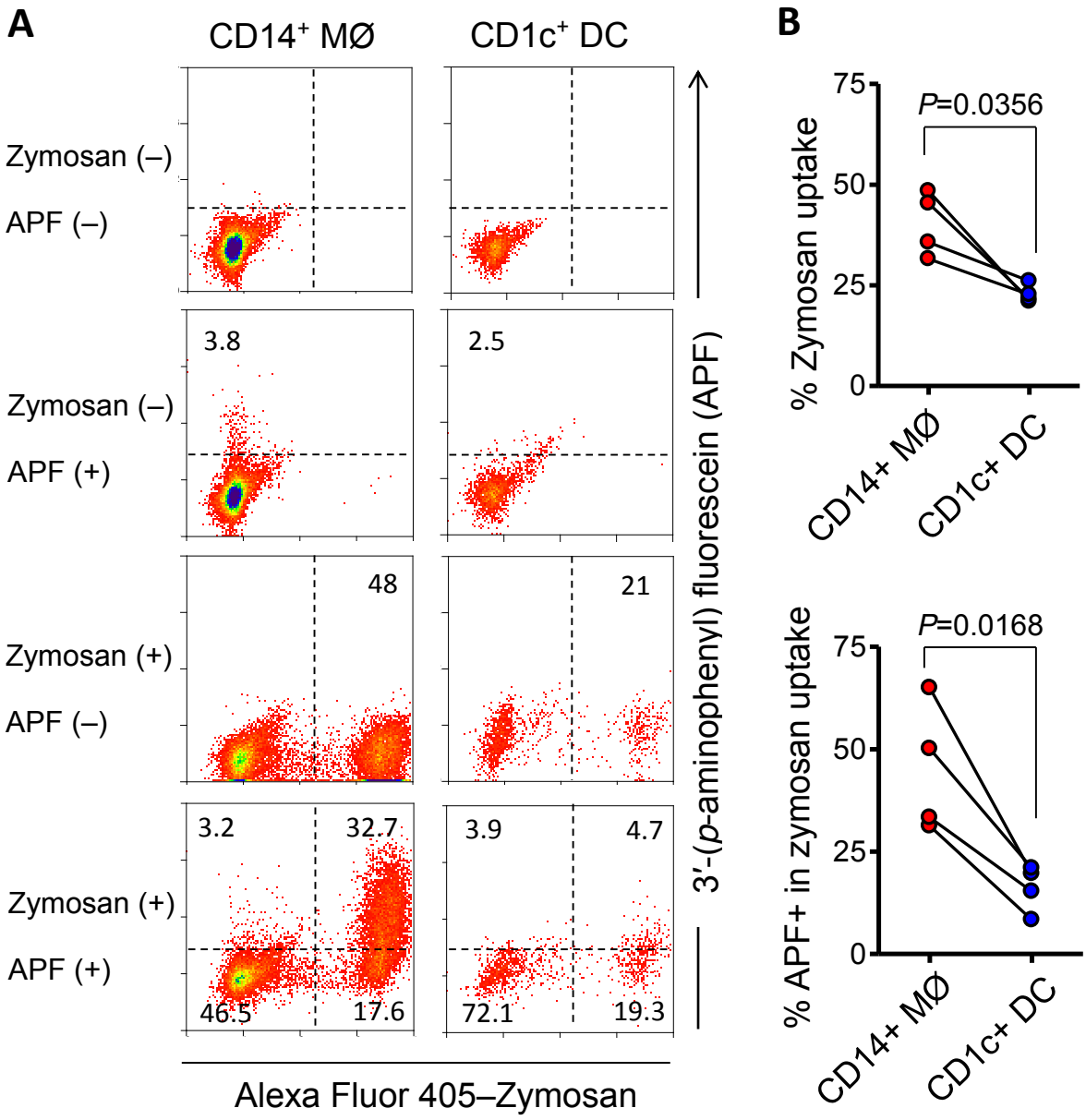

Figure 3.14 Phagocytosis and respiratory burst responses following *ex vivo* challenges with zymosan particles

(A) Representative flow-cytometric density plots showing the generation of reactive oxygen radicals from peritoneal MØ/DC, detected by 3'-(p-aminophenyl) fluorescein (APF), following challenges with Alexa Fluor 405-conjugated zymosan particles *ex vivo* or cultured in medium only. The percentages of cells found in each of specified gate are indicated. **(B)** Quantification of zymosan particles uptake by respective monocytic cells (upper graph) and positive APF staining (%) within the cells phagocytosing zymosan particles (lower graph). Data are representative of 4 new-starter PD patients and were analysed by paired *t*-test.

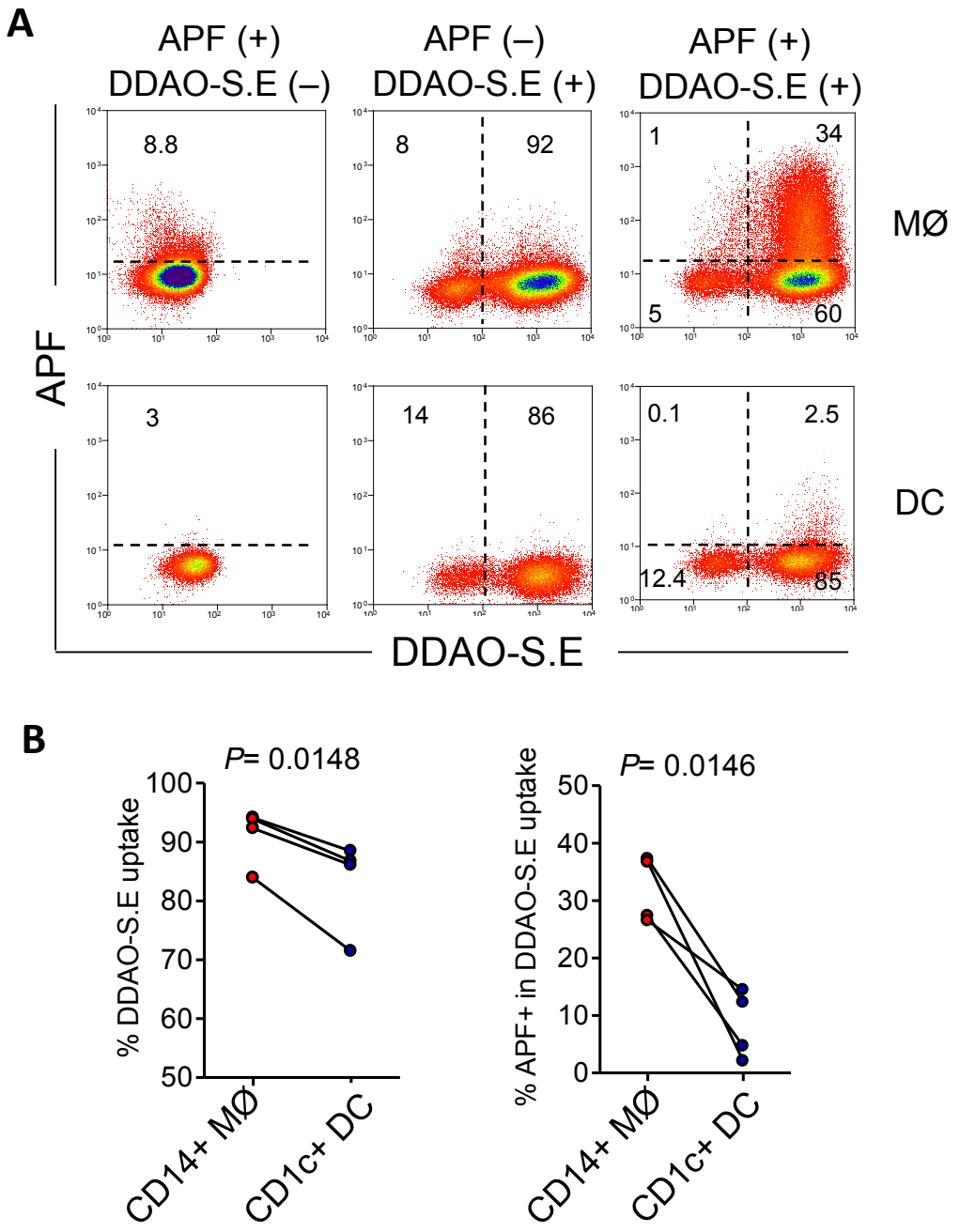

Figure 3.15 Phagocytosis and respiratory burst responses following *ex vivo* challenges with *Staphylococcus epidermidis* (S.E)

(A) Representative flow-cytometric density plots showing the generation of reactive oxygen species from peritoneal MØ/DC, detected by 3'-(p-aminophenyl) fluorescein (APF), following challenges with DDAO-conjugated S.E *ex vivo* or cultured in medium only. The percentages of cells found in each of specified gate are indicated. **(B)** Quantification of bacterial uptake by the respective MØ/DC subset (left graph) and positive APF staining (%) within the cells phagocytosing DDAO-S.E (right graph). Data are representative of 4 stable PD patients and were analysed by paired *t*-test.

3.2.9 Flow-cytometric cell sorting of human peritoneal MØ and DC subsets

To purify the respective peritoneal $CD14^+$ MØs and $CD1c^+$ DCs, a flow-cytometric cell sorting approach was performed (Fig. 3.16A). The purity of each post-sorted subset was generally >95%. The cells were stained with Microscopy Hemacolor (Merck) and the morphology was shown in Fig. 3.16B.

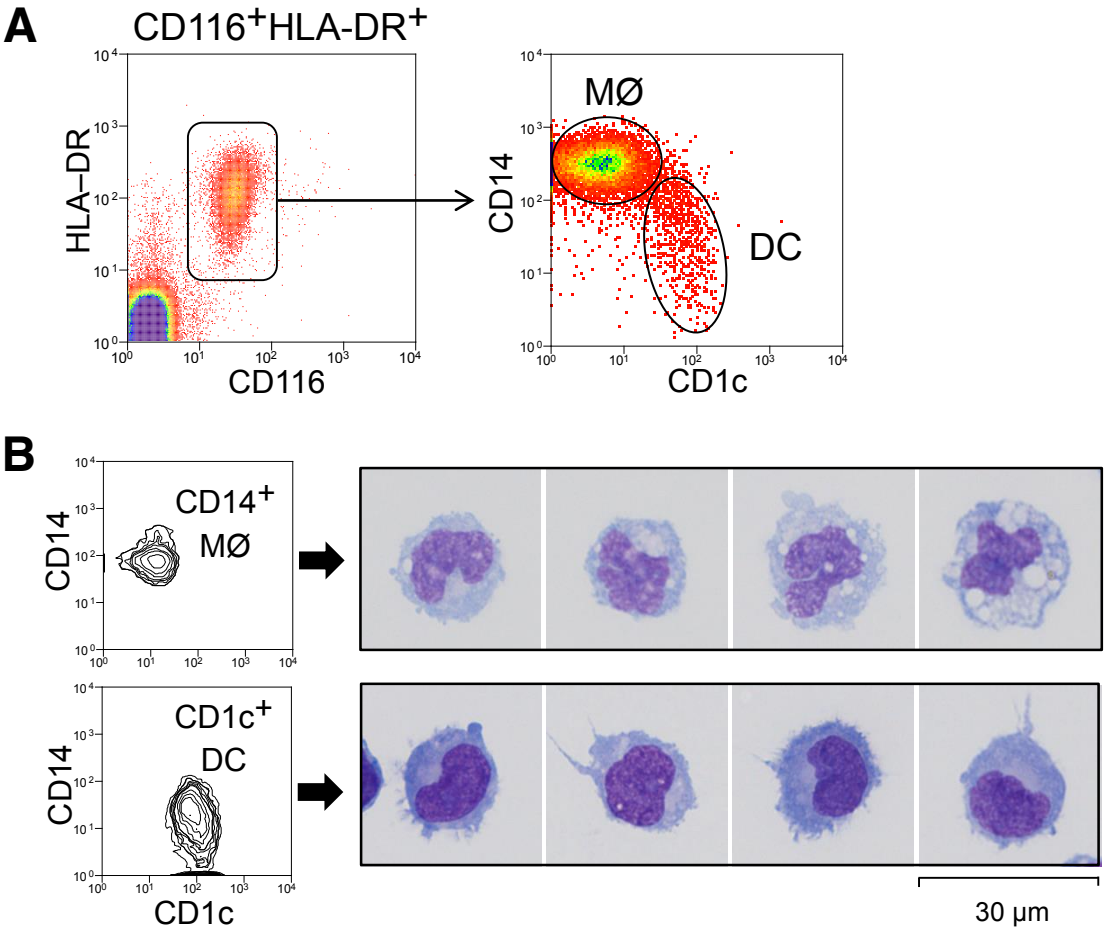

Figure 3.16 Cell sorting of human peritoneal MØ/DC and their morphology

(A) Representative density plots depict the purification strategy of $CD14^+$ MØs and $CD1c^+$ DCs from peritoneal effluent cells by flow cytometry. Cells were gated on $CD116^+HLA\text{-}DR^+$, then separated into two. **(B)** Plots shown were the post-sorted cells (the purity >95%). Purified cells were cytospun, air-dried and stained with Microscopy Hemacolor. The morphology of cells was shown (scale bar denotes 30 μ m). Data represent one of 4 stable PD patients.

3.2.10 Antigen processing and presenting assay

MØs and DCs are generally considered professional antigen-presenting cells (APCs). To test their ability to uptake, process and present specific antigen to responder T cells, a modified *in vitro* assay of cross presentation was conducted. The results suggested both cell types are effective antigen processing and presenting cells, albeit $CD1c^+$ DCs are slightly more efficient than $CD14^+$ MØs in this regard (Fig. 3.17).

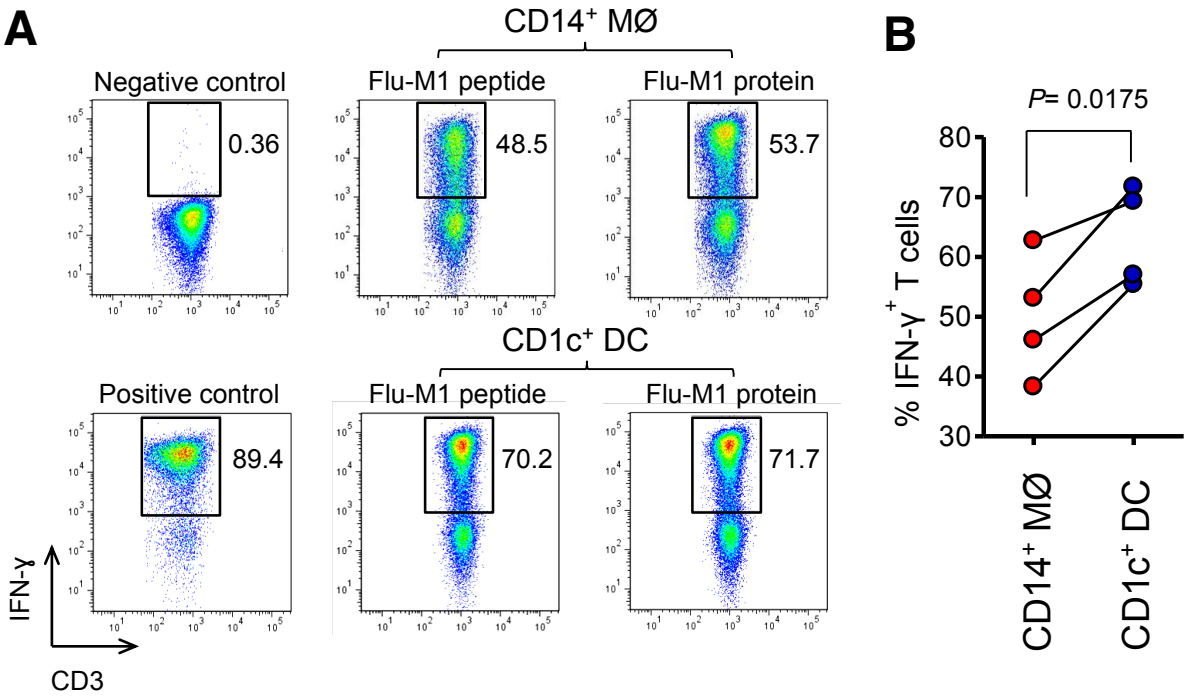

Figure 3.17 Human antigen processing and presenting assay

(A) Representative density plots show flow-cytometric determination of intracellular IFN-γ production by responder $CD8^+$ T cells specific for M1p58-66. Plots display responder T cells after co-culture with $CD14^+$ MØ or $CD1c^+$ DC (from $HLA\text{-}A2^+$ stable PD patients), which were loaded with soluble Flu-M1 protein, or pulsed with Flu-M1p58-66 peptide (at an APC: responder ratio of 1:1-2). PMA (10 µg/ml) + Ionomycin (1µM) was used as a positive control. Data are representative of 1 from 4 stable PD patients. **(B)** Quantification of intracellular IFN-γ expression from responder T cells derived from antigen processing and presentation assay based on loading Flu-M1 protein antigen on the respective APCs ($CD14^+$ MØ or $CD1c^+$ DC). Data are representative of 4 stable PD patients and were analyzed by paired *t*-test.

3.3 Discussion

In this chapter, the results shown demonstrate that human peritoneal mononuclear phagocytes within the PD effluents from PD patients are a highly heterogeneous population. Distinct peritoneal monocytic subsets might represent different developmental origins, differentiation pathways or activation/maturation status. Importantly, for the first time, we could identify human peritoneal DCs in PD effluents, which are morphologically, phenotypically and functionally distinct from traditional peritoneal MØs.

The application of a wide range of cell-specific fluorochrome-conjugated antibodies and polychromatic flow cytometry enabled the analysis of the composition of leukocyte subpopulations within the PD effluents. In this project, I have established a novel flow-cytometric gating strategy to successfully discriminate monocytic cells ($CD116^{+}HLA\text{-}DR^{+}CD14^{+/low/-}$) from other $CD116^{+}HLA\text{-}DR^{-}$ myeloid subsets, such as $CD16^{+}CD66^{+}$ neutrophils and $CCR3^{+}Siglec\text{-}8^{+}$ eosinophils, within the PD effluents. From the peritoneal monocytic cells, two distinct subsets - $CD14^{+}CD1c^{low/-}$ MØs and $CD14^{low/-}$ $CD1c^{+}$ DCs could be identified, for the first time in the context of PD. Interestingly, a very recent study also discovered these two monocytic subsets wihin tumor ascites from the advanced ovarian cancer patients, using a different flow-cytometric approach with direct gating on the $CD11c^{+}HLA\text{-}DR^{+}$ population and subsequent separation into $CD14^{+}$ MØs and $CD1c^{+}$ DCs (Segura et al., 2013). From my own comparison analysis, both methods generated the same results: specific identification of two discrete monocytic subsets. Based on the immunophenotyping in this study, $CD1c^{+}$ DCs are $CD11c^{high}CD206^{high}CD226^{+}CD301^{high}Fc\varepsilon R1\alpha^{high}$, whereas $CD14^{+}$ MØs are $CD11b^{high}$ $CD16^{+}CD36^{high}CD64^{high}CD163^{high}MerTK^{+}$. Notably, these unique surface marker profiles were seen both under uninfected and infected conditions, albeit with different

extents of expression levels. The comparisons of gene expression profiles between peritoneal $CD14^+$ MØs and $CD1c^+$ DCs derived from tumour ascites, as well as compared to different blood monocyte subsets and blood $CD1c^+$ DC precursors, suggested that peritoneal $CD14^+$ MØs and $CD1c^+$ DCs are more likely monocyte-derived (Segura et al., 2013). However, this inference should be validated on healthy individuals and patients under different clinical settings (i.e. uninfected and infected PD patients).

Another noteworthy observation in PD patients is the heterogeneous status of peritoneal MØ activation or maturation. The flow-cytometric analysis has demonstrated the differential expression patterns of CD16 and CD206 on peritoneal MØs within the PD effluents. Sub-stratification based on these two surface markers has permitted further separation of peritoneal MØ/DCs into six subtypes. Interestingly, these subtypes displayed differential expression levels of HLA-DR, CD86 and CD163, which may reflect different stages of MØ/DC activation or maturation. For example, the $CD14^+CD16^+CD206^+$ subtype has the highest HLA-DR/CD86/CD163 expression within $CD14^+$ MØs, suggesting that this subtype is likely more mature peritoneal MØs. Conversely, the $CD14^+CD16^{low/-}CD206^-$ subtype with the lowest expression levels of HLA-DR/CD86/CD163, could be newly recruited monocyte-derived MØs as they are phenotypically close to 'classical' $CD14^+CD16^{low/-}$ blood monocytes. Surprisingly, $CD14^{low}CD16^+$ MØs were hardly found in the peritoneal cavity, in all PD effluent samples studied. The possible explanation is 'non-classical' $CD14^{low}CD16^+$ blood monocytes either not being recruited into peritoneal cavity or differentiating into other phenotypes after migration. The fact that peritoneal $CD14^+$ MØs from all PD effluents are mostly $CCR2^+$ suggested that these cells might originate from $CD14^+CD16^-$ blood monocytes ($CCR2^+$), rather than $CD14^{low}CD16^+$ blood monocytes ($CCR2^{low/-}$).

Altogether, these data provided new insights into the heterogeneity of phenotypes and activation/maturation of peritoneal MØ/DCs within PD effluent. In the next chapter, the issue of how these phenotypes as well as activation/maturation status is influenced by the time on PD therapy, and by acute PD-related peritonitis, will be explored.

Apart from phenotypic heterogeneity and plasticity, peritoneal monocytic subsets displayed distinct functional characteristics. Firstly, both $CD14^+$ MØs and $CD1c^+$ DCs could produce significant amounts of pro-inflammatory cytokines such as TNF-α, IL-1β, IL-6 and IL-12p40/p70 in response to *ex vivo* stimulation with lipopolysaccaride (LPS) and Staphylococcus epidermidis supernatant (SES). These cytokines have recently been suggested to drive Th1 responses leading to chronic peritoneal injury/fibrosis as a consequence of repeat inflammation in a mouse peritonitis model (Fielding et al., 2014). Secondly, $CD14^+$ MØs have superior phagocytic capability in response to *ex vivo* zymosan particles or *Staphylococcus epidermidis* challenges, compared to $CD1c^+$ DCs. After uptake of zymosan particles or bacteria, $CD14^+$ MØs could generate more respiratory burst response than $CD1c^+$ DCs. Finally, in the assay of antigen cross-presentation, preliminary observations suggested $CD1c^+$ DCs are more efficient than $CD14^+$ MØs in influenza M1 protein uptake, processing and presentation of peptides to the responder CD8 T lymphocytes specific for M1p58-66.

Collectively, through phenotypic and functional characterization, the results in this chapter have advanced our understanding of human peritoneal MØ/DC biology in the context of PD therapy.

Chapter Four

Kinetics and distributions of peritoneal myeloid subsets during the course of peritoneal dialysis

4.1 Introduction

Like any tissue, the homeostatic environment of the peritoneal cavity is tightly regulated. However, in the context of peritoneal dialysis (PD), the intraperitoneal immune system is perturbed. Initially, catheter insertion is anticipated to induce a surgical injury-related inflammatory response, followed by the resolution of this acute response. Meanwhile, the catheter tube component within the peritoneal cavity might induce a foreign-body response (Flessner et al., 2010), which would further complicate the inflammatory scenario during the post-surgery/pre-dialysis period. When the dialysis ensues (normally about one month after catheterization), patients begin daily exchange of dialysis fluid. Earlier evidence revealed that this continuous dialysis process altered the resident leukocyte compositions in the peritoneal cavity over time (McGregor et al., 1989). Based on a novel immunophenotyping approach (established in Chapter 3), in the work presented in this Chapter, the kinetics and distributions of peritoneal myeloid subsets as well as MØ/DC phenotypes have been monitored from one week after catheterization to PD commencement ("pre-dialysis period"), and then to the end of the first year of PD therapy ("post-dialysis period"). These data in combination with patient information have been used to address the following research questions:

- What are the main features of the peritoneal inflammatory response induced by the catheter insertion surgery?
- How do peritoneal myeloid subsets as well as the MØ/DC phenotypes change after dialysis intervention?
- Do patients with different clinical outcomes during the course of PD therapy have distinct peritoneal immune characteristics?

In the second part of this chapter, two different clinical cohorts of PD patients have been investigated. These are, first, patients diagnosed with acute PD-related peritonitis and, second, stable dialysis patients (under dialysis for at least one year). Previous studies have shown that MØs are the predominant leukocytes within PD dialysate from stable patients (Goldstein et al., 1984). Upon PD-related peritonitis, a large number of neutrophils accumulate in the peritoneal cavity during the early time period following infection (Lin et al., 2013). However, the distribution of MØ/DC subsets during peritonitis has not been well characterised. Here, the compositions of myeloid cells as well as MØ/DC subsets have been analysed in "cloudy" effluents from the first day of peritonitis episodes, and compared with data from "clean" effluents from uninfected stable dialysis patients. Several research questions have been considered:

- What are the key features of the inflammatory response upon acute PD-related peritonitis, in terms of peritoneal myeloid subsets as well as MØ/DC phenotype/activation, compared to uninfected status?
- Do peritonitis patients with technique failure have distinct distributions of peritoneal myeloid subsets as well as MØ/DC phenotype/activation?
- Is there any pathogen-specific distribution of peritoneal myeloid subsets and MØ/DC phenotype/activation upon acute PD-related peritonitis?
- Do stable dialysis patients with or without a history of peritonitis have different peritoneal immune characteristics?

Overall, the aim is to understand how the kinetics and distributions of peritoneal myeloid subsets and MØ/DC subsets change under different clinical scenarios during PD therapy, and to determine whether or not the alterations of peritoneal MØ/DC phenotype and activation have associations with patients' clinical outcomes.

4.2 Results

4.2.1 Clinical outcomes of new-starter PD patients with 1-year follow-up

To investigate the cellular distribution of peritoneal MØ/DC subsets and their respective kinetic change during the course of PD therapy, 50 new-starter PD patients were enrolled and longitudinally followed for at least 1 year (summarized in Fig. 4.1). Discontinuation of PD therapy within the study period has been documented and is mainly attributed to receiving transplantation (n = 12), non-death technique failure from any aetiology (shifting to haemodialysis) (n = 19), or deaths from any reason (n = 3). Also, follow-up on one patient was lost due to his transfer to another institute (Fig. 4.1). Of 50 new-starters, 44 patients successfully commenced maintenance dialysis, while 5 patients could not start dialysis owing to catheter dysfunction refractory to treatment. One patient maintained a well preserved residual kidney function and no need for dialysis throughout the study period. After dialysis initiation, another 12 patients left PD within the initial 3-month period (3 receiving transplantation, 1 cancer death, 8 non-death technique failure). The reasons for technique failure included irreversible catheter dysfunction (n = 4), ultrafiltration failure (n = 2), unresolved peritonitis (n = 1) and abdominal hernia (n = 1). During the subsequent 3 months, 4 patients were transplanted, 1 patient moved to another institution, 1 patient died from unresolved peritonitis and 3 patients experienced non-death technique failure (1 peritonitis, 1 dialysis inadequacy, 1 abdominal hernia), leaving 23 patients remaining on PD after 6-month dialysis. From 6 month to the end of the first year, 9 patients left PD (5 transplantation, 1 cardiovascular death, 3 peritonitis-related technique failure). By the end of the first year, 14 patients remained on PD therapy.

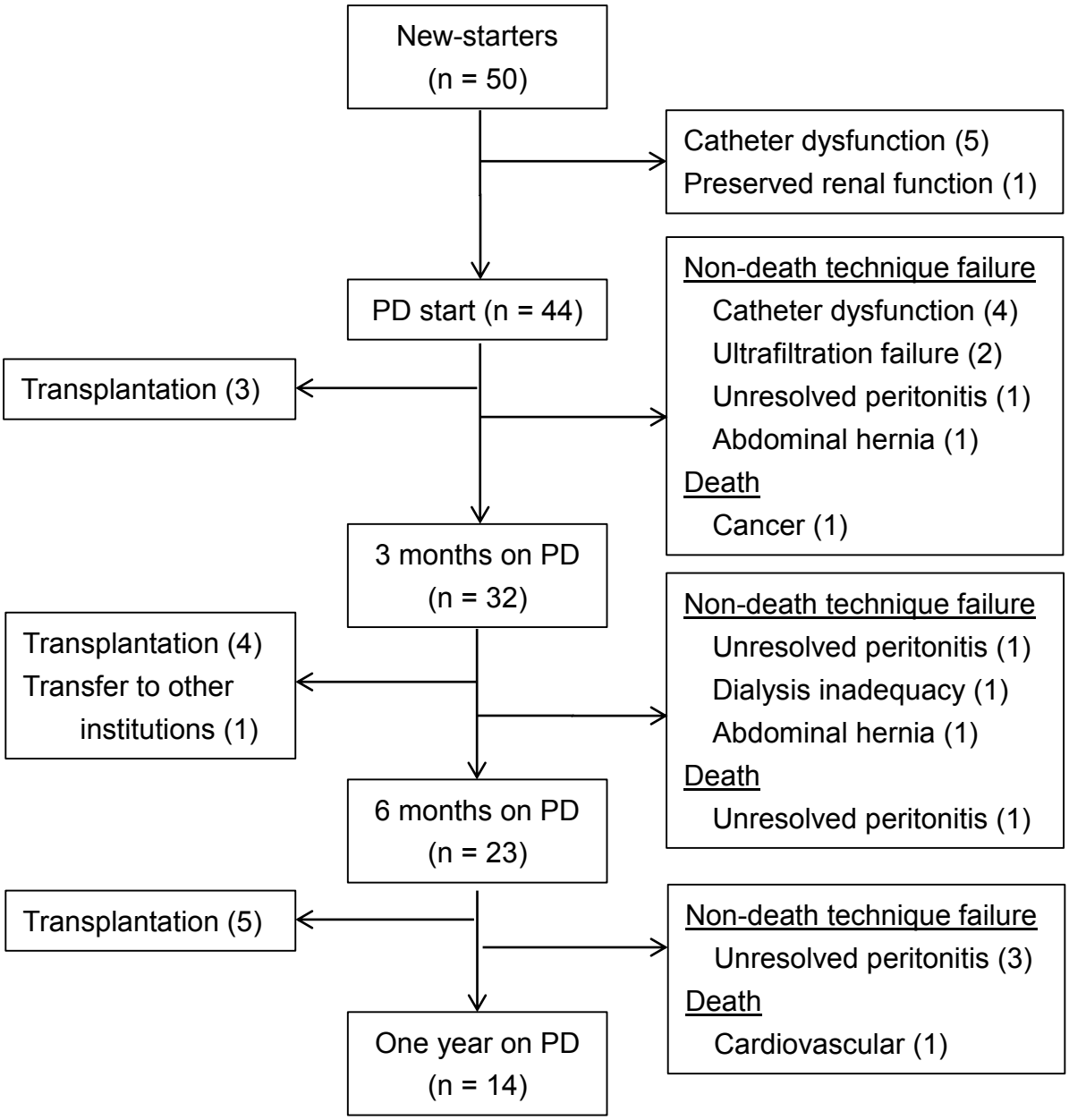

Figure 4.1 Flow diagram of longitudinal outcomes of new-starter PD patients during 1-year follow-up

A total of 50 new-starter PD patients were enrolled in this study. The reasons for dropout from this cohort during 1-year follow-up period included receiving transplantation (n = 12), transferring to other institutions (n = 1), non-death technique failure (n = 19), death (n = 3). The number in each parenthesis denotes the number of patients under this defined category.

4.2.2 Kinetic changes of major peritoneal myeloid cells during the 1st year of PD therapy

For new-starter PD patients, the compositions of myeloid subpopulations in peritoneal effluents have been analysed from one week after PD catheter implantation to the end of the first year of treatment. Each patient would have six time points of PD fluid sampling if he/she could maintain PD therapy for at least one year. In total, 171 PD effluent samples have been analysed: 50 samples from *1st flush*, 37 samples from *2nd flush*, 39 samples from *PD start*, 20 samples from *PD for 3 months*, 15 samples from *PD for 6 months,* and 10 samples from *PD for 1 year.* As shown in Fig 4.2, total peritoneal effluent cells as well as major peritoneal myeloid subsets (neutrophils: $CD116^{+}HLA\text{-}DR^{-}CD16^{+}$; eosinophils: $CD116^{+}HLA\text{-}DR^{-}CD16^{-}$ with characteristic FSc/SSc profile; and monocytic cells: $CD116^{+}HLA\text{-}DR^{+}CD14^{+/low/-}$, see Fig. 3.2) changed over time during the 1st year of PD therapy. Generally, the cell number of each subset declined during the post-surgery/pre-dialysis period, from 1st peritoneal flush to the start of PD. After dialysis initiation, peritoneal neutrophils and eosinophils were significantly depleted (Fig. 4.3). By contrast, monocytic cells gradually became the predominant cell type (40~ 70 % of total effluent cells) in the peritoneal cavity, as they decreased at a relatively slow rate.

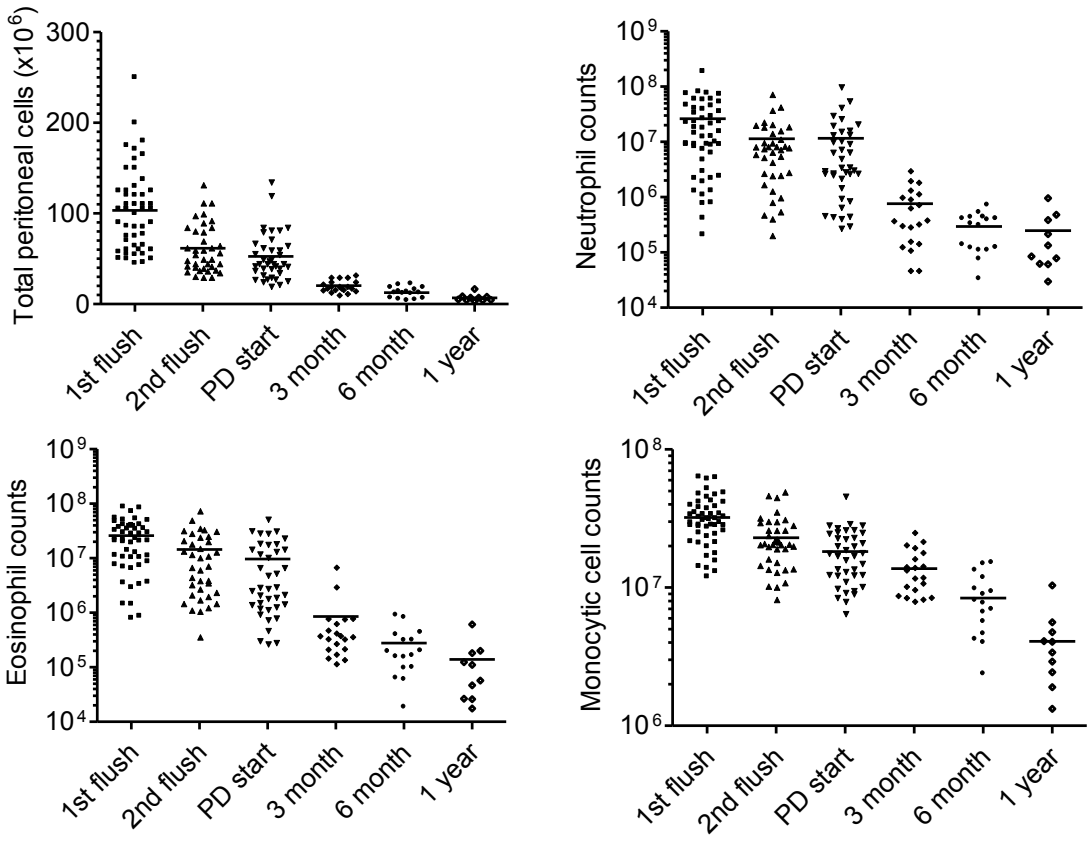

Figure 4.2 Changes in the numbers of major peritoneal myeloid cells during the 1st year of PD therapy

Numbers of total peritoneal cells, neutrophils, eosinophils, and monocytic cells changed during the 1-year follow-up period. Data are representative of 171 PD samples from 50 patients at different time points (50 samples from *1st flush*, 37 samples from *2nd flush*, 39 samples from *PD start*, 20 samples from *PD for 3 months*, 15 samples from *PD for 6 months*, and 10 samples from *PD for 1 year*). Horizontal bar in each group represents the mean.

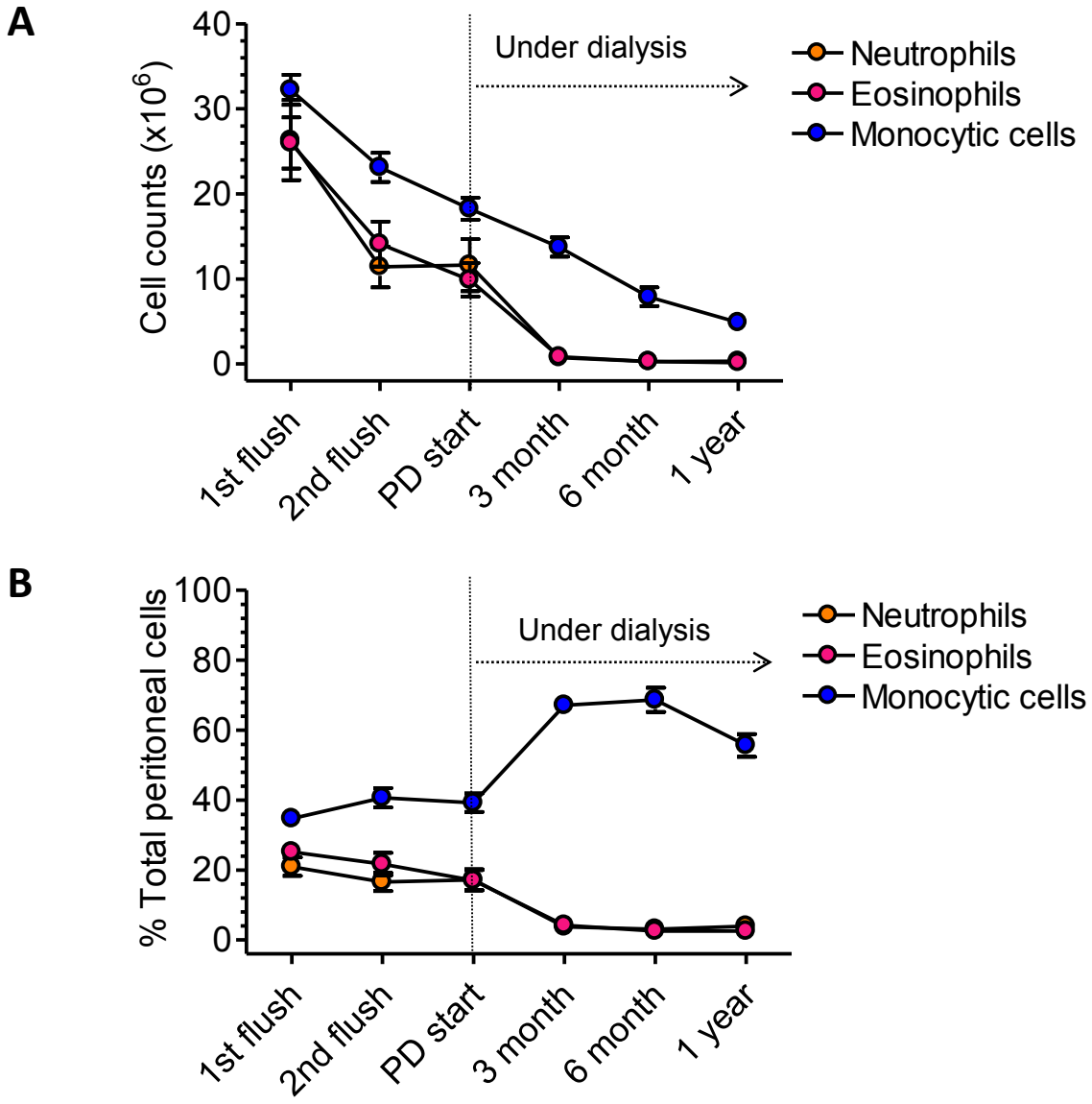

Figure 4.3 Kinetic changes of major peritoneal myeloid subsets during the 1st year of PD therapy

Graphs showing (A) the numbers and (B) the proportion of peritoneal neutrophils, eosinophils, and monocytic cells changed during the 1-year follow-up period. Data are representative of 171 PD samples from 50 patients at different time points (50 samples from *1st flush*, 37 samples from *2nd flush*, 39 samples from *PD start*, 20 samples from *PD for 3 months*, 15 samples from *PD for 6 months*, and 10 samples from *PD for 1 year*). Error bars in each group denote the standard error of mean.

4.2.3 Kinetic changes of peritoneal macrophage and dendritic cell subsets during the 1st year of PD therapy

Peritoneal monocytic cells comprise $CD14^+$ MØs and $CD1c^+$ DCs, and could be further phenotypically stratified into six subtypes based on differential expressions of CD16 and CD206 (see Chapter 3, Fig. 3.7). Longitudinal analysis showed that $CD14^+$ MØs decreased continuously along the course of PD therapy, while $CD1c^+$ DCs maintained a stable number during the pre-dialysis as well as early dialysis period, then declined at a relatively slow rate as dialysis continued (Fig. 4.4A). This distinctive kinetic change resulted in a relative increase of the proportion of $CD1c^+$ DCs and a decrease in the proportion of $CD14^+$ MØ within the peritoneal monocytic cell population (Fig. 4.4B). This is easily visualised as an alteration in the ratio of $CD14^+$ MØ to $CD1c^+$ DC during pre-dialysis as well as early dialysis period, then reaching a relative stable figure after 6-month dialysis (Fig. 4.4C).

Subsequent kinetic investigation of six peritoneal MØ/DC subsets revealed that all subsets decreased in number during the course of 1st-year PD therapy (Fig. 4.5A). In terms of the proportion of each subset, the most interesting finding was that $CD14^+CD16^+CD206^+$ cells (blue, solid line), initially the major subset, gradually declined in number, while $CD14^+CD16^+CD206^-$ cells (orange, dashed line) increased after dialysis initiation, becoming the largest cell subtype (Fig. 4.5B).

Altogether, these findings demonstrate that the dialysis process has altered the peritoneal immune system by changing the distributions of peritoneal myeloid subsets as well as MØ/DC phenotypes.

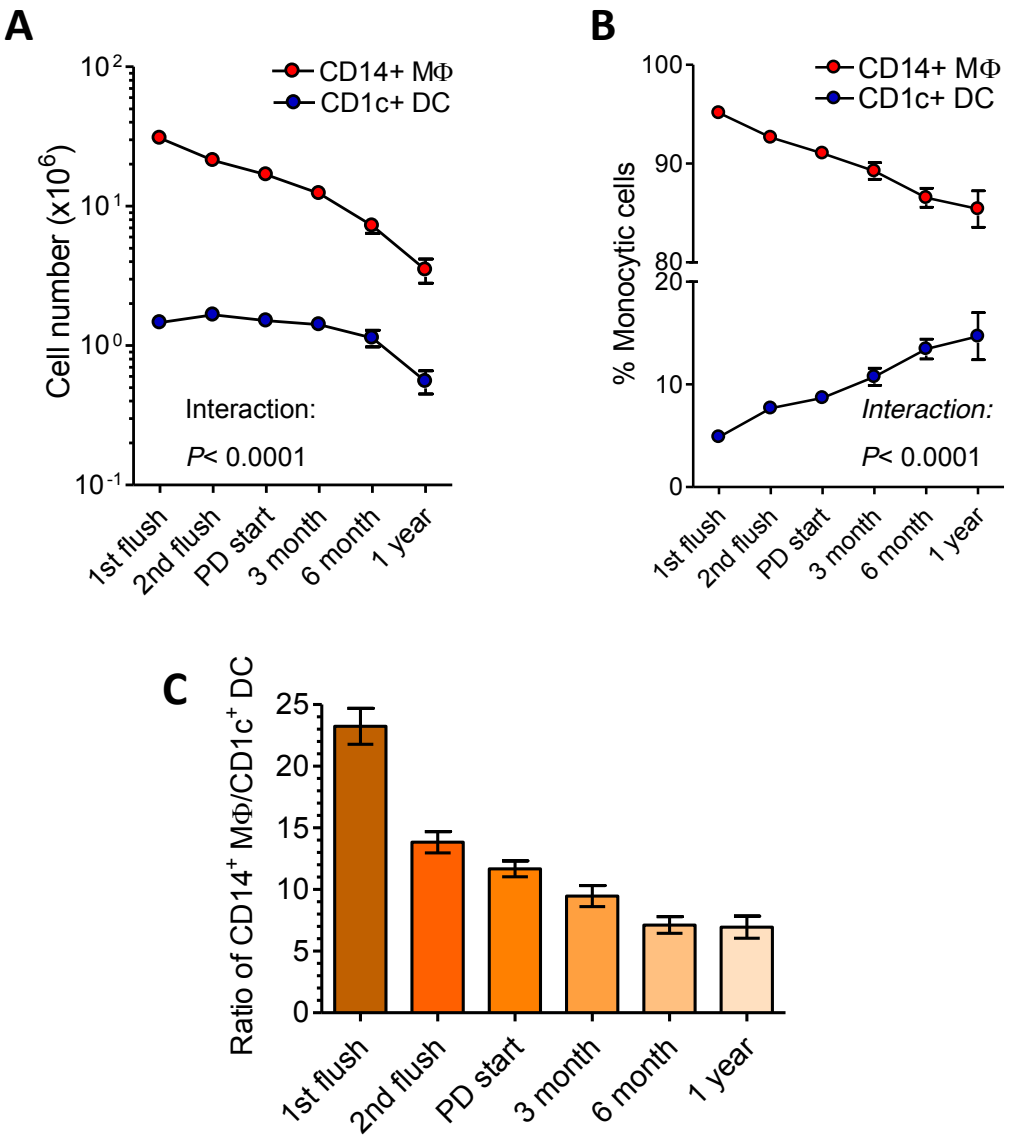

Figure 4.4 Differential kinetic changes of CD14⁺ MØ sand CD1c⁺ DC during the 1st year of PD therapy

Graph showing **(A)** the numbers and **(B)** the proportion of $CD14^+$ MØ sand $CD1c^+$ DC within peritoneal monocytic population changed during the 1st year of PD therapy. **(C)** The ratio of $CD14^+$ MØs over $CD1c^+$ DC showed an initial decline and then gradually stabilised after 6-month therapy. Data are representative of 171 PD samples from 50 patients at six time points. Data are shown as mean ± SEM. Data are analysed by two-way ANOVA and interaction statistics *P*-values are indicated.

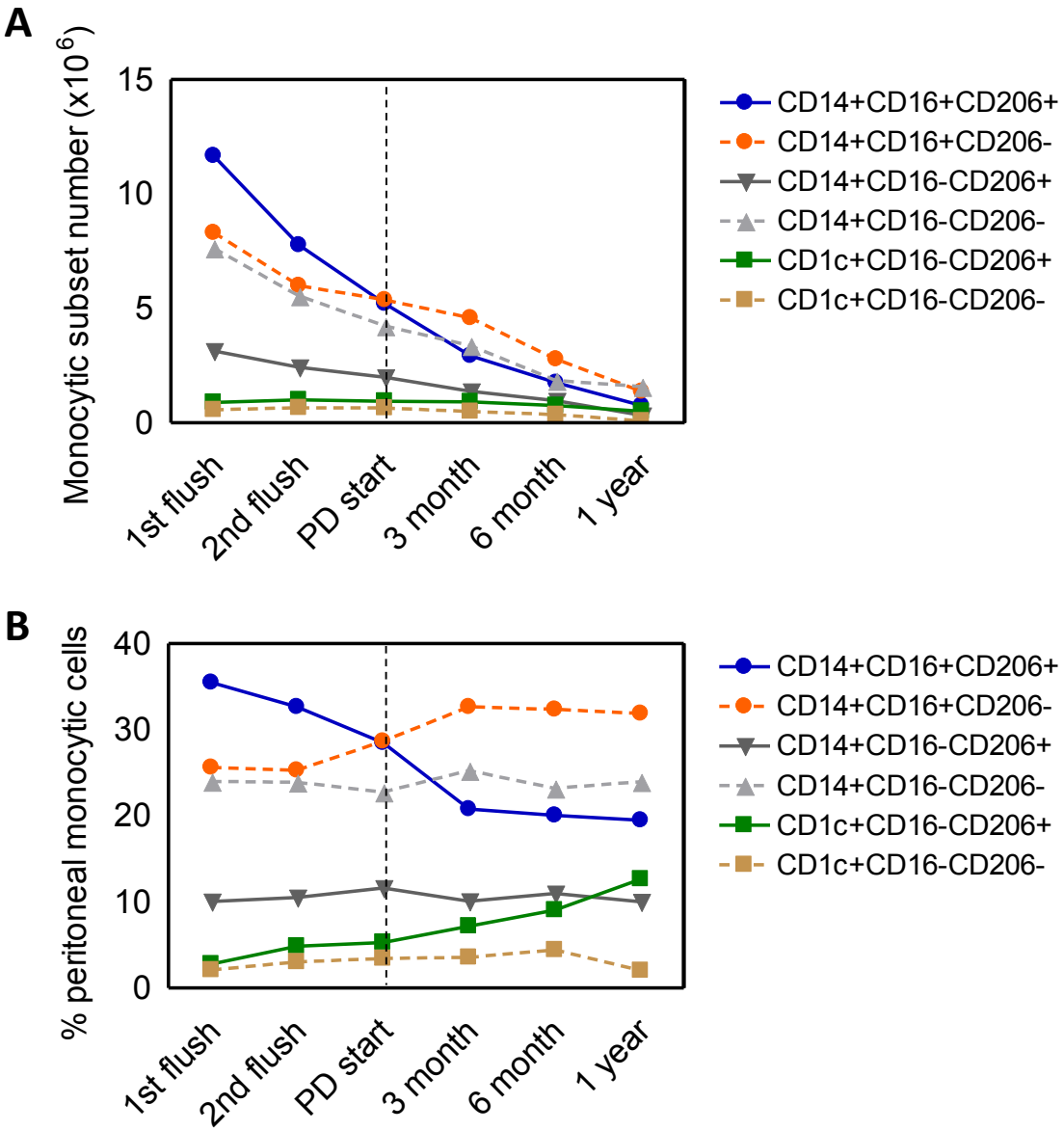

Figure 4.5 Individual kinetic changes of six peritoneal monocytic subsets during the 1st year of PD therapy

Graphs showing **(A)** the cell number of each peritoneal monocytic subset changed during the 1st year of PD therapy. **(B)** The proportion of Individual subset changed during the study period illustrating distinctive kinetic distribution. Data are representative of 171 PD samples from 50 patients at six time points.

4.2.4 Minimal local proliferation of peritoneal MØs and DCs alongside post-surgery inflammatory recruitment

Recently, our group showed in experimental peritonitis mouse models that peritoneal resident MØs as well as discrete recruited inflammatory MØs could display local proliferative activity during the early resolution phase of specific inflammation (Davies et al., 2011 and 2013), providing evidence of distinctive cellular kinetics during tissue inflammation. The observation of a kinetic change in peritoneal MØs during the catheter-induced inflammation/resolution process, raises a question as to whether these MØs are all recruited from the periphery, or whether to some extent, local proliferation also contributes to the peritoneal MØ pool. To answer this question, intracellular Ki67 expression (proliferation marker) and DNA content (Davies et al., 2011) of peritoneal MØs and DCs were examined in PD effluents from 1st flush, 2nd flush and 1st exchange at PD start (Fig. 4.6). The results suggested that the majority of peritoneal MØs and DCs were within G_0 phase of cell cycle. Very few proliferating cells (< 0.1% of cells, defined as cells within S-G_2-M phase) were found in either subset (Fig. 4.6A & B). There was no significant difference in proliferative activity between the three time points (Fig 4.6C). These preliminary observations implied that the peritoneal MØ/DC pool during the post-surgery period originates principally via inflammatory recruitment from the periphery, with limited contribution from local proliferation.

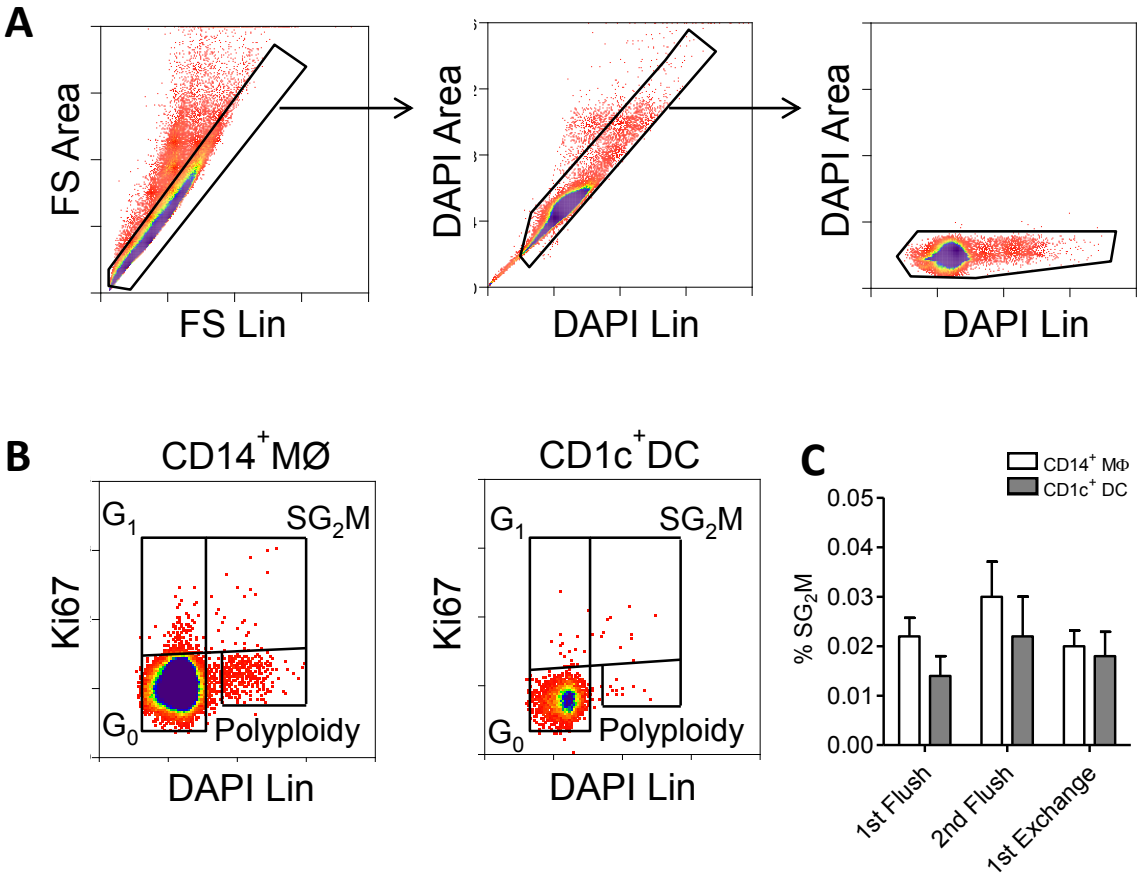

Figure 4.6 Minimal proliferative activity of peritoneal MØ/DC during post-surgery inflammation

(A) Flow-cytometric gating strategy used to serially exclude doublets before accurate analysis of DNA content and proliferation of specific subset (Davies et al., 2011). **(B)** Representative density plots of DAPI staining for DNA content and intracellular Ki67 expression (proliferation marker) in $CD14^+$ MØs and $CD1c^+$ DCs, respectively. The majority of either MØs or DCs, were within G_0 phase, while only very few cells under S-G_2-M phase, suggesting that minimal proliferative activity had occurred. Data are derived from the 2nd PD flush of one new-starter patient. **(C)** Graph showing the percentage of respective MØs and DCs under S-G_2-M phase at three time-point sample analysis. Data are derived from the analysis of 15 samples in total (n = 5 per time point). Data are shown as mean ± SEM.

4.2.5 Is the catheter-induced peritoneal inflammatory response associated with early non-peritonitis technique failure in new-starter PD patients?

The fact that PD catheter insertion elicits a sterile inflammatory response, represents the patient's immune system response to surgical injury as well as catheter tubing itself. During inflammation, peritoneal exudates containing fibrins accumulate in the peritoneal cavity, in severe cases, resulting in catheter occlusion. That is the reason why catheter dysfunction is one of the major causes for early technique failure in PD (Béchade et al., 2013; Kolesnyk et al., 2010; Quinn et al., 2010). In this cohort, 9 patients suffered from catheter dysfunction-related technique failure (5 patients before dialysis and 4 patients soon after dialysis start). Compared to patients without early technique failure (n = 32), those with catheter failure (n = 9) had significantly higher peritoneal neutrophils and higher MØ to DC ratio at the 1st PD flush (Fig. 4.7). Notably, a higher percentage of $CD16^+$ in $CD14^+$ MØs was also observed in patients with catheter failure (Fig. 4.8A). In terms of MØ/DC subtypes, the most significant difference between two groups was a higher proportion and higher numbers of $CD14^+CD16^+CD206^-$ subtype (Fig. 4.8B & C) in patients with catheter failure than those without early technique failure.

Additionally, compared to patients maintaining dialysis for 1 year (n = 14), those with post-dialysis non-peritonitis technique failure (n = 7, 4 for catheter dysfunction, 3 for membrane dysfunction including ultrafiltration failure and dialysis inadequacy) had distinct pre-dialysis inflammatory kinetics with a relatively slower rate of decline in the ratios of MØ to DC (Fig. 4.9).

Collectively, these preliminary observations implied that severe or delayed resolution of catheter-induced inflammation may be associated with higher risk of developing early non-peritonitis technique failure in new-starter PD patients.

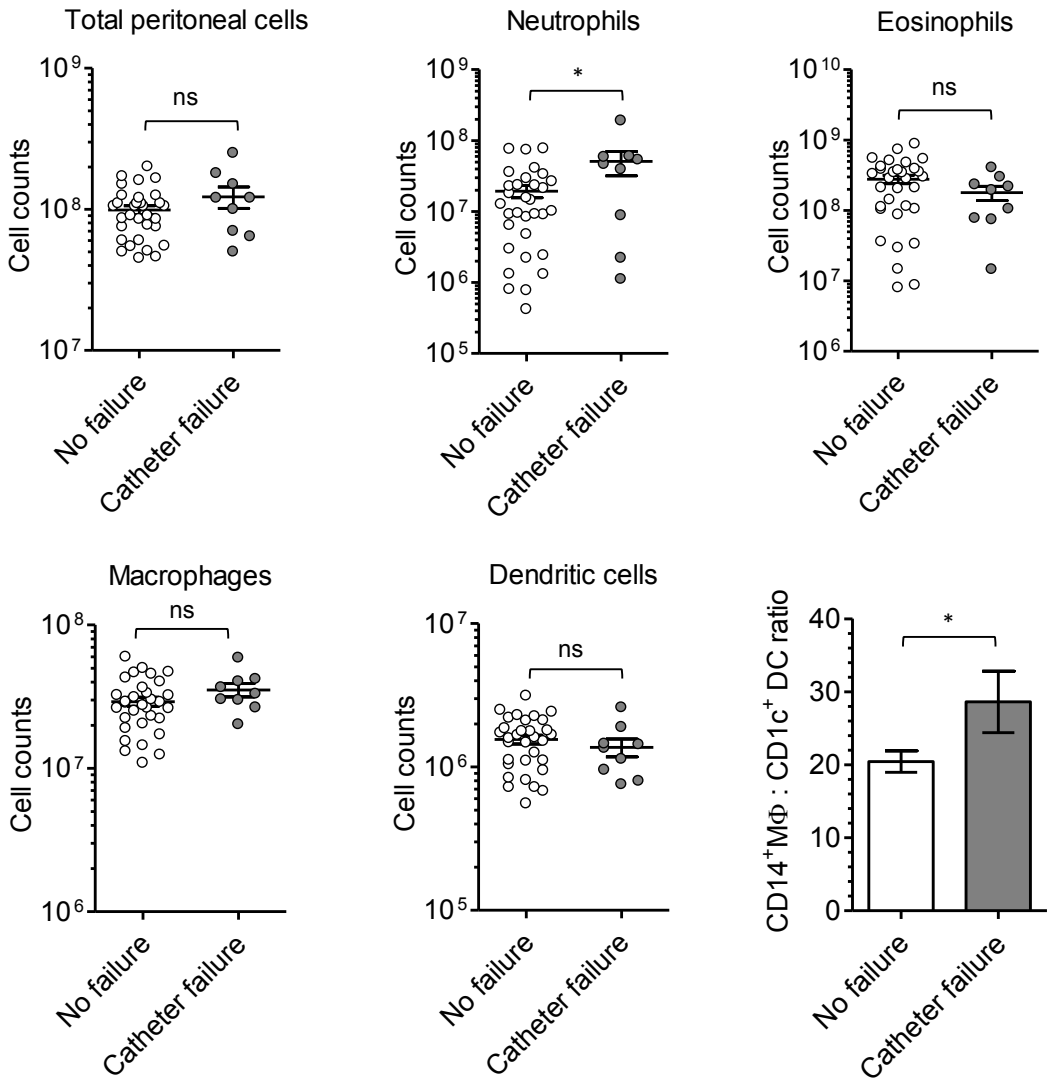

Figure 4.7 Comparisons of peritoneal myeloid cells from the 1st flush PD effluents between new-starter PD patients without early technique failure *versus* those with catheter-related technique failure

Graphs showing the comparisons of total peritoneal cells, peritoneal neutrophils, eosinophils, macrophages and dendritic cells (in number) from 1st PD flush effluent samples between new-starter patients without early technique failure (n = 32) *versus* with catheter failure (n = 9). Horizontal bars represent the mean. The ratio of $CD14^+$ MØ to $CD1c^+$ DC was compared between two outcomes (right lower graph). Data are shown as mean ± SEM. Data are analysed by Student's *t*-test (if parametric) or Mann Whitney *U* test (if nonparametric). (ns= $P > 0.05$, *= $P \leq 0.05$, **= $P \leq 0.01$ and ***= $P \leq 0.001$)

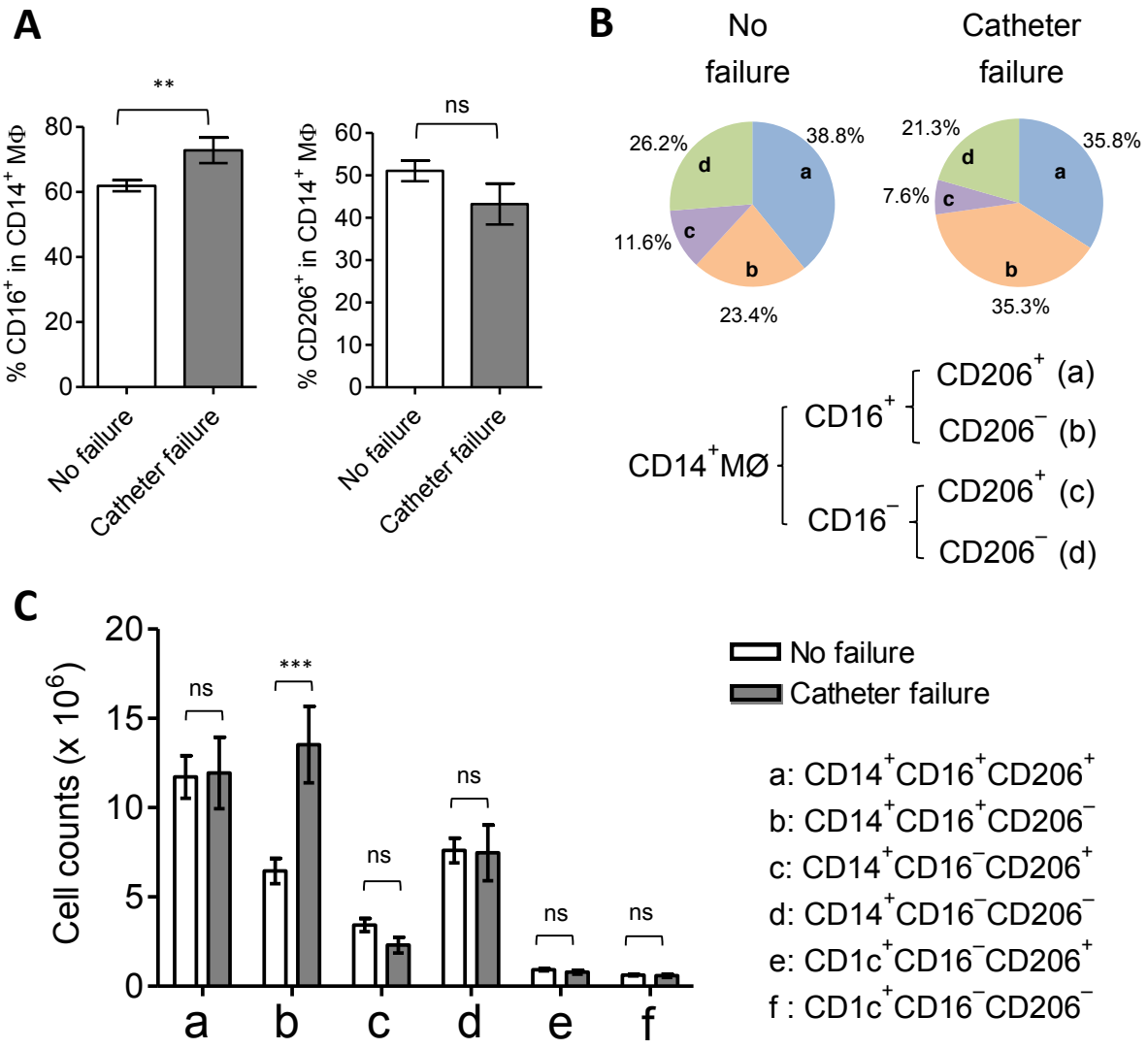

Figure 4.8 Differential distributions of peritoneal MØ/DC subsets from the 1st flush PD effluents between new-starter PD patients with and without catheter failure

(A) Graphs showing the proportion of $CD16^+$ (left) or $CD206^+$ (right) expression on $CD14^+$ MØ. **(B)** Pie charts demonstrating the proportion of four peritoneal MØ subsets. **(C)** Graph depicting actual number of each peritoneal monocytic subset from the 1st flush PD effluents of new-starter patients. Comparisons were performed between patients with catheter failure (n = 9) and those without technique failure (n = 32). Data are shown as mean ± SEM. Data are analysed by Student's *t*-test (if parametric) or Mann Whitney *U* test (if nonparametric). (ns= $P > 0.05$, *= $P \leq 0.05$, **= $P \leq 0.01$ and ***= $P \leq 0.001$)

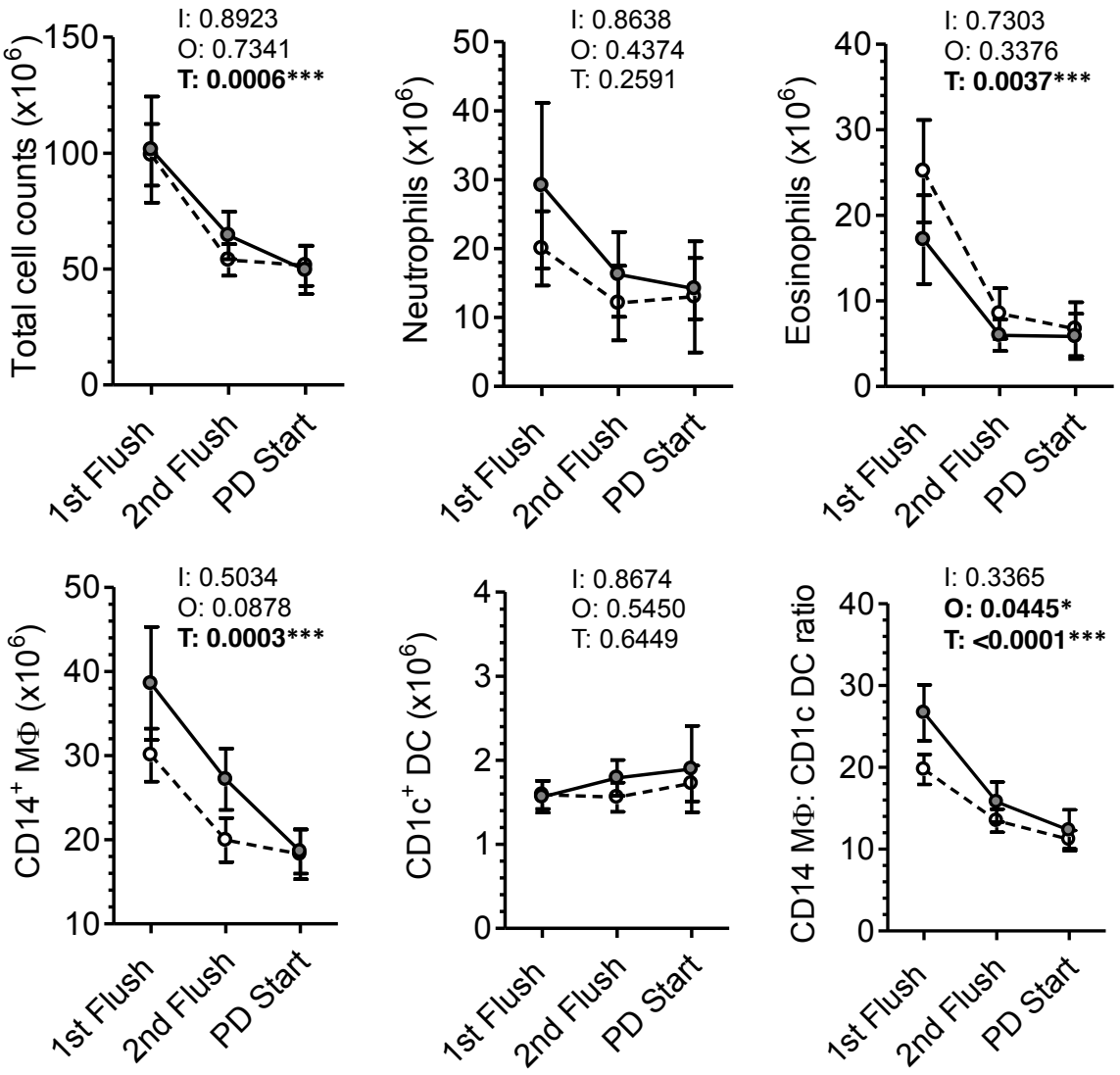

Figure 4.9 Comparisons of kinetic changes of peritoneal myeloid cells during pre-dialysis period between new-starter PD patients with and without non-peritonitis technique failure

Graphs showing the kinetic changes of the numbers of peritoneal neutrophils, eosinophils, MØs, DCs as well as MØ to DC ratio during the pre-dialysis period. Comparisons were made between new-starter PD patients with non-peritonitis technique failure (gray dots with solid line, n = 7) and those without failure (white dots with dashed line, n =14) within the first year of PD therapy. Error bars denote standard error of mean. Data are analysed by two-way ANOVA. (I: interaction, O: catheter outcomes, T: time factor; the numbers shown denote *P*-values)

4.2.6 Association between peritoneal immune characteristics and the risk for developing first episode of peritonitis during the 1st year PD therapy

Peritonitis remains the most frequent cause of technique failure in PD despite the observed decline in incidence over the past decades (Davenport et al., 2009). Several epidemiological studies have looked for the risk factors or predictors for developing first peritonitis episode in incident PD patients (Chow et al., 2005; Nessim et al., 2009, Matin et al., 2011). These studies mainly focused on the demographic as well as clinical characteristics, i.e., age at PD start, gender, race/ethic, primary cause of ESRF, diabetic status, socioeconomic circumstance. However, little is known with regards to the association between peritoneal immune characteristics and the risk for developing PD-related peritonitis.

In this cohort, of 44 successfully commenced PD patients, 8 patients developed first peritonitis episode during the 1st year of PD therapy. Only 12 patients maintained dialysis for more than one year without experiencing any peritonitis event. To investigate whether or not peritoneal immune characteristics at the start of PD could predict the risk for developing first peritonitis episode within the 1st year of PD therapy, the distributions of peritoneal myeloid cells as well as MØ/DC phenotypes at the start of PD were compared between patients who had first peritonitis episode (n = 8) and those free from peritonitis for one year (n = 12). The results were shown in Table 4.1. There is no significant difference between two groups regarding the peritoneal immune characteristics presented in this study.

Table 4.1 Comparisons of clinical and peritoneal immune characteristics at the start of PD between patients free from peritonitis and patients developing first peritonitis episode within the 1st year of PD therapy

Parameters	Patients free from peritonitis (n =12)	Patients having peritonitis (n = 8)	*P*-value
Clinical characteristics			
Age at PD start (year-old)	56.33 ± 4.96	60.13 ± 5.96	0.6322
Gender (% female)	16.7	50	0.1110
Diabetes (%)	41.7	12.5	0.1632
Peritoneal immune characteristics			
Total peritoneal cells ($x10^6$)	55.93 ± 8.71	44.19 ± 7.00	0.3470
Neutrophils ($x10^6$)	13.53 ± 8.03	8.84 ± 5.01	0.6664
Eosinophils ($x10^6$)	9.56 ± 3.81	8.12 ± 4.04	0.8034
Macrophages ($x10^6$)	18.13 ± 2.67	16.38 ± 2.49	0.6561
Dendritic cells ($x10^6$)	1.60 ± 0.20	1.51 ± 0.15	0.7436
MØ to DC ratio	12.07 ± 1.23	10.83 ± 1.20	0.4991
% $CD16^+$ in MØ	61.50 ± 3.43	61.47 ± 4.70	0.9962
% $CD206^+$ in MØ	50.68 ± 5.00	45.57 ± 2.67	0.4449
% $CD16^+CD206^+$ in MØ	42.57 ± 5.52	36.25 ± 5.96	0.4581
% $CD16^+CD206^-$ in MØ	27.72 ± 4.88	25.93 ± 3.58	0.7918
% $CD16^-CD206^+$ in MØ	10.83 ± 2.18	15.25 ± 3.23	0.2530
% $CD16^-CD206^-$ in MØ	18.87 ± 2.67	22.56 ± 4.12	0.4398
$CD14^+CD16^+$ MØ ($x10^6$)	10.85 ± 1.45	10.40 ± 1.94	0.8520
$CD14^+CD206^+$ MØ ($x10^6$)	9.15 ± 1.19	7.35 ± 1.08	0.3068
$CD14^+CD16^+CD206^+$ MØ ($x10^6$)	6.74 ± 0.01	5.24 ± 0.96	0.3191
$CD14^+CD16^+CD206^-$ MØ ($x10^6$)	4.30 ± 0.87	5.17 ± 1.03	0.5329
$CD14^+CD16^-CD206^+$ MØ ($x10^6$)	2.22 ± 0.33	2.11 ± 0.28	0.8229
$CD14^+CD16^-CD206^-$ MØ ($x10^6$)	4.87 ± 1.28	3.86 ± 0.58	0.5495
$CD1c^+CD206^+$ DC ($x10^6$)	0.94 ± 0.11	0.97 ± 0.86	0.8528
$CD1c^+CD206^-$ DC ($x10^6$)	0.66 ± 0.11	0.54 ± 0.08	0.427

Data are expressed as mean ± standard error of mean. Group differences are assessed by Student's *t*-test (if parametric) or Mann Whitney *U* test (if nonparametric) for continuous variables and chi-square test for categorical variables.

4.2.7 Differential distributions of peritoneal myeloid cells and MØ/DC subsets between infected PD effluents from acute peritonitis patients and uninfected PD fluids from stable dialysis patients

In the second part of this chapter, a cohort of PD patients experiencing acute PD-related peritonitis was enrolled. A total of 37 acute bacterial peritonitis episodes were recorded during the study period. Microbiological data showed that 26 episodes were gram positive bacteria, 8 episodes were gram negative bacteria, and 3 episodes with mixed gram positive/negative bacteria. Notably, 30 episodes had been successfully treated, while 7 episodes had unresolved peritonitis leading to technique failure or peritonitis-related death. Meanwhile, a total of 37 uninfected PD fluid samples (overnight long-dwell bags) were collected from 37 patients under stable dialysis for more than one year. History of peritonitis and the number of peritonitis episodes were recorded. Of them, 17 patients had a history of peritonitis (9 patients with a single episode and 8 patients with more than one episode).

The results shown in Fig 4.11 revealed that peritoneal neutrophils, eosinophils, MØs, DCs, significantly increased in the infected fluid samples from day 1 bacterial peritonitis, compared to uninfected fluid samples from stable dialysis patients. Interestingly, in patients with acute peritonitis, the increase in $CD14^+$ MØs was much greater than $CD1c^+$ DCs, and the ratio of MØ to DC also increased significantly, from 6.6 ± 0.6 fold in uninfected samples to 110.1 ± 15.4 fold in peritonitis samples. Additionally, the percentage of $CD16^+$ or $CD206^+$ expression in $CD14^+$ MØs was much lower in the presence of peritonitis (Fig. 4.11A). With regards to MØ subtypes, the proportion of $CD14^+CD16^-CD206^-$ subset was significantly higher in the infected fluid samples compared to uninfected fluid samples (Fig. 4.11B). All six MØ/DC subtypes increased in number during acute bacterial peritonitis (Fig. 4.11C).

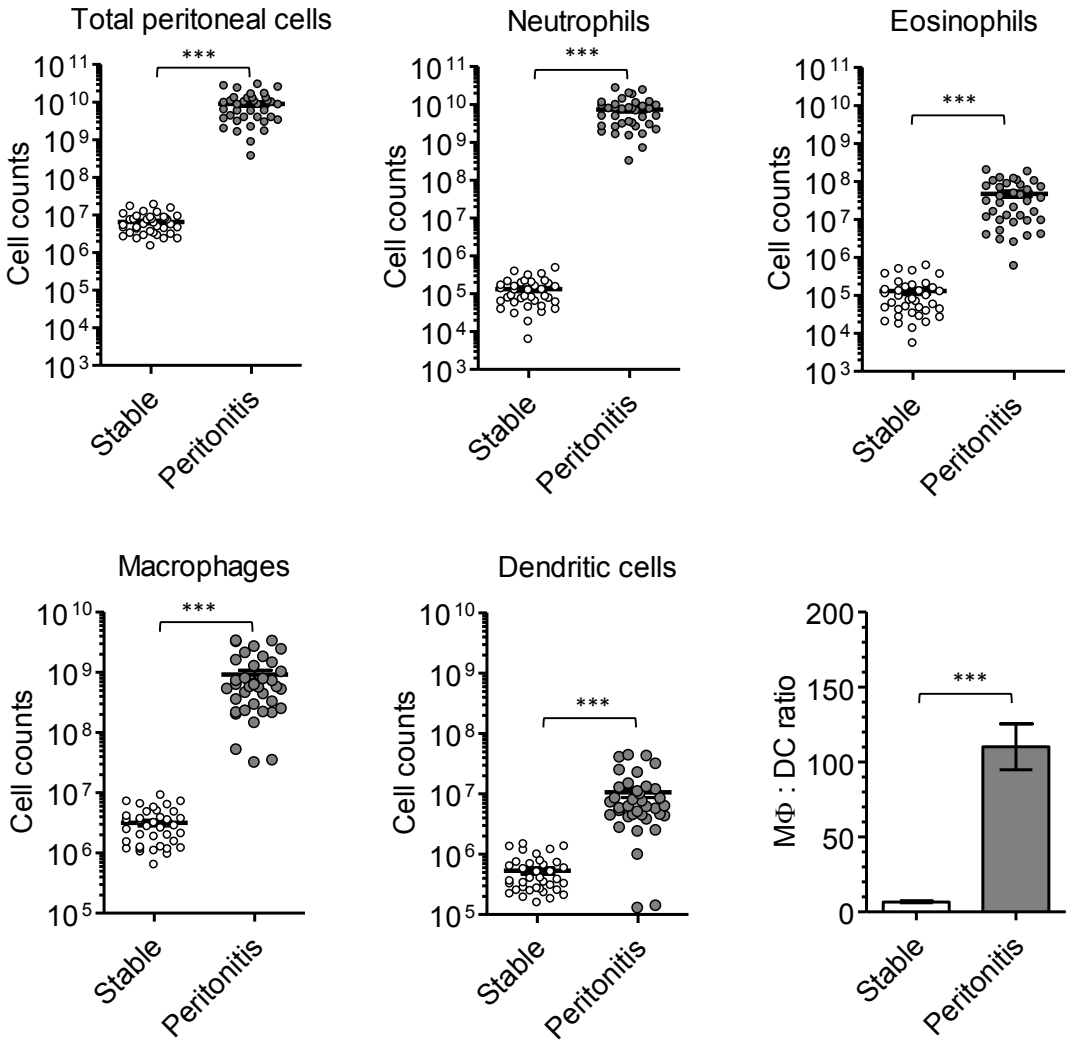

Figure 4.10 Comparisons of major peritoneal myeloid cells between infected PD effluents from day 1 acute bacterial peritonitis and uninfected fluids from stable dialysis patients

Graphs showing the comparisons of total peritoneal cells, peritoneal neutrophils, eosinophils, MØs and DCs (in number) within infected PD fluids on day 1 acute bacterial peritonitis (n = 37) *versus* uninfected fluids from stable dialysis patients (n = 37). The ratio of $CD14^+$ MØ to $CD1c^+$ DC was compared between two groups (right lower panel). Data are shown as mean ± SEM. Data are analysed by Student's *t*-test (if parametric) or Mann Whitney *U* test (if nonparametric). (ns= $P > 0.05$, *= $P \leq 0.05$, **= $P \leq 0.01$ and ***= $P \leq 0.001$)

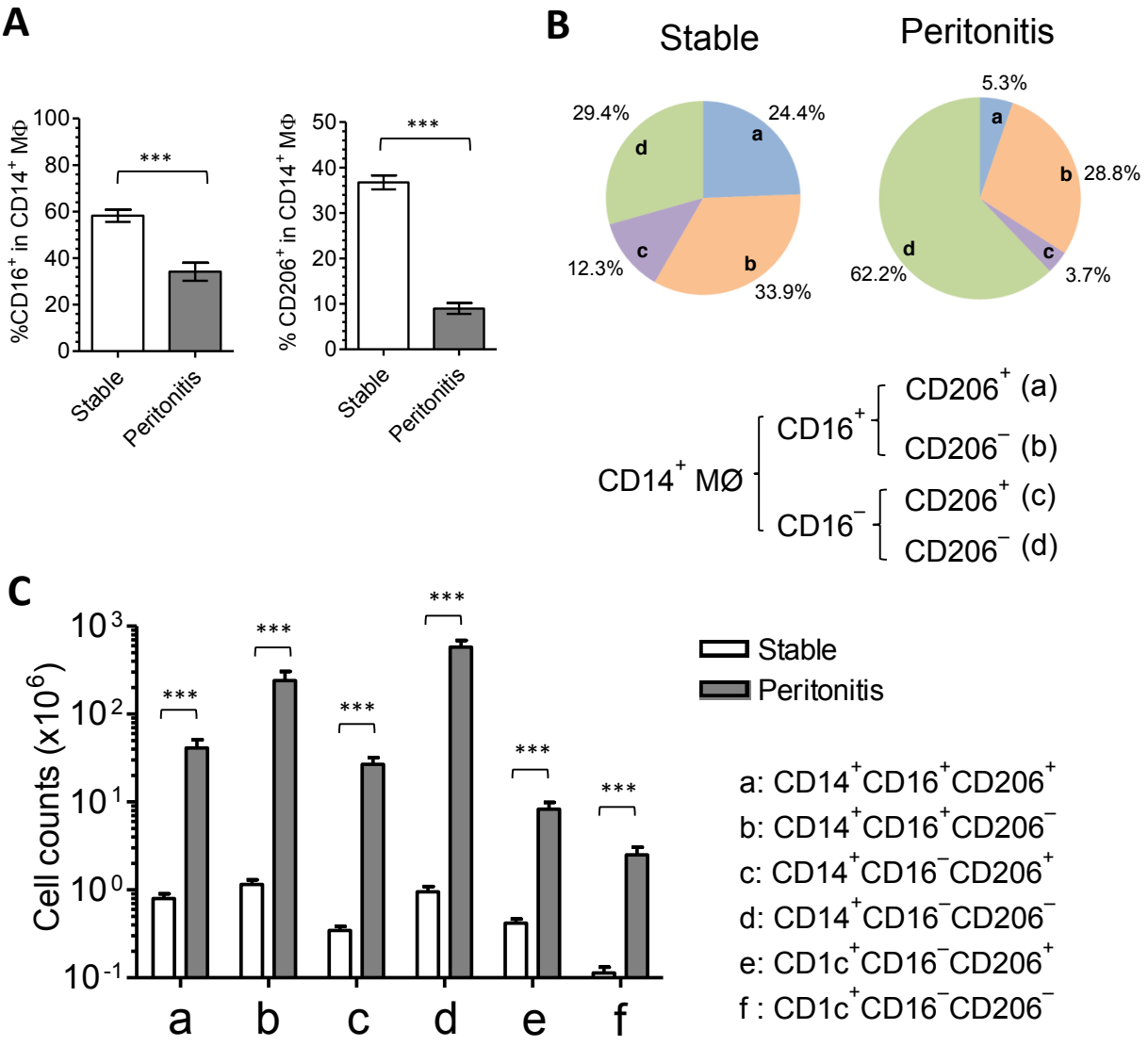

Figure 4.11 Differential distributions of peritoneal MØ/DC subsets between PD patients with bacterial peritonitis *versus* the stable dialysis patients

(A) Graphs showing the proportion of $CD16^+$ (left) or $CD206^+$ (right) expression on $CD14^+$ MØ. **(B)** Pie charts illustrating the distribution of individual MØ subset. **(C)** Graph depicting actual number of each MØ/DC subset within infected PD effluents on day 1 bacterial peritonitis (n = 37) *versus* uninfected fluids from stable dialysis patients (n = 37). Data are shown as mean ± SEM. Data are analysed by Student's *t*-test (if parametric) or Mann Whitney *U* test (if nonparametric). (ns= $P > 0.05$, *= $P \leq 0.05$, **= $P \leq 0.01$ and ***= $P \leq 0.001$)

4.2.8 Differential distributions of peritoneal myeloid cells and MØ/DC subsets between patients with and without treatment failure upon bacterial peritonitis

The reasons for treatment failure upon PD-related bacterial peritonitis may be multi-factorial, including antibiotic efficacy, pathogen virulence, and host immunity. It is assumed that impaired or dysregulated host peritoneal immune response to invaded pathogens may play a contributive role. Here, the aim is to examine whether peritonitis patients with unresolved peritonitis leading to technique failure or infectious deaths, have distinctive recruitment of peritoneal myelomonocytic cells during bacterial peritonitis. To answer this question, the cellular constituents of PD effluent samples from the day 1 bacterial peritonitis were compared between episodes with treatment failure (n = 7) and those successfully treated (n = 30). As shown in Fig. 4.12, unresolved/refractory peritonitis episodes were associated with significantly higher numbers of peritoneal neutrophils, eosinophils, MØs and DCs as well as higher ratio of MØ to DC than successfully treated ones. Although there was no significant difference of the percentage of $CD16^+$ or $CD206^+$ in $CD14^+$ MØs between two groups (Fig. 4.12A), there were significant increase in the numbers of $CD14^+CD16^-$ ($CD206^{+ \text{ or } -}$) MØs in peritonitis patients with poor outcomes, compared to successfully treated group (Fig. 4.13B & C).

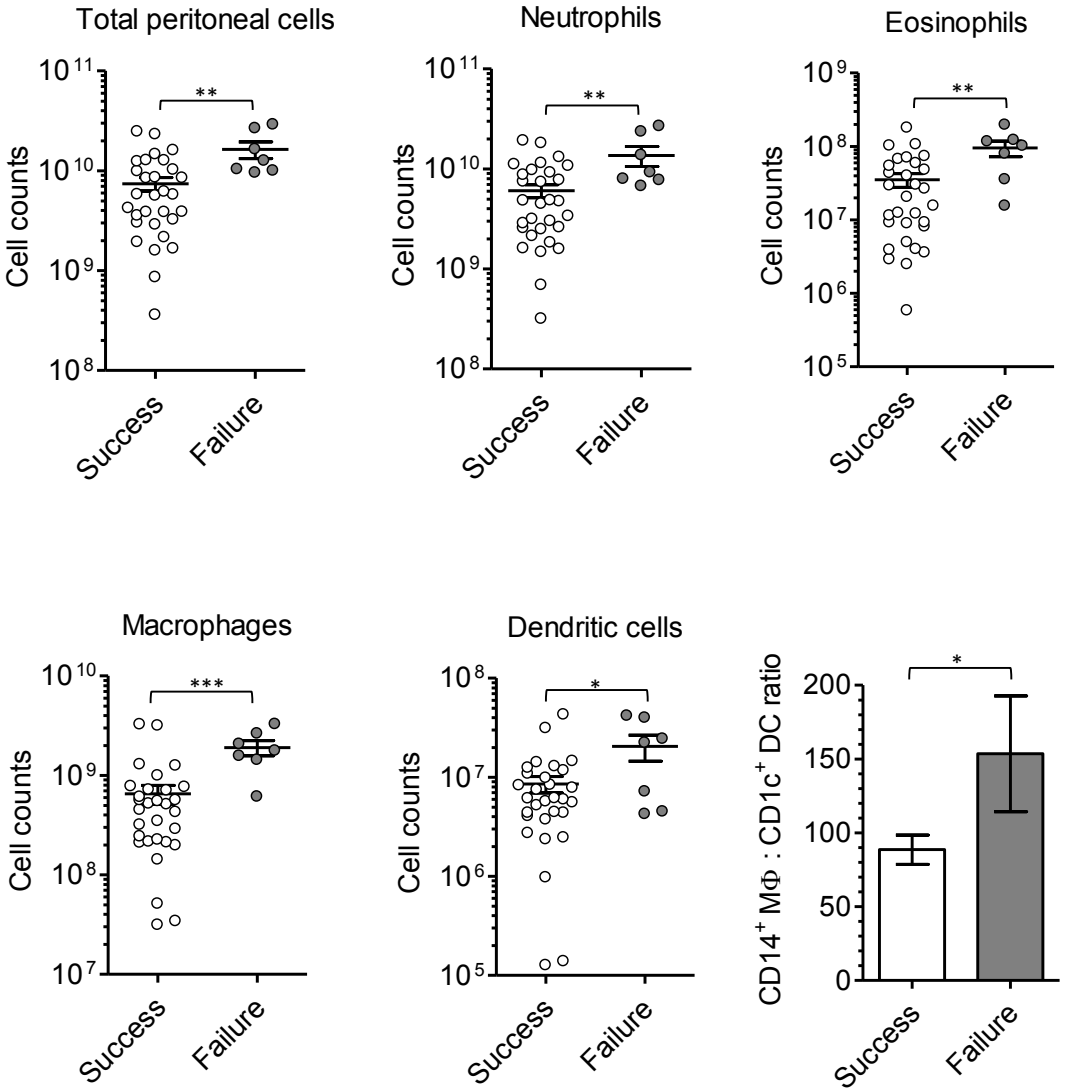

Figure 4.12 Comparisons of major peritoneal myeloid cells between bacterial peritonitis episodes with treatment success *versus* those with treatment failure

Graphs showing the comparisons of total peritoneal cells, peritoneal neutrophils, eosinophils, macrophages and dendritic cells (in number) within PD effluents from the 1st day of acute bacterial peritonitis episodes between "treatment success" group (n = 30) *versus* "treatment failure" group (n = 7). The ratio of $CD14^+$ MØ to $CD1c^+$ DC was also compared between two outcomes. Data are shown as mean ± SEM. Data are analysed by Student's *t*-test (if parametric) or Mann Whitney *U* test (if nonparametric). (ns= $P > 0.05$, *= $P \leq 0.05$, **= $P \leq 0.01$ and ***= $P \leq 0.001$)

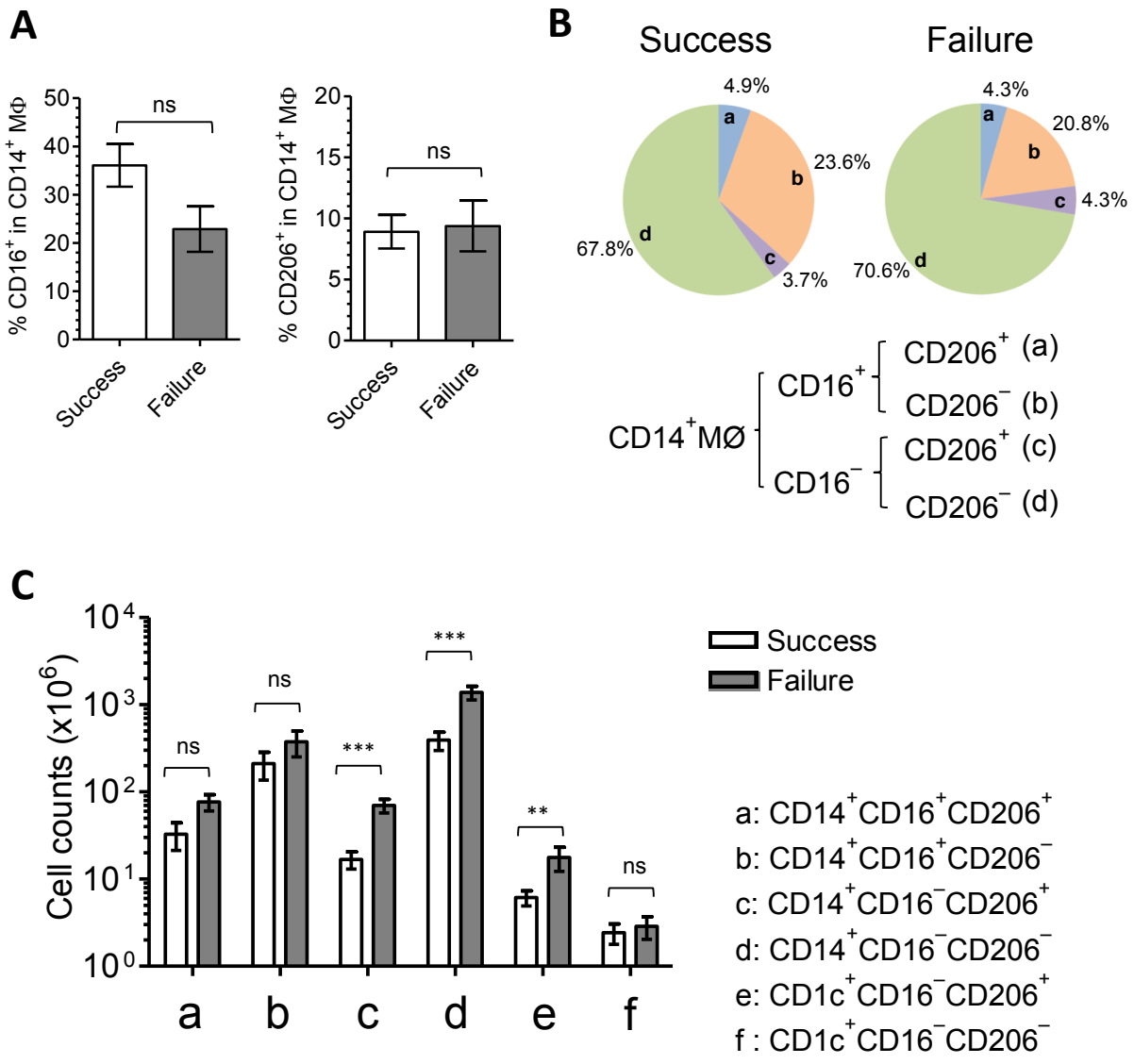

Figure 4.13 Differential distributions of peritoneal MØ/DC subsets between bacterial peritonitis with treatment success *versus* treatment failure

(A) Graphs showing the proportion of $CD16^+$ (left) or $CD206^+$ (right) expression on $CD14^+$MØ. **(B)** Pie charts demonstrating the distribution of individual MØ subset. **(C)** Graph depicting actual number of each peritoneal monocytic subset within PD effluents from the 1st day of acute bacterial peritonitis episodes. The comparisons were performed between "treatment success" group (n = 29) *versus* "treatment failure" group (n = 9). Data are shown as mean ± SEM. Data are analysed by Student's *t*-test (if parametric) or Mann Whitney *U* test (if nonparametric). (ns= $P > 0.05$, *= $P \leq 0.05$, **= $P \leq 0.01$ and ***= $P \leq 0.001$)

4.2.9 Pathogen-specific distributions of peritoneal myeloid cells and MØ/DC subsets during acute bacterial peritonitis

A recent study suggested that pathogen-specific inflammatory characteristics (an "immune fingerprint") based on leukocyte subsets (particular T lymphocyte subsets) and cytokine profiles in PD effluent fluids could distinguish culture-positive from culture-negative peritonitis, as well as gram positive peritonitis from gram negative peritonitis (Lin et al., 2013). Here, the distribution of peritoneal myelomonocytic cells during peritonitis was compared between culture-positive peritonitis (n = 37) and culture-negative peritonitis (n = 5). As shown in Figure 4.14, PD effluents from culture-positive peritonitis had significantly higher numbers of total peritoneal cells and neutrophils, compared to those from culture-negative peritonitis. Additionally, culture-positive peritonitis had a trend to lower proportion of $CD16^+$ or $CD206^+$ in $CD14^+$ MØs (Fig. 4.15A), and more specifically, a higher proportion of $CD16^-$ $CD206^-$ (Fig. 4.15B), than those in culture-negative peritonitis. There was a general trend that culture-positive peritonitis had higher numbers of each MØ/DC subtype than culture-negative peritonitis (Fig. 4.15C).

Next, the comparisons among gram positive peritonitis (n = 26) and gram negative peritonitis (n = 8) and mixed gram positive/negative bacterial peritonitis (n = 3) were conducted. The results showed a trend of higher numbers of each myeloid subset in the mixed gram positive/negative peritonitis, compared to either gram positive or negative peritonitis. No significant differences in numbers of peritoneal neutrophils, eosinophils, MØs and DCs between gram positive and gram negative peritonitis were found (Fig. 4.16). However, those with gram negative peritonitis had a trend for a lower proportion of $CD16^+$ in $CD14^+$ MØ and higher proportion of $CD16^-CD206^-$ than those with gram negative peritonitis (Fig. 4.17).

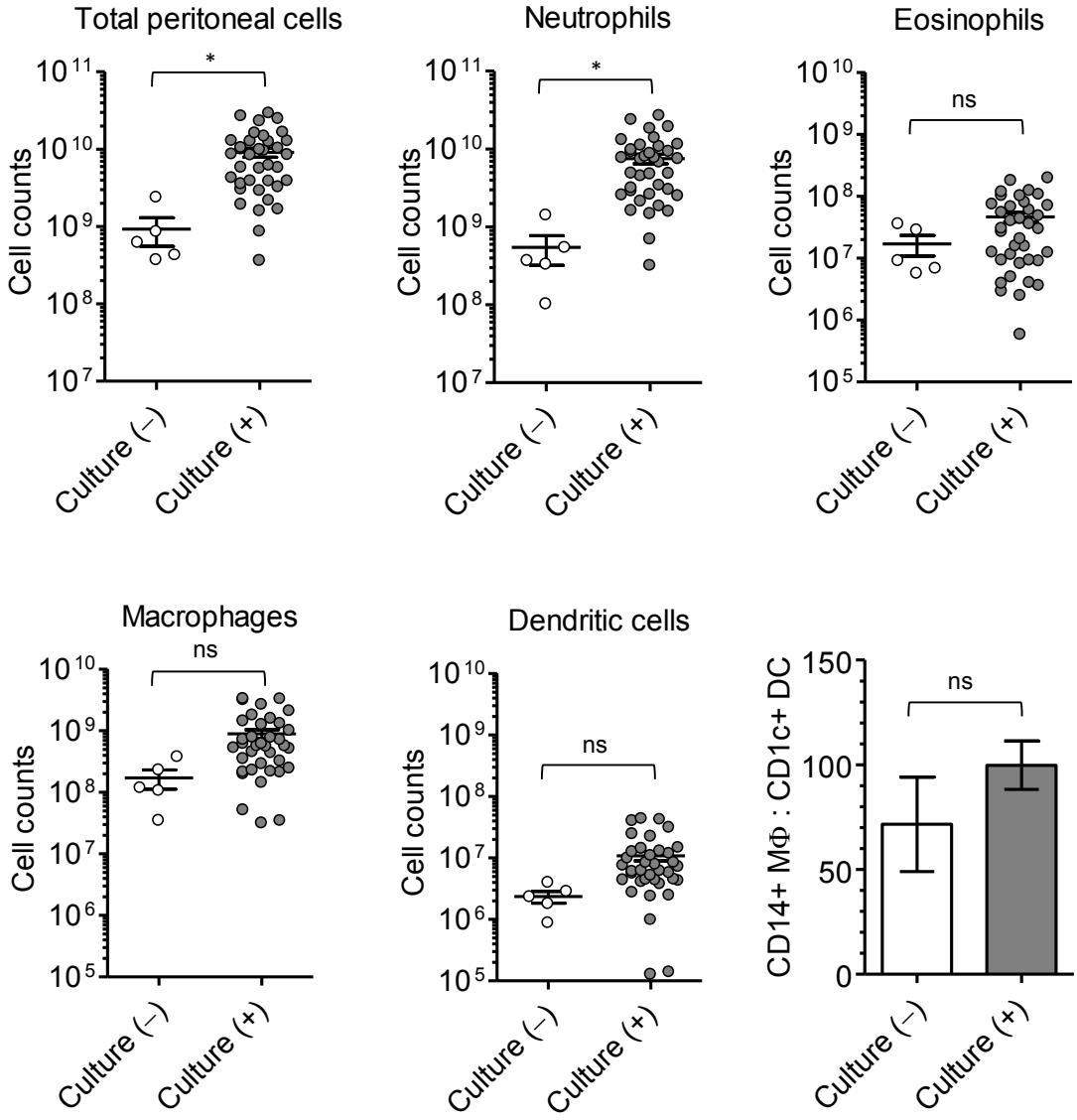

Figure 4.14 Comparisons of major peritoneal myeloid cells between culture-negative *versus* culture-positive peritonitis

Graphs showing the comparisons of total peritoneal cells, peritoneal neutrophils, eosinophils, macrophages and dendritic cells (in number) within PD effluents from the 1st day of PD-related peritonitis between culture-negative peritonitis (n = 5) and culture-positive peritonitis (n = 37). The ratio of $CD14^+$ MØ to $CD1c^+$ DC was compared between two groups (right lower panel). Data are shown as mean ± SEM. Data are analysed by Student's *t*-test (if parametric) or Mann Whitney *U* test (if nonparametric). (ns= $P > 0.05$, *= $P \leq 0.05$, **= $P \leq 0.01$ and ***= $P \leq 0.001$)

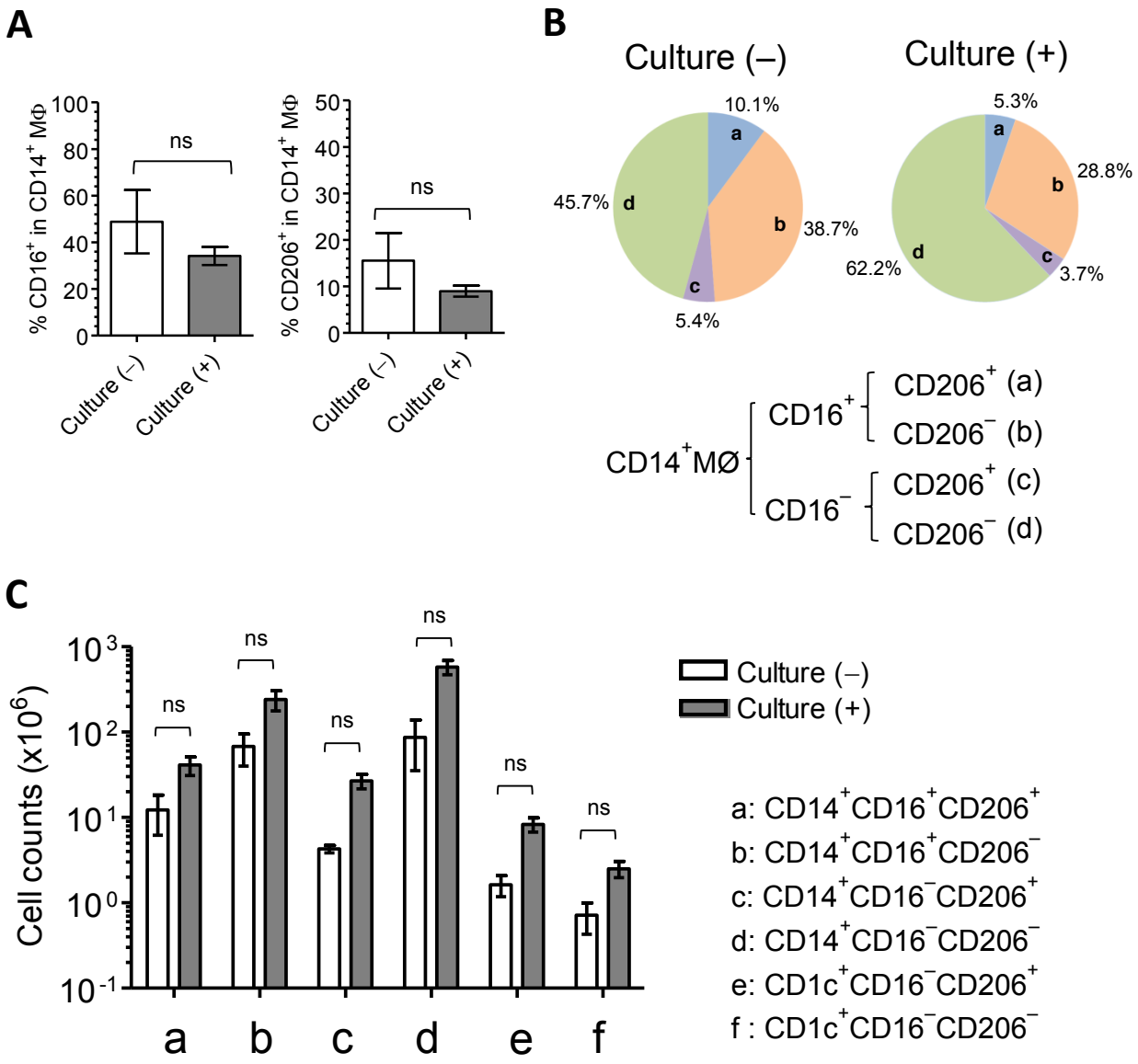

Figure 4.15 Differential distributions of peritoneal MØ/DC subsets between culture-negative and culture-positive bacterial peritonitis

(A) Graphs showing the proportion of $CD16^+$ (left) or $CD206^+$ (right) expression on $CD14^+$ MØ. Horizontal bars represent the mean. **(B)** Pie charts demonstrating the distribution of individual MØ subset. **(C)** Graph depicting actual number of each peritoneal monocytic subset within PD effluents from the 1st day of PD-related peritonitis. The comparisons were performed between culture-negative (n = 5) *versus* culture-positive peritonitis (n = 37). Data are shown as mean ± SEM. Data are analysed by Student's *t*-test (if parametric) or Mann Whitney *U* test (if nonparametric). (ns= $P > 0.05$, *= $P \leq 0.05$, **= $P \leq 0.01$ and ***= $P \leq 0.001$)

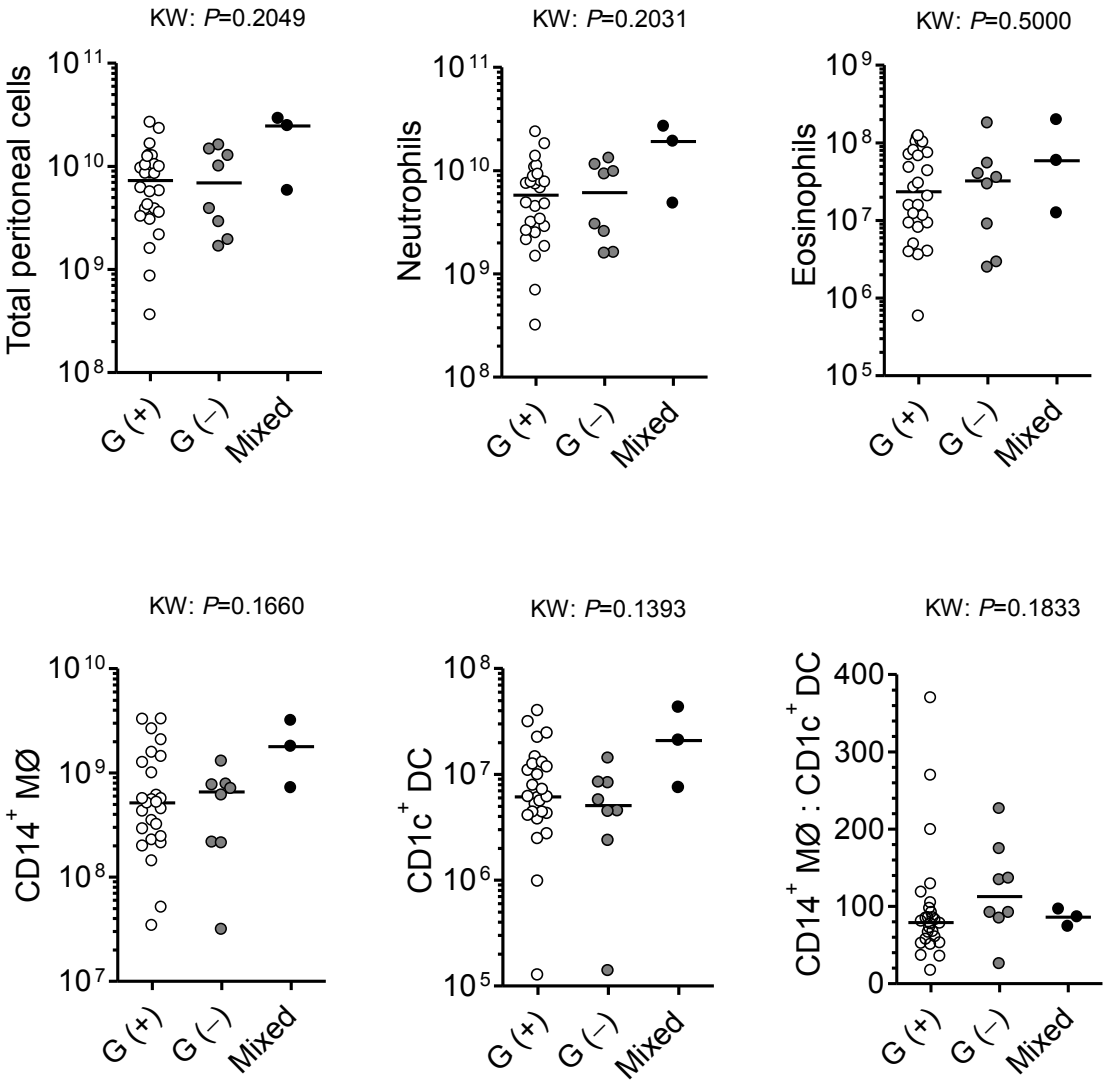

Figure 4.16 Comparisons of major peritoneal myeloid cells among gram-positive, gram-negative and mixed bacterial peritonitis

Graphs showing the comparisons of total peritoneal cells, peritoneal neutrophils, eosinophils, macrophages and dendritic cells (in number) within PD effluents from the 1st day of bacterial peritonitis among gram-positive (n = 8), gram-negative and mixed bacterial peritonitis (n = 20). The ratio of $CD14^+$ MØ to $CD1c^+$ DC was also compared. Horizontal bars denote the median. Data are analysed for statistical significance by Kruskal-Wallis (KW) test and Dunn's multiple comparison post-tests (asterisks) are indicated where significant (ns= $P > 0.05$, *= $P \leq 0.05$, **= $P \leq 0.01$ and ***= $P \leq 0.001$)

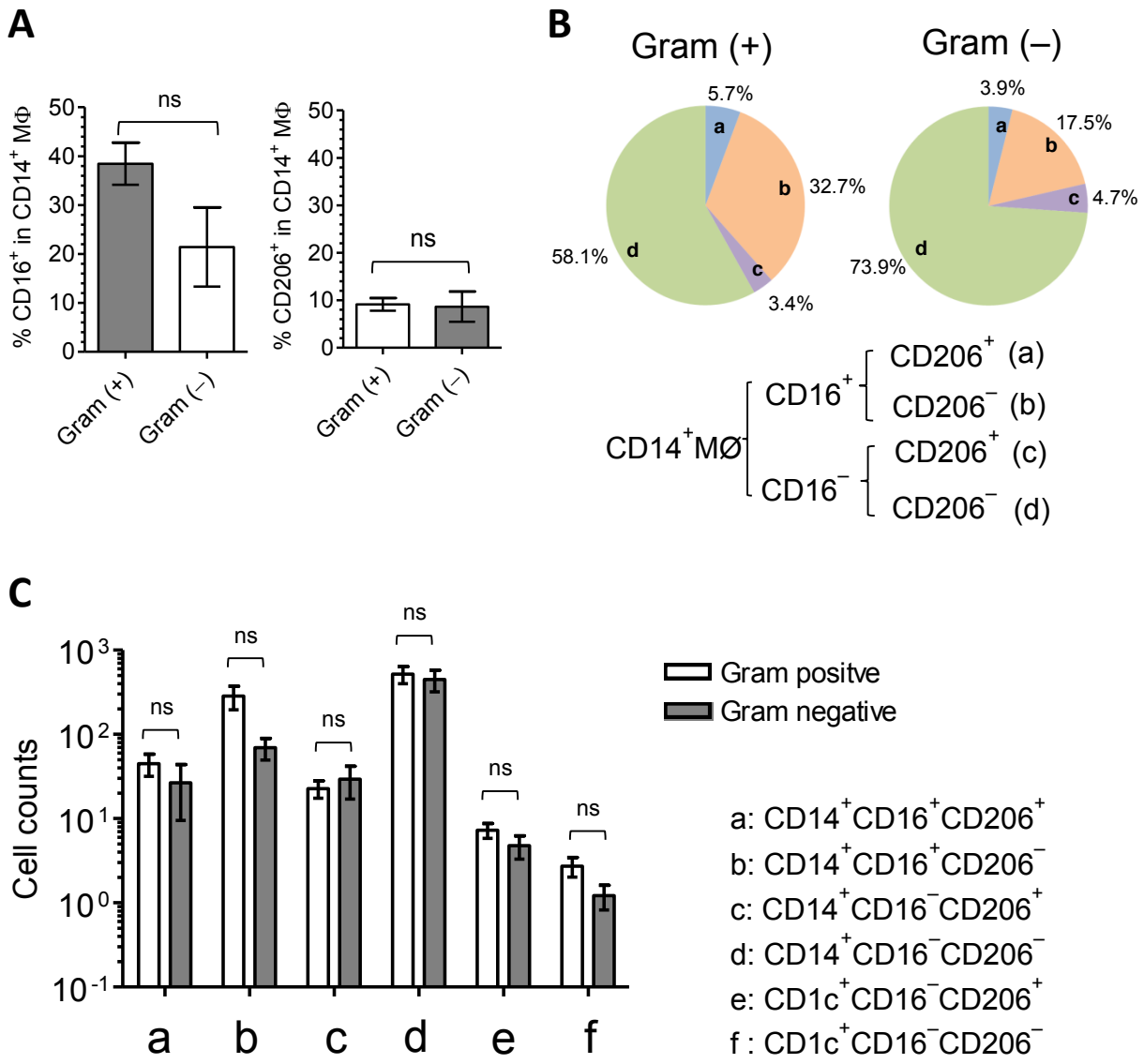

Figure 4.17 Differential distributions of peritoneal MØ/DC subsets between gram-positive and gram-negative bacterial peritonitis

(A) Graphs showing the proportion of $CD16^+$ (left) or $CD206^+$ (right) expression on $CD14^+$ MØ. **(B)** Pie charts demonstrating the distribution of individual MØ subset. **(C)** Graph depicting actual number of each peritoneal monocytic subset within PD effluents from the 1st day of bacterial peritonitis. The comparisons were performed between gram-negative (n = 5) *versus* gram-positive bacterial peritonitis (n = 24). Data are shown as mean ± SEM. Data are analysed by Student's *t*-test (if parametric) or Mann Whitney *U* test (if nonparametric). (ns= $P > 0.05$, *= $P \leq 0.05$, **= $P \leq 0.01$ and ***= $P \leq 0.001$)

4.2.10 Impact of peritonitis history on the distributions of peritoneal myeloid cells and MØ/DC subsets in patients under stable dialysis

Clinically, some PD patients might experience one or more episodes of peritonitis during maintenance dialysis, while others could remain free from peritonitis for years. Earlier study revealed that stable PD patients who had a peritonitis history would have a distinct immunological profile of peritoneal MØ, compared to patients free from peritonitis (Lin et al., 1990). Whether or not the history of peritonitis would change the distribution of peritoneal myeloid cells and MØ/DC phenotypes is unclear. Here, a comparison of stable dialysis patients (defined as maintaining PD for at least one year) without history of peritonitis and those with only one episode or multiple episodes of peritonitis showed that there is a higher number of peritoneal MØs as well as higher MØ to DC ratio in patients with multiple episodes of peritonitis, compared to those without any history of peritonitis (Fig. 4.18). However, there is no difference between those with single peritonitis episode and those without any history of peritonitis in terms of each myeloid subset. Compared with no history of peritonitis, those with history of peritonitis (including single and multiple episodes) had a trend of increase in the proportion and also the number of $CD14^{+}CD16^{+}CD206^{-}$ subtype (Fig. 4.19).

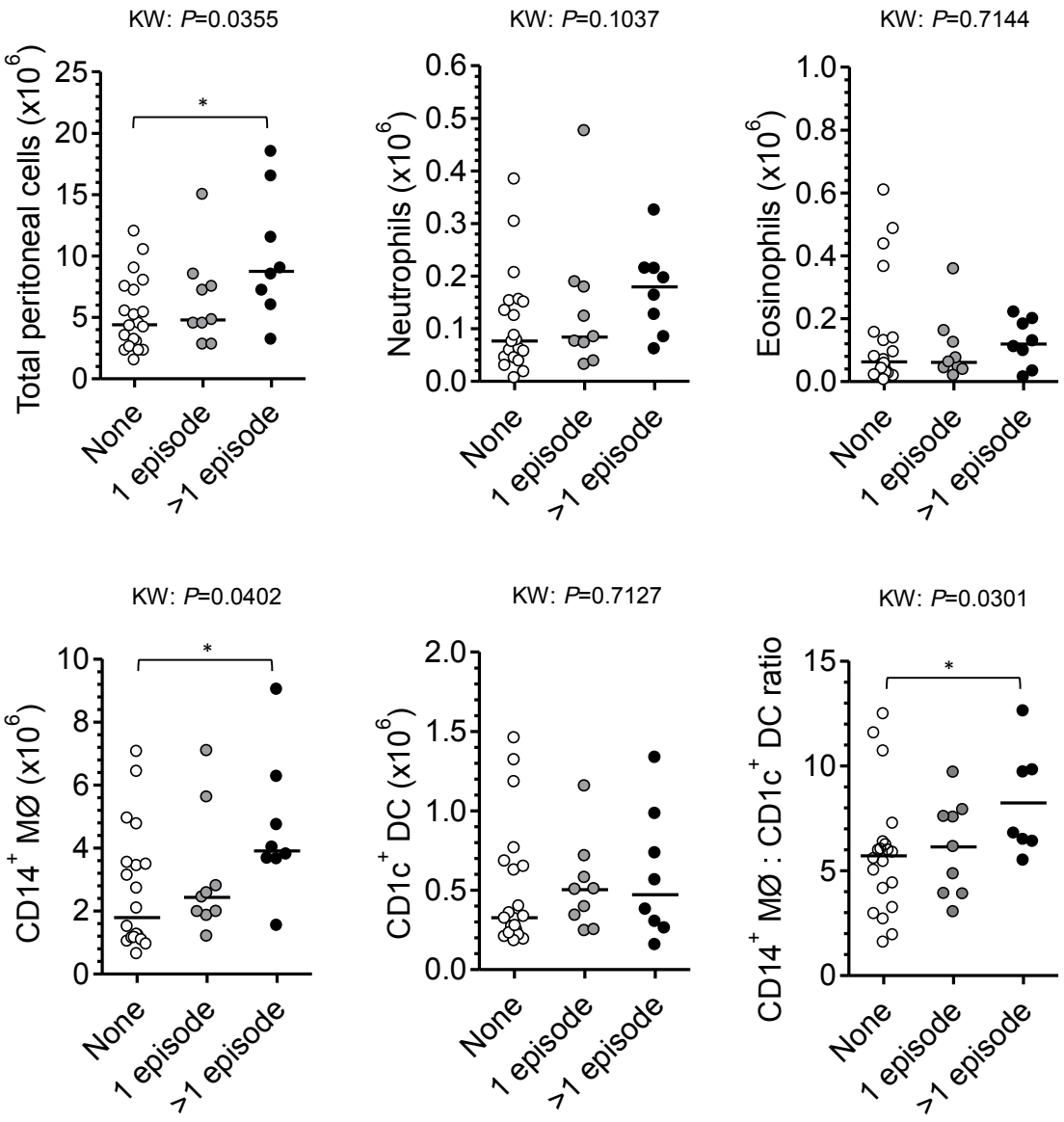

Figure 4.18 Comparisons of major peritoneal myeloid cells and MØ/DC subsets between stable dialysis patients without history of peritonitis, with only one episode of peritonitis and with more than one episode of peritonitis

Graphs showing the comparisons of peritoneal neutrophils, eosinophils, macrophages and dendritic cells (in number) within PD effluents from stable dialysis patients without history of peritonitis (n = 20), with only one episode of peritonitis (n = 9) and with more than one episode of peritonitis (n = 8). The ratio of $CD14^+$ MØ to $CD1c^+$ DC was also compared. Horizontal bars denote the median. Data are analysed for statistical significance by Kruskal-Wallis (KW) test and Dunn's multiple comparison post-tests (asterisks) are indicated where significant (ns= $P > 0.05$, *= $P \leq 0.05$, **= $P \leq 0.01$ and ***= $P \leq 0.001$)

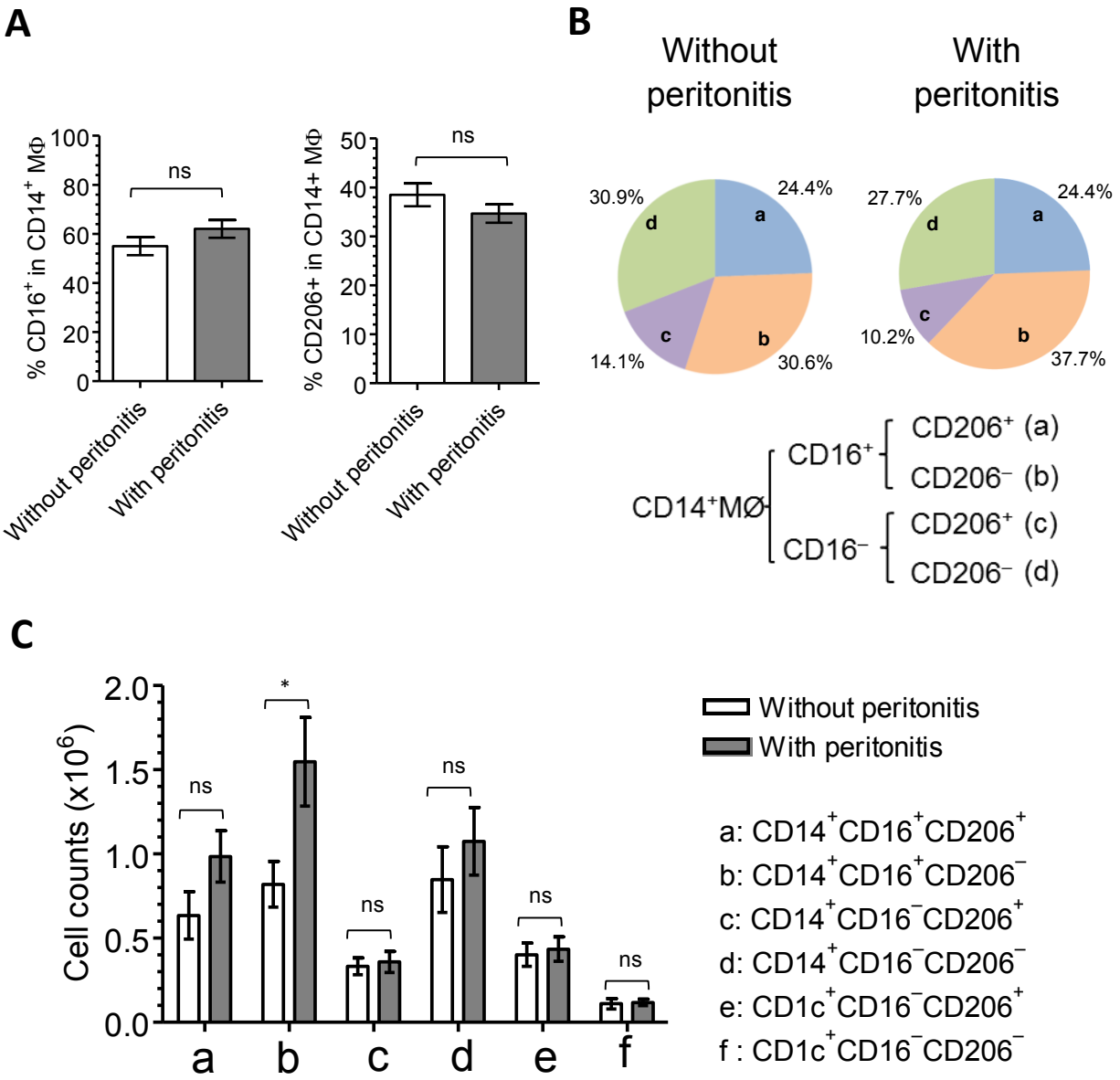

Figure 4.19 Differential distributions of major peritoneal MØ/DC subsets between stable dialysis patients without history of peritonitis and those with history of peritonitis

(A) Graphs showing the proportion of $CD16^+$ (left) or $CD206^+$ (right) expression on $CD14^+$ MØ. **(B)** Pie charts demonstrating the distribution of individual MØ subset. **(C)** Graph depicting actual number of each peritoneal monocytic subset within PD effluents from stable dialysis patients without and with peritonitis. The comparisons were performed between those without peritonitis history (n = 20) *versus* those with peritonitis history (n = 17). Data are shown as mean ± SEM. Data are analysed by Student's *t*-test (if parametric) or Mann Whitney *U* test (if nonparametric). (ns= $P > 0.05$, *= $P \leq 0.05$, **= $P \leq 0.01$ and ***= $P \leq 0.001$)

4.3 Discussion

The results in this chapter have demonstrated that the intervention of PD therapy in ESRD patients has changed the peritoneal immune system and altered the composition of peritoneal myeloid subsets and the MØ/DC phenotypes as well as their activation/maturation status. Individual clinical circumstance, such as post-catheter implantation in new-starters, during acute PD-related peritonitis, or under long-term stable dialysis, displayed unique distributions of myeloid subpopulations and distinct MØ/DC phenotypic changes. These observations also suggested that the altered constituents of peritoneal myeloid cells as well as the variable MØ/DC phenotypes and activation/ maturation status might represent different situations of intraperitoneal inflammation, which in turn could be linked to different patients' clinical outcomes.

In new-starter patients, the compositions of peritoneal myeloid cells and MØ/DC phenotypes have been greatly altered by the commencement of PD. Mononuclear phagocytes become the predominant leukocytes in the peritoneal cavity after dialysis. Perhaps the most interesting finding is the distinctive kinetics of $CD14^+$ MØs and $CD1c^+$ DCs during the course of PD therapy. $CD1c^+$ DCs maintained a relatively stable number in the pre-dialysis phase and appeared more resistant to the dialysis depletion, which was in contrast to $CD14^+$ MØs, implying these two monocytic subsets might have distinctive recruitment and/or differentiation processes during homeostasis and inflammation. Indeed, a significantly greater number of $CD14^+$ MØs were recruited during an episode of peritonitis, compared to $CD1c^+$ DCs. In the future, it may be of interest to explore the underlying mechanisms controlling the trafficking of the respective cell types, or differentiation pathways, in a particular clinical setting.

Regarding the MØ subtypes, the results suggested that the mature $CD16^{+}CD206^{+}$ MØs considerably decreased after dialysis intervention, replaced by the relatively immature $CD16^{+}CD206^{-}$ MØs. This phenomenon could be explained by the maturation process of newly recruited MØs being perturbed under continuous dialysis process, possibly due to dilution of the growth factors that stimulate MØ maturation. Upon peritonitis, $CD16^{-}CD206^{-}$ MØs became the major subtype. As these MØs were phenotypically close to circulating classical blood monocytes, it is suggested that the latter were heavily recruited into peritoneal cavity upon PD-related peritonitis. The fate of these recruited MØs, either becoming activated or differentiated into other subsets, is difficult to determine owing to the practice of continuous fluid exchanges in the context of PD.

In the aspect of the associations between the peritoneal immune characteristics and patient outcomes, the relatively small size of this cohort did limit the interpretation of the results. However, some of the preliminary observations are noteworthy. For example, the ratio of MØ to DC could be a potential indicator of the severity of intraperitoneal inflammation. Higher MØ/DC ratio was associated with poor patient outcomes as demonstrated in new-starter patients (catheter failure *versus* no failure) and in peritonitis cases (treatment failure *versus* treatment success). The value of the differential expression of CD16 and CD206 in $CD14^{+}$ MØs (or the distribution of MØ subtypes) in predicting patient outcomes is not prominent in the present study, although it is worth pointing out some alterations possibly correlating to clinical outcomes. For example, the increased proportion of $CD16^{-}CD206^{-}$ MØs ("monocyte-like") has been noted in peritonitis cases with culture-positive (*versus* culture-negative), gram-negative (*versus* gram-positive) as well as treatment failure (*versus* treatment success), suggesting the "skewed" pattern of peritoneal MØ

activation/maturation might reflect a unique inflammatory scenario. Larger size of patient cohorts would be needed to justify these complex relationships. As for stable dialysis patients, there seemed to be a trend that patients experiencing multiple peritonitis episodes may have a higher number of peritoneal MØs and a higher ratio of MØ to DC, compared to those without any history of peritonitis. This preliminary observation could be explained by the fact that patients have had multiple episodes of peritonitis would acquire a more inflamed peritoneum with more inflammatory monocyte/MØ infiltration and then release into the peritoneal cavity. Indeed, a recent observational study revealed that stable dialysis patients with past history of peritonitis had higher levels of dialysate MCP-1, a major inflammatory chemokine for monocyte migration, compared to those with no history of peritonitis (Malik et al., 2007). Interestingly, both peritoneal macrophage infiltration (Sawai et al., 2011) and dialysate MCP-1 level (Malik et al., 2007) are positively correlated with higher peritoneal solute transport rate in new-starter PD patients and in stable dialysis patients, respectively. Hence, the increased MØ accumulation (and also the MØ to DC ratio) within PD effluents may reflect chronic inflammation of the patient's peritoneal membranes as a sequela of repeated peritonitis. However, it has to be mentioned that even in patients without any history of peritonitis, there is a substantial variation of peritoneal MØ number accumulating within PD effluents, suggesting that other factors such as uraemic background, time and/or types of dialysis fluids use, may also contribute to local peritoneal inflammation in long-term PD patients.

Chapter Five

Characterisation of 'dendritic cell-like' subsets in murine peritoneal cavity

5.1 Introduction

Dendritic cells (DCs) are professional antigen-presenting cells (APCs), acting as central regulators between innate and adaptive immune system. Recently, subsets of heterogeneous DC populations in lymphoid and non-lymphoid tissues have been defined in mice and humans (Merad et al., 2013; Schlitzer and Ginhoux 2014), however, the DC phenotype in the mouse peritoneal cavity and its role in the clinically relevant experimental peritonitis models remains poorly understood. In parallel with the novel identification of human peritoneal DCs within the dialysate of PD patients (see Chapter 3 and 4), it is important to investigate the immunobiology of mouse peritoneal DC subsets in order to understand possible variations between humans and mice in terms of cellular kinetics during peritonitis as well as their phenotypes and functions. Moreover, the interspecies comparisons will be useful in the future for defining the role of peritoneal DCs in pathological conditions including acute peritonitis and repeated peritonitis-related peritoneal fibrosis.

In the peritoneal cavity of mice, the initial observations of Steinman's group identified a relatively rare population with high MHCII expression and weak CD11c expression, but this was masked by the relative high autofluorescence of resident macrophages ('ResMØs') (Witmer-Pack et al., 1993). Recently, a 12/15-LOX^{-} myeloid cell type in the naïve peritoneal cavity has been characterised by our group, with a distinct F4/80$^{int/low}$MHCII^{+} and high expression of CD116 (GM-CSF receptor alpha-chain) and CD206 (macrophage mannose receptor). These cells were able to mount effective inflammatory responses (Rosas et al., 2007; Dioszeghy et al., 2008) and present model antigens to naïve CD4^{+} T cells, which led to their tentative classification as 'DC-like' cells (Dioszeghy et al., 2008). However, we could not clearly identify these 'DC-like'

cells within the bulk population of infiltrating MØs in the inflammatory settings (named as inflammatory macrophages, 'InfMØs') due to their overlapping immunophenotypes ($F4/80^{int/low}MHCII^{+}$). Subsequently, the presence and function of these cells has been ratified by other groups, however, the inability to discriminate these cells from monocyte-derived $MHCII^{+}$ InfMØs, has led to the ambiguity and confusion of whether these cells represent a mix of '*bona-fide*' DC and $MHCII^{+}$ MØ populations during inflammation (Ghosn et al., 2010; Cassado Ados et al., 2011; Nguyen et al., 2012).

Since these peritoneal DC subsets remain poorly defined, the functional roles and cellular kinetics of these particular cell types during tissue homeostasis as well as intraperitoneal inflammation-resolution process are also not well characterized.

Hence, the specific aims of this chapter are:

1. To validate a select panel of surface markers for phenotypic determination of peritoneal 'DC-like' subsets during homeostasis and inflammation.
2. To investigate the respective cellular kinetics of distinct peritoneal MØ/DC subpopulations in relevant experimental peritonitis models, including acute SES-induced peritonitis and acute zymosan-induced peritonitis.
3. Finally, to assess each individual subset's responsiveness to external microbial product stimulation, capacity to clear apoptotic cells and their capability of processing and presenting antigen to helper T cells.

Together, these data will help to delineate the nature of the DC network in the murine peritoneal cavity and will inform as to whether mouse peritoneal DCs exhibit similarities with the newly identified human peritoneal DCs, and hence whether mice are a useful animal model for the study of human diseases.

5.2 Results

5.2.1 Phenotypic identification of murine peritoneal 'DC-like' subsets under steady state

Myelomonocytic cells in the mouse peritoneal cavity can be subdivided based on expression of CD11b and F4/80 (Rosas et al., 2007; Dioszeghy et al., 2008; Ghosn et al., 2010). In the steady state, apart from the large number of $CD11b^{high}F4/80^{high}MHCII^{low/-}$ ResMØs, a minor population has been noted with a $CD11b^{int}F4/80^{int\text{-}low}MHCII^{+}$ phenotype (Fig. 5.1A). This rare population, considered to be 'DC-like' because of their ability to present antigen to naïve T cells (Dioszeghy et al., 2008), is phenotypically heterogeneous and not readily defined by CD11c, a traditional surface marker for DCs. More importantly, these cells could not be clearly discriminated from recruited InfMØs during inflammation in our previous studies (Rosas et al., 2007; Dioszeghy et al., 2008). By analysis of published microarray data comparing peritoneal '$F4/80^{low}MHCII^{+}$' cells (most likely a mixed population, containing InfMØs and 'DC-like' cells) with '$F4/80^{int}MHCII^{+}$' cells (predominantly comprising InfMØs) 5 days after the induction of inflammation with thioglycollate broth, a series of differentially expressed genes were identified (Table 1, data analysis performed by Dr. Peter Giles). Notably, $F4/80^{low}MHCII^{+}$ cells were associated with higher expression of *Cd226* and *Cd209a*. Based on the differential surface expression of CD11c and CD226, three putative peritoneal 'DC-like' subsets could be separated: $CD226^{+}CD11c^{+}$, $CD226^{+}CD11c^{low}$ and $CD11c^{+}CD226^{low}$ (Fig. 5.1A). Interestingly, $CD226^{+}$ cells were associated with higher CD11b, but heterogeneous CD209a and CD11c. Whilst $CD11c^{+}CD226^{low}$ cells were primarily $CD209^{+}$ and had lower CD11b than their $CD226^{+}$ counterparts (Fig. 5.1B). Thus neither CD11c nor CD209a allowed

definitive identification of a discrete DC population, but $CD11c^{+}CD226^{low}$ expression did appear to define one population of cells.

Further immunophenotyping depicts that all three putative peritoneal 'DC-like' populations and ResMØs, express co-stimulatory molecules CD80 and CD86 (Fig. 5.2), however, only the 'DC-like' cells express CD206 (macrophage mannose receptor) (also shown by Dioszeghy et al., 2008), CD301 (macrophage galactose-type C-type lectin, MGL1/MGL2) and CCR2. Of the three subsets, $CD11c^{+}CD226^{low}$ cells have more uniformly high CD209a (DC-SIGN) expression. By contrast, ResMØs express higher levels of MerTK, CD36, CD64 (FcγRI) and CD73 than all three 'DC-like' subsets, suggesting that these markers are more 'MØ-associated'.

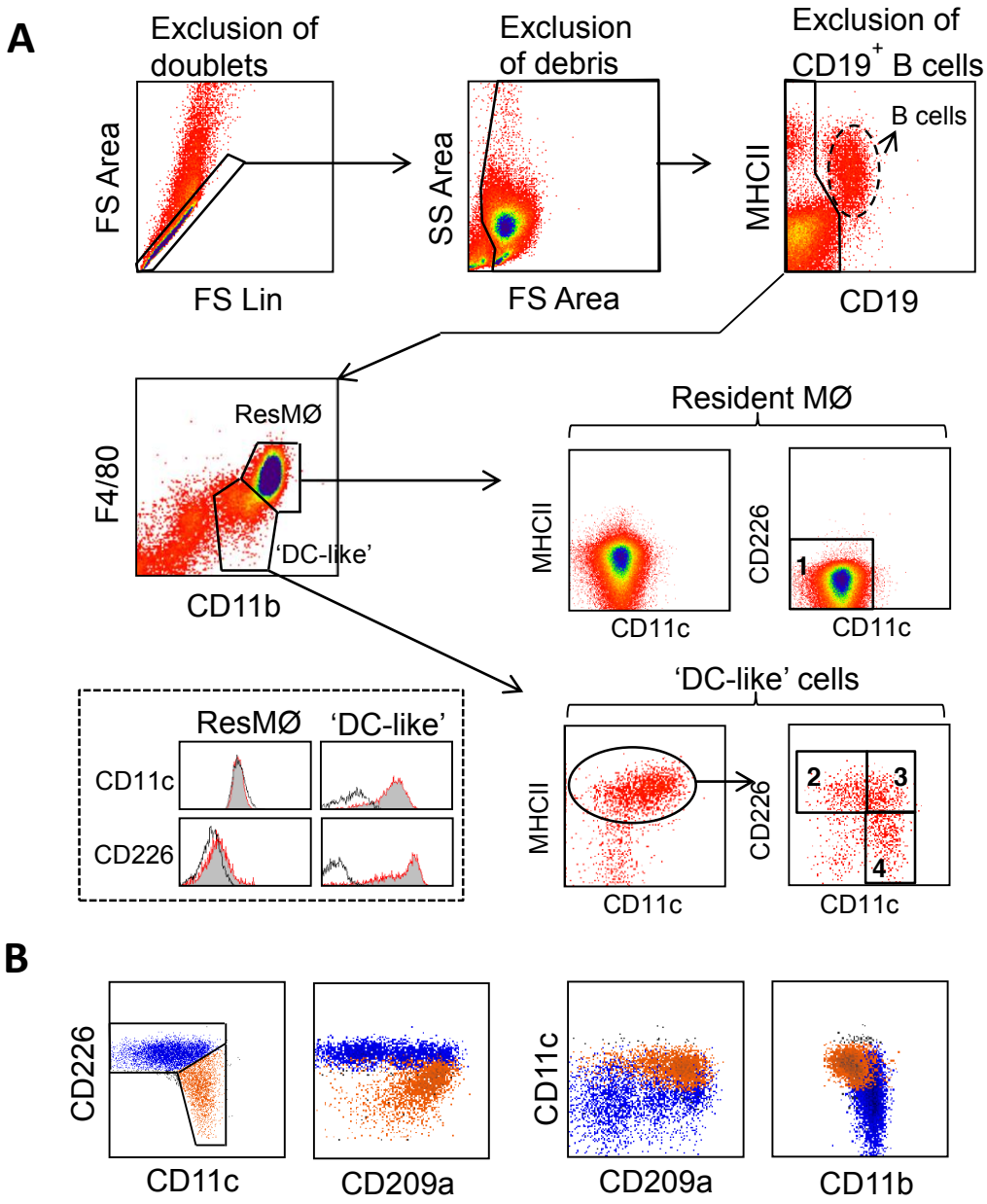

Figure 5.1 Phenotypic identification of peritoneal 'DC-like' subsets in the naïve murine peritoneal cavity

(A) Flow-cytometric analysis of peritoneal cells from naïve mice. Density plots shown were gating strategies to identify ResMØs ($CD11b^{high}F4/80^{high}MHCII^{low/-}$) and 'DC-like' cells ($CD11b^{int}F4/80^{int\text{-}low}MHCII^{+}$). The latter were readily subdivided into three subsets: $CD226^{+}CD11c^{low}$, $CD226^{+}CD11c^{+}$and $CD11c^{+}CD226^{low}$. Histogram plots depicted expression level of CD11c and CD226 on ResMØs and 'DC-like' cells. Shaded histograms depict receptor specific staining and bold lines denote isotype control staining. **(B)** Multi-colour analysis highlighting heterogeneity of CD226 and CD209a expression. Data are representative of two independent experiments with C57BL/6 mice.

Table 5.1 Differentially expressed genes between peritoneal F4/80^{low}MHCII^{+} MØs and F4/80^{int}MHCII^{+} MØs during thioglycollate peritonitis (Gautier 2012). Only genes showing a >5-fold difference in expression are shown.

Probe ID	*P*-value	Abs FC	Symbol	Description
10576784	*1.29E-08*	*19.56224*	*Cd209a*	*CD209a antigen*
10483046	1.29E-08	18.37917	Dpp4	dipeptidylpeptidase 4
10457168	*2.14E-08*	*14.52031*	*Cd226*	*CD226 antigen*
10414262	2.07E-08	13.73705	Ear2	eosinophil-associated, ribonuclease A family, member 2
10419154	1.26E-07	12.46663	Ear1	eosinophil-associated, ribonuclease A family, member 1
10541581	5.55E-08	11.95879	Clec4b1	C-type lectin domain family 4, member b1
10419156	2.14E-08	11.52477	Ear10	eosinophil-associated, ribonuclease A family, member
10576829	1.25E-08	11.52477	Cd209c	CD209c antigen
10598175	1.31E-08	11.26155	Ear10	eosinophil-associated, ribonuclease A family, member
10538791	1.13E-07	10.0329	Tnip3	TNFAIP3 interacting protein 3
10415392	2.71E-08	9.781122	Ltb4r1	leukotriene B4 receptor 1
10399691	8.32E-09	9.042155	Id2	inhibitor of DNA binding 2
10497345	3.02E-08	8.574188	751864	predicted gene, 751864
10351644	9.29E-07	7.835362	Cd244	CD244 natural killer cell receptor 2B4
10548552	1.54E-07	7.799239	Klra2	killer cell lectin-like receptor, subfamily A, member 2
10548314	2.69E-06	7.464264	Klrb1b	killer cell lectin-like receptor subfamily B member 1B
10352000	5.36E-07	7.143676	Kmo	kynurenine 3-monooxygenase (kynurenine 3-
10538802	4.07E-08	6.868523	A930038C07Rik	RIKEN cDNA A930038C07 gene
10538356	2.07E-08	6.528116	Chn2	chimerin (chimaerin) 2
10362896	1.54E-07	6.483023	Cd24a	CD24a antigen
10597743	3.13E-08	6.379014	Cx3cr1	chemokine (C-X3-C) receptor 1
10548105	4.94E-07	6.276673	Ccnd2	cyclin D2
10364038	4.73E-08	6.247735	Upb1	ureidopropionase, beta
10499189	1.53E-08	6.218931	Fcrls	Fc receptor-like S, scavenger receptor
10548345	1.98E-06	6.090947	Klrk1	killer cell lectin-like receptor subfamily K, member 1
10555297	2.48E-08	5.656854	Kcne3	potassium voltage-gated channel, Isk-related subfamily,
10530827	1.49E-07	5.451551	Spink2	serine peptidase inhibitor, Kazal type 2
10538150	6.04E-07	5.36409	Tmem176a	transmembrane protein 176A
10439542	2.31E-06	5.278032	Zdhhc23	zinc finger, DHHC domain containing 23
10470529	3.44E-07	5.074738	Olfm1	olfactomedin 1
10569646	2.71E-08	5.063026	Ccnd1	cyclin D1
10351792	1.89E-06	5.039684	Slamf9	SLAM family member 9

Abs FC, absolute fold change

Note: Microarray data analysis is performed by Dr. Peter Giles. CEL files were downloaded from GEO (GSE15907) before expression summarization using the RMA algorithm in R (Irizarry et al., 2003). Differentially expressed genes were identified using limma (Smyth GK 2005) with *P*-values corrected for multiple testing and false discovery (Benjamini Y and Hochberg Y 1995).

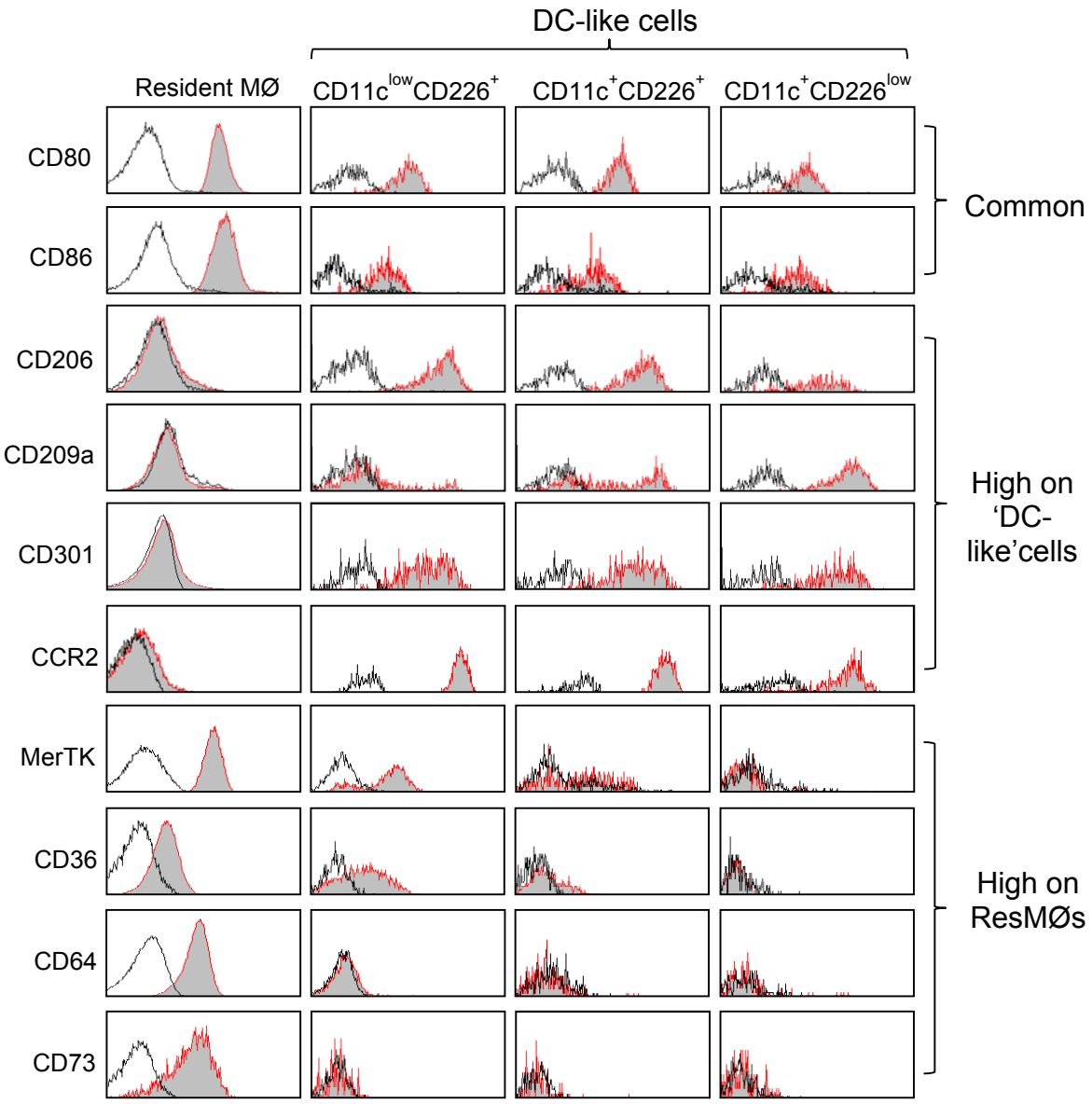

Figure 5.2 Phenotypic comparisons between peritoneal resident MØs and three 'DC-like' subsets from naïve mice

Flow-cytometric analysis of select marker expression by peritoneal ResMØs and three 'DC-like' subsets. Representative histogram plots were pre-gated on the respective cells based on definitive phenotypic markers after exclusion of doublets, debris and $CD19^+$ B cells (as shown in Fig. 5.1A). Shaded histograms depict receptor specific staining and bold lines denote isotype control staining. Data are representative of two independent experiments with a total of four C57BL/6 mice.

5.2.2 Phenotypic discrimination between murine peritoneal 'DC-like' subsets and recruited monocyte-derived macrophages during inflammation

Previously, our group and others have characterized a $CD11b^{int}F4/80^{int}MHC^{+\text{ to low/}-}$ monocytic population during experimental peritonitis (Rosas et al., 2007; Ghosn et al., 2010). We denoted them as 'inflammatory MØs (InfMØs)', to distinguish them from $CD11b^{high}F4/80^{high}$ ResMØs, and because of their large accumulation within the peritoneal cavity upon elicited peritonitis. Adoptive transfer experiments and bone marrow chimera studies suggested that these cells are peripherally recruited, with limited self-renewal ability (Davies et al., 2011 & 2013). However, a lack of definitive markers has led to ambiguity, and confusion of these cells with monocyte-derived InfMØs and potential 'DC-like' cells during inflammation (Ghosn et al., 2010; Nguyen et al., 2012). Here, using the combination of CD11c and CD226, this mixed MØ/DC population, defined as $CD11b^{int}F4/80^{int\text{ to }low}Tim4^{-}$ (Tim4 is a useful marker for distinguishing the majority of ResMØs from InfMØ/DCs, Davies et al., 2011), could be separated into $CD226^{-}CD11c^{-}$ InfMØs as well as three 'DC-like' subsets ($CD226^{+}CD11c^{+}$/$CD226^{+}CD11c^{low}$/$CD11c^{+}CD226^{low}$) (Fig. 5.3). Further phenotyping depicts that the marker expression profiles of three peritoneal 'DC-like' populations and ResMØs under inflammation are similar with those under naïve status except for the decreased expression of CD73 on ResMØs (Fig. 5.4). Of note, InfMØs express CD206 and CCR2 like the 'DC-like' cells, while they express MerTK, CD36 and CD64, similar to ResMØs.

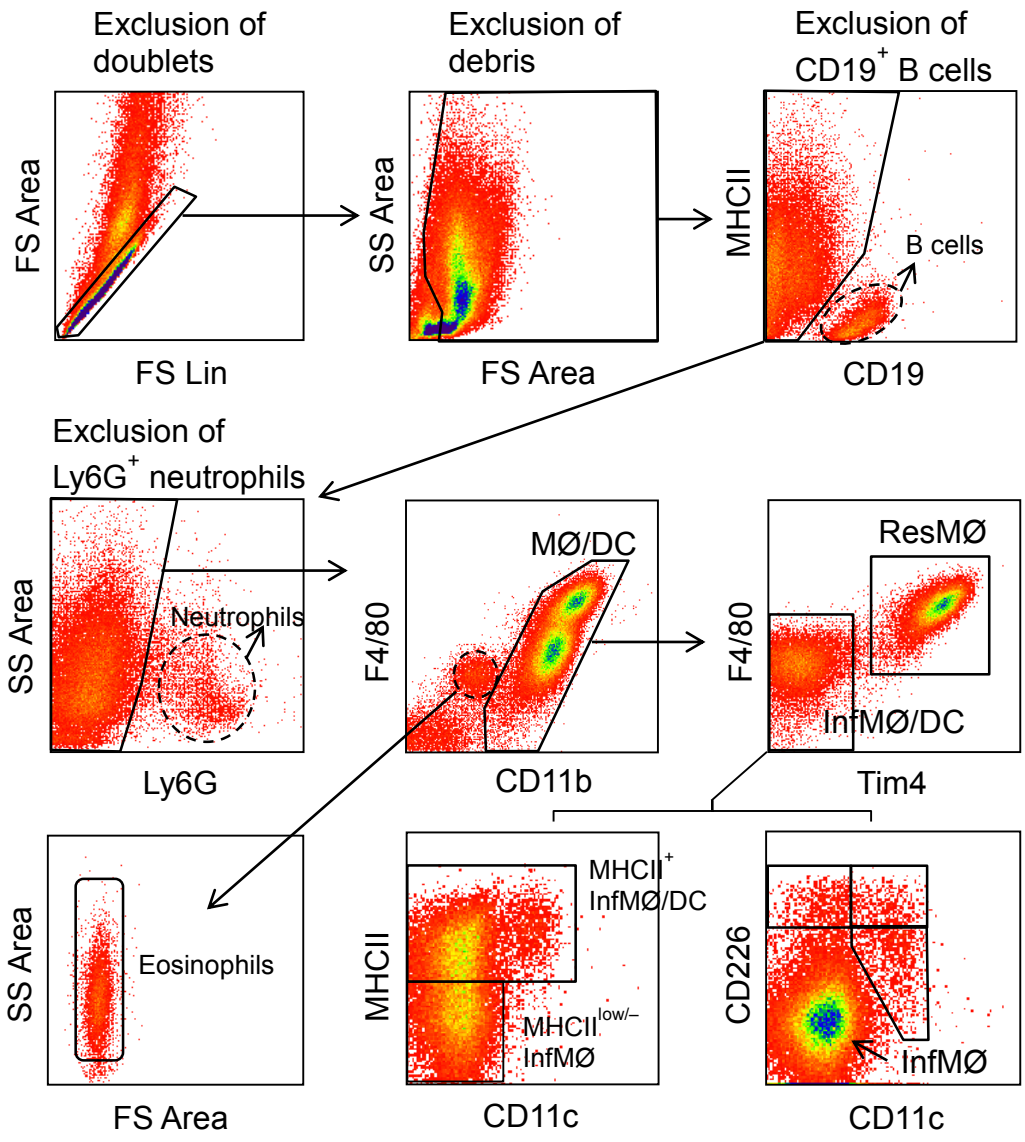

Figure 5.3 Phenotypic discrimination of 'DC-like' cells from monocyte-derived inflammatory MØs during peritoneal inflammation

Flow-cytometric analysis of peritoneal cells from mice 3 days after intraperitoneal staphylococcus epidermidis supernatant (SES) challenge. Density plots show MØ/DC populations were pre-gated on $CD11b^{+}F4/80^{high/low}$ cells (central plot) after exclusion of doublets, cellular debris, $CD19^{+}$ B cells, $Ly6G^{+}$ neutrophils and eosinophils (Davies et al., 2011). Within these cells, individual MØ/DC subset could be further separately identified: ResMØs ($CD11b^{high}F4/80^{high}Tim4^{-}$), InfMØs ($CD11b^{int}F4/80^{int}Tim4^{-}MHCII^{+/-}CD11c^{-}CD226^{-}$) and three 'DC-like' subsets ($CD11b^{int}F4/80^{int\text{-}low}Tim4^{-}MHCII^{+}$ with $CD226^{+}CD11c^{low}$, $CD226^{+}CD11c^{+}$ and $CD11c^{+}CD226^{low}$). Data are representative of two independent experiments with C57BL/6 mice.

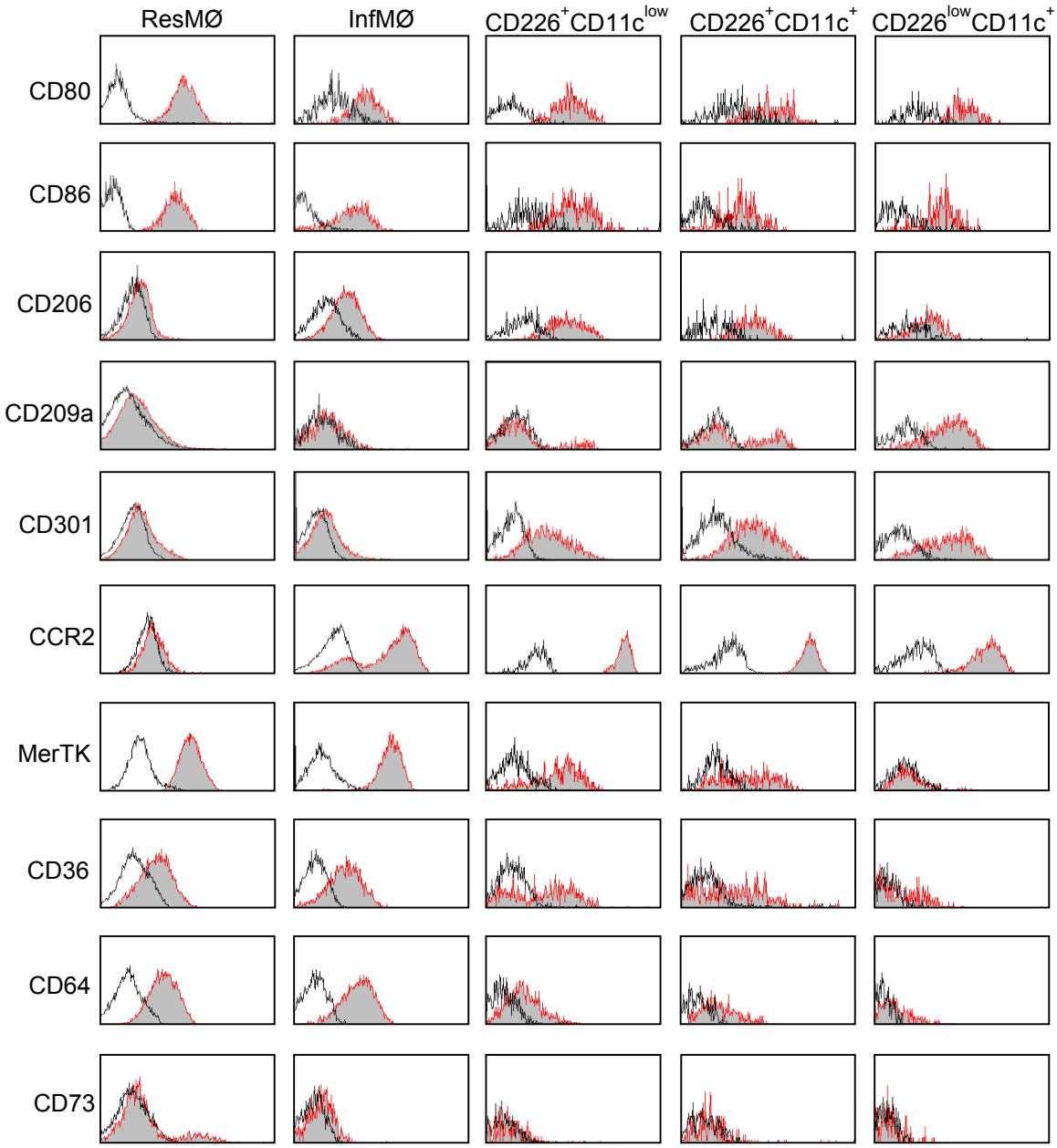

Figure 5.4 Phenotypic comparisons between peritoneal resident MØs, inflammatory MØs and three 'DC-like' subsets from inflamed mice

Flow-cytometric analysis of select marker expression by peritoneal ResMØs, InfMØs and three 'DC-like' subsets. Representative histogram plots were pre-gated on respective MØ/DC subsets based on definitive phenotypic markers after exclusion of doublets, debris, $CD19^+$ B cells and $Ly6G^+$ neutrophils (as shown in Fig. 5.3). Shaded histograms depict receptor specific staining and bold lines denote isotype control staining. Data are representative of two independent experiments with a total of four C57BL/6 mice.

5.2.3 Cellular kinetics of different peritoneal MØ/DC subsets during acute experimental peritonitis

In an acute *Staphylococcus epidermidis* cell-free supernatant (SES)-induced sterile peritonitis model (Hurst et al., 2001), neutrophils ($CD11b^{+}F4/80^{-}Ly6G^{+}$) are rapidly recruited into the peritoneal cavity during the first few hours, but numbers subside after 24 hours (Hurst et al, 2001) (Fig. 5.5). In contrast, the numbers of ResMØs decline initially but gradually recover in a similar way to that seen in zymosan-peritonitis (Davies et al., 2011 & 2013). InfMØs, which were found to lack CD226 and CD11c expression in the SES-peritonitis model ($CD11b^{int}F4/80^{int}CD11c^{-}CD226^{-}$, Fig. 5.5A), accumulated in the peritoneal cavity after SES administration (Fig. 5.5B). All three putative 'DC-like' subsets noted in naïve peritoneal cavity could be identified during the inflammatory response (Fig. 5.5A), based on the same phenotypic strategy. During inflammation, numbers of $CD11c^{low}CD226^{+}$ and $CD11c^{+}CD226^{low}$ cells initially decreased following SES administration (4 hours after inflammatory challenge) and then increased later on (72 hours after inflammatory challenge) (Fig. 5.5B). To test whether these cellular kinetics can be found in a different inflammatory setting, low dose ($2x10^{6}$ particles) and high dose ($2x10^{7}$ particles) zymosan-induced peritonitis models were examined, and similar results were obtained albeit with different magnitudes of the inflammatory recruitment. (Fig. 5.6A & B).

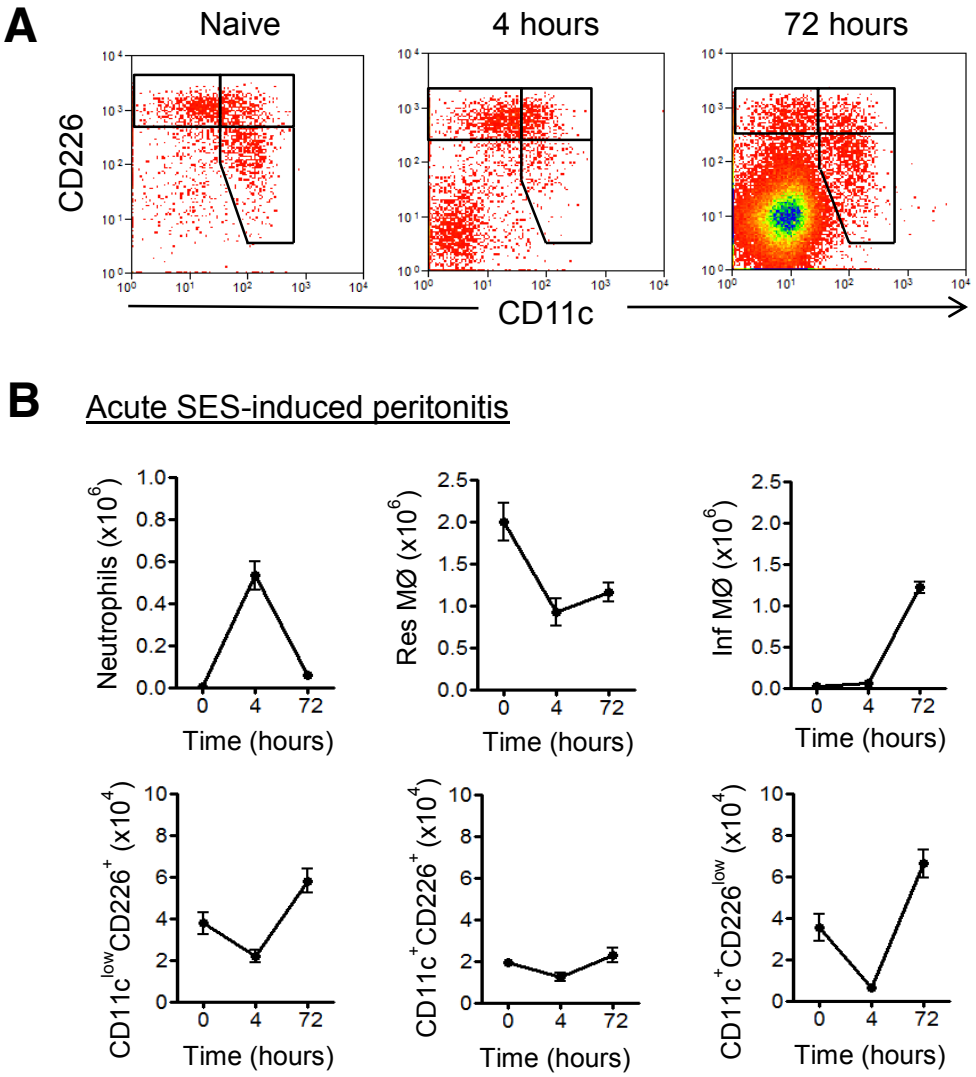

Figure 5.5 Cellular kinetics of peritoneal myeloid subsets during acute SES-induced peritoneal inflammation

(A) Representative flow-cytometric analysis showing the kinetic changes of InfMØs ($F4/80^{int}CD11b^{int}CD11c^{-}CD226^{-}$) and three 'DC-like' cells ($CD226^{+}CD11c^{+}$, $CD226^{+}CD11c^{low}$, $CD11c^{+}CD226^{low}$) during acute SES-induced peritoneal inflammation. (**B**) Graphs showing the absolute numbers of neutrophils ($F4/80^{-}Ly6G^{+}$), ResMØs ($F4/80^{high}CD11b^{high}$), InfMØs and three DC subsets (as defined above) observed during acute SES-induced peritoneal inflammation. Data (mean ± SEM) are derived from 5- to 6- week-old C57BL/6 mice (n = 4 per group) and are derived from one of two independent experiments.

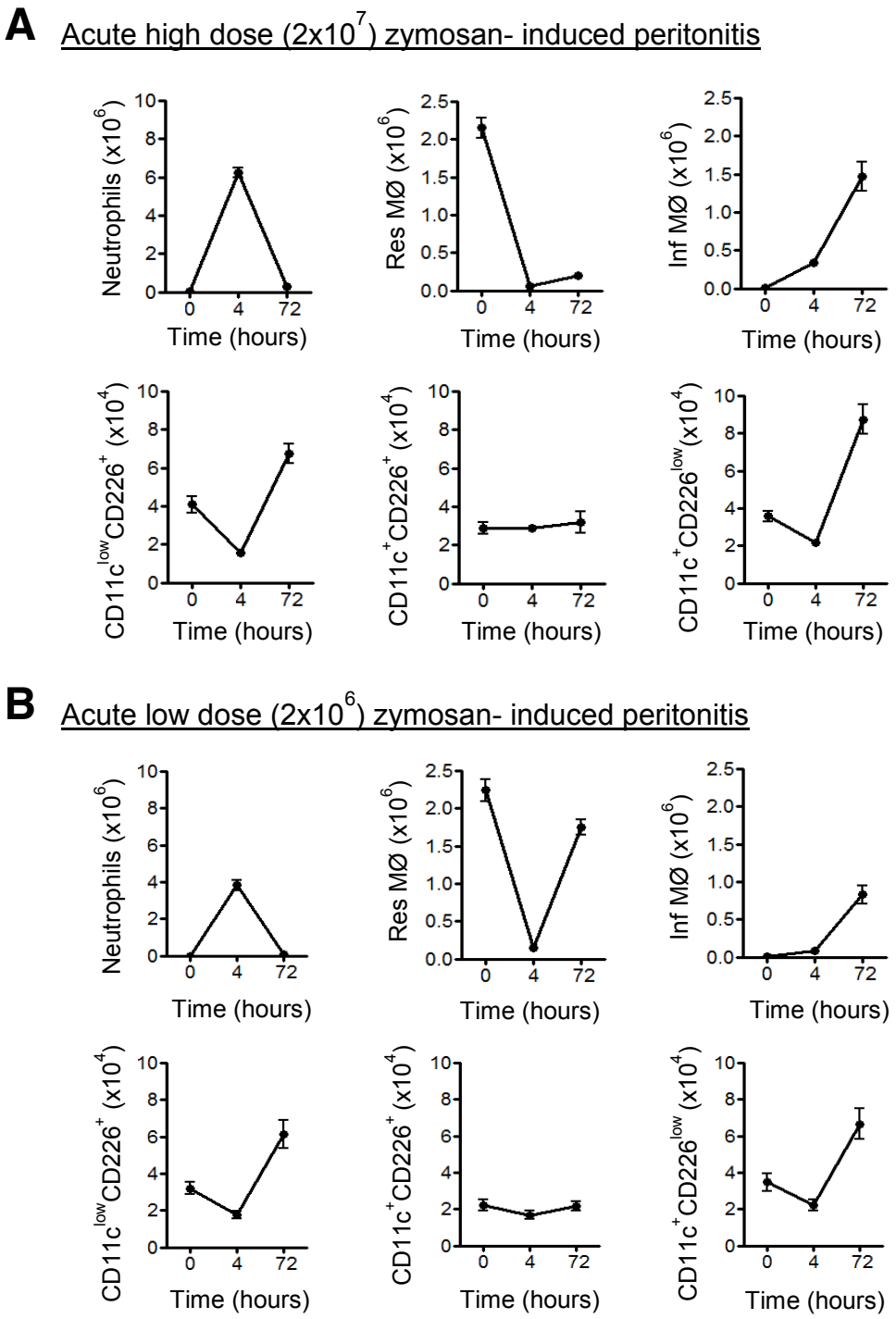

Figure 5.6 Cellular kinetics of peritoneal myeloid subsets during acute zymosan-induced peritoneal inflammation

(A) Graphs showing the absolute numbers of neutrophils, ResMØs, InfMØs and three DC subsets observed during acute high dose zymosan ($2x10^7$ particles)-induced peritoneal inflammation. Data (mean ± SEM) are derived from 5- to 6- week-old C57BL/6 mice (n = 4 per group) and from one experiment. **(B)** Similar results from another experiment with low dose zymosan ($2x10^6$ particles) challenge. Data (mean ± SEM) are derived from 5- to 6- week-old C57BL/6 mice (n = 3-5 per group).

5.2.4 Peritoneal DC-like subsets are recruited from the periphery during acute experimental peritonitis

To determine whether the expansion of peritoneal 'DC-like' cells seen at later time points following acute experimental peritonitis is due to recruitment from the periphery, an intraperitoneal adoptive transfer experiment was performed (Fig. 5.7). Briefly, donor ($CD45.1^+$) peritoneal cells were harvested and pooled, then transferred intraperitoneally into ($CD45.2^+$) congenic mice one day before i.p. SES challenges. Recipient mice without SES challenges were treated as controls (Fig. 5.7A). The respective numbers of $CD45.1^+$ (donor) and $CD45.2^+$ (host) cells in each peritoneal MØ/DC subset were measured 4 days after intraperitoneal adoptive transfer (both SES-challenged and unchallenged mice) (Fig. 5.7B). The results showed that the proportion of donor 'DC-like' cells dropped considerably after SES challenges, suggesting that these cells were either dead or lost to retrieval through increased adhesion or emigration, with less local expansion during the resolution phase of inflammation, compared to ResMØs (Davies et al., 2011) (Fig. 5.7C). Notably, all three donor 'DC-like' subsets showed similar reduction after SES challenges, while host 'DC-like' subsets after SES challenges have similar (or even higher) numbers, compared to those unchallenged (Fig. 5.7D) These findings are compatible with the kinetic studies of these MØ/DC subsets in previous experimental peritonitis models, demonstrating that these 'DC-like' cells are basically recruited from the periphery during inflammation.

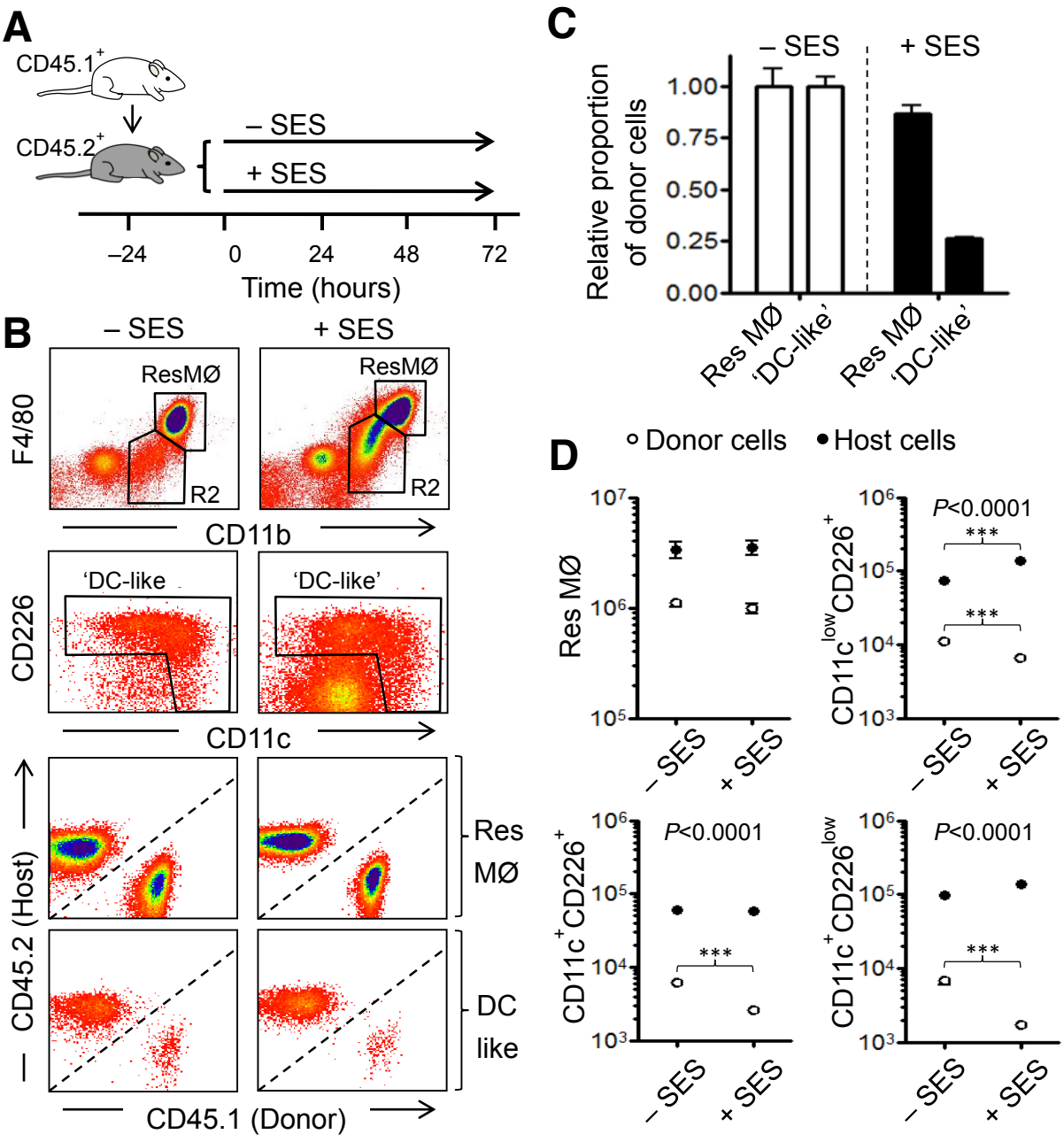

Figure 5.7 Peritoneal 'DC-like' cells are recruited from the periphery during acute SES-induced peritonitis

(A) Schematic representation of the adoptive transfer strategy used to study to determine the origin of peritoneal 'DC-like' cells during peritonitis. One day after adoptive transfer of naïve peritoneal cells between CD45 allotype-mismatched animals, mice were either injected intraperitoneally with SES or were left unchallenged, and were sacrificed on Day 3. **(B)** Representative flow-cytometric plots showing the relative contribution of donor and host cells to the ResMØs and 'DC-like' populations 4 days after adoptive transfer. 'R2' represents $CD11b^{int}F4/80^{int/low}$ population, which further

subdivided into three subsets of DC and InfMØs based on CD11c and CD226 expression. Data are derived from 1 of 4 individual 129S6/SvEv mice. **(C)** Bar graphs showing the relative proportion of $CD45.1^+$ donor cells in the peritoneal cavity of unchallenged and SES-challenged $CD45.2^+$ host mice 4 days after intraperitoneal adoptive transfer (normalized to unchallenged mice). Data represents the mean ± SEM and are derived from 8 individual 129S6/SvEv mice (n = 4 per group). **(D)** Graphs showing the number of recoverable donor (white symbols) and host (black symbols) ResMØs and 'DC-like' subsets in the peritoneal lavage of the mice shown in (C) above. Data represents mean ± SEM. Data was analyzed for statistical significance by two-way ANOVA after log transformation and interaction statistics *P*-values and Bonfferoni post-tests (asterisks) are indicated where significant.

5.2.5 Limited evidence of local proliferation of peritoneal DC-like subsets during acute experimental peritonitis

Previous mouse studies have demonstrated that tissue ResMØs, such as peritoneal ResMØs have distinct self-renewal ability during the resolution phase of certain inflammatory circumstances (Jenkins et al., 2011; Davies et al., 2011). Subsequent study also provided evidence that a discrete subset of peripherally recruited monocyte-derived MØs, Ly-6B^{+} MØs, could proliferate at the recovery phase during tissue inflammation (Davies et al., 2013). Here, a similar flow-cytometric method was applied using DPAI (4',6-Diamidino-2-phenylindole) for measuring DNA content and intracellular Ki-67 staining for measuring active cell division, to investigate the proliferative potential of these peritoneal 'DC-like' cells, compared to ResMØs and InfMØs (MHCII^{+} and MHCII^{-}) (Davies et al., 2011; and Fig. 5.8). The data indicated that whilst ResMØs were experiencing substantial proliferation 3 days after low dose zymosan-induced peritonitis, there was only limited evidence of proliferation in the 'DC-like' subsets and InfMØs, suggesting that recruitment from the periphery may be the major source of these cells during peritonitis.

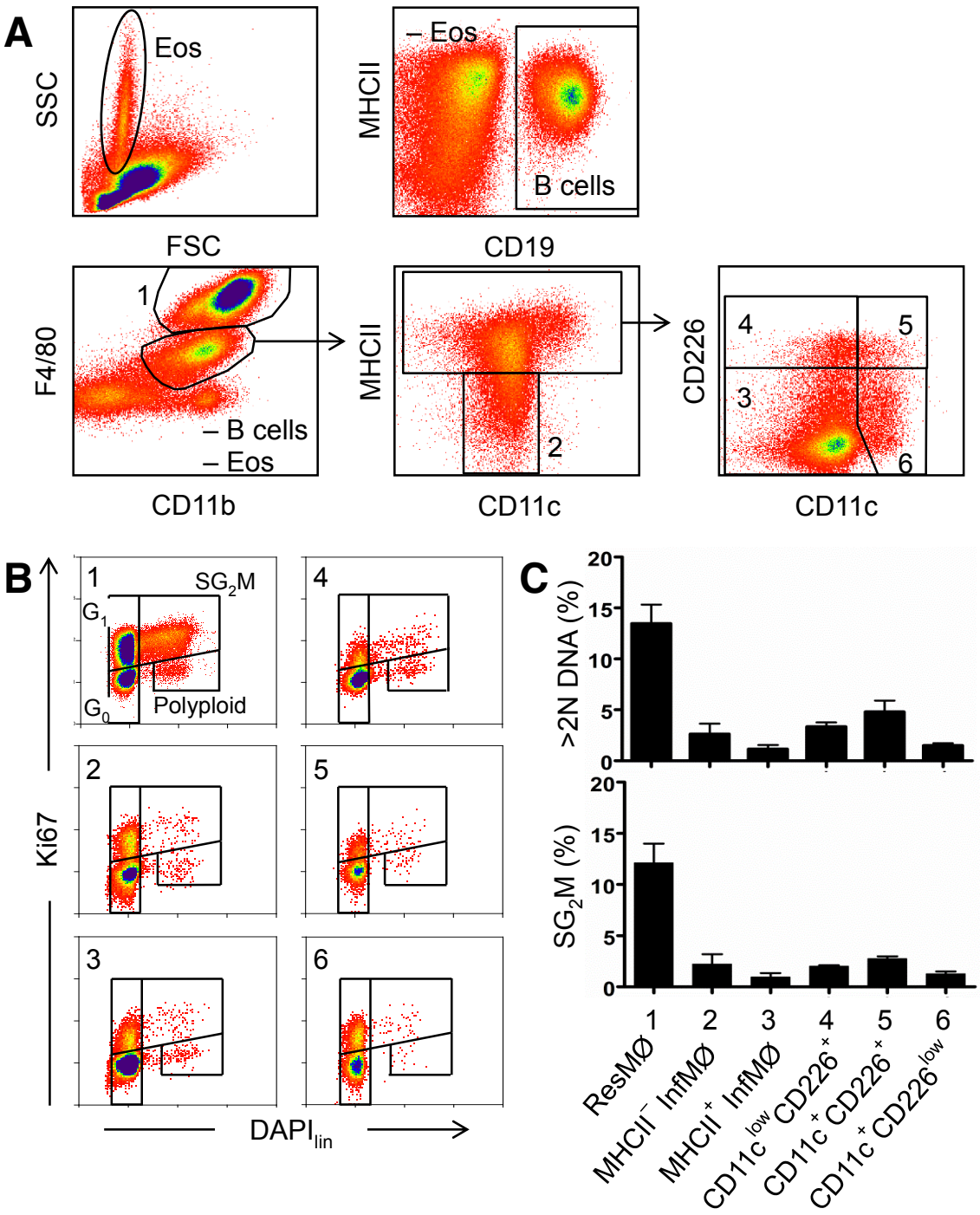

Figure 5.8 Limited evidence of proliferation during peritonitis of murine peritoneal 'DC-like' subsets

(A) Peritoneal cells from mice 3 days after low dose zymosan-induced peritonitis ($2x10^6$ particles) were analysed by flow cytometry for evidence of cell cycle. Peritoneal MØ/DCs were gated by exclusion of eosinophils (upper left panel) and $CD19^+$ B cells (upper right panel), before selectively gating on $F4/80^{high}$ ResMØs (gate 1, lower left panel) and $F4/80^{+/low}$ InfMØ/DCs, which were further divided into $MHCII^-$ InfMØs (gate 2, lower middle panel) and $MHCII^+$ cells. The $MHCII^+$ cells (lower middle panel)

were further divided into MHCII^{+}CD226^{-}CD11c^{-} InfMØs (gate 3, lower right panel), and the 3 previously described 'DC-like' populations (gates 4-6, lower right panel). **(B)** The cells were assessed for active cell division during peritonitis as previously described (Davies et al., 2011) by measuring Ki67 expression and DNA content. **(C)** Quantification of the data indicated that whilst ResMØs were experiencing substantial proliferation as previously observed, there was only limited evidence of proliferation in the 'DC-like' subsets indicating that recruitment from the periphery may be the major source of these cells during peritonitis. Data represents the mean ± SEM of three C57BL/6 mice from one of two similar experiments.

5.2.6 CCR2-dependent homeostasis and inflammatory recruitment of peritoneal 'DC-like' subsets

As shown in Figure 5.2 & 5.4, peritoneal 'DC-like' subsets express the highest levels of the chemokine receptor CCR2 of all leukocytes, not only in the peritoneal cavity of naive, but also inflamed mice. Kinetic studies and adoptive transfer experiments indicate that 'DC-like' cells are relatively transient in the peritoneal cavity during inflammation and replenished predominantly from the periphery, and in contrast to ResMØs, do not largely arise through local proliferation (Section 5.2.3, 5.2.4 and 5.2.5). As CCR2 is a major chemokine receptor that regulates monocyte migration (Serbina and Pamer 2006), the expression of CCR2 suggests that CCR2 may be of importance for these cells to enter into peritoneal cavity under tissues homeostasis and during inflammation. To test this hypothesis, CCR2-deficient mice (*Ccr2*$^{-/-}$) were compared to wild type controls (*Ccr2*$^{+/+}$, C57BL/6 CD45.1 strain), for the presence and numbers of 'DC-like' cells, amongst all myeloid cells. As shown in Fig. 5.9, dramatically decreased numbers of peritoneal 'DC-like' cells (CD11b^{int}MHCII^{+}) were noted in naïve *Ccr2*$^{-/-}$ mice, compared to wild type mice (Fig. 5.9A). Specifically, all three DC subsets decreased significantly in *Ccr2*$^{-/-}$ mice, compared to *Ccr2*$^{+/+}$ mice. There were no differences in ResMØ numbers between these two strains under homeostatic conditions.

At 72 hours after SES challenge, the numbers of MHCII^{+} CD11c^{-}CD226^{-} InfMØs as well as peritoneal 'DC-like' cells (CD11b^{int}MHCII^{+}) significantly decreased in *Ccr2*$^{-/-}$ mice, compared to wild type mice (Fig. 5.10). Interestingly, the number of ResMØs in *Ccr2*$^{-/-}$ mice is significantly greater than that in *Ccr2*$^{+/+}$ mice, suggesting that altered expansion of ResMØs during the resolution phase of acute SES-induced peritonitis in *Ccr2*$^{-/-}$ mice or increased recovery due to lower tissue adhesion, or emigration as a consequence of activation.

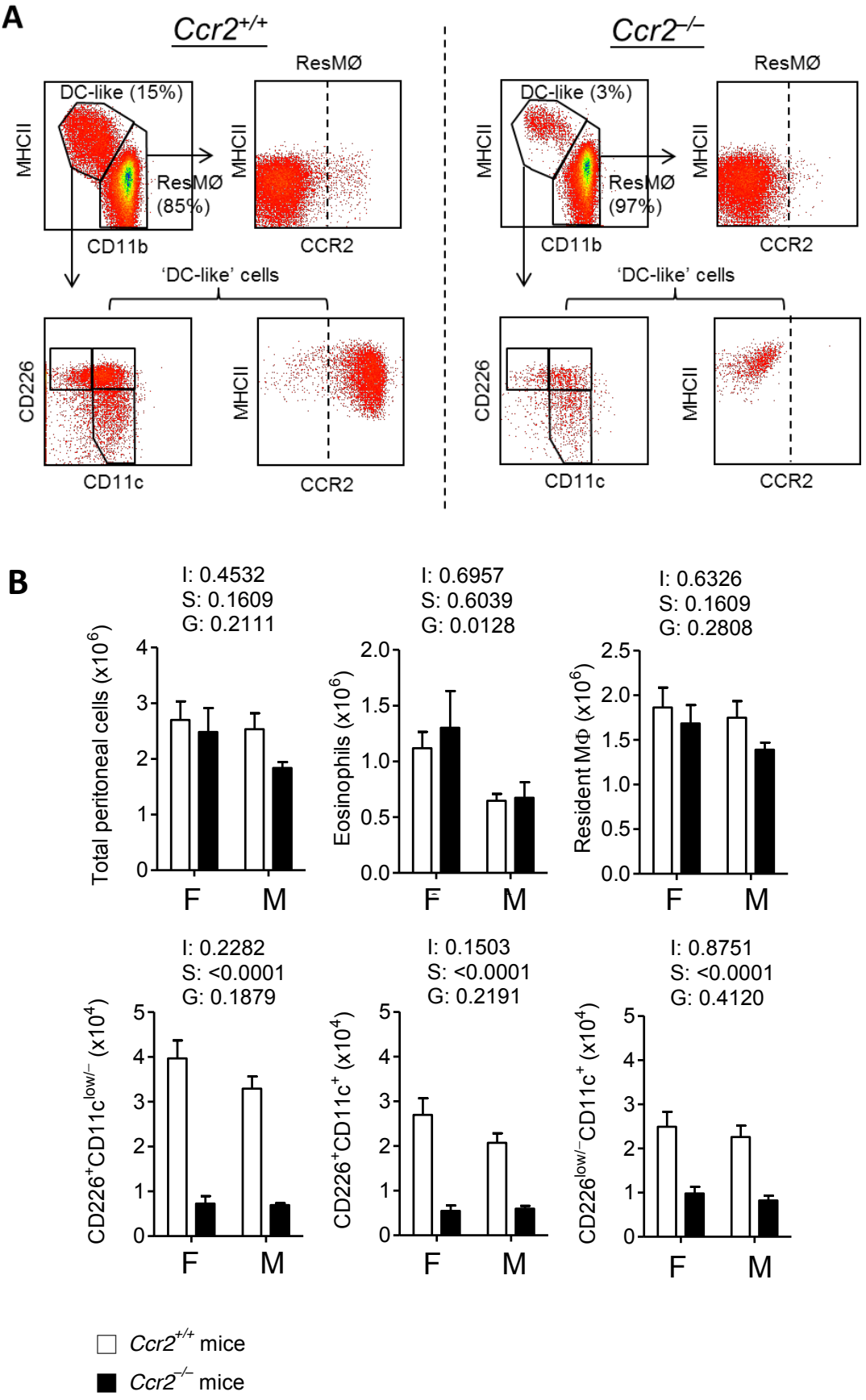

(Figure legend in on the next page)

Figure 5.9 Myeloid cell compositions in the naïve peritoneal cavity of *Ccr2*$^{-/-}$ mice, compared to wild-type *Ccr2*$^{+/+}$ mice

(A) Representative density plots showing peritoneal ResMØs (CD11b^{high}MHCII^{-}) and three 'DC-like' subsets (CD11b^{int}MHCII^{+} with CD11c^{low}CD226^{+}, CD11c^{+}CD226^{+} or CD11c^{+}CD226^{low}) from naïve C57BL/6 CD45.1 (*Ccr2*$^{+/+}$) mice (left panels) and *Ccr2*$^{-/-}$ mice (right panels). Myelomonocytic cells (MØs + DCs) are pre-gated by CD19^{-}CD11b^{+}F4/80$^{high\text{-}to\text{-}low}$ cells. In naïve *Ccr2*$^{+/+}$ mice, three 'DC-like' subsets are CCR2$^{high/+}$, while ResMØs are mostly CCR2^{-}. Dashed lines denote the level of isotype controls. In naïve *Ccr2*$^{-/-}$ mice, the proportion of three 'DC-like' subsets within the MØ/DC pool is decreased and they are basically CCR2^{-}. Data are derived from one of two similar experiments. **(B)** Bar graphs depicting significantly decreased numbers of all three 'DC-like' subsets in *Ccr2*$^{-/-}$ mice, compared to *Ccr2*$^{+/+}$ mice. No gender difference was noted in this regard. Additionally, no differences in total cell number, eosinophils, ResMØ numbers were noted between *Ccr2*$^{+/+}$ and *Ccr2*$^{-/-}$ mice under naive status. Data is representative of two independent experiments (n = 5 per group, n = 20 in total). Data are shown as mean and error bars denote SEM. Data are analysed by two-way ANOVA tests (I: Interaction, S: mouse strain, G: Gender; the numbers denote *P*-value; F: female, M: male).

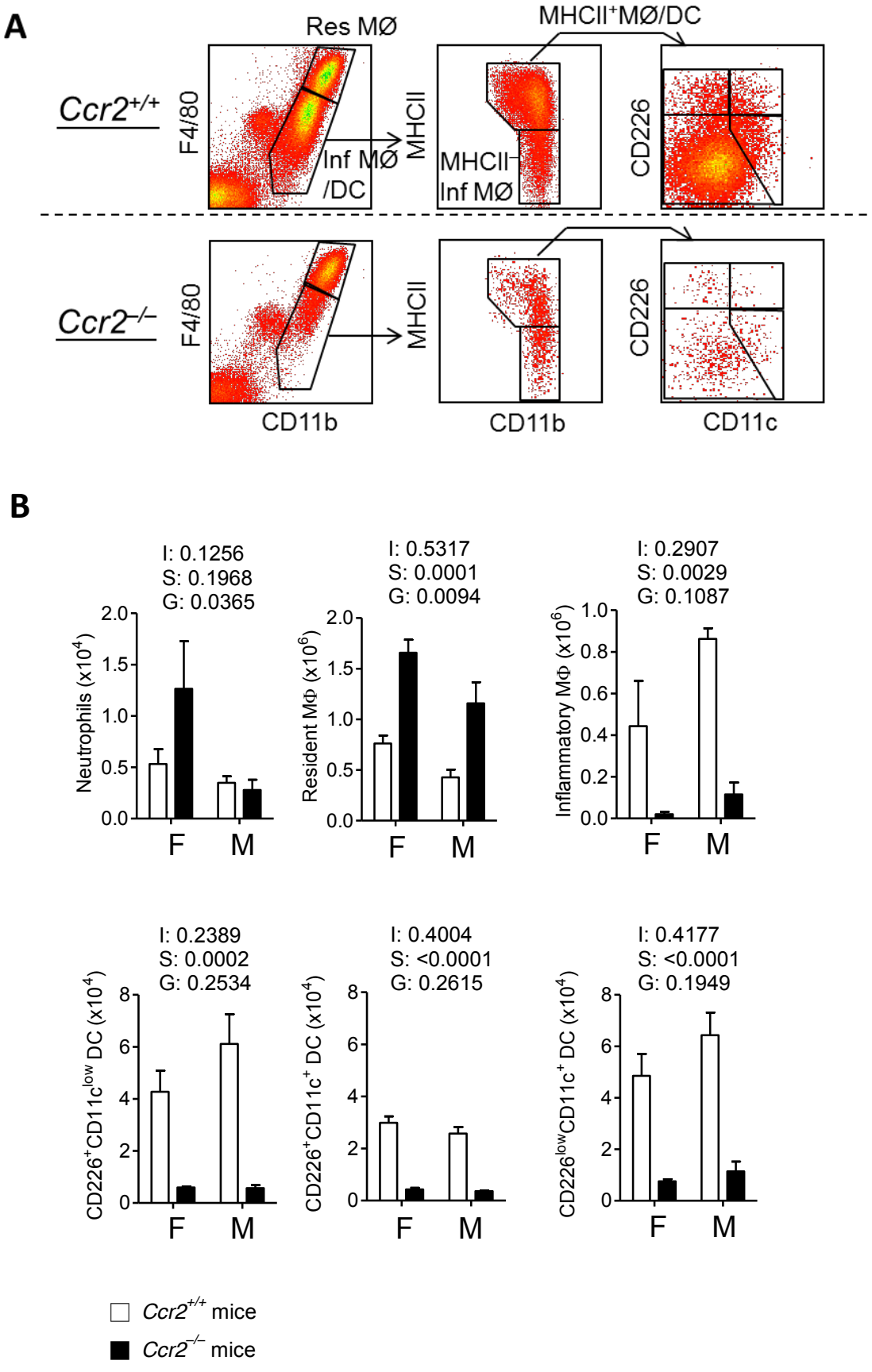

(Figure legend in on the next page)

Figure 5.10 Myeloid cell compositions in the peritoneal cavity from 72h post-SES challenge *Ccr2*$^{-/-}$ mice and wild-type *Ccr2*$^{+/+}$ mice

(A) Representative density plots showing peritoneal ResMØs (CD11b^{high}F4/80^{high}), InfMØs (CD11b^{int}F4/80^{int}MHCII$^{+/-}$ with CD226$^{low/-}$CD11c$^{low/-}$) and three 'DC-like' subsets (CD11b^{int}F4/80^{int}MHCII^{+} with CD11c^{low}CD226^{+}, CD11c^{+}CD226^{+} or CD11c^{+}CD226 ^{low}) from 72 hours after SES challenge in C57BL/6 CD45.1 (*Ccr2*$^{+/+}$) mice (upper panels) and *Ccr2*$^{-/-}$ mice (lower panels). Myelomonocytic cells are gated as CD19^{-}Ly6G^{-}CD11b^{+}F4/80$^{high\text{-}to\text{-}low}$ cells. In *Ccr2*$^{-/-}$ mice, the proportion/number of CD11b^{+}F4/80$^{int\text{-}to\text{-}low}$ InfMØ/DCs decreased, compared to *Ccr2*$^{+/+}$ mice. Data are derived from one of two similar experiments. **(B)** Bar graphs depicting significantly decreased numbers of InfMØs and all three 'DC-like' subsets in *Ccr2*$^{-/-}$ mice, compared to *Ccr2*$^{+/+}$ mice. No gender difference was noted in this regard. The number of ResMØs in *Ccr2*$^{-/-}$ mice is significantly higher than in *Ccr2*$^{+/+}$ mice. Additionally, no differences in the number of total cells, neutrophils, or eosinophils were noted between *Ccr2*$^{+/+}$ mice and *Ccr2*$^{-/-}$ mice at 72 hours after SES challenge. Data represents one of two similar experiments (n = 3-4, per group, n = 13 in total). Data are shown as mean and error bars denote SEM. Statistical analysis was based on two-way ANOVA tests (I: Interaction, S: mouse strain, G: Gender; the numbers denote *P*-value; F: female, M: male).

5.2.7 Role of IL-10 on the inflammatory recruitment of peritoneal 'DC-like' subsets

IL-10 has recently been reported to control the differentiation of peritoneal 'DC-like' cells during inflammation from peripheral monocytes (Nguyen et al, 2012), however, this study was unable to distinguish peritoneal 'DC-like' cells from concurrently infiltrating monocyte-derived InfMØs. To determine the differential influence of IL-10 on peritoneal 'DC-like' cells and InfMØs, SES-induced peritonitis was undertaken using *Il10*$^{-/-}$mice, compared to wild type controls (*Il10*$^{+/+}$). Three days after SES administration, InfMØs (CD11b^{int}F4/80^{int}CD11c^{-}CD226^{-}) from *Il10*$^{-/-}$ mice exhibited more MHCII expression compared to the *Il10*$^{+/+}$ mice (Fig. 5.11A). The numbers of neutrophils, InfMØs and 'DC-like' subsets were significantly increased in *Il10*$^{-/-}$ mice, compared to the controls (Fig. 5.11B). ResMØ numbers were similar between *Il10*$^{+/+}$ and *Il10*$^{-/-}$ mice (Fig. 5.11B). To control for the exaggerated inflammatory response observed in the *Il10*$^{-/-}$ mice, we expressed the numbers of the DC subsets as a ratio to InfMØs. Whilst the numbers of DCs were higher in the IL-10-deficient mice compared to controls (Fig. 5.11B, lower row), relative to the InfMØs, the proportion of DCs was actually lower in the IL-10-deficient mice (Fig. 5.11C).

Together, these data indicate that IL-10 plays an important role in limiting both the recruitment of InfMØs and 'DC-like' cells, although with a potentially greater impact on InfMØs recruitment and MHCII expression. Furthermore, there was no evidence of the proposed increase in 'differentiation of APCs' in the absence of IL-10, reported by Nguyen et al (2012).

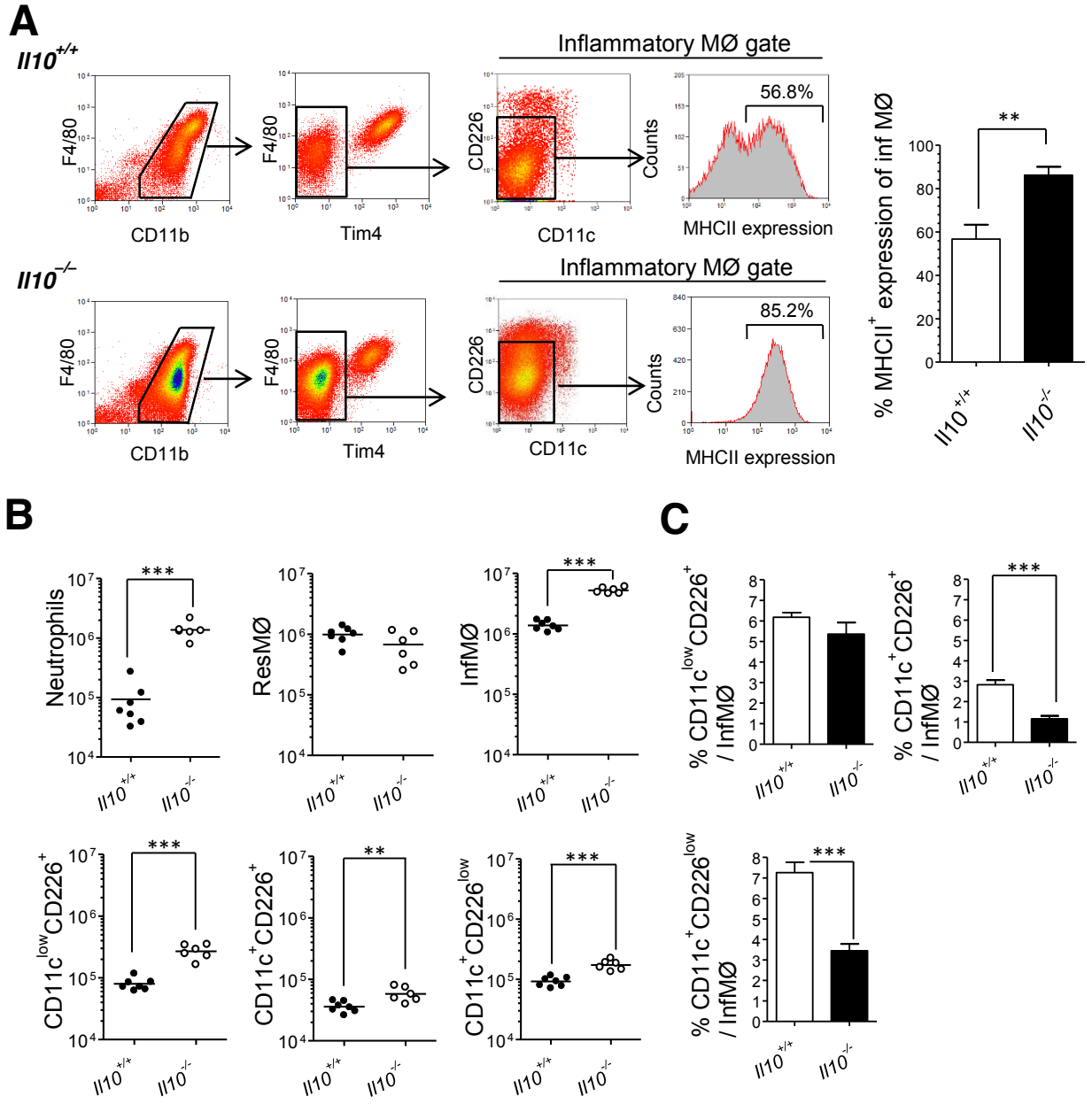

Figure 5.11 IL-10 limits inflammatory response in acute SES-induced peritonitis model

(A) Representative density plots showing the gating of monocyte-derived InfMØs ($CD11b^{int}F4/80^{int/low}Tim4^{-}CD11c^{-}CD226^{-}$) and the proportion of positive MHCII expression at 72 hours post-SES challenge in wild type (*Il10*$^{+/+}$, upper panels) and IL-10 knockout (*Il10*$^{-/-}$, lower panels) C57BL/6 mice. Cells were pre-gated by the exclusion of doublets, $Ly6G^{+}$ neutrophils and $CD19^{+}$ B cells. Tim4 antibody was applied to assure the specific exclusion of the majority of $Tim4^{+}$ ResMØs (Davies et al., 2011). Comparison of high MHCII expression of InfMØs between *Il10*$^{+/+}$ and *Il10*$^{-/-}$ mice was shown in the bar graph (far right). Data shown is represented as mean ± SEM of 6-7 mice per group, combined from two independent experiments. Data are analysed

by Student's *t*-test. (**B**) Graphs showing the comparisons of actual numbers of individual peritoneal population between *Il10*$^{+/+}$ and *Il10*$^{-/-}$ mice at 72 hours post-SES challenge. Data were derived from same animals shown in (A). Data are analysed by Student's *t*-test. **(C)** Bar graphs showing the comparisons of the ratio of individual peritoneal 'DC-like' subset over InfMØs (expressed as percentage) between *Il10*$^{+/+}$ and *Il10*$^{-/-}$ mice. Data shown is represented as mean ± SEM of 6-7 mice per group, combined from two independent experiments. Data are analysed by Student's *t*-test.

5.2.8 Differential cytokine responses among distinct peritoneal MØ/DC subsets upon *ex vivo* microbial product stimulation

To explore the functional differences among these monocytic subsets, intracellular staining of peritoneal cells for TNF-α, IL-6 and IL-12p40 after 6 hours *ex vivo* stimulation with SES was undertaken to determine the pro-inflammatory cytokine production of individual monocytic subpopulations (Fig. 5.12A). The results showed that both ResMØs and three 'DC-like' subsets can generate significant amounts of TNF-α and IL-6 after SES stimulation (Fig. 5.12B). Notably, compared to ResMØs, 'DC-like' cells have significantly greater potential for IL-12p40 production, particularly the $CD11c^{+}CD226^{low}$ subset (two-way ANOVA test with Bonferroni post-tests, $p < 0.001$). Similar results were revealed in cells either from naïve mice (Fig. 5.12B, left panels) or and from mice 72 hours after SES injection, where $MHCII^{+}$ and $MHCII^{-}$ InfMØs were also assessed (Fig. 5.12B, right panels). Similarly, these differential cytokine responses of the peritoneal MØ/DC subsets could be generated upon LPS stimulation (Fig. 5.12C). Additionally, the ability of these monocytic subsets to produce anti-inflammatory cytokine IL-10 was examined (Fig. 5.13A). Interestingly, ResMØs generated the highest amount of IL-10 upon *ex vivo* stimulation by SES or LPS for 6 hours, and the $CD11c^{+}CD226^{low}$ subset exhibited very minimal IL-10 production (Fig. 5.13B).

Collectively, these data demonstrated that in response to microbial product stimulation, pro-inflammatory and anti-inflammatory cytokines can be differentially generated by distinct peritoneal MØ/DC subsets.

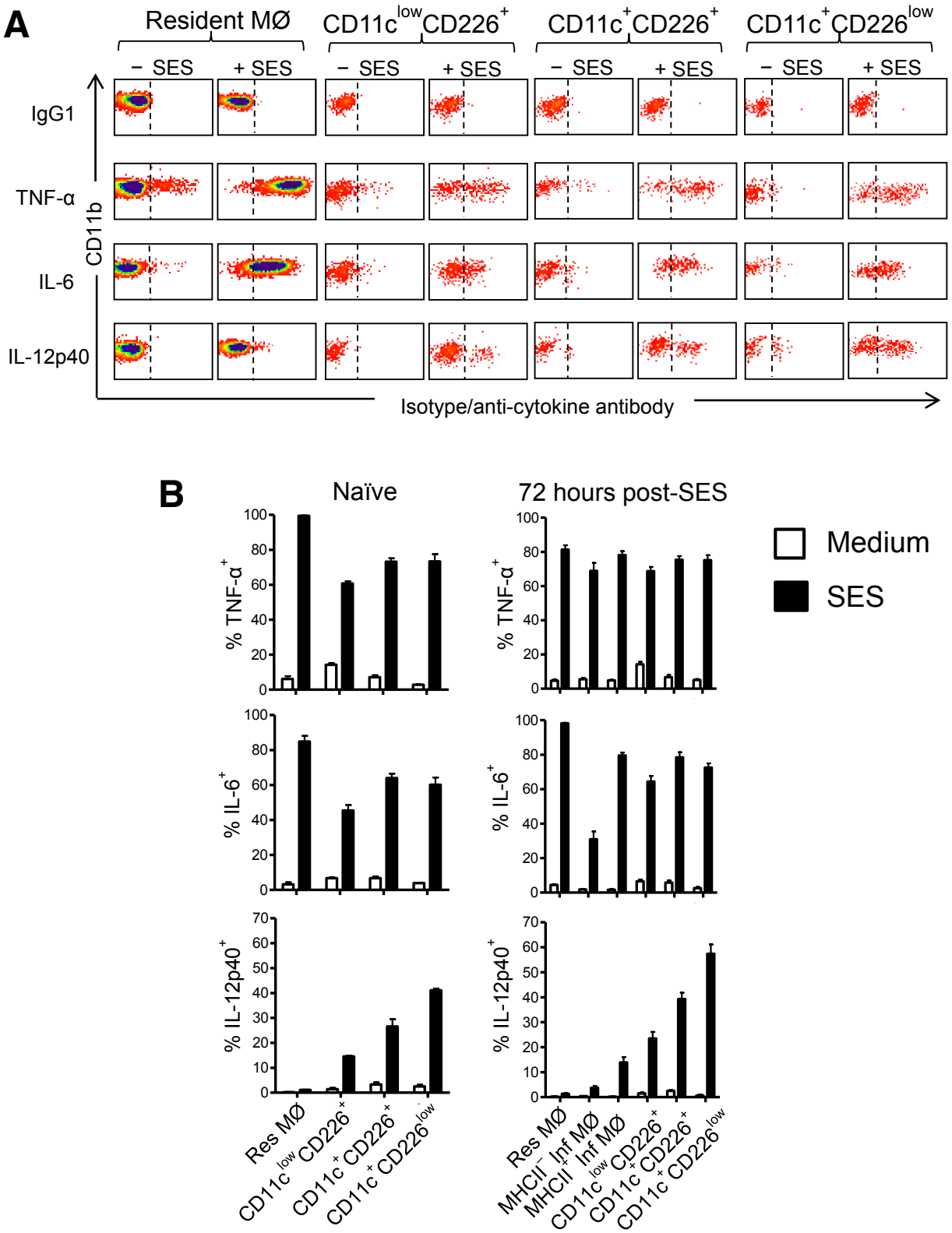
A
Resident MØ
CD11c^low CD226^+
CD11c^+ CD226^+
CD11c^+ CD226^low
− SES
+ SES
IgG1
TNF-α
IL-6
IL-12p40
CD11b
Isotype/anti-cytokine antibody
B
Naïve
72 hours post-SES
Medium
SES
% TNF-α^+
% IL-6^+
% IL-12p40^+
Res MØ
CD11c^low CD226^+
CD11c^+ CD226^+
CD11c^+ CD226^low
MHCII^− Inf MØ
MHCII^+ Inf MØ

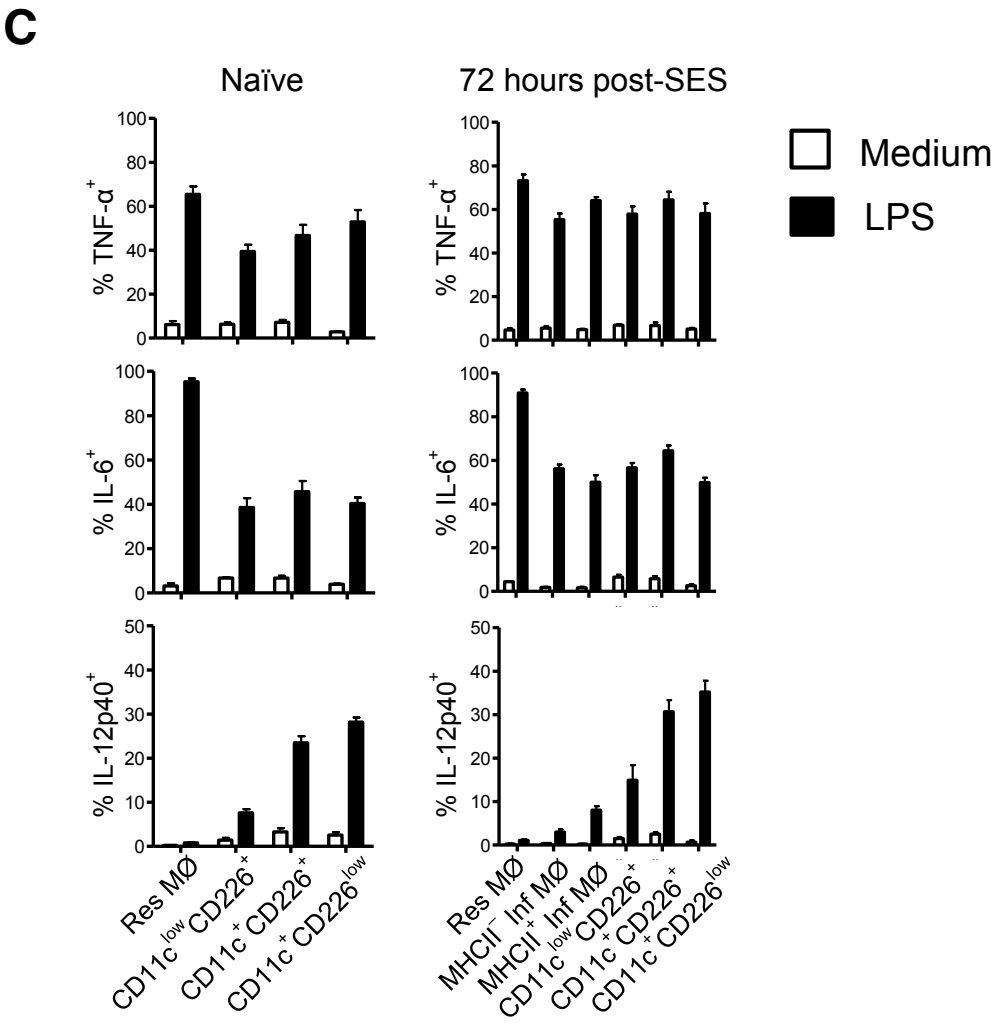

Figure 5.12 Peritoneal MØ/DC subsets exhibit differential pro-inflammatory cytokine production following SES or LPS exposure

(A) Representative density plots depicting the flow-cytometric determination of intracellular cytokine production (TNF-α, IL-6, IL-12p40) by peritoneal MØ/DC subsets from naive C57BL/6 mice, after *ex vivo* stimulation with SES (1: 10 dilution) for 6 hours. (**B**) Bar graphs comparing the intracellular cytokine production (TNF-α, IL-6, IL-12p40) among individual subsets of peritoneal monocytic cells from C57BL/6 mice, both naïve (left panels) and 72 hours post-intraperitoneal SES challenge (right panels). Positive intracellular cytokine production was determined by comparison with isotype controls. Data represent mean ± SEM and are derived from one of two similar experiments (n = 4-5 in each experiment). **(C)** Similar experiment was undertaken to detect differential cytokine production among the respective cells from C57BL/6 mice, both naïve (left panels) and 72 hours post-intraperitoneal SES challenge (right panels). Data represent mean ± SEM and are derived from one of two similar experiments (n = 4-5 in each experiment).

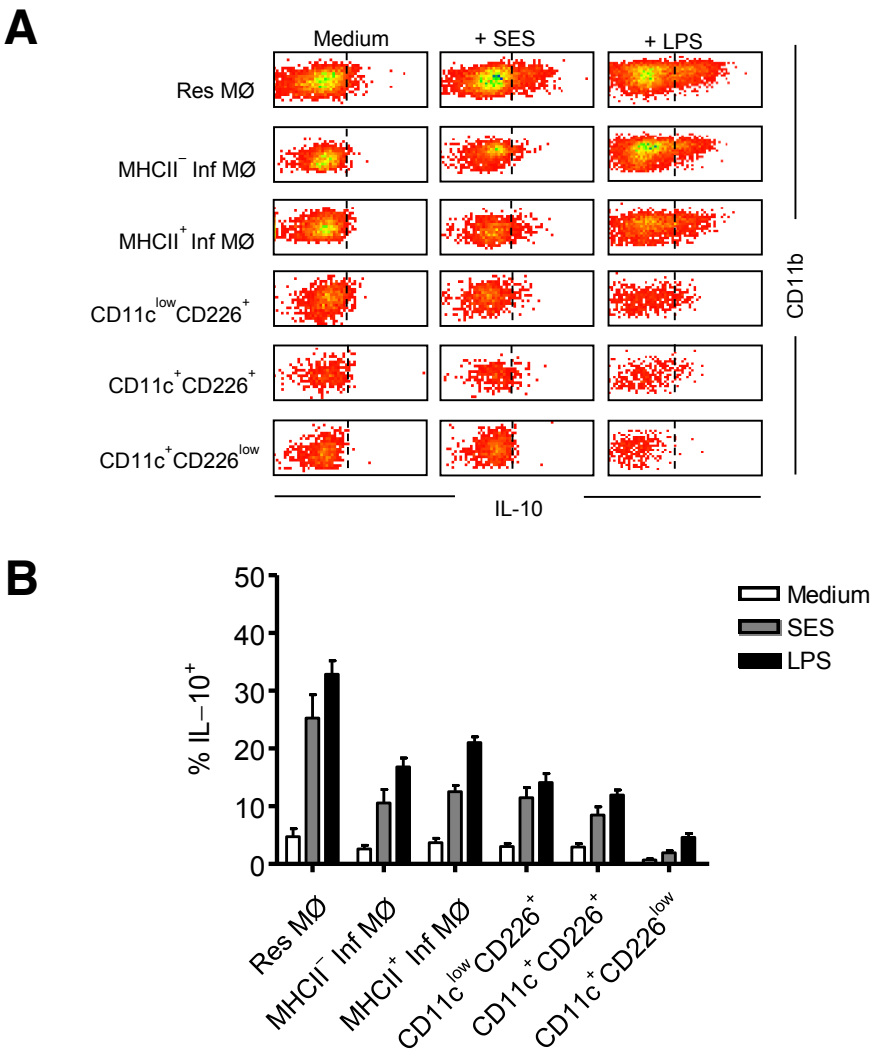

Figure 5.13 Peritoneal MØ/DC subsets exhibit differential IL-10 production following SES or LPS exposure

(A) Representative density plots depicting the flow-cytometric determination of intracellular IL-10 production by peritoneal MØ/DC subsets from naive C57BL/6 mice, after *ex vivo* stimulation with SES (1: 10 dilution) or LPS for 6 h. (**B**) Bar graphs comparing the intracellular IL-10 production among individual subsets of peritoneal monocytic cells from C57BL/6 mice, both naïve (left panels) and 72 hours post-intraperitoneal SES challenge (right panels). Positive intracellular cytokine production was determined by comparison with isotype controls. Data represents the mean ± SEM of C57BL/6 female mice (n = 5) from one of two identical experiments giving similar results.

5.2.9 Differential capacity for *in vivo* apoptotic thymocyte clearance among distinct peritoneal MØ/DC subsets

It has been recognised that mononuclear phagocytes play an important role in apoptotic and necrotic cell clearance. To determine the role of these peritoneal DC in apoptotic cell uptake during homeostasis and under inflammatory conditions, a previously established protocol was modified to assess the capability of apoptotic thymocyte clearance by each monocytic subset (Taylor et al., 2000; Uderhardt et al., 2012). Briefly, thymocytes from CD45.1$^+$ 129 S6/SvEv mice were recovered then apoptosis was induced by *ex vivo* dexamethasone treatment for 4 hours. About one-third to one-half of treated thymocytes became apoptotic, which could be estimated by flow cytometry using NIM-DAPI solution (containing nuclear isolation medium, NIM-II and DAPI) to detect DNA degradation (Fig. 5.14). These CD45.1$^+$ apoptotic thymocytes were intraperitoneally transferred to CD45.2$^+$ cogenic mice, in either naïve mice or 3 days after SES injection. After 30 minutes retention (*in vivo* phagocytosis), the peritoneal cells were harvested and assessed by flow cytometry (Fig. 5.15A & B). To assure what we measure is genuine phagocytosis, only internalized apoptotic thymocytes within each MØ/DC subset were assessed, through the exclusion of surface CD45.1$^+$ cells (adhered or partially digested apoptotic thymocytes) and exclusion of the doublets.

Amongst myelomonocytic subpopulations in the naïve peritoneal cavity, ResMØs display the highest capability of apoptotic thymocyte clearance, while the CD11c$^+$CD226^{low} subset show the lowest ability (Fig. 5.15C). At 72 hours after SES challenge, ResMØs still have the highest phagocytic capacity among six defined subpopulations. InfMØs (MHCII$^{+\text{ or }-}$) are less capable than ResMØs, but better than 'DC-like' cells. CD11c$^+$CD226^{low} cells remain the least efficient cell type in terms of apoptotic cell clearance (Fig. 5.16).

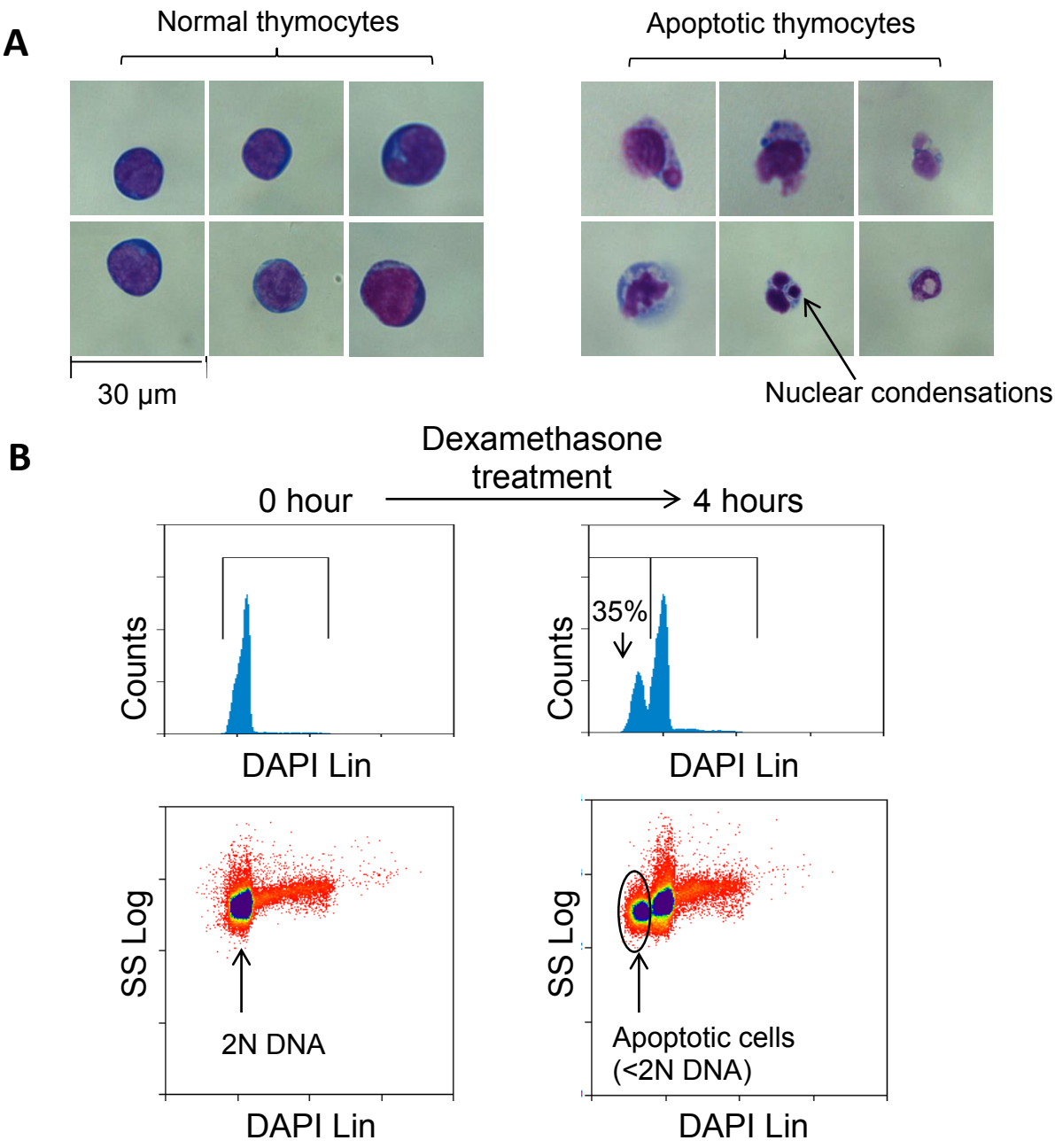

Figure 5.14 Glucocorticoid-induced thymocyte apoptosis

(**A**) The morphology of individual cytospun normal thymocytes (left) and apoptotic thymocytes after *ex vivo* glucocorticoid treatment for 4 hours (right) is shown (scale bar represents 30 µm). Data is representative of two independent experiments. (**B**) Representative histograms and density plots showing apoptotic thymocytes with DNA degradation (<2N DNA, also called 'sub-G_0') after glucocorticoid treatment for 4 hours. Data represents one of four experiments.

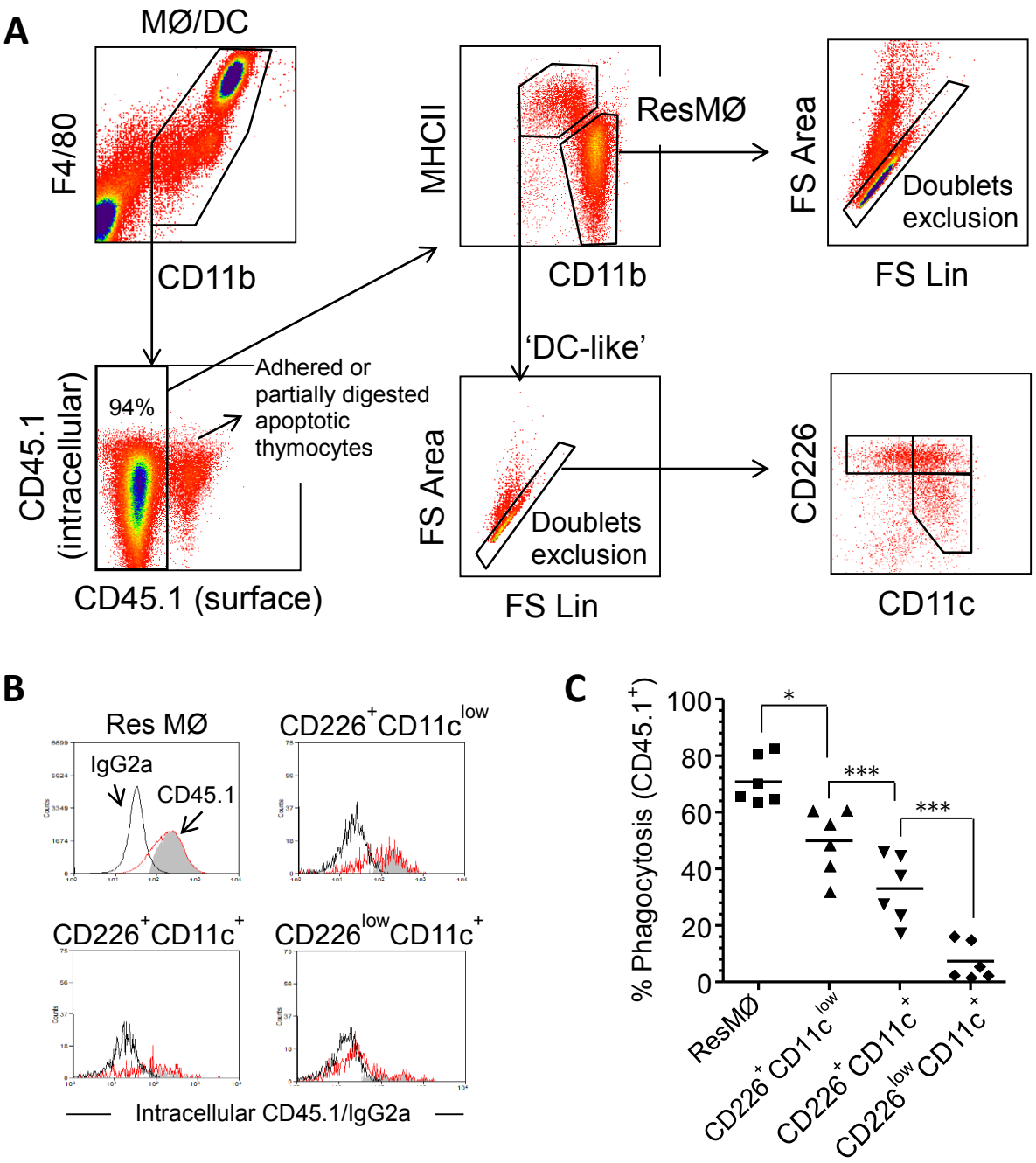

Figure 5.15 Peritoneal MØ/DC subsets from naïve status exhibit differential capability of apoptotic thymocyte clearance

(A) Representative plots depicting the flow-cytometric identification of peritoneal MØ/DC subsets from naive CD45.2$^+$ 129S6/SvEv mice, after intraperitoneal injection of CD45.1$^+$ apoptotic thymocytes for 30 minutes. Peritoneal MØ/DC subsets are gated on CD11b$^+$F4/80$^{high-low}$ and surface-staining CD45.1 cells. **(B)** Histograms showing the proportion of phagocytosed CD45.1$^+$ thymocytes within individual peritoneal MØ/DC subsets. **(C)** Graphs comparing the capability of apoptotic thymocyte clearance (% phagocytosis) among individual peritoneal monocytic subsets. Data represent the mean and are derived from one of two similar experiments (n = 5).

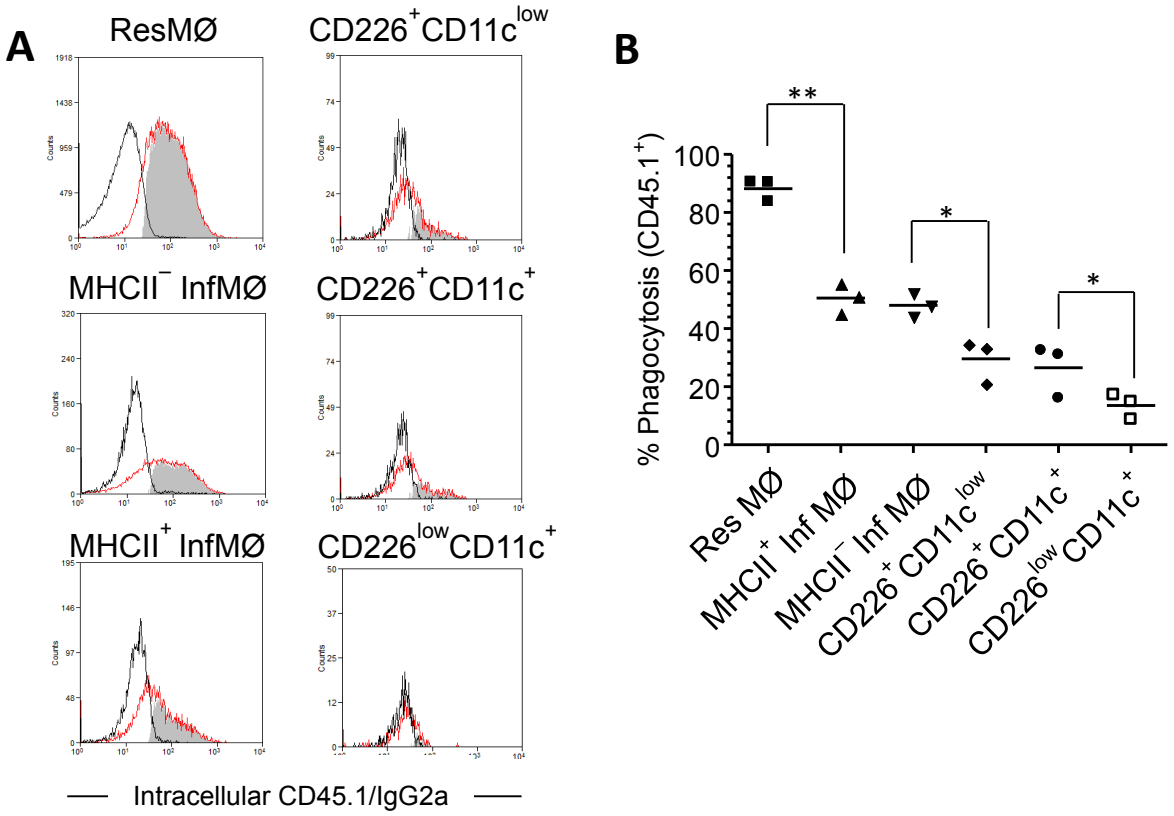

Figure 5.16 Peritoneal MØ/DC subsets from 72h after SES-induced peritonitis exhibit differential capability of apoptotic thymocyte clearance

(A) Representative histograms showing the proportion of phagocytosed CD45.1$^+$ thymocytes within individual peritoneal MØ/DC subsets from CD45.2$^+$ 129S6/SvEv mice at 72 hours after SES-induced peritonitis **(B)** Graphs comparing the capability of apoptotic thymocyte clearance (% phagocytosis) among individual peritoneal monocytic subsets. Data represent the mean and are derived from one of two similar experiments (n = 3).

5.2.10 Fluorescence-activated cell sorting and morphological analysis of murine peritoneal MØ/DC subsets

To understand the morphological appearance of individual peritoneal MØ/DC subsets, a flow-cytometric cell sorting approach for the purification of these cell typeswas performed, firstly from naïve C57BL/6 mice, was performed (Fig. 5.17A). After sorting, the isolated single cell populations were checked for the purity by flow cytometry (Fig. 5.17A, 2nd panel from above).The following highest sort purities were achieved: ResMØ: 98.56%; MHCII^{+} InfMØ: 99.72%; CD11c^{low}CD226^{+}: 94.29%; CD11c^{+}CD226^{+}: 89.86%; CD11c^{+}CD226^{low}: 88.89%. In addition, cytospin preparations were made and the sorted cytospun cells were stained with Microscopy Hemacolour cell stain (Merck), visualized on a Leica DMLB microscope (Leica) and images were captured using a Leica DFC490 digital camera (Leica) and processed using QWin Software (Leica). The morphology of ResMØs and three 'DC-like' subsets stained with Microscopy Hemacolor (Merck) was as shown in Fig. 5.17A (3rd panel from abovetop). Compared to ResMØs, 'DC-like' cells have round or bean-shaped nuclei that are unilobar, ('monocytic appearance'). Of note, CD11c^{+}CD226^{low} subset has the least cytoplasm among three 'DC-like' cells. Secondly, MHCII^{+} InfMØs was sorted from 72 hours post-SES challenged C57BL/6 mice (Fig. 5.17B, left panel). The purity of this cell type was generally > 98%. The morphology of MHCII^{+} InfMØs was as shown in Fig. 5.17B (right panel). They displayed an appearance consistent with more-likely mature 'macrophage appearance', similar to that of ResMØs.

Additionally, these purified individual peritoneal MØ/DC subsets have been used for *in vitro* functional assay (undertaken by Dr. Marcela Rosas) to examine their ability of processing and presenting antigen to helper T cells (see Appendix 2).

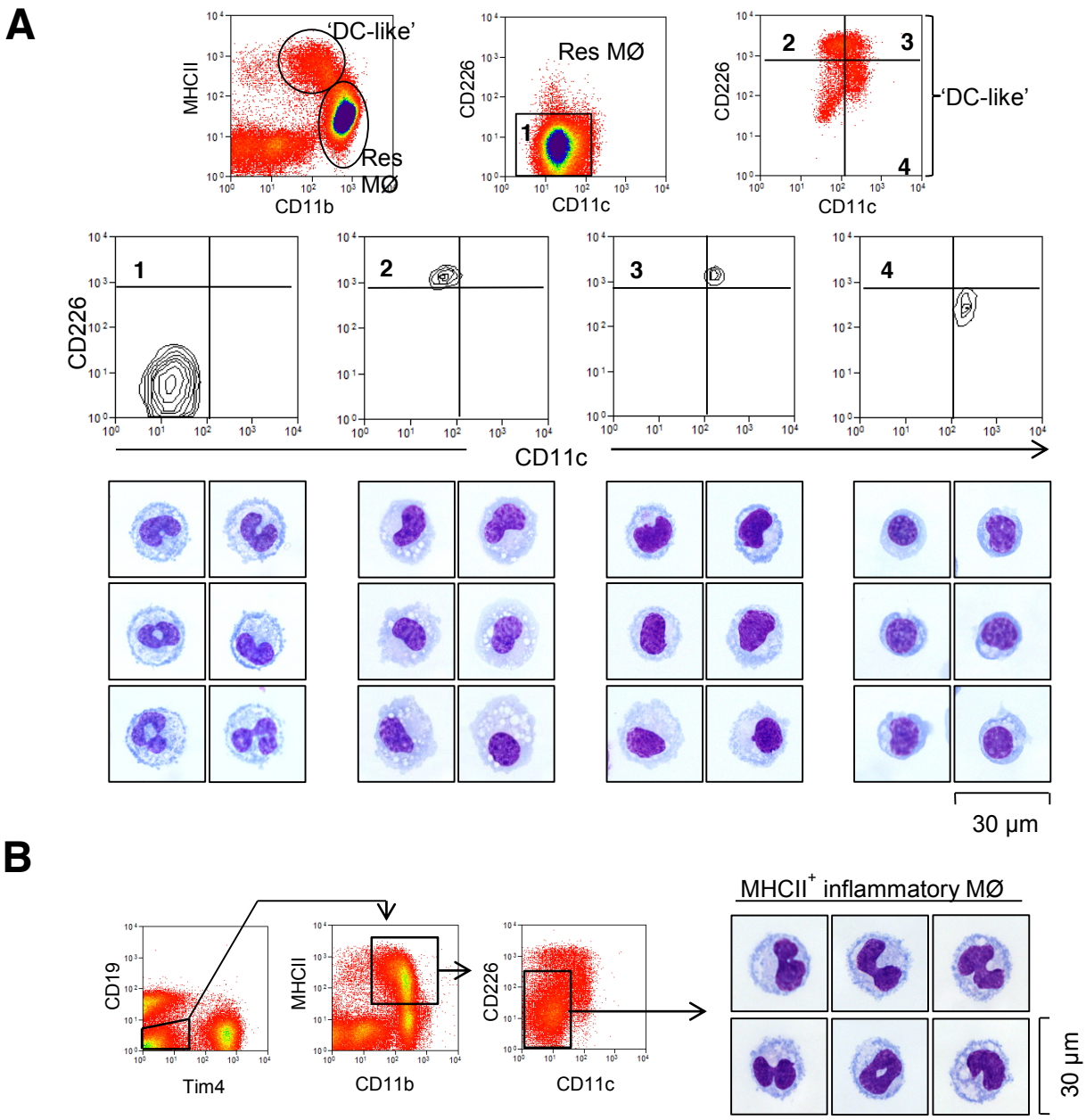

Figure 5.17 Fluorescence-activated cell sorting and morphological analysis of individual peritoneal MØ/DC subset

(A) Representative plots showing the flow-cytometric sorting strategies of ResMØs (**1:**$CD19^{-}CD11b^{high}MHCII^{-}$) and three 'DC-like' subsets ($CD19^{-}CD11b^{int}MHCII^{+}$ with **2:**$CD11c^{low}CD226^{+}$, **3:**$CD11c^{+}CD226^{+}$ and **4:**$CD11c^{+}CD226^{low}$) from cells pooled from 10 naïve C57BL/6 mice. The purity of each post-sorted cell subset is shown. The morphology of individual cytospun cells is shown (scale bar represents 30 µm). **(B)** Dot plots showing the flow-cytometric sorting strategy of peritoneal $MHCII^{+}$ InfMØs ($CD19^{-}Tim4^{-}CD11b^{+}MHCII^{+}CD11c^{-}CD226^{-}$) from 72 hours post-SES challenged C57BL/6 mice. The morphology of cytospun $MHCII^{+}$ InfMØs is shown (scale bar represents 30 µm). Data is representative of two independent experiments.

5.3 Discussion

In this chapter, a select surface marker panel has been successfully applied for defining 'DC-like' subsets within the mouse peritoneal cavity. This decisive phenotyping has permitted for the first time a study of the origins and kinetics of these cells during inflammation, an assessment of their response to microbial products, stimuli and an evaluation of their specialised functions such as apoptotic cell clearance as well as antigen processing and presentation. Although tentatively classified into three 'DC-like' subsets, it appears to be two main subsets according to their morphology and immunophenotype, one which has a $CD226^{low}CD11c^{+}$ phenotype with a slightly smaller size and less cytoplasm, to be more reminiscent of a conventional DC. The other subset is defined by high expression of CD226, but is notably heterogeneous in the expression of traditional DC-markers- CD209a (DC-SIGN) and CD11c. Importantly, the expression of CD226 and CD11c is largely restricted to these 'DC-like' subsets in both steady-state and inflamed peritoneum, allowing definitive discrimination of these cells from the large numbers of potentially $MHCII^{+}$ InfMØs recruited during inflammation.

The kinetic studies depicted found that resident peritoneal 'DC-like' cells disappeared after inflammatory insult (4 hours post-immune challenge), which could be possibly explained by leaving through lymphatic drainage to local lymph nodes, then followed by the accumulation of 'DC-like' cells during the early resolution phase (at 48-72 hours post-inflammatory challenge). The latter were primarily recruited from the periphery with limited local proliferation. This inflammatory recruitment process is consistent with their high expression of CCR2. Recent studies of assumed DC in the peritoneum, based on the use of a $MHCII^{high}CD11c^{+}$ phenotype, confirmed the importance of CCR2

for the recruitment of at least these cells (Goldszmid et al., 2012; Newson et al., 2014). Indeed, the results from CCR2-deficiency mice in this project also confirmed that CCR2 is critical for these 'DC-like' cells in both homing to the peritoneal cavity under the both steady state and during the inflammatory recruitment. Notably, this $CCR2^{+}$ phenotype was conserved across species, with expression observed on human $CD1c^{+}$ peritoneal DCs (Fig. 3.5). The observation of significant recruitment of these human peritoneal DCs (Fig. 4.10) in response to infectious peritonitis suggests that similar inflammatory kinetics upon during peritonitis may exist in both species.

As a known regulatory of inflammatory responses, IL-10 is a keystone to limiting inflammation in the peritoneal cavity (Ajuebor et al., 1999). A recent study of an infectious peritonitis model assessed the regulatory role of IL-10 on the differentiation of peritoneal $MHCII^{+}$ and $MHCII^{-}$ MØs (Nguyen et al., 2012). My data reproduces these observations, confirming that MHCII expression by InfMØs is an indicator of the inflammatory process and the state of InfMØ activation, which is regulated by IL-10. However, the presence of peritoneal 'DC-like' cells during an acute inflammatory response is seemingly less dependent of IL-10, than InfMØs (Fig. 5.11 C). Additionally, we found that $MHCII^{+}$ InfMØs were actually quite poor at the processing and presentation of antigen to T cells when compared to 'DC-like' subsets (see Appendix 2, 'antigen processing and presentation assays' were performed by Dr. Marcela Rosas), which contrasts with the conclusion of previous study (Nguyen et al., 2012). The reason for this discrepancy is unclear, but perhaps includes contamination of $MHCII^{+}$ InfMØs with the previously unidentifiable peritoneal 'DC-like' cells, in the earlier study (Nguyen et al, 2012).

Regarding the responsiveness *ex vivo* to microbial-derived stimuli (SES and LPS), all peritoneal 'DC-like' subsets from either naïve or inflamed mice were predisposed to

produce IL-12, but under inflamed conditions, $MHCII^+$ InfMØs also represented a significant potential source of IL-12, especially given their relatively high numbers in an inflammatory context. Importantly, in a repeat-hit SES-induced chronic peritonitis model, the capability of pro-inflammatory cytokine production (TNF-α, IL-6, IL-12) from InfMØ/DCs may play a contributive role in the process of Th1-driven peritoneal fibrosis (Fielding et al., 2014). Conversely, InfMØs were less disposed to the production of IL-10 after LPS or SES stimulation than ResMØs, but least likely to produce IL-10 was the $CD11c^+CD226^{low}$ DC subset.

Previous study has shown that peritoneal ResMØs were effective at phagocytosing apoptotic cells *in vivo* (Taylor et al., 2000; Uderhardt et al., 2012). The results in this project, by comparisons of different MØ/DC subsets from either naïve or from inflamed mice, have demonstrated that on a single cell basis of all cell types, ResMØs are the most efficient for clearance of apoptotic cells and the $CD11c^+CD226^{low}$ DC subset were the poorest in this regard.

In summary, 'DC-like' subsets in the mouse peritoneal cavity have been characterized phenotypically and functionally. More importantly, their respective cellular kinetics during acute peritonitis has been investigated. Together with human data from PD patients, it is likely that these mouse peritoneal 'DC-like' subsets could be the homologues of newly identified human peritoneal $CD1c^+$ DCs. However, it will need detailed transcriptional mapping between the two species to provide further evidence of their corresponding relationships.

Chapter Six

General discussion

6.1 The identities of peritoneal macrophages and dendritic cells

6.1.1 Peritoneal MØs: "resident" *versus* "recruited"

In the murine peritoneal cavity, $CD11b^{high}F4/80^{high}$ MØs, have been recognized as the major tissue-resident MØ subset in the steady state (Rosas et al., 2007; Dioszeghy et al., 2008). These ResMØs are found to be mainly prenatal in origin (Yona et al., 2013), with the ability to maintain basal numbers by self-renewal, and display a unique proliferative capability for repopulation during the resolution phase of specific inflammatory responses (Davies et al., 2011 & 2013). By contrast, $CD11b^{+}F4/80^{int/low}$ MØs, are known to accumulate in the peritoneal cavity during inflammation, denoted here as 'InfMØs'. They are hematopoietic in origin, primarily recruited from the circulating Ly-$6C^{+}$ monocytes in a CCR2-dependent manner (Yona et al., 2013). In this project, I attempted to identify the potential human analogous ResMØs within the PD effluents and discriminate them from InfMØs by examining a wide range of relevant myelomonocytic markers (Davies et al., 2011; Rosas et al., 2014). Nevertheless, the corresponding human ResMØs still could not be clearly recognised from the patients' PD effluents under different clinical situations. One possible explanation is that the surface markers used in this project show lack of specificity to phenotypically discriminate ResMØs from InfMØs, and the markers found to be useful in mouse ResMØ phenotyping, including F4/80, Tim-4 and CD73, are not expressed in a similar pattern on their human counterparts. Another explanation could be related to the "disappearance reaction" of tissue ResMØs. This reaction has been noted in several murine models of experimental inflammation, and the proposed mechanisms include increased tissue adherence, migration through the draining lymphatic system, and cell death (Barth et al., 1995; Rosen et al., 1990). In the

context of PD, ResMØs could 'disappear' after catheter-related surgical insult or be depleted by the repetitive flushing and continuous dialysis exchange during the course of PD therapy. Indeed, one recent murine study investigated the effect of the catheter implantation-induced peritoneal inflammatory response, showing that decrease in number of ResMØs during the post-surgery period (Min et al., 2012). The fact that almost all $CD14^+$ MØs harvested from PD fluids in this study are $CCR2^+$, also suggests that these cells are mainly derived from the periphery (most likely from $CD14^+CD16^-$ classical blood monocytes), and indirectly implies that recoverable ResMØs are lost under PD therapy. Finally, recent fate-mapping models revealed that in some murine tissues such as intestine, skin, heart, the prenatally-derived tissue ResMØs become substantially replaced by the circulating Ly-$6C^+$($CCR2^+$) classical monocytes, from neonatal period to adulthood (Tamoutounour et al., 2013; Molawi et al., 2014; Bain et al., 2014). This tissue-specific replenishment over time could probably be explained by the diminished proliferative capability of prenatally-derived MØs during ageing process, thereby gradually insufficient to maintain normal tissue homeostasis. Accordingly, it is possible, given the age of the PD patients recruited for this study (mean age 55 years in the new-starters), that the identified peritoneal MØs may be monocyte-derived. In summary, $CD14^+$ MØs harvested from PD effluent in this project are most likely monocyte-derived InfMØs, so the true phenotypic identity of human ResMØs remains elusive. However, the results shown in this study have provided three possibilities of ResMØ identity in humans: 1) In the normal human peritoneal cavity, prenatally-derived ResMØs do exist and self-renew, just like their murine counterparts, but inflammation and/or dialysis washout bias to a circulating precursor-derived cell type ('monocyte-derived MØ'). In the future, maybe we can address this point by studying the peritoneal cells recovered at laparoscopic donor nephrectomy or cholecystectomy which will minimise the impact of surgery-induced

inflammation and dialysis 2) Human peritoneal ResMØs may start as self-renewing like in mice, but over the much longer human lifespan, there is a shift to monocyte-derived, with potential implications for tissue homeostasis during the ageing process. Perhaps future ageing experiments with longitudinal follow-up in mouse models may provide some clues in this regard. In humans, it will be interesting to investigate the peritoneal MØs from pediatric patients, to be able to compare the immunophenotypes with those from old patients. 3) It is also possible that over the much longer gestational period, the embryonic seeded (yolk sac/fetal liver-derived) peritoneal ResMØs in humans have been mostly replaced by the circulating precursor-derived MØs before birth, unlike what we found in mice.

6.1.2 Peritoneal DC population

Since Steinman's classical proposal describing DC's in the 1970's, several DC subsets in lymphoid and non-lymphoid tissues have been described with distinctive phenotypes and functions, both in mice and humans (Merad et al., 2013; Schlitzer and Ginhoux 2014). Although recent fate-mapping experiments in mice have delineated the ontogeny of DC, segregated from the monocyte-MØ lineage (Geissmann et al., 2010; Merad et al., 2013; Schlitzer and Ginhoux 2014), the *in vitro* (Pickl et al., 1996) *in vivo* studies have demonstrated that monocytes can differentiate into DCs in inflammatory contexts (Serbina et al., 2006; León et al., 2007; Greter et al., 2012). To avoid confusion, it has been argued that *bona-fide* DCs should be restricted to "FLT3L/FLT3-dependent DC subsets, thereby all the non-FLT3L/FLT3-dependent DC-like subsets should be regarded as monocyte-derived (Jenkins and Hume 2014). However, in inflammatory scenarios, the term 'inflammatory DC (InfDC)' has been adopted for describing the DC pool in the inflamed tissues (Segura and Amigorena et al., 2014). These tissue infiltrating InfDCs are thought to be mainly derived from circulating monocytes (Osterholzer et al., 2009; Nakano et al., 2009; León et al., 2007; Zigmond et al., 2012; Goldszmid et al., 2012). So far, there is no clear evidence showing that blood DC precursors (FLT3/FLT3L-dependent DCs) contribute to InfDCs during inflammation (Plantinga et al., 2013).

In humans, several tissue DC subsets have been defined, principally myeloid DCs (BDCA-1^+/$CD1c^+$ DCs and BDCA-3^+/$CD141^+$ DCs) and plasmacytoid DCs ($CD123^+CD303^+$ DCs) (Ziegler-Heitbrock et al., 2010). Each DC subset demonstrates a distinctive functional profile (Schlitzer et al., 2014). These DC subsets exist in a variety of human tissues/organs, including intestinal mucosa (Watchmaker et al., 2014), intra-articular fluid (Moret et al., 2013), kidney (Kassianos et al., 2013), and

liver (Kelly et al., 2014). In this study, we identified, for the first time, $CD1c^+$ DCs within the PD effluents from PD patients. A similar observation of this novel cell type has been reported by another group very recently, but from a very different clinical situation (tumor ascites) and using a different flow-cytometric gating approach (Segura et al., 2013). Both sets of data demonstrate that $CD1c^+$ DCs are the predominant DC subtype within the "peritoneal DC pool", at least under these inflamed conditions. Functionally, these DCs display a superior capability for antigen presentation and T cell stimulation (CD4 T cell stimulation in Segura et al., 2013; CD8 T cell stimulation in this study). The origin of these cells is difficult to address but could be directly from transmigration of blood $CD1c^+$ DC precursors or from *in situ* differentiation of the recruited monocytes. The transcriptome analysis has shown that peritoneal $CD1c^+$ DCs from tumour ascites are more close to blood $CD14^+$ monocytes than $CD1c^+$ DC precursors (Segura et al., 2013). However, this does not preclude the possibility of dual sources from the peripheral circulation.

In mice, this study characterises two main 'DC-like' subsets ($CD226^+CD11c^{+/low}$ and $CD11c^+CD226^{low}$) in the naïve or inflamed peritoneal cavity. The $CD226^+$ cells are reminiscent of the previously described $CD11b^+F4/80^+MHCII^+$ 'small MØs' (Rosas et al., 2007; Dioszeghy et al., 2008; Ghosn et al., 2010). Notably, $CD226^+$ cells express some 'MØ-associated' surface markers such as MerTK and, when inflamed, CD64 (Gautier et al., 2012), and share functional properties with both MØs and DCs. Hence, it could be argued that $CD226^+$ cells are an 'intermediate' subtype between MØs and DCs. Intriguingly, one recent paper revealed that 'small MØs' could locally differentiate into ResMØs in a tissue-specific C/EBPβ-dependent pathway (Cain et al., 2013), suggesting that at least in some instances, 'small MØs' or $CD226^+$ cells can be immediate precursors of ResMØs. On the other hand, $CD11c^+CD226^{low}$ cells are

morphologically, phenotypically and functionally more like *bona-fide* DCs despite their relatively low CD11c expression, compared to classical splenic DCs. The fact that $CD226^{+}$ cells and $CD11c^{+}CD226^{low}$ cells are $CCR2^{high/+}$ and could be recruited into the peritoneal cavity in a similar way as InfMØs during experimental peritonitis, indicated that these 'DC-like' cells are likely Ly-$6C^{+}$($CCR2^{+}$) monocyte-derived. Recent evidence using intravenous Ly-$6C^{+}$ monocyte transfer experiments disclosed that after peritonitis is elicited, donor Ly-$6C^{+}$ monocytes can migrate into the peritoneal cavity and differentiate into both InfMØs and $CD11c^{+}MHCII^{+}$ DCs (Goldszmid et al., 2012). However, our data from naïve *Gata6* knockout mice showed a significant increase (4-5 fold) of $CD226^{+}$ cells, but not $CD11c^{+}CD226^{low}$ cells, accompanying the decrease of ResMØs, compared to the wild type littermates (Rosas et al., 2014 and unpublished data). These observations suggested that $CD226^{+}$ cells and $CD11c^{+}CD226^{low}$ cells have distinct developmental cues. Whether or not $CD226^{+}$ cells could differentiate into $CD11c^{+}CD226^{low}$ cells *in situ* under steady-state or inflamed conditions remains to be elucidated.

6.1.3 Comparisons between human and murine peritoneal MØ/DC subsets

The phenotypic comparisons between mice and humans revealed characteristic surface marker expression conserved across both species. Specifically, peritoneal MØs (ResMØs/InfMØs in mice as well as $CD14^+$ MØs in humans) express relatively high levels of CD36, CD64 and MerTK, while peritoneal DCs ($CD226^+$ DCs and $CD11c^+$ DCs in mice as well as $CD1c^+$ DCs in humans) express relatively high levels of CD206, CD226 and CD301. These characteristic 'MØ or DC-specific' surface marker panels could be useful for future immunophenotyping. In both species, all peritoneal MØ/DC subsets could generate substantial amounts of pro-inflammatory cytokines such as TNF-α, IL-1β and IL-6 upon *ex vivo* LPS or SES stimulation. However, murine DC-like cells display significantly greater potential for IL-12p40 production, compared to ResMØs or InfMØs. In PD patients, both $CD14^+$ MØs and $CD1c^+$ DCs generate similar extent of IL-12 upon stimulation. Functionally, Human $CD14^+$ MØs have superior capability of phagocytosis (*Staphylococcus epidermidis* or zymosan particles) than $CD1c^+$ DCs. Similarly, murine ResMØs or InfMØs are more efficient at phagocytosis of apoptotic thymocytes than DC-like subsets. On the other hand, human $CD1c^+$ DCs have a superior ability to process and present antigen than $CD14^+$ MØs, and the capability of antigen processing and presentation is mostly restricted to peritoneal 'DC-like' cells in mice.

Taken together, murine $CD11c^+CD226^{low}$ cells are phenotypically and functionally more likely analogous to subsets of human $CD1c^+$ DCs, whereas $CD226^+$ cells are phenotypically and functionally 'intermediate' between MØ and DC. To confirm the potential corresponding relationships between humans and mice, it will be necessary to perform cross-species mapping of gene expression profiles derived from the transcriptome analysis of multiple peritoneal MØ/DC subsets.

6.1.4 Future directions

To identify *bona fide* human peritoneal ResMØs, further analysis of peritoneal cells from healthy individuals, possibly *via* laparoscopic surgery or perhaps from pediatric/young adult PD patients, will be needed. It should be kept in mind, however, that even minimally-invasive surgery can cause blood dissemination within the peritoneal cavity, and potentially induce inflammatory response and change the MØ phenotype. Because genetic lineage tracing is not feasible in humans, it would be difficult to prove that human peritoneal ResMØs (if identified) are prenatal in origin. However, recent studies on human skin from patients receiving sex-mismatched hematopietic stem cell transplantation have provided indirect evidence that at least some steady-state human skin ResMØs are long lived (possibly embryo-derived) and could persist more than one year post-transplantation independently of donor monocyte input. Conversely, steady-state human skin DCs are almost completely supplied from the donors' circulating precursors within 40 days after transplantation (Haniffa et al., 2009; McGovern et al., 2014). Perhaps, this strategy will enable us to further clarify the developmental origins of human peritoneal MØ/DC subsets in the future. In addition, it will be of interest to perform transcriptome analysis of the isolated human peritoneal $CD14^+$ MØs and $CD1c^+$ DCs from PD effluent. Then we can compare the published data using tumour ascites as a different source of peritoneal cells (Segura et al., 2013) to tell how the two microarray datasets may have similarities or differences in terms of gene expression profiles from the respective MØ and DC subsets.

In mice, there are some issues raised in this project. Firstly, it is unclear that for how long peritoneal ResMØs can maintain the required tissue cell number by self-renewal under steady state. It has been demonstrated that the proliferative capability of

peritoneal ResMØs gradually declines from newborns (2-week-old) to young adults (12-16-week-old) (Davies et al., 2011). However, it is still unclear to what extent the prenatally-derived tissue ResMØs can be replaced by monocyte-derived MØs during ageing. To address this issue, it would be necessary to conduct further experiments, for example using BM chimerism (*Ccr2*$^{-/-}$/*Ccr2*$^{+/+}$) with longer time point follow-up. Secondly, we still don't know whether the recruited InfMØs can genuinely differentiate into ResMØs during the resolution phase of the elicited inflammation, and if so, how they can compare the prenatally-derived ResMØs. To decipher this point will probably need further BM chimerism experiments (CD45.1/CD45.2) and sorting of the respective ResMØs (CD45.1^{+} and CD45.2^{+}) at the latter time points of the elicited peritonitis for transcriptomic comparisons. Finally, it remains obscure to what extent peritoneal DC-like subsets (CD226^{+} or CD11c^{+}CD226^{low}) are FLT3/FLT3L-dependent. Future lineage tracing studies, and the use of *Flt3* and/or *Flt3l* knockout mice, may be helpful in clarifying this concern.

6.2 Alterations of peritoneal MØ/DC phenotypes and activation/ maturation status during PD therapy

PD is a well-established renal replacement therapy for kidney failure patients, however its' short-term and long-term influences on the peritoneal immune system have concerned the PD community. Mononuclear phagocytes are immune cells with high plasticity, which promptly respond to the microenvironmental changes *in vitro* or *in vivo*. In this study, one of the main objectives was to understand how the peritoneal mononuclear phagocytes are modified during the treatment course of PD, including PD-related peritonitis, and whether alterations observed correlated with clinical outcomes of PD patients.

6.2.1 Altered distribution of peritoneal MØ/DC during PD therapy

In this study, the longitudinal analysis of myelomonocytic subsets within the PD flushes/effluents from 'new-starter' patients revealed that peritoneal $CD14^+$ MØs and $CD1c^+$ DCs display distinct cellular kinetics along the PD course, implying that differential factors may control the recruitment or the differentiation process of the respective MØ/DC subsets. It was anticipated that CCR2 ligands (e.g. CCL2/MCP-1) would play a crucial role in the process of monocyte recruitment (predominantly inflammatory, but possibly also homeostatic) based on previous mouse work by our group and others (Goldszmid et al., 2012). On the other hand, GM-CSF might be essential for the (monocyte → DC) differentiation process, as GM-CSF is an important growth factor for DC differentiation *in vitro*. FLT3 ligand, another growth factor critical for DC development, may also be involved in this process. Although these chemokines/growth factors could be diluted by the instilled PD fluids, it is

possible that local concentrations remain high enough within the peritoneum (particular in the interstitial layer), leading to continuous leukocyte transmigration and/or *in situ* differentiation. Interestingly, the ratio of $CD14^+$ MØ to $CD1c^+$ DC may be a good indicator of the status of intra-peritoneal inflammation, as shown by the decline of the ratio from one week after catheter insertion (20-25:1) to 3-6 month maintenance dialysis (5-10:1) and which dramatically increases during acute peritonitis (up to nearly 100:1). During acute bacterial peritonitis, $CD14^+$ monocytes are rapidly recruited into the peritoneal cavity, presumably depending on the chemotactic gradient generated by the inflamed peritoneum, including for example CCL2/MCP-1 secreted from peritoneal mesothelial cells (Li et al., 1998). Intriguingly, the increase in $CD1c^+$ DC number is very limited during peritonitis. One possible explanation is that the local chemokine and cytokine microenvironment during peritonitis may favour monocyte transmigration, rather than DC migration and/or *in situ* monocyte-to-DC differentiation. Hence, the ratio of MØ to DC drastically increases during inflammation. Importantly, preliminary observation showed that patients with adverse outcomes (catheter failure or peritonitis failure) had higher ratios of MØ to DC than those with good prognosis, suggesting that higher ratios are associated with more severe intra-peritoneal inflammation. Notably, there is a trend towards a higher number of peritoneal MØs and also a higher ratio of MØ to DC in stable dialysis patients with a history of multiple peritonitis episodes, compared to those without any history of peritonitis. These observations could be a consequence of chronic peritoneal inflammation with increased infiltration of monocyte-MØs after repeated peritonitis, and possibly would lead to to accumulating membrane fibrosis and technique failure in the longer term, similar to the results found in the repeat-hit SES-induced peritoneal fibrosis mouse model (Fielding et al., 2014).

6.2.2 Altered activation/maturation status of peritoneal MØ during PD therapy

Another impact of PD therapy on peritoneal MØ biology is altered MØ activation/maturation status. We observed heterogeneous surface marker expression in peritoneal $CD14^+$ MØs from serial PD effluents of 'new-starter' patients,, probably reflecting different stages of MØ activation and maturation. Notably, the number and the proportion of $CD206^+$ MØs (also with higher expression of HLA-DR, CD86 and CD163, denoted as 'mature MØ' phenotype) declined after dialysis intervention, indicating that continuous dialysis exchanges may hinder the maturation process of recruited monocytes turning into tissue MØs, perhaps owing to the diluted cytokines, insufficient for the maturation requirement.

Previously, two studies have shown that peritoneal MØs from uninfected PD effluent samples display a M2-like phenotype ($CD163^+$ or $CD206^+$) with 'anti-inflammatory' IL-10 production after *ex vivo* LPS stimulation (Xu et al., 2007) or with increased mRNA expression of 'pro-fibrotic' genes such as TGF-β1, MMP-9, CCL18 (Bellon et al., 2009). Our results demonstrate that peritoneal MØs from uninfected PD effluent samples differentially expressed CD16 and CD206, and could generate significant amounts of 'pro-inflammatory' cytokines such as TNF-α, IL-1β, IL-6 as well as IL-12 upon *ex vivo* LPS or SES stimulation. Altogether, these findings suggest that peritoneal MØs are highly heterogeneous *in vivo* and retain phenotypic plasticity in response to micro-environmental changes, and that the classical M1/M2 paradigm may be inadequate in this context. This contrasts with the presence of 'M1-MØs' or 'classically activated MØs' during acute bacterial peritonitis. In the context of the post-surgery period, the catheter-related sterile inflammatory response, either from surgical injury or from catheter-induced foreign body reaction, enriches the cavity with both $CD206^+$ and $CD206^-$ MØs. Hence, it is difficult to fit this scenario into

either the M1 or the M2 category. Moreover, the fact that the proportion of $CD206^+$ cells within $CD14^+$ MØs is significantly reduced after the commencement of dialysis implies that CD206 may be more appropriately used here as a "maturation marker" for MØs, rather than a definitive "M2-specific marker". Perhaps the genuine 'M2-MØs' *in vivo*, based on the rigorous definition, can only be found in extremes of clinical scenario, similar to the conditioned *in vitro* polarised microenvironment (Murray et al., 2014).

As for the relationship between MØ activation and clinical outcomes, peritonitis patients with treatment failure displayed a trend of lower proportion of $CD16^+$ cells within $CD14^+$ MØs and a significantly higher number of the $CD14^+CD16^-$($CD206^{+\text{ or }-}$) subtype, compared to those who were successfully treated. As described, this $CD14^+CD16^-$ subtype may represent newly recruited classical monocyte/MØs within the peritoneal cavity. Therefore, the high amplitude of inflammatory recruitment of this cell type may be associated with adverse outcomes. In new-starter patients, those suffering from catheter failure had a higher percentage of $CD16^+$ cells within $CD14^+$ MØs and a significantly higher number of $CD14^+CD16^+CD206^-$ subtype at the time of the *1st flush* (one week after surgery), compared to those with good catheter outcomes. Similarly, stable dialysis patients with a history of multiple peritonitis episodes had a higher percentage of $CD16^+$ within $CD14^+$ MØs and a significantly higher number of the $CD14^+CD16^+CD206^-$ subtype, than those without any history of peritonitis. These $CD14^+CD16^+CD206^-$ cells are possibly derived from transmigration of $CD14^+CD16^+$ blood monocytes or from up-regulated CD16 expression of $CD14^+CD16^-$ blood monocytes after recruitment. Nevertheless, the increase in this subtype may reflect a unique inflammatory status, i.e., catheter-related sterile inflammation or chronic (non-infectious) inflammation.

6.2.3 Future directions

These studies have demonstrated the impact of PD therapy on the peritoneal MØ/DC phenotype, and activation/maturation within the peritoneal cavity. However, there are some issues that need to be addressed. Firstly, PD patients have a complex uraemic background which has been suggested to influence the MØ/DC biology. For example, a recent study showed that the uraemic toxin, indoxyl sulphate, alone could stimulate MØ function, e.g. inducing ROS and nitric oxide release; and also enhance peritoneal MØ activation in response to LPS challenge with increased TNF-α/IL-6 production (Adesso et al., 2013). Additionally, it has been shown that advanced glycation end product (AGE)-modified beta-2 microglobulin, which is frequently accumulated in uraemic dialysis patients, could activate peritoneal MØs by increasing TNF-α/IL-1β secretion (Rashid et al, 2006). In the future, it would be interesting to measure PD effluent levels of these "uraemic factors", and investigate their associations with the altered MØ/DC activation/differentiation, pro-inflammatory cytokines changes and peritoneal membrane dysfunction in long-term PD patients. With regard to the potential effects of dialysis fluids on peritoneal MØ/DC biology, a series of studies have revealed that conventional acidic lactate-buffered PD solutions would compromise MØ function, compared to new biocompatible PD fluids such as neutral pH solutions buffered with bicarbonate/lactate (Mackenzie et al., 1998 & 2000, Jones et al., 2002). Furthermore, a study has suggested that conventional PD solutions would impair monocyte-to-DC differentiation and also inhibit the LPS-induced maturation of monocyte-derived DCs. The evaluation of PD fluids revealed that sodium acetate and glucose degradation products are the key components which would inhibit the acquisition of DC marker expression (CD1a, CD209) and impair LPS-stimulated NF-kB activation (Puiq-Kroger et al., 2003). Because the PD effluent

cells analysed in this project are generally derived from conventional PD fluids, which means the MØ/DC biology data shown in this project would possibly be influenced by those PD fluid components. Nonetheless it would need to compare different types of dialysis fluids in the future, to clarify to what extent the altered MØ/DC biology due to different PD fluids is correlated to PD patient outcomes, particularly long-term membrane function.

In this project, I stratified peritoneal MØs into multiple subtypes based on the CD16 and CD206 expression, representing different stages of MØ activation and maturation. However, it is unclear whether the distinct activation/maturation status is committed to different functional properties. For example, it has been shown that blood $CD14^{+}CD16^{+}$ monocytes produce more inflammatory cytokines upon LPS challenge but exhibit less capability to generate ROS, compared to blood $CD14^{+}CD16^{-}$ monocytes (Cros et al., 2010). It will be of interest to know whether such functional distinction exists in the context of PD between $CD16^{+}$ MØs and $CD16^{-}$ MØs. Similarly, whether $CD206^{+}$ MØs are functionally different from $CD206^{-}$ MØs remains to be determined. Finally, understanding the factors by which MØ activation/maturation is controlled could be important for developing novel therapeutic strategies to modify disease outcomes in the future.

6.3 From peritonitis to peritoneal fibrosis: defining the roles of peritoneal MØ and DC in PD patients

Peritonitis remains one of the major reasons for technique failure or death in PD patients, despite advances in connective technology and antimicrobial treatment. One of the key determinants is that renal failure patients are relatively immunocompromised and vulnerable to microbial attack. Hence, the study of PD patients' peritoneal immune system is pertinent to understand the host-pathogen interaction and further delineate possible links to clinical outcomes. In the context of MØ and DC, our human and mouse studies have provided a broad insight as to how these cell types contribute to peritoneal immunity upon infectious challenge. In general, peritoneal MØ/DC serve as the frontline cell types to sense invading pathogens though their abundant PRRs on their cell surface, triggering chemokine and cytokine production, and attracting massive numbers of neutrophils and monocyte/MØs into the peritoneal cavity. The recruited neutrophils and InfMØs substantially participate in phagocytosis and microbial killing. MØs also play a predominant role in the clearance of apoptotic cells, and in the resolution of acute inflammation. In fact, the term "resolution-phase MØs" has been used in mouse experimental peritonitis models to describe this type of MØs, to distinguish from "pro-inflammatory MØs" (Stables et al., 2011). Although the transcriptome analysis of these two cell types shows differentially expressed gene signatures (Stables et al., 2011), these data should be interpreted with caution as both these classes of MØs comprise a mixed population when sorted. Hence, the phenotype of MØ (and/or DC) actually involved in the resolution process remains elusive. In PD patients, we only studied peritoneal MØs from day 1 peritonitis patients, which are recognized as 'pro-inflammatory' type MØs. In the future, it will be of interest to know how the MØ

phenotype changes during the course of PD-related peritonitis by serial follow-up of PD effluent from the same patient until the episode has resolved or the treatment failed. Then we can possibly identify 'high risk' patients who may have defects in the transition from 'inflammation' to 'resolution', thereby suffering from adverse outcomes. Similarly, it could also be important to identify patients with impaired monocyte/MØ function, who may be at high risk for developing peritonitis and are potentially associated with poor prognosis.

Peritoneal DCs, despite overlapping phenotypically with MØs, display distinctive functional properties. For instance, they are less capable of phagocytosis, but significantly more efficient at processing and presenting antigen. The latter provides for superior T cell stimulation, presumably leading to the development of effective protective immunity against infections. However, like MØs, peritoneal DCs can generate significant amounts of pro-inflammatory cytokines in response to external microbial stimuli, potentially contributing to tissue damage in persistent or recurrent inflammation.

What are the roles of peritoneal MØs and DCs in the development of peritoneal fibrosis in PD patients? This is a complex issue as peritoneal fibrosis is contributed to by many factors, including genetic predisposition, uraemic background, pre-existing comorbidities, and most importantly, exposure to non-physiologic PD fluids and infectious events. Although the 'multi-hit' SES mouse model has provided a novel insight into how the immune cells and related cytokines play their roles in the development of repeated infection-related peritoneal fibrosis (Fielding et al., 2014), whether or not MØ and DC participate in 'non-infectious type' peritoneal fibrosis as well as fulminant encapsulating peritoneal sclerosis (EPS) remains to be determined. In a recent global transcriptome analysis of peritoneal tissues from patients with

encapsulating peritoneal sclerosis (EPS), compared to PD patients without EPS or uraemic patients without history of PD, the canonical pathway analysis of differentially expressed genes has revealed enrichment in several pathways relating to MØ/DC function and activation/maturation, highlighting the critical role of these immune cell types in the process of peritoneal fibrosis (Reimold et al., 2013). Hence, exploring the underlying mechanisms controlling peritoneal MØ/DC biology and the potential crosstalk between MØ/DC and other cell types such as mesothelial cells and fibroblasts will pave the way for the development of novel therapeutic strategies to retard this devastating complication of PD in the future.

Bibliography

Adesso S, Popolo A, Bianco G, Sorrentino R, Pinto A, Autore G, Marzocco S. (2013) The uremic toxin indoxyl sulphate enhances macrophage response to LPS. *PLoS One* 8:e76778

Adolfs MJ, Fieren MW, Bonta IL. (1985) Infectious-inflammatory changes in cyclic AMP levels and in their regulation by prostaglandins in human peritoneal macrophages. *Prostaglandins Leukot Med* 18:217-226

Ajami B, Bennett JL, Krieger C, Tetzlaff W, Rossi FM. (2007) Local self-renewal can sustain CNS microglia maintenance and function throughout adult life. *Nat Neurosci* 10:1538-1543

Albanese AM, Albanese EF, Miño JH, Gómez E, Gómez M, Zandomeni M, Merlo AB. (2009) Peritoneal surface area: measurements of 40 structures covered by peritoneum: correlation between total peritoneal surface area and the surface calculated by formulas. *Surg Radiol Anat* 31:369-377

Alobaidi HM, Coles GA, Davies M, Lloyd D. (1986) Host defence in continuous ambulatory peritoneal dialysis: the effect of the dialysate on phagocyte function. *Nephrol Dial Transplant* 1:16-21

Andreesen R, Brugger W, Scheibenbogen C, Kreutz M, Leser HG, Rehm A, Löhr GW. (1990) Surface phenotype analysis of human monocyte to macrophage maturation. *J Leukoc Biol* 47:490-497

Aschoff L. Das reticulo-endotheliale system. (1924) *Ergeb. Inn. Med. Kinderheilkd* 26:1-118

Auffray C, Fogg D, Garfa M, Elain G, Join-Lambert O, Kayal S, Sarnacki S, Cumano A, Lauvau G, Geissmann F. (2007) Monitoring of blood vessels and tissues by a population of monocytes with patrolling behavior. *Science* 317:666-670

Austyn JM, Gordon S. (1981) F4/80, a monoclonal antibody directed specifically against the mouse macrophage. *Eur J Immunol* 11:805-815

Autissier P, Soulas C, Burdo TH, Williams KC. (2010) Evaluation of a 12-color flow cytometry panel to study lymphocyte, monocyte, and dendritic cell subsets in humans. *Cytometry A* 77:410-419

Bain CC, Scott CL, Uronen-Hansson H, Gudjonsson S, Jansson O, Grip O, Guilliams M, Malissen B, Agace WW, Mowat AM. (2013) Resident and pro-inflammatory macrophages in the colon represent alternative context-dependent fates of the same Ly-6C^{hi} monocyte precursors. *Mucosal Immunol* 6:498-510

Bain CC, Bravo-Blas A, Scott CL, Perdiguero EG, Geissmann F, Henri S, Malissen B, Osborne LC, Artis D, Mowat AM. (2014) Constant replenishment from circulating monocytes maintains the macrophage pool in the intestine of adult mice. *Nat Immunol* 15:929-937

Barth MW, Hendrzak JA, Melnicoff MJ, Morahan PS. (1995) Review of the macrophage disappearance reaction. *J Leukoc Biol* 57:361-367

Béchade C, Guittet L, Evans D, Verger C, Ryckelynck JP, Lobbedez T. (2013) Early failure in patients

starting peritoneal dialysis: a competing risks approach. *Nephrol Dial Transplant* 29:2127-2135

Bellon T, Martínez V, Lucendo B, del Peso G, Castro MJ, Aroeira LS, Rodríguez-Sanz A, Ossorio M, Sánchez-Villanueva R, Selgas R, Bajo MA. (2009) Alternative activation of macrophages in human peritoneum: implications for peritoneal fibrosis. *Nephrol Dial Transplant* 26:2995-3005

Benjamini Y, Hochberg Y. (1995) Controlling the false discovery rate: a practical and powerful approach to multiple testing. *Journal of the Royal Statistical Society*, Series B. 57:289-300

Betjes MG, Haks MC, Tuk CW, Beelen RH. (1991) Monoclonal antibody EBM11 (anti-CD68) discriminates between dendritic cells and macrophages after short-term culture. *Immunobiology* 183:79-87

Betjes MG, Tuk CW, Struijk DG, Krediet RT, Arisz L, Beelen RH. (1993) Antigen-presenting capacity of macrophages and dendritic cells in the peritoneal cavity of patients treated with peritoneal dialysis. *Clin Exp Immunol* 94:377-384

Biswas SK, Mantovani A. (2010) Macrophage plasticity and interaction with lymphocyte subsets: cancer as a paradigm. *Nat Immunol* 11:889-896

Brown GD, Gordon S. Immune recognition. (2001) A new receptor for beta-glucans. *Nature* 413:36-37

Brown GD, Taylor PR, Reid DM, Willment JA, Williams DL, Martinez-Pomares L, Wong SY, Gordon S. (2002) Dectin-1 is a major beta-glucan receptor on macrophages. *J Exp Med* 196:407-412

Cain DW, O'Koren EG, Kan MJ, Womble M, Sempowski GD, Hopper K, Gunn MD, Kelsoe G. (2013) Identification of a tissue-specific, C/EBPβ-dependent pathway of differentiation for murine peritoneal macrophages. *J Immunol* 191:4665-4675

Cárcamo C, Fernández-Castro M, Selgas R, Jiménez C, Molina S, Vara F. (1996) Long-term continuous ambulatory peritoneal dialysis reduces the expression of CD11b, CD14, CD16, and CD64 on peritoneal macrophages. *Perit Dial Int* 16:582-589

Cassado Ados A, de Albuquerque JA, Sardinha LR, Buzzo Cde L Faustino L Nascimento R, Ghosn EE, Lima MR, Alvarez JM, Bortoluci KR. (2011) Cellular renewal and improvement of local cell effector activity in peritoneal cavity in response to infectious stimuli. *PLoS One* 6:e22141

Chana KK, Fenwick PS, Nicholson AG, Barnes PJ, Donnelly LE. (2014) Identification of a distinct glucocorticosteroid-insensitive pulmonary macrophage phenotype in patients with chronic obstructive pulmonary disease. *J Allergy Clin Immunol* 133:207-216

Chaudhary K, Sangha H, Khanna R. (2011) Peritoneal dialysis first: rationale. *Clin J Am Soc Nepphrol* 6:447-456

Choi P, Nemati E, Banerjee A, Preston E, Levy J, Brown E. (2004) Peritoneal dialysis catheter removal for acute peritonitis: a retrospective analysis of factors associated with catheter removal and prolonged postoperative hospitalization. *Am J Kidney Dis* 43:103-111

Chorro L, Sarde A, Li M, Woollard KJ, Chambon P, Malissen B, Kissenpfennig A, Barbaroux JB, Groves R, Geissmann F. (2009) Langerhans cell (LC) proliferation mediates neonatal

development, homeostasis, and inflammation-associated expansion of the epidermal LC network. *J Exp Med* 206:3089-3100

Chow KM, Szeto CC, Leung CB, Kwan BC, Law MC, Li PK. (2005) A risk analysis of continuous ambulatory peritoneal dialysis-related peritonitis. *Perit Dial Int* 25:374-379

Cichocki T, Hanicki Z, Sulowica W, Smolenski O, Kopec J, Zembala M. (1983) Output of peritoneal cells into peritoneal dialysate. Cytochemical and functional studies. *Nephron* 35:175–182

Cisse B, Caton ML, Lehner M, Maeda T, Scheu S, Locksley R, Holmberg D, Zweier C, den Hollander NS, Kant SG, Holter W, Rauch A, Zhuang Y, Reizis B. (2008) Transcription factor E2-2 is an essential and specific regulator of plasmacytoid dendritic cell development. *Cell* 135:37-48

Cohn ZA, Benson B. (1965) The differentiation of mononuclear phagocytes. Morphology, cytochemistry, and biochemistry. *J Exp Med* 121:153-170

Cohn ZA, Hirsch JG, Fedorko ME. (1966) The in vitro differentiation of mononuclear phagocytes. IV. The ultrastructure of macrophage differentiation in the peritoneal cavity and in culture. *J Exp Med* 123:747-756

Cohn ZA, Fedorko ME, Hirsch JG. (1966) The in vitro differentiation of mononuclear phagocytes. V. The formation of macrophage lysosomes. *J Exp Med* 123:757-766

Corcoran L, Ferrero I, Vremec D, Lucas K, Waithman J, O'Keeffe M, Wu L, Wilson A, Shortman K. (2003) The lymphoid past of mouse plasmacytoid cells and thymic dendritic cells. *J Immunol* 170:4926-4932

Cresswell P. (1985) Intracellular class II HLA antigens are accessible to transferrin-neuraminidase conjugates internalized by receptor-mediated endocytosis. *Proc Natl Acad Sci U S A* 82:8188-8192

Cros J, Cagnard N, Woollard K, Patey N, Zhang SY, Senechal B, Puel A, Biswas SK, Moshous D, Picard C, Jais JP, D'Cruz D, Casanova JL, Trouillet C, Geissmann F. (2010) Human $CD14^{dim}$ monocytes patrol and sense nucleic acids and virus TLR 7 and TLR8 receptors. *Immunity* 33:375-386

Cunningham RS. (1926) The physiology of the serous membranes. *Physiol Rev* 6:242-256

Czernielewski JM, Demarchez M. (1987) Further evidence for the self-reproducing capacity of Langerhans cells in human skin. *J Invest Dermatol* 88:17–20

Damsker JM, Hansen AM, Caspi RR. (2010) Th1 and Th17 cells: adversaries and collaborators. *Ann N Y Acad Sci* 1183:211-221

Daugirdas JT, Leehey DJ, Popli S, Hoffman W, Zayas I, Gandhi VC, Ing TS. (1987) Induction of peritoneal fluid eosinophilia and/or monocytosis by intraperitoneal air injection. *Am J Nephrol* 7:116-120

Davenport A. (2009) Peritonitis remains the major clinical complication of peritoneal dialysis: The London UK, Peritonitis Audit 2002-2003. *Perit Dial Int* 29:297-302

Davey MS, Lin CY, Roberts GW, Heuston S, Brown AC, Chess JA, Toleman MA, Gahan CG, Hill C, Parish T, Williams JD, Davies SJ, Johnson DW, Topley N, Moser B, Eberl M. (2011) Human

neutrophil clearance of bacterial pathogens triggers anti-microbial γδ T cell responses in early infection. *PLoS Pathog* 7:e1002040

Davies LC, Rosas M, Smith PJ, Fraser DJ, Jones SA, Taylor PR. (2011) A quantifiable proliferative burst of tissue macrophage restores homeostatic macrophage populations after acute inflammation. *Eur J Immunol* 41:2155-2164

Davies LC, Rosas M, Jenkins SJ, Liao CT, Scurr MJ, Brombacher F, Fraser DJ, Allen JE, Jones SA, Taylor PR. (2013) Distinct bone marrow-derived and tissue-resident macrophage lineages proliferate at key stages during inflammation. *Nat Commun* 4:1886

Davies LC, Jenkins SJ, Allen JE, Taylor PR. (2013) Tissue-resident macrophages. *Nat Immunol* 14:986-995

Davies SJ, Suassuna J, Ogg CS, Cameron JS. (1989) Activation of immunocompetent cells in the peritoneum of patients treated with CAPD. *Kidney Int* 36:661-668

Davies SJ, Yewdall VM, Ogg CS, Cameron JS. (1990) Peritoneal defence mechanisms and Staphylococcus aureus in patients treated with continuous ambulatory peritoneal dialysis (CAPD). *Perit Dial Int* 10:135-140

Davies SJ, Mushahar L, Yu Z, Lambie M. (2011) Determinants of peritoneal membrane function over time. *Semin Nephrol* 31:172-182

Davies SJ. (2014) Peritoneal solute transport and inflammation. *Am J Kidney Dis* 64:978-986

de Fijter CW, Verbrugh HA, Peters ED, Oe PL, van der Meulen J, Verhoef J, Donker AJ. (1993) In vivo exposure to the currently available peritoneal dialysis fluids decreases the function of peritoneal macrophages in CAPD. *Clin Nephrol* 39:75-80

Diao J, Winter E, Chen W, Cantin C, Cattral MS. (2004) Characterisation of distinct conventional and plasmacytoid dendritic cell-committed precursors in murine bone marrow. *J Immunol* 173:1826-1833

Diaz-Buxo JA. (1998) Management of peritoneal catheter malfunction. *Perit Dial Int* 18:256-259

Dicarlo FJ, Fiore JV. (1958) On the composition of zymosan. *Science* 127:756-757

Dioszeghy V, Rosas M, Maskrey BH, Colmont C, Topley N, Chaitidis P, Kühn H, Jones SA, Taylor PR, O'Donnell VB. (2010) 12/15-Lipoxygenase regulates the inflammatory response to bacterial products in vivo. *J Immunol* 181:6514-6524

Doyle AG, Herbein G, Montaner LJ, Minty AJ, Caput D, Ferrara P, Gordon S. (1994) Interleukin-13 alters the activation state of murine macrophages in vitro: comparison with interleukin-4 and interferon-gamma. *Eur J Immunol* 24:1441-1445

Duffield JS, Lupher M, Thannickal VJ, Wynn TA. (2013) Host responses in tissue repair and fibrosis. *Annu Rev Pathol* 8:241-276

Dudziak D, Kamphorst AO, Heidkamp GF, Buchholz VR, Trumpfheller C, Yamazaki S, Cheong C, Liu K, Lee HW, Park CG, Steinman RM, Nussenzweig MC. (2007) Differential antigen processing by dendritic cell subsets in vivo. *Science* 315:107-111

Eberl M, Roberts GW, Meuter S, Williams JD, Topley N, Moser B. (2009) A rapid crosstalk of human gammadelta T cells and monocytes drives the acute inflammation in bacterial infections. *PLoS Pathog* 5:e1000308

Ebert RH, Florey HW. (1939) The Extravascular Development of the Monocyte Observed In vivo. *Br J Exp Pathol* 20: 342–356

Edwards JP, Zhang X, Frauwirth KA, Mosser DM. (2006) Biochemical and functional characterization of three activated macrophage populations. *J Leukoc Biol* 80:1298-1307

Ejaz AA. (1998) Peritoneal fluid eosinophilia. *Nephrol Dial Transplant* 13:2463-2464

Elliott MR, Ravichandran KS. Clearance of apoptotic cells: implications in health and disease. *J Cell Biol* 189:1059-1070

Esperanca MJ, Collins DL. (2010) Peritoneal dialysis efficiency in relation to body weight. (1966) *J Pediatr Surg* 1:162-169

Fabriek BO, Dijkstra CD, van den Berg TK. (2005) The macrophage scavenger receptor CD163. *Immunobiology* 210:153-160

Fakhri O, Al-Mondhiry H, Rifaat UN, Khalil MA, Ai-Rawi AM. (1978) Output of peritoneal cells during peritoneal dialysis. *J Clin Pathol* 31:645–647

Fancke B, Suter M, Hochrein H, O'Keeffe M. (2008) M-CSF: a novel plasmacytoid and conventional dendritic cell poietin. *Blood* 111:150-159

Fielding CA, Jones GW, McLoughlin RM, McLeod L, Hammond VJ, Uceda J, Williams AS, Lambie M, Foster TL, Liao CT, Rice CM, Greenhill CJ, Colmont CS, Hams E, Coles B, Kift-Morgan A, Newton Z, Craig KJ, Williams JD, Williams GT, Davies SJ, Humphreys IR, O'Donnell VB, Taylor PR, Jenkins BJ, Topley N, Jones SA. (2014) Interleukin-6 signaling drives fibrosis in unresolved inflammation. *Immunity* 40:40-50

Flanigan MJ, Freeman RM, Lim VS. (1985) Cellular response to peritonitis among peritoneal dialysis patients. *Am J Kidney Dis* 6:420-424

Flessner ML, Li X, Potter R, He Z. (2010) Foreign-body response to sterile catheters is variable over 20 weeks. *Adv Perit Dial* 26:101-104

Flessner ML, Credit K, Richardson K, Potter R, Li X, He Z, Hoskins G, Henegar J. (2010) Peritoneal inflammation after twenty-week exposure to dialysis solution: effect of solution versus catheter-foreign body response. *Perit Dial Int* 30:284-293

Floyd H, Ni J, Cornish AL, Zeng Z, Liu D, Carter KC, Steel J, Crocker PR. (2000) Siglec-8. A novel eosinophil-specific member of the immunoglobulin superfamily. *J Biol Chem* 275:861-866

Fogg DK, Sibon C, Miled C, Jung S, Aucouturier P, Littman DR, Cumano A, Geissmann F. (2006) A clonogenic bone marrow progenitor specific for macrophages and dendritic cells. *Science* 311:83-87

Gautier EL, Shay T, Miller J, Greter M, Jakubzick C, Ivanov S, Helft J, Chow A, Elpek KG, Gordonov S, Mazloom AR, Ma'ayan A, Chua WJ, Hansen TH, Turley SJ, Merad M, Randolph GJ; Immunological Genome Consortium. (2012) Gene-expression profiles and transcriptional

regulatory pathways that underlie the identity and diversity of mouse tissue macrophages. *Nat Immunol* 13:1118-1128

Ganguly R, Milutinovich J, Lazzell V, Waldman RH. (1980) Studies of human peritoneal cells: A normal saline lavage technique for the isolation and characterization of cells from peritoneal dialysis patients. *J Reticuloendothel Soc* 27:303–310

García-López E, Lindholm B, Davies S. (2012) An update on peritoneal dialysis solutions. *Nat Rev Nephrol* 8:224-233

Geissmann F, Jung S, Littman DR. (2003) Blood monocytes consist of two principal subsets with distinct migratory properties. *Immunity* 19:71-82

Geissmann F, Manz MG, Jung S, Sieweke MH, Merad M, Ley K. (2010) Development of monocytes, macrophages, and dendritic cells. *Science* 327:656-661

Geissmann F, Gordon S, Hume DA, Mowat AM, Randolph GJ. (2010) Unravelling mononuclear phagocyte heterogeneity. *Nat Rev Immunol* 10:453-460

Ghosen EE, Cassado AA, Govoni GR, Fukuhara T, Yang Y, Monack DM, Bortoluci KR, Almeida SR, Herzenberg LA, Herzenberg LA. (2010) Two physically, functionally, and developmentally distinct peritoneal macrophage subsets. *Proc Natl Acad Sci U S A* 107:2568-2573

Ghosh HS, Cisse B, Bunin A, Lewis KL, Reizis B. (2010) Continuous expression of the transcription factor e2-2 maintains the cell fate of mature plasmacytoid dendritic cells. *Immunity* 33:905-916

Ginhoux F, Greter M, Leboeuf M, Nandi S, See P, Gokhan S, Mehler MF, Conway SJ, Ng LG, Stanley ER, Samokhvalov IM, Merad M. (2010) Fate mapping analysis reveals that adult microglia derive from primitive macrophages. *Science* 330:841-845

Ginhoux F, Jung S. (2014) Monocytes and macrophages: developmental pathways and tissue homeostasis. *Nat Rev Immunol* 14:392-404

Gokal R, Ramos JM, Ward MK, Kerr DN. (1981) "Eosinophilic" peritonitis in continuous ambulatory peritoneal dialysis (CAPD). *Clin Nephrol* 15:328-330

Goldstein CS, Bomalaski JS, Zurier RB, Neilson EG, Douglas SD. (1984) Analysis of peritoneal macrophages in continuous ambulatory peritoneal dialysis patients. *Kidney Int* 26:733-740

Goldszmid RS, Caspar P, Rivollier A, White S, Dzutsev A, Hieny S, Kelsall B, Trinchieri G, Sher A. (2012) NK cell-derived interferon-γ orchestrates cellular dynamics and the differentiation of monocytes into dendritic cells at the site of infection. *Immunity* 36:1047-1059

Gordon S, Crocker PR, Morris L, Lee SH, Perry VH, Hume DA. (1986) Localization and function of tissue macrophages. *Ciba Found Symp* 118:54-67

Gordon S. (2002) Pattern recognition receptors: doubling up for the innate immune response. *Cell* 111:927-930

Gordon S, Taylor PR. (2005) Monocyte and macrophage heterogeneity. *Nat Rev Immunol* 5:953-964

Gordon S, Martinez FO. (2010) Alternative activation of macrophages: mechanism and functions. *Immunity* 32:593-604

Greter M, Helft J, Chow A, Hashimoto D, Mortha A, Agudo-Cantero J, Bogunovic M, Gautier EL, Miller J, Leboeuf M, Lu G, Aloman C, Brown BD, Pollard JW, Xiong H, Randolph GJ, Chipuk JE, Frenette PS, Merad M. (2012) GM-CSF controls nonlymphoid tissue dendritic cell homeostasis but is dispensable for the differentiation of inflammatory dendritic cells. *Immunity* 36:1031-1046

Greter M, Lelios I, Pelczar P, Hoeffel G, Price J, Leboeuf M, Kündig TM, Frei K, Ginhoux F, Merad M, Becher B. (2012) Stroma-derived interleukin-34 controls the development and maintenance of langerhans cells and the maintenance of microglia. *Immunity* 37:1050-1060

Guilliams M, Bruhns P, Saeys Y, Hammad H, Lambrecht BN. (2014) The function of Fcγ receptors in dendritic cells and macrophages. *Nat Rev Immunol* 14:94-108

Guilliams M, Ginhoux F, Jakubzick C, Naik SH, Onai N, Schraml BU, Segura E, Tussiwand R, Yona S. (2014) Dendritic cells, monocytes and macrophages: a unified nomenclature based on ontogeny. *Nat Rev Immunol* 14:571-578

Hamann J, Koning N, Pouwels W, Ulfman LH, van Eijk M, Stacey M, Lin HH, Gordon S, Kwakkenbos MJ. (2007) EMR1, the human homolog of F4/80, is an eosinophil-specific receptor. *Eur J Immunol* 37:2797-2802

Hamilton JA, Whitty G, Masendycz P, Wilson NJ, Jackson J, De Nardo D, Scholz GM. (2008) The critical role of the colony-stimulating factor-1 receptor in the differentiation of myeloblastic leukemia cells. *Mol Cancer Res* 6:458-467

Haniffa M, Ginhoux F, Wang XN, Bigley V, Abel M, Dimmick I, Bullock S, Grisotto M, Booth T, Taub P, Hilkens C, Merad M, Collin M. (2009) Differential rates of replacement of human dermal dendritic cells and macrophages during hematopoietic stem cell transplantation. *J Exp Med* 206:371-385

Hart PH, Jones CA, Finlay-Jones JJ. (1992) Peritoneal macrophages during peritonitis. Phenotypic studies. *Clin Exp Immunol* 88:484-491

Hashimoto D, Miller J, Merad M. (2011) Dendritic cell and macrophage heterogeneity in vivo. *Immunity* 35:323-335

Hashimoto D, Chow A, Noizat C, Teo P, Beasley MB, Leboeuf M, Becker CD, See P, Price J, Lucas D, Greter M, Mortha A, Boyer SW, Forsberg EC, Tanaka M, van Rooijen N, García-Sastre A, Stanley ER, Ginhoux F, Frenette PS, Merad M. (2013) Tissue-resident macrophages self-maintain locally throughout adult life with minimal contribution from circulating monocytes. *Immunity* 38:792-804

Heath WR, Carbone FR. (2001) Cross-presentation in viral immunity and self-tolerance. *Nat Rev Immunol* 1:126-134

Hettinger J, Richards DM, Hansson J, Barra MM, Joschko AC, Krijgsveld J, Feuerer M. (2013) Origin of monocytes and macrophages in a committed progenitor. *Nat Immunol* 14:821-830

Hildner K, Edelson BT, Purtha WE, Diamond M, Matsushita H, Kohyama M, Calderon B, Schraml BU, Unanue ER, Diamond MS, Schreiber RD, Murphy TL, Murphy KM. (2008) Batf3

deficiency reveals a critical role for CD8α$^+$ dendritic cells in cytotoxic T cell immunity. *Science* 322:1097-1100

Höchstetter R, Dobos G, Kimmig D, Dulkys Y, Kapp A, Elsner J. (2000) The CC chemokine receptor 3 CCR3 is functionally expressed on eosinophils but not on neutrophils. *Eur J Immunol* 30:2759-2764

Hoeffel G, Wang Y, Greter M, See P, Teo P, Malleret B, Leboeuf M, Low D, Oller G, Almeida F, Choy SH, Grisotto M, Renia L, Conway SJ, Stanley ER, Chan JK, Ng LG, Samokhvalov IM, Merad M, Ginhoux F. (2012) Adult Langerhans cells derive predominantly from embryonic fetal liver monocytes with a minor contribution of yolk sac-derived macrophages. *J Exp Med* 209:1167-1181

Hruza Z. (1977) Connective tissue. In: Kaley G, Altura BM, eds. Microcirculation, Vol. I, Baltimore, MD: University Park Press, pp.167-183

Humayun HM, Ing TS, Daugirdas JT, Gandhi VC, Popli S, Robinson JA, Hano JE, Zayas I. (1981) Peritoneal fluid eosinophilia in patients undergoing maintenance peritoneal dialysis. *Arch Intern Med* 141:1172-1173

Hume DA, Gordon S. Mononuclear phagocyte system of the mouse defined by immunohistochemical localization of antigen F4/80. (1983) Identification of resident macrophages in renal medullary and cortical interstitium and the juxtaglomerular complex. *J Exp Med* 157:1704-1709

Hume DA, Ross IL, Himes SR, Sasmono RT, Wells CA, Ravasi T. (2002) The mononuclear phagocyte system revisited. *J Leukoc Biol* 72:621-627

Hurst SM, Wilkinson TS, McLoughlin RM, Jones S, Horiuchi S, Yamamoto N, Rose-John S, Fuller GM, Topley N, Jones SA. (2001) IL-6 and its soluble receptor orchestrate a temporal switch in the pattern of leukocyte recruitment seen during acute inflammation. *Immunity* 14:705–714

Irizarry RA, Bolstad BM, Collin F, Cope LM, Hobbs B, Speed TP. (2003) Summaries of Affymetrix GeneChip probe level data. *Nucleic Acids Res* 31:e15

Jenkin C, Benacerraf B. (1960) In vitro studies on the interaction between mouse peritoneal macrophages and strains of Salmonella and Escherichia coli. *J Exp Med* 112:403-417

Jenkins SJ, Ruckerl D, Cook PC, Jones LH, Finkelman FD, van Rooijen N, MacDonald AS, Allen JE. (2011) Local macrophage proliferation, rather than recruitment from the blood is a signature of TH2 inflammation. *Science* 322:1284-1288

Joffre OP, Segura E, Savina A, Amigorena S. (2012) Cross-presentation by dendritic cells. *Nat Rev Immunol* 12:557-569

Jones S, Holmes CJ, Mackenzie RK, Stead R, Coles GA, Williams JD, Faict D, Topley N. (2002) Continuous dialysis with bicarbonate/lactate-buffered peritoneal dialysis fluids results in a long-term improvement in ex vivo peritoneal macrophage function. *J Am Soc Nephrol* 13:S97-103

Jongbloed SL, Kassianos AJ, McDonald KJ, Clark GJ, Ju X, Angel CE, Chen CJ, Dunbar PR, Wadley RB, Jeet V, Vulink AJ, Hart DN, Radford KJ. (2010) Human CD141+ (BDCA-3)+ dendritic cells (DCs) represent a unique myeloid DC subset that cross-presents necrotic cell antigens. *J Exp Med* 207:1247-1260

Jörres A, Topley N, Witowski J, Liberek T, Gahl GM. (1993) Impact of peritoneal dialysis solutions on peritoneal immune defense. *Perit Dial Int* 13:S291-294

Kassianos AJ, Wang X, Sampangi S, Muczynski K, Healy H, Wilkinson R. (2003) Increased tubulointerstitial recruitment of human CD141(hi) CLEC9A(+) and CD1c(+) myeloid dendritic cell subsets in renal fibrosis and chronic kidney disease. *Am J Physiol Renal Physiol* 305:1391-1401

Kathuria P, Twardowski ZJ, Nichols WK. (2009) Peritoneal dialysis access and exit-site care including surgical aspects. In: Nolph and Gokal's Textbook of Peritoneal Dialysis, 3rd edition. Chapter 14, pp. 410-435

Kelly A, Fahey R, Fletcher JM, Keogh C, Carroll AG, Siddachari R, Geoghegan J, Hegarty JE, Ryan EJ, O'Farrelly C. (2014) $CD141^+$ myeloid dendritic cells are enriched in healthy human liver. *J Hepatol* 60:135-142

Kim YL. (2009) Update on mechanisms of ultrafiltration failure. *Perit Dial Int* 29:S123-127

Kolesnyk I, Dekker FW, Boeschoten EW, Krediet RT. (2010) Time-dependent reasons for peritoneal dialysis technique failure and mortality. *Perit Dial Int* 30:170-177

Lambie M, Chess J, Donovan KL, Kim YL, Do JY, Lee HB, Noh H, Williams PF, Williams AJ, Davison S, Dorval M, Summers A, Williams JD, Bankart J, Davies SJ, Topley N; Global Fluid Study Investigators. (2013) Independent effects of systemic and peritoneal inflammation on peritoneal dialysis survival. *J Am Soc Nephrol* 24:2071-2080

Lavin Y, Winter D, Blecher-Gonen R, David E, Keren-Shaul H, Merad M, Jung S, Amit I. (2014) Tissue-resident macrophage enhancer landscapes are shaped by the local microenvironment. *Cell* 159:1312-1326

Lee HA. (1967) Evaluation of peritoneal dialysis and haemodialysis in paediatrics. *Isr J Med Sci* 3:28-44

León B, López-Bravo M, Ardavín C. (2007) Monocyte-derived dendritic cells formed at the infection site control the induction of protective T helper 1 responses against Leishmania. *Immunity* 26:519-531

Lewis SL, Norris PJ, Holmes CJ. (1990) Phenotypic characterization of monocytes and macrophages from CAPD patients. *ASAIO Trans* 36:575-577

Lewis SL, Holmes CJ. (1991) Host defense mechanisms in the peritoneal cavity of continuous ambulatory peritoneal dialysis patients. 1. *Perit Dial Int* 11:14-21

Lewis SL, Kutvirt SG, Cooper CL, Bonner PN, Holmes CJ. (1993) Characteristics of peripheral and peritoneal lymphocytes from continuous ambulatory peritoneal dialysis patients. *Perit Dial Int* 13:S273-277

Li FK, Davenport A, Robson RL, Loetscher P, Rothlein R, Williams JD, Topley N. (1998) Leukocyte migration across human peritoneal mesothelial cells is dependent on directed chemokine secretion and ICAM-1 expression. *Kidney Int* 4:2170-2183

Li PK, Szeto CC, Piraino B, Bernardini J, Figueiredo AE, Gupta A, Johnson DW, Kuijper EJ, Lye WC, Salzer W, Schaefer F, Struijk DG; International Society for Peritoneal Dialysis. (2010) Peritoneal dialysis-related infections recommendations: 2010 update. *Perit Dial Int* 30:393-423

Liaskou E, Zimmermann HW, Li KK, Oo YH, Suresh S, Stamataki Z, Qureshi O, Lalor PF, Shaw J, Syn WK, Curbishley SM, Adams DH. (2013) Monocyte subsets in human liver disease show distinct phenotypic and functional characteristics. *Hepatology* 57:385-398

Lin CY, Ku WL, Huang TP. (1990) Serial peritoneal macrophage function studies in new and established continuous ambulatory peritoneal dialysis patients. *Am J Nephrol* 10:368-373

Lin CY, Roberts GW, Kift-Morgan A, Donovan KL, Topley N, Eberl M. (2013) Pathogen-specific local immune fingerprints diagnose bacterial infection in peritoneal dialysis patients. *J Am Soc Nephrol* 24: 2002-2009

Liu K, Victora GD, Schwickert TA, Guermonprez P, Meredith MM, Yao K, Chu FF, Randolph GJ, Rudensky AY, Nussenzweig M. (2009) In vivo analysis of dendritic cell development and homeostasis. *Science* 324:392-397

Lucas T, Waisman A, Ranjan R, Roes J, Krieg T, Müller W, Roers A, Eming SA. (2010) Differential roles of macrophages in diverse phases of skin repair. *J Immunol* 184:3964-3977

MacKenzie RK, Holmes CJ, Moseley A, Jenkins JP, Williams JD, Coles GA, Faict D, Topley N. (1998) Bicarbonate/lactate- and bicarbonate-buffered peritoneal dialysis fluids improve ex vivo peritoneal macrophage TNF-α secretion. *J Am Soc Nephrol* 9:1499-1506

Mackenzie RK, Jones S, Moseley A, Holmes CJ, Argyle R, Williams JD, Coles GA, Pu K, Faict D, Topley N. (2000) In vivo exposure to bicarbonate/lactate- and bicarbonate-buffered peritoneal dialysis fluids improves ex vivo peritoneal macrophage function. *Am J Kidney Dis* 35:112-121

Mactier RA, Khanna R, Twardowski ZJ, Nolph KD. (1987) Role of peritoneal cavity lymphatic absorption in peritoneal dialysis. *Kidney Int* 32:165-172

Maddox Y, Foegh M, Zeligs B, Zmudka M, Bellanti J, Ramwell P. (1984) A routine source of human peritoneal macrophages. *Scand J Immunol* 19:23-29

Maldonado RA, von Andrian UH. (2010) How tolerogenic dendritic cells induce regulatory T cells. *Adv Immunol* 108:111-165

Malik AR, Little MA, Henriksson M, Tam FW, Brown EA. (2007) Peritonitis, peritoneal inflammation and membrane permeability: a longitudinal study of dialysate and serum MCP-1 in stable patients on peritoneal dialysis. *J Nephrol* 20:340-349

Mantovani A, Sica A, Sozzani S, Allavena P, Vecchi A, Locati M. (2004) The chemokine system in diverse forms of macrophage activation and polarization. *Trends Immunol* 25:677-686

Mantovani A, Sica A, Locati M. (2005) Macrophage polarization comes of age. *Immunity* 23:344-346

Marcus CC. (1962) Cytology of the pelvic peritoneal cavity in benign and malignant disease. *Obstet Gynecol* 20:701-712

Martin LC, Caramori JC, Fernandes N, Divino-Filho JC, Pecoits-Filho R, Barretti P; Brazilian Peritoneal Dialysis Multicenter Study BRAZPD Group. (2011) Geographic and educational factors and risk of the first peritonitis episode in Brazilian Peritoneal Dialysis study (BRAZPD) patients. *Clin J Am Soc Nephrol* 6:1944-1951

Martinez FO and Gordon S. (2014) The M1 and M2 paradigm of macrophage activation: time for reassessment. *F1000Prime Rep* 6:13

McCormick BB, Bargman JM. (2007) Noninfectious complications of peritoneal dialysis: implications for patient and technique survival. *J Am Soc Nephrol* 18:3023-3025

McCully ML, Chau TA, Luke P, Blake PG, Madrenas J. (2005) Characterization of human peritoneal dendritic cell precursors and their involvement in peritonitis. *Clin Exp Immunol* 139:513-525

McCully ML, Madrenas J. (2006) Dendritic cells as arbiters of peritoneal immune responses. *Perit Dial Int* 26:8-25

McGovern N, Schlitzer A, Gunawan M, Jardine L, Shin A, Poyner E, Green K, Dickinson R, Wang XN, Low D, Best K, Covins S, Milne P, Pagan S, Aljefri K, Windebank M, Saavedra DM, Larbi A, Wasan PS, Duan K, Poidinger M, Bigley V, Ginhoux F, Collin M, Haniffa M. (2014) Human dermal $CD14^{+}$ cells are a transient population of monocyte-derived macrophages. *Immunity* 41:465-477

McGowan L, Davis RH, Stein DB, Bebon S, Vaskelis P. (1967) Cytologic differential of pelvic cavity aspiration specimens in normal women. *Obstet Gynecol* 30: 821-829

McGregor SJ, Brock JH, Briggs JD, Junor BJ. (1987) Bactericidal activity of peritoneal macrophages from continuous ambulatory dialysis patients. *Nephrol Dial Transplant* 2:104-108

McGregor SJ, Brock JH, Briggs JD, Junor BJ. (1989) Longitudinal study of peritoneal defense mechanisms in patients on continuous ambulatory peritoneal dialysis (CAPD). *Perit Dial Int* 9:115-119

McGregor SJ, Topley N, Jörres A, Speekenbrink AB, Gordon A, Gahl GM, Junor BJ, Briggs JD, Brock JH. (1996) Longitudinal evaluation of peritoneal macrophage function and activation during CAPD: maturity, cytokine synthesis and arachidonic acid metabolism. *Kidney Int* 49:525-533

McKenna HJ, Stocking KL, Miller RE, Brasel K, De Smedt T, Maraskovsky E, Maliszewski CR, Lynch DH, Smith J, Pulendran B, Roux ER, Teepe M, Lyman SD, Peschon JJ. (2000) Mice lacking flt3 ligand have deficient hematopoiesis affecting hematopoietic progenitor cells, dendritic cells, and natural killer cells. *Blood* 95:3489-3497

McKnight AJ, Gordon S. (1998) The EGF-TM7 family: unusual structures at the leukocyte surface. *J Leukoc Biol* 63:271-280

Meixlsperger S, Leung CS, Rämer PC, Pack M, Vanoaica LD, Breton G, Pascolo S, Salazar AM, Dzionek A, Schmitz J, Steinman RM, Münz C. (2013) CD141+ dendritic cells produce prominent amounts of IFN-α after dsRNA recognition and can be targeted via DEC-205 in humanized mice. *Blood* 121:5034-5044

Melnicoff MJ, Horan PK, Breslin EW, Morahan PS. (1988) Maintenance of peritoneal macrophages in the steady state. *J Leukoc Biol* 44:367–375

Merad M, Manz MG, Karsunky H, Wagers A, Peters W, Charo I, Weissman IL, Cyster JG, Engleman EG. (2002) Langerhans cells renew in the skin throughout life under steady-state conditions. *Nat Immunol* 3:1135-1141

Merad M, Sathe P, Helft J, Miller J, Mortha A. (2013) The dendritic cell lineage: ontogeny and function of dendritic cells and their subsets in the steady state and the inflamed setting. *Annu Rev Immunol* 31:563-604

Metchnikoff, E. (1892) Leçons sur la pathologie comparée de l'inflammation. Masson, Paris

Metlay JP, Witmer-Pack MD, Agger R, Crowley MT, Lawless D, Steinman RM. (1990) The distinct leukocyte integrins of mouse spleen dendritic cells as identified with new hamster monoclonal antibodies. *J Exp Med* 171:1753-1771

Meuter S, Eberl M, Moser B. (2010) Prolonged antigen survival and cytosolic export in cross-presenting human gammadelta T cells. *Proc Natl Acad Sci U S A* 107:8730-8735

Mills CD, Kincaid K, Alt JM, Heilman MJ, Hill AM. (2000) M-1/M-2 macrophages and the Th1/Th2 paradigm. *J Immunol* 164:6166-6173

Min SY, Fu Y, Hutcheson J, Wu T, Khobahy E, Zhu J, Vanarsa K, Du Y, Park MJ, Park HS, Saxena R, Kim HY, Mohan C. (2012) Peritoneal catheter implantation elicits IL-10-producing immune-suppressor macrophages through a MyD88-dependent pathway. *Clin Immunol* 143:59-72

Miyajima A, Kitamura T, Harada N, Yokota T, Arai K. (1992) Cytokine receptors and signal transduction. *Annu Rev Immunol* 10:295-331

Mokoena T, Gordon S. (1985) Human macrophage activation. Modulation of mannosyl, fucosyl receptor activity in vitro by lymphokines, gamma and alpha interferons, and dexamethasone. *J Clin Invest* 75:624-631

Molawi K, Wolf Y, Kandalla PK, Favret J, Hagemeyer N, Frenzel K, Pinto AR, Klapproth K, Henri S, Malissen B, Rodewald HR, Rosenthal NA, Bajenoff M, Prinz M, Jung S, Sieweke MH. (2014) Progressive replacement of embryo-derived cardiac macrophages with age. *J Exp Med* 211:2151-2158

Moret FM, Hack CE, van der Wurff-Jacobs KM, de Jager W, Radstake TR, Lafeber FP, van Roon JA. (2013) Intra-articular CD1c-expressing myeloid dendritic cells from rheumatoid arthritis patients express a unique set of T cell-attracting chemokines and spontaneously induce Th1, Th17 and Th2 cell activity. *Arthritis Res Ther*15:R155

Mosser DM, Edwards JP. (2008) Exploring the full spectrum of macrophage activation. *Nat Rev Immunol* 8:958-969

Moughal NA, McGregor SJ, Brock JH, Briggs JD, Junor BJ. (1991) Expression of transferrin receptors by monocytes and peritoneal macrophages from renal failure patients treated by continuous ambulatory peritoneal dialysis (CAPD). *Eur J Clin Invest* 21:592-596

Moulding DA, Hart CA, Edwards SW. (1999) Regulation of neutrophil FcgammaRIIIb (CD16) surface expression following delayed apoptosis in response to GM-CSF and sodium butyrate. *J Leukoc Biol* 65:875-882

Murray PJ, Allen JE, Biswas SK, Fisher EA, Gilroy DW, Goerdt S, Gordon S, Hamilton JA, Ivashkiv LB, Lawrence T, Locati M, Mantovani A, Martinez FO, Mege JL, Mosser DM, Natoli G, Saeij JP, Schultze JL, Shirey KA, Sica A, Suttles J, Udalova I, van Ginderachter JA, Vogel SN, Wynn TA. (2014) Macrophage activation and polarization: nomenclature and experimental guidelines. *Immunity* 41:14-20

Myers MA, McPhail LC, Snyderman R. (1985) Redistribution of protein kinase C activity in human monocytes: correlation with activation of the respiratory burst. *J Immunol* 135:3411-3416

Naik SH, Metcalf D, van Nieuwenhuijze A, Wicks I, Wu L, O'Keeffe M, Shortman K. (2006) Intrasplenic steady-state dendritic cell precursors that are distinct from monocytes. *Nat Immunol* 7:663-671

Naik SH, Sathe P, Park HY, Metcalf D, Proietto AI, Dakic A, Carotta S, O'Keeffe M, Bahlo M, Papenfuss A, Kwak JY, Wu L, Shortman K. (2007) Development of plasmacytoid and conventional dendritic cell subtypes from single precursor cells derived in vitro and in vivo. *Nat Immunol* 8:1217-1226

Naito M, Umeda S, Yamamoto T, Moriyama H, Umezu H, Hasegawa G, Usuda H, Shultz LD, Takahashi K. (1996) Development, differentiation, and phenotypic heterogeneity of murine tissue macrophages. *J Leukoc Biol* 59:133-138

Nakano H, Lin KL, Yanagita M, Charbonneau C, Cook DN, Kakiuchi T, Gunn MD. (2009) Blood-derived inflammatory dendritic cells in lymph nodes stimulate acute T helper type 1 immune responses. *Nat Immunol* 10:394-402

Nessim SJ, Bargman JM, Austin PC, Nisenbaum R, Jassal SV. (2009) Predictors of peritonitis in patients on peritoneal dialysis: results of a large, prospective Canadian database. *Clin J Am Soc Nephrol* 4:1195-1200

Nguyen HH, Tran BT, Muller W, Jack RS. (2012) IL-10 acts as a developmental switch guiding monocyte differentiation to macrophages during a murine peritoneal infection. *J Immunol* 189:3112-3120

Noorman F, Braat EA, Barrett-Bergshoeff M, Barbé E, van Leeuwen A, Lindeman J, Rijken DC. (1997) Monoclonal antibodies against the human mannose receptor as a specific marker in flow cytometry and immunohistochemistry for macrophages. *J Leukoc Biol* 61:63-72

Nuchtern JG, Bonifacino JS, Biddison WE, Klausner RD. (1989) Brefeldin A implicates egress from endoplasmic reticulum in class I restricted antigen presentation. *Nature* 339:223-226

Onai N, Obata-Onai A, Schmid MA, Ohteki T, Jarrossay D, Manz MG. (2007) Identification of clonogenic common Flt3+M-CSFR+ plasmacytoid and conventional dendritic cell progenitors in mouse bone marrow. *Nat Immunol* 8:1207-1216

Onai N, Kurabayashi K, Hosoi-Amaike M, Toyama-Sorimachi N, Matsushima K, Inaba K, Ohteki T. (2013) A clonogenic progenitor with prominent plasmacytoid dendritic cell developmental potential. *Immunity* 38:943-957

Osterholzer JJ, Chen GH, Olszewski MA, Curtis JL, Huffnagle GB, Toews GB. (2009) Accumulation of CD11b+ lung dendritic cells in response to fungal infection results from the CCR2-mediated recruitment and differentiation of Ly-6Chigh monocytes. *J Immunol* 183:8044-8053

Parwaresch, MR, Wacker, HH. (1984) Origin and kinetics of resident tissue macrophages. Parabiosis studies with radiolabelled leucocytes. *Cell Tissue Kinet* 17:25–39

Pawlaczyk K, Kuzlan M, Wieczorowska-Tobis K, Pawlik-Juzków H, Breborowicz A, Knapowski J, Oreopoulos DG. (1996) Species-dependent topography of the peritoneum. *Adv Perit Dial* 12:3-6

Pelayo R, Hirose J, Huang J, Garrett KP, Delogu A, Busslinger M, Kincade PW. (2005) Derivation of 2 categories of plasmacytoid dendritic cells in murine bone marrow. *Blood* 105:4407-4415

Perry VH, Hume DA, Gordon S. (1985) Immunohistochemical localization of macrophages and microglia in the adult and developing mouse brain. *Neuroscience* 15:313-326

Peterson PK, Gaziano E, Suh HJ, Devalon M, Peterson L, Keane WF. (1985) Antimicrobial activities of dialysate-elicited and resident human peritoneal macrophages. *Infect Immun* 49:212-218

Pickl WF, Majdic O, Kohl P, Stöckl J, Riedl E, Scheinecker C, Bello-Fernandez C, Knapp W. 91996) Molecular and functional characteristics of dendritic cells generated from highly purified CD14+ peripheral blood monocytes. *J Immunol* 157:3850-3859

Plantinga M, Guilliams M, Vanheerswynghels M, Deswarte K, Branco-Madeira F, Toussaint W, Vanhoutte L, Neyt K, Killeen N, Malissen B, Hammad H, Lambrecht BN. (2013) Conventional and monocyte-derived CD11b(+) dendritic cells initiate and maintain T helper 2 cell-mediated immunity to house dust mite allergen. *Immunity* 38:322-335

Pollard JW. (2009) Trophic macrophages in development and disease. *Nat Rev Immunol* 9:259-270

Poon IK, Lucas CD, Rossi AG, Ravichandran KS. (2014) Apoptotic cell clearance: basic biology and therapeutic potential. *Nat Rev Immunol* 14:166-180

Popovich RP, Moncrief JW, Nolph KD, Ghods AJ, Twardowski ZJ, Pyle WK. (1978) Continuous ambulatory peritoneal dialysis. *Ann Intern Med* 88:449-456

Putnam TJ. (1923) The living peritoneum as a dialyzing membrane. *Am J Physiol* 63:548-565

Puig-Kröger A, Pello OM, Selgas R, Criado G, Bajo MA, Sánchez-Tomero JA, Alvarez V, del Peso G, Sánchez-Mateos P, Holmes C, Faict D, López-Cabrera M, Madrenas J, Corbí AL. (2003)

Peritoneal dialysis solutions inhibit the differentiation and maturation of human monocyte-derived dendritic cells: effect of lactate and glucose-degradation products. *J Leukoc Biol* 73:482-492

Quinlan C, Cantwell M, Rees L. (2010) Eosinophilic peritonitis in children on chronic peritoneal dialysis. *Pediatr Nephrol* 25:517-522

Quinn RR, Ravani P, Hochman J. (2010) Technique failure in peritoneal dialysis patients: insights and challenges. *Perit Dial Int* 30:161-162

Rashid G, Korzets Z, Bernheim J. (2006) Advanced glycation end products stimulate tumor necrosis factor-alpha and interleukin-1 beta secretion by peritoneal macrophages in patients on continuous ambulatory peritoneal dialysis. *Isr Med Assoc J* 8:36-39

Rippe B. (1993) A three-pore model of peritoneal transport. *Perit Dial Int* 13:S35-S38

Roberts GW, Baird D, Gallagher K, Jones RE, Pepper CJ, Williams JD, Topley N. (2009) Functional effector memory T cells enrich the peritoneal cavity of patients treated with peritoneal dialysis. *J Am Soc Nephrol* 20:1895-1900

Rouzer CA, Scott WA, Kempe J, Cohn ZA. (1980) Prostaglandin synthesis by macrophages requires a specific receptor-ligand interaction. *Proc Natl Acad Sci U S A* 77:4279-82

Rosas M, Gordon S, Taylor PR. (2007) Characterisation of the expression and function of the GM-CSF receptor alpha-chain in mice. *Eur J Immunol* 37:2518-2528

Rosas M, Thomas B, Stacey M, Gordon S, Taylor PR. (2010) The myeloid 7/4-antigen defines recently generated inflammatory macrophages and is synonymous with Ly-6B. *J Leukoc Biol* 88:169-180

Rosas M, Davies LC, Giles PJ, Liao CT, Kharfan B, Stone TC, O'Donnell VB, Fraser DJ, Jones SA, Taylor PR. (2014) The transcription factor Gata6 links tissue macrophage phenotype and proliferative renewal. *Science* 344: 645-648

Rosen H, Gordon S. (1990) Adoptive transfer of fluorescence-labeled cells shows that resident peritoneal macrophages are able to migrate into specialized lymphoid organs and inflammatory sites in the mouse. *Eur J Immunol* 20:1251-1258

Satpathy AT, Wu X, Albring JC, Murphy KM. (2012) Re(de)fining the dendritic cell lineage. *Nat Immunol* 13:1145-1154

Sawai A, Ito Y, Mizuno M, Suzuki Y, Toda S, Ito I, Hattori R, Matsukawa Y, Gotoh M, Takei Y, Yuzawa Y, Matsuo S. (2011) Peritoneal macrophage infiltration is correlated with baseline peritoneal solute transport rate in peritoneal dialysis patients. *Nephrol Dial Transplant* 26:2322-2332

Sawyer RT, Strausbauch PH, Volkman A. (1982) Resident macrophage proliferation in mice depleted of blood monocytes by strontium-89. *Lab. Invest* 46:165-170

Schenk U, Kiefer T, Hübel E, Weber J, Mettang T, Passlick-Deetjen J, Kuhlmann U. (1994) In vitro effects of amino-acid-based versus glucose-based continuous ambulatory peritoneal dialysis fluids on peritoneal macrophage function. *Nephron* 68:338-346

Schlitzer A, McGovern N, Teo P, Zelante T, Atarashi K, Low D, Ho AW, See P, Shin A, Wasan PS, Hoeffel G, Malleret B, Heiseke A, Chew S, Jardine L, Purvis HA, Hilkens CM, Tam J, Poidinger M, Stanley ER, Krug AB, Renia L, Sivasankar B, Ng LG, Collin M, Ricciardi-Castagnoli P, Honda K, Haniffa M, Ginhoux F. (2013) IRF4 transcription factor-dependent CD11b+ dendritic cells in human and mouse control mucosal IL-17 cytokine responses. *Immunity* 38:970-983

Schlitzer A, Ginhoux F. (2014) Organization of the mouse and human DC network. *Curr Opin Immunol* 26:90-99

Schmidt T, Zundorf J, Gruger T, Brandenburg K, Reiners AL, Zinserling J, Schnitzler N. (2012) CD66b overexpression and homotypic aggregation of human peripheral blood neutrophils after activation by a gram-positive stimulus. *J Leukoc Biol* 91:791-802

Schulz C, Gomez Perdiguero E, Chorro L, Szabo-Rogers H, Cagnard N, Kierdorf K, Prinz M, Wu B, Jacobsen SE, Pollard JW, Frampton J, Liu KJ, Geissmann F. (2012) A lineage of myeloid cells independent of Myb and hematopoietic stem cells. *Science* 336:86-90

Segura E, Touzot M, Bohineust A, Cappuccio A, Chiocchia G, Hosmalin A, Dalod M, Soumelis V, Amigorena S. (2013) Human inflammatory dendritic cells induce Th17 cell differentiation. *Immunity* 38:336-348

Serbina NV, Pamer EG. (2006) Monocyte emigration from bone marrow during bacterial infection requires signals mediated by chemokine receptor CCR2. *Nat Immunol* 7:311-317

Serbina NV, Jia T, Hohl TM, Pamer EG. (2008) Monocyte-mediated defense against microbial pathogens. *Annu Rev Immunol* 26:421-452

Shi C, Pamer EG. (2011) Monocyte recruitment during infection and inflammation. *Nat Rev Immunol* 11:762-774

Shraml BU, van Blijswijk J, Zelenay S, Whitney PG, Filby A, Acton SE, Rogers NC, Moncaut N, Carvajal JJ, Reis e Sousa C. (2013) Genetic tracing via DNGR-1 expression history defines dendritic cells as a hematopoietic lineage. *Cell* 154:843-858

Smalley DM, Ley K. (2005) L-selectin: mechanisms and physiological significance of ectodomain cleavage. *J Cell Mol Med* 9:255-266

Smyth GK, Michaud J, Scott HS. (2005) Use of within-array replicate spots for assessing differential expression in microarray experiments. *Bioinformatics* 21:2067-2075

Smyth GK. (2005) In: Bioinformatics and computational biology solutions using R and Bioconductor, eds. Gentleman R, Carey V, Huber W, Irizarry RA, Dudoit S. (Springer, New York), pp. 397-420

Starling EH, Tubby AH. (1894) The influence of mechanical factors on lymph production. *J Physiol* 16:140-148

Stein M, Keshav S, Harris N, Gordon S. (1992) Interleukin 4 potently enhances murine macrophage mannose receptor activity: a marker of alternative immunologic macrophage activation. *J Exp Med* 176(1):287-292

Steinman RM, Cohn ZA. (1973) Identification of a novel cell type in peripheral lymphoid organs of mice. I. Morphology, quantitation, tissue distribution. *J Exp Med* 137:1142-1162

Steinman RM, Witmer MD. (1978) Lymphoid dendritic cells are potent stimulators of the primary mixed leukocyte reaction in mice. *Proc Natl Acad Sci U S A* 75:5132-5136

Stout RD, Watkins SK, Suttles J. (2009) Functional plasticity of macrophages: in situ reprogramming of tumor-associated macrophages. *J Leukoc Biol* 86:1105-1109

Suzuki S, Honma K, Matsuyama T, Suzuki K, Toriyama K, Akitoyo I, Yamamoto K, Suematsu T, Nakamura M, Yui K, Kumatori A. (2004) Critical roles of interferon regulatory factor 4 in $CD11b^{high}$ $CD8\alpha^{-}$ dendritic cell development. *Proc Natl Acad Sci U S A* 101:8981-8986

Sawai A, Ito Y, Mizuno M, Suzuki Y, Toda S, Ito I, Hattori R, Matsukawa Y, Gotoh M, Takei Y, Yuzawa Y, Matsuo S. (2011) Peritoneal macrophage infiltration is correlated with baseline peritoneal solute transport rate in peritoneal dialysis patients. *Nephrol Dial Transplant* 26:2322-2332

Szeto CC, Kwan BC, Chow KM, Law MC, Pang WF, Chung KY, Leung CB, Li PK. (2009) Recurrent and relapsing peritonitis: causative organisms and response to treatment. *Am J Kidney Dis* 54:702-710

Tamoutounour S, Guilliams M, Montanana Sanchis F, Liu H, Terhorst D, Malosse C, Pollet E, Ardouin L, Luche H, Sanchez C, Dalod M, Malissen B, Henri S. (2013) Origins and functional specialization of macrophages and of conventional and monocyte-derived dendritic cells in mouse skin. *Immunity* 39:925-938

Taylor PR, Gordon S, Martinez-Pomares L. (2005) The mannose receptor: linking homeostasis and immunity through sugar recognition. *Trends Immunol* 26:104-110

Teitelbaum I, Burkart J. (2003) Peritoneal dialysis. *Am J Kidney Dis* 42:1082-1096

Tokgoz B. (2009) Clinical advantages of peritoneal dialysis. *Perit Dial Int* 29:S59-S61

Topley N, Alobaidi HM, Davies M, Coles GA, Williams JD, Lloyd D. (1988) The effect of dialysate on peritoneal phagocyte oxidative metabolism. *Kidney Int* 34:404-411

Twardowski ZJ, Nolph KD, Khanna R, Prowant BF, Ryan LP, Moore HL, Nielsen MP. (1987) Peritoneal equilibration test. *Perit Dial Bull* 7:138-147

Twardowski ZJ. (1990) PET--a simpler approach for determining prescriptions for adequate dialysis therapy. *Adv Perit Dial* 6:186-191

Uderhardt S, Herrmann M, Oskolkova OV, Aschermann S, Bicker W, Ipseiz N, Sarter K, Frey B, Rothe T, Voll R, Nimmerjahn F, Bochkov VN, Schett G, Krönke G. (2012) 12/15-lipoxygenase orchestrates the clearance of apoptotic cells and maintains immunologic tolerance. *Immunity* 36:834-846

Underhill DM, Ozinsky A. (2002) Phagocytosis of microbes: complexity in action. *Annu Rev Immunol* 20:825-852

Underhill DM. (2003) Macrophage recognition of zymosan particles. *J Endotoxin Res* 9:176-180

UK Renal Registry- The Sixteenth Annual Report. The Renal Association. December 2013: https://www.renalreg.org/reports/2013-the-sixteenth-annual-report/

Valle MT, Degl'Innocenti ML, Giordano P, Kunkl A, Costantini MT, Perfumo F, Manca F, Gusmano R. (1989) Analysis of cellular populations in peritoneal effluents of children on CAPD. *Clin Nephrol* 32:235-238

van Biesen W, Heimburger O, Krediet R, Rippe B, La Milia V, Covic A, Vanholder R; ERBP working group on peritoneal dialysis. (2010) Evaluation of peritoneal membrane characteristics: clinical advice for prescription management by the ERBP working group. *Nephrol Dial Transplant* 25:2052-2062

van de Laar L, Coffer PJ, Woltman AM. (2012) Regulation of dendritic cell development by GM-CSF: molecular control and implications for immune homeostasis and therapy. *Blood* 119:3383-3393

van Furth R, Cohn ZA, Hirsch JG, Humphry JH, Spector WG, Langevoort HL. (1972) The mononuclear phagocyte system: a new classification of macrophages, monocytes, and their precursor cells. *Bull World Health Organ* 46: 845-852

van Furth R. (1980) The mononuclear phagocyte system. *Verh Dtsch Ges Pathol* 64:1-11

van Gorp H, Delputte PL, Nauwynck HJ. (2010) Scavenger receptor CD163, a Jack-of-all-trades and potential target for cell-directed therapy. *Mol Immunol* 47:1650-1660

van Lookeren Campagne M, Wiesmann C, Brown EJ. (2007) Macrophage complement receptors and pathogen clearance. *Cell Microbiol* 9:2095-2102

Verbrugh HA, Keane WF, Hoidal JR, Freiberg MR, Elliott GR, Peterson PK. (1983) Peritoneal macrophages and opsonins: antibacterial defense in patients undergoing chronic peritoneal dialysis. *J Infect Dis* 147:1018-1029

Villadango JA, Schnorrer P. (2007) Intrinsic and cooperative antigen-presenting functions of dendritic-cell subsets in vivo. *Nat Rev Immunol* 7:543-555

Volkman A, Gowans JL. (1965) The Origin of Macrophages from Bone Marrow in the Rat. *Br J Exp Pathol* 46: 62–70

Wang HH, Lin CY, Huang TP. (2003) Patterns of CD4/CD8 T-cell ratio in dialysis effluents predict the long-term outcome of peritonitis in patients undergoing peritoneal dialysis. *Nephrol Dial Transplant* 18:1181-1189

Wang HH, Lin CY. (2005) Interleukin-12 and -18 levels in peritoneal dialysate effluent correlate with the outcome of peritonitis in patients undergoing peritoneal dialysis: implications for the Type I/Type II T-cell immune response. *Am J Kidney Dis* 46:328-338

Wang Y, Szretter KJ, Vermi W, Gilfillan S, Rossini C, Cella M, Barrow AD, Diamond MS, Colonna M. (2012) IL-34 is a tissue-restricted ligand of CSF1R required for the development of Langerhans cells and microglia. *Nat Immunol* 13:753-760

Waskow C, Liu K, Darrasse-Jèze G, Guermonprez P, Ginhoux F, Merad M, Shengelia T, Yao K, Nussenzweig M. (2008) The receptor tyrosine kinase Flt3 is required for dendritic cell development in peripheral lymphoid tissues. *Nat Immunol* 9:676-683

Watchmaker PB, Lahl K, Lee M, Baumjohann D, Morton J, Kim SJ, Zeng R, Dent A, Ansel KM, Diamond B, Hadeiba H, Butcher EC. (2014) Comparative transcriptional and functional profiling defines conserved programs of intestinal DC differentiation in humans and mice. *Nat Immunol* 15:98-108

Wegner G. (1877) Chirurgische bemerkingen uber die peritoneal Hole, mit Besonderer Berucksichtigung der ovariotomie. *Arch Klin Chir* 20:51-59

Whitby JL, Rowley D. (1959) The role of macrophages in the elimination of bacteria from the mouse peritoneum. *Br J Exp Pathol* 40:358-370

Witmer-Pack MD, Crowley MT, Inaba K, & Steinman RM. (1993) Macrophages, but not dendritic cells, accumulate colloidal carbon following administration in situ. *J Cell Sci* 105:965-973

Wynn TA, Chawla A, Pollard JW. (2013) Macrophage biology in development, homeostasis and disease. *Nature* 496:445-455

Xu W, Schlagwein N, Roos A, van den Berg TK, Daha MR, van Kooten C. (2007) Human peritoneal macrophages show functional characteristics of M-CSF-driven anti-inflammatory type 2 macrophages. *Eur J Immunol* 37:1594-1599

Yona S, Kim KW, Wolf Y, Mildner A, Varol D, Breker M, Strauss-Ayali D, Viukov S, Guilliams M, Misharin A, Hume DA, Perlman H, Malissen B, Zelzer E, Jung S. (2013) Fate mapping reveals origins and dynamics of monocytes and tissue macrophages under homeostasis. *Immunity* 38:79-91

Ziegler-Heitbrock HW, Ulevitch RJ. (1993) CD14: cell surface receptor and differentiation marker. *Immunol Today* 14:121-125

Ziegler-Heitbrock L, Ancuta P, Crowe S, Dalod M, Grau V, Hart DN, Leenen PJ, Liu YJ, MacPherson G, Randolph GJ, Scherberich J, Schmitz J, Shortman K, Sozzani S, Strobl H, Zembala M, Austyn JM, Lutz MB. (2010) Nomenclature of monocytes and dendritic cells in blood. *Blood* 116: e74-80

Zigmond E, Varol C, Farache J, Elmaliah E, Satpathy AT, Friedlander G, Mack M, Shpigel N, Boneca IG, Murphy KM, Shakhar G, Halpern Z, Jung S. (2012) Ly-6C^{hi} monocytes in the inflamed colon give rise to pro-inflammatory effector cells and migratory antigen-presenting cells. *Immunity* 37:1076-1090

Appendix 1. Clinical characteristics of the study patients

(A) Clinical characteristics of new-starter PD patients (n = 50) in this study

Age at PD start (year-old)	55.18 ± 15.87
Gender (F/M)	18/32
Primary renal disease	
Diabetic kidney disease	15
Glomerulonephritis	12
Hypertensive renovascular disease	5
Cystic kidney disease	3
Myeloma kidney	2
Pyelonephritis	1
Interstitial nephritis	1
Congenital renal dysplasia	1
Nephrectomy	1
Unknown	9

(B) Clinical characteristics of stable patients and peritonitis patients in the study

	Stable patients (n = 37)	Peritonitis patients (n = 37)
Age at PD start (year-old)	63.81 ± 14.50	63.95 ± 15.00
Gender (F/M)	6/31	13/24
Primary renal disease		
Diabetic kidney disease	11	8
Glomerulonephritis	7	6
Hypertensive renovascular disease	4	5
Pyelonephritis	2	2
Interstitial nephritis	1	0
Obstructive uropathy	1	0
Nephrectomy	1	3
Cystic kidney disease	0	3
Unknown	10	10

Appendix 2. Antigen processing and presentation assay in mice

Note: This extract from a manuscript in preparation was written by Dr. Marcela Rosas and Prof. Philip Taylor. The experiments and data analysis were performed by Dr. Marcela Rosas.

Materials & Methods

Antigen processing and presentation assay

Bone marrow-derived dendritic cells (BMDC) from 129S6SvEv mice were differentiated in 20 ng/ml GM-CSF for seven days. B3Z, a CD8 $^{+}$ T-cell hybridoma specific for the ovalbumim$^{257-264}$ peptide (SIINFEKL) in the context of K^b, was provided by Nilabh Shastri (University of California, Berkeley, CA) (Karttunen et al., 1992). BO-97.11, a $CD4^+$ T-cell hybridoma that responds to the peptide ovalbumin$^{323-339}$ (ISQAVHAAHAEINEAGR) presented by I-A^b, was a gift from Philippa Marrack (National Jewish Center for Respiratory Medicine, Denver, CO) (Hugo et al., 1992). Purified APCs (10^4 cells per well) were co-cultured with BO97.11 cells at a 1:1 ratio in a 96-well flat-bottom plate in 40µl complete RPMI with or without 5 mg/ml EWE (see below). In control experiments $5x10^4$ BMDC, were used in a 1:1 ratio with either B3Z or BO97.11 cells with EWE or ovalbumin. To ensure antigen internalization and processing was occurring, BMDC were fixed with 1% paraformaldehyde for 10 minutes, which was then quenched with an equal volume of 0.1M glycine in PBS (pH 7.0) for 10 minutes (all at room temperature). APC were washed three times with medium before coculture with the T-cell hybridomas. The ovalbumin peptides indicated above (2µM) were used as controls. After 24 hours of culture at 37^{o}C, IL-2 in the supernatants was measured by ELISA on triplicate samples (R&D systems).

Preparation of EWE

To prepare EWE (Boes et, al., 2003), egg white was recovered through a small hole in the end of a fresh chicken egg and diluted to 50 ml with PBS. The egg white was repeatedly passed through decreasing needle sizes (21G to 25G) and then a 0.2 µm filter before storage at -80^{o}C.

Results

To determine if the peritoneal 'DC-like' cells were competent APCs we established a specific assay. To ensure that we directly measured antigen processing and not presentation of unprocessed 'low quality' antigen preparations, we prepared a fresh egg white extract (EWE)

as a source of ovalbumin (Boes et, al., 2003) (**Supplementary Fig. 1A**). BMDC were used live or fixed in antigen presentation assays with EWE and commercial ovalbumin to specific T cell hybridomas B3Z (MHCI-restricted (Karttunen et al., 1992)) and BO-97.11 (MHCII-restricted (Hugo et al., 1992). Commercial ovalbumin, but not EWE, could be presented by fixed BMDC (**Supplementary Fig. 1B**), so we used EWE to assess antigen processing and presentation.

Three 'DC-like' subsets and ResMØs were purified (See section 5.2.10). All putative APCs could process EWE and present to BO-97.11 $CD4^+$ T cells, as determined by IL-2 production. (**Supplementary Fig. 1C**). As previously noted (Dioszeghy et al., 2008), the $MHCII^{low/-}$ ResMØs had no significant activity in this assay. Compared to putative APCs, $MHCII^+$ InfMØs had only a minimal capacity to present ovalbumin to the BO-97.11 hybridoma (**Supplementary Fig. 1D**).

References

Karttunen J, Sanderson S, & Shastri N (1992) Detection of rare antigen-presenting cells by the lacZ T-cell activation assay suggests an expression cloning strategy for T-cell antigens. *Proc Natl Acad Sci U S A* 89(13):6020-6024.

Hugo P, Kappler JW, Godfrey DI, & Marrack PC (1992) A cell line that can induce thymocyte positive selection. *Nature* 360(6405):679-682.

Dioszeghy V, *et al*. (2008) 12/15-Lipoxygenase regulates the inflammatory response to bacterial products in vivo. *J Immunol* 181(9):6514-6524.

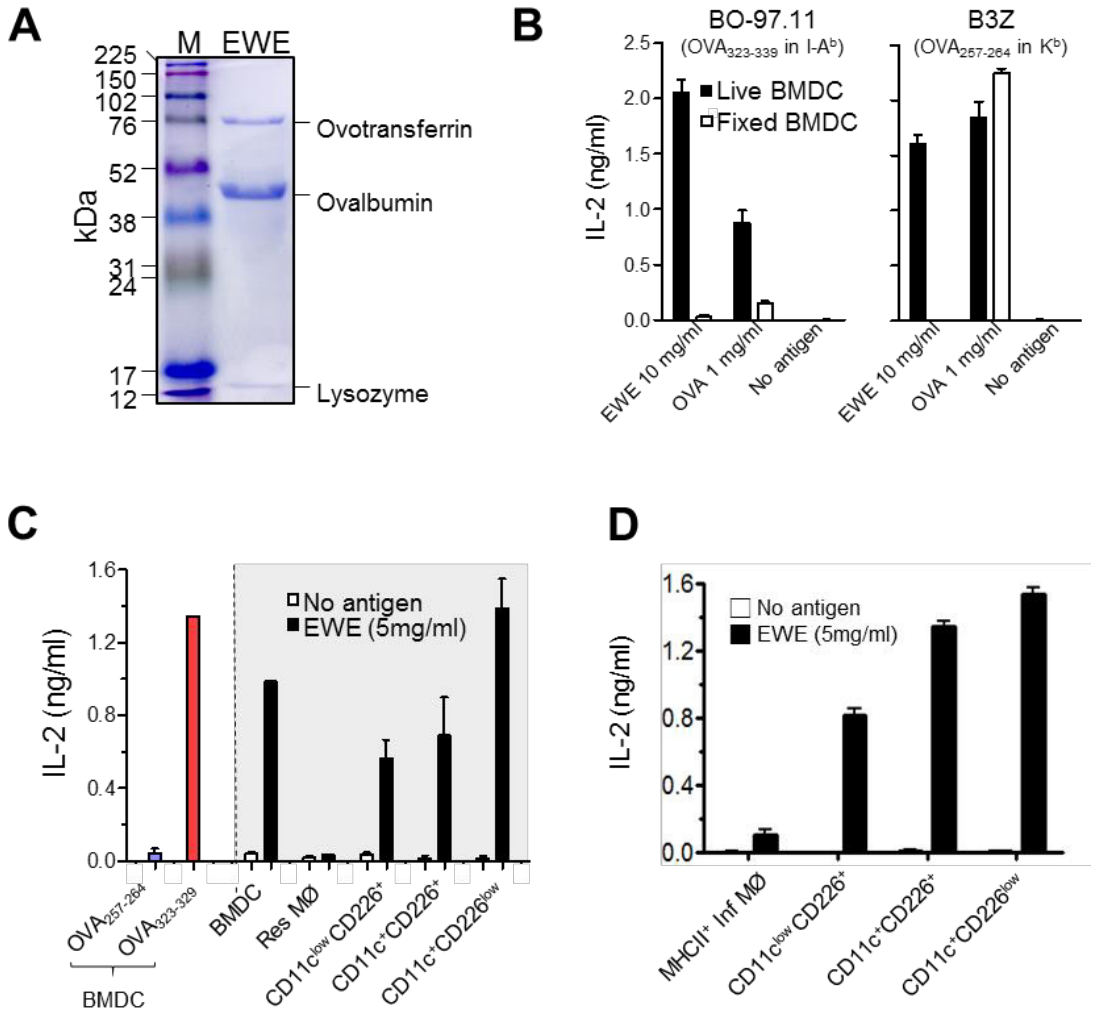

Supplementary Figure 1 All 'DC-like' subsets are effective at antigen processing and presentation. A) Coomassie stained SDS PAGE gel showing the protein content of EWE (5 µg resolved on a 12% SDS PAGE gel). Ovalbumin (OVA) (~45 KDa) is the major constituent of egg white. **B**) EWE was compared to a commercial preparation of OVA in antigen processing and presentation assays. The ability of BMDC (both live and paraformaldehyde fixed) to process and present both sources of OVA to BO-97.11 and B3Z cells as a measure of presentation on MHCII and MHCI, respectively. The fixed BMDC were able to present commercial OVA, particularly to the B3Z cells, indicating the presence of degraded protein and peptides and hence not an effective measure of antigen processing. The EWE, however, was only presented to either reporter cell when the BMDC were live, indicating that antigen processing was required. **C**) The ability of the purified cellular subsets from naïve C57BL/6 mice to process and present EWE on MHCII to BO-97.11 cells was assessed and compared to BMDC and BMDC pulsed with specific peptide. All three subsets of APCs were found to be competent at antigen processing and presentation. Data shows mean±SEM of IL-2 production by the BO-97.11 T cell hybridoma from two independent experiments, which were pooled after normalization of the data to the peptide pulsed BMDC control. **D**) Similar APC assay was performed using purified three 'DC-like' subsets as well as MHCII$^+$ InfMØs from 72 hours post-SES challenged C57BL/6 mice. Bar graph depicting the IL-2 production of BO-97.11 cells after culture with the indicated cell subsets and EWE. Data represents the mean±SEM of one of two identical experiments.